Insights on type I IFN signaling and regulation : studies of disease-associated TYK2 variants and of the negative regulators USP18/ISG15

Zhi Li

THESE DE DOCTORAT DE L'UNIVERSITE PARIS 6
PIERRE ET MARIE CURIE

Specialité : Physiologie, Physiopathologie et Thérapeutique

présentée par

Zhi LI

Unité de Signalisation des Cytokines

pour obtenir le grade de

DOCTEUR DE L' UNIVERSITE PARIS 6 PIERRE ET MARIE CURIE

Insights on type I IFN signaling and regulation: studies of disease-associated TYK2 variants and of the negative regulators USPl8/ISGl5

Soutenue le 12 octobre 2017

Devant le jury composé de :

Prof. Benoit SALOMON	Président
Dr. Iris BEHRMANN	Rapporteur
Dr. Stefan N. CONSTANTINESCU	Rapporteur
Dr. Gilles UZE	Examinateur
Dr. Pierre GENIN	Examinateur
Dr. Sandra PELLEGRINI	Directeur de thèse

ACKNOWLEDGEMENTS

Foremost, I would like to express my sincere gratitude to my advisor Dr. Sandra Pellegrini for having recruited me to her lab then accepted me as her Ph.D student and for her time and patience during all the time of research and of writing of this thesis. I have learned a lot working with her during these years.

I would like to thank all the members of my thesis committee for having accepted to evaluate my work: Prof. Benoit SALOMON as the president of the committee, Dr. Iris BEHRMANN and Dr. Stefan N. CONSTANTINESCU as *rapporteurs*, Dr. Gilles UZE and Dr. Pierre GENIN as *examinateurs*.

Special thanks to Josiane Ragimbeau for sharing with me her wisdom of science and of life.

I am very grateful to the present and past members of the lab: Josiane, Béatrice B, Frédérique, Françoise, Béatrice C, Priyanka, Erminia, Giulia, Véronique, Mark, Umeshree, Ignacio, Hana, Shen, Chau, Lasse, Arthur, Mathilde, Federica, Coralie, Alexandra, Milica, Manolo, Philippe, Betty, Corinna as well as Marie-Luce and Bérengère, Marie-Christine for all their support, insightful conversations and good mood during these years. It has been a real pleasure working with you all.

I thank Dr. Andres Alcover, Dr. Vincenzo Di Bartolo, Dr. Emmanuel Laplantine for insightful discussion and advice.

Many thanks to Hélène Quach, Jérémy Manry, Eddi Loh from Human Evolutionary Genetics Unit, for the conversations on SNP genotyping and LD interpretation. Many thanks to Valérie, Andrée, Isabelle from the preparation lab for their precious help.

I thank all the collaborators and CNRS for the support.

Last but not the least, I would like to thank my parents, my family and my friends for the love, trust and support they have given to me.

TABLE OF CONTENTS

ACKNOWLEDGEMENTS 1
TABLE OF CONTENTS 2
LIST OF ABBREVIATIONS 5
LIST OF FIGURES IN INTRODUCTION 7
RÉSUMÉ 8
INTRODUCTION 11
Part I - TYK2, from structure-function to diseases 12
1. Structural studies of the four JAK family members 12
1.1 The TK domain 16
1.2 The kinase-like domain 21
1.3 The N-terminal region 24
1.4 The JAK-receptor interaction 27
2. TYK2-activating cytokines 31
2.1 Type I IFN 31
2.2 IL-12 and IL-23 33
2.3 IL-10, IL-22, IL-26 and IFN-λ 35
2.4 The IL-6 family 38
2.5 IL-4 and IL-13 40
3. Tyk2 mouse models 41
4. TYK2-deficient patients 43
4.1 TYK2, cognate cytokine receptors and cytokine signaling 43
5. TYK2 and diseases 48
5.1 TYK2 variants associated with autoimmune diseases 48

Part II - Type I IFN and its physiopathological role 52
1. IFN induction 52
1.1 Constitutive IFN 52
1.2 Pathogen-induced IFN 52
2. IFN activities through ISGs: a double-edged sword 54
2.1 Direct antiviral activity 54
2.2 Orchestrators of innate and adaptive immunity 55
2.3 Anti-proliferative activity 56
2.4 Detrimental effects of ISGs 56
2.4.1 IFN and infectious diseases 57
2.4.2 IFN and autoimmune disease 57
2.4.3 Interferonopathies 58
3. Negative regulation of IFN signaling 60
3.1 Internalization, ubiquitination and degradation of IFNAR1 60

4. ISG15 and USP18 63
4.1 The ubiquitin-like ISG15 63
4.1.1 ISGylation 63
4.1.2 Extracellular ISG15 63
4.1.3 Antiviral role of ISG15 64
4.2 USP18 65
4.2.1 Usp18-deficient mice 65
4.2.2 USP18 as inhibitor of IFN signaling 66
4.2.3 USP18 and virus infection in mice 66
OBJECTIVES 68
MATERIALS AND METHODS 71
RESULTS 75
Part I - Functional study of natural TYK2 variants associated with AID 77
Part I-1. Functional impact of Rs12720356 (TYK2-I684S) and rs34536443 (TYK2-P1104A) 78
Two rare disease-associated TYK2 variants are catalytically impaired but signaling competent (Li et al., J. Immunol 2013) 78
Additional results 79
Part I-1 Further studies of rs12720356 (TYK2-I684S) and rs34536443 (TYK2-P1104A) 80
Part I-2. Functional impact of rs2304256 (V362F) and rs12720270 87
Part I-3. Functional study of the TYK2 FERM domain 95

Part II - Negative regulation of IFN signaling, from patients to mechanism 104
PartII-1. Studies of patients 105
USP18-deficient patients 106
ISG15-deficient patients 108
ISG15 deficiency and increased viral resistance in humans but not mice (Nature communications 2016) 111
Part II-2 Mechanistic studies of USP18 function in negative regulation of IFN signaling 113
DISCUSSION AND PERSPECTIVES 117
What have we learned from the AID-associated TYK2-I684S and TYK2 -P1104A ? 118
Is TYK2 rs2304256 (V362F) causal in AID ? 122
Why and how TYK2 FERM domain binds to PI(3)P ? 125
USP18, ISG15 and species-specific interaction of USP18/ISG15 128
A novel negative regulatory role of STAT2 131

REFERENCES.. 133
RÉSUMÉ 146

LIST OF ABBREVIATIONS

AGS	Aicardi-Goutières syndrome
AID	autoimmune diseases
AS	ankylosing spondylitis
BCG	Bacille Calmette-Guérin vaccine
BMM	bone marrow macrophages
CCR	CC-chemokine receptor
CDK	cyclin dependent kinase
cGAS	Cyclic GMP-AMP synthase
CXCL	CXC-chemokine ligand
DCs	dendritic cells
eQTL	expression quantitative trait locus
EBV-B	Epstein-Barr *Virus (*EBV)-immortalized B cell
FAK	focal adhesion kinase
FERM	band 4.1, ezrin, radixin, moesin
GAS	IFN-γ activation sequence
HVS-T	Herpes virus saimiri-transformed human T lymphocyte
IBD	inflammatory bowel disease
ICD	intracellular domain
IFI16	γ-IFN-inducible protein 16
IFN	interferon
IFNAR	interferon receptor
IFNLR	interferon-λ receptor
ILCs	and innate lymphoid cells
IRFs	interferon regulatory factors
IRSE	interferon-stimulated response element
ISG	interferon-stimulated gene
ISGF3	interferon-stimulated gene factor 3
JAK	Janus kinases
JH	JAK homology
KI	Knockin
KL	kinase-like
KO	Knockout
LCMV	lymphocytic choriomeningitis virus
LFA1	lymphocyte function-associated antigen 1
MAF	minor allele frequency
MAVS	mitochondrial antiviral signaling
MDA5	melanoma differentiation-associated gene 5

MEF	mouse embryonic fibroblast
MFI	mean fluorescence intensity
MS	multiple sclerosis
MyD88	myeloid differentiation primary response gene 88
NFκB	nuclear factor κB
NKT	natural killer T cells
PAMPs	pathogen-associated molecular patterns
pDC	Plasmacytoid dendritic cell
PDL1	programmed cell death ligand 1
PH	pleckstrin-homology
PHA	phytohemagglutinin
PI3K	phosphoinositide-3 kinase
PIAS	protein inhibitors of activated STAT
PRRs	pattern-recognition receptors
Ps	psoriasis
PTPN	Protein tyrosine phosphatase, non-receptor type
RA	rheumatoid arthritis
RT-PCR	retro-transcriptional polymerase chain reaction
SH2	Src homology 2
SHP	SH2-containing protein tyrosine phosphatase
SLE	systemic lupus erythematosus
SNPs	single nucleotide polymorphisms
SOCS	suppressor of cytokine signaling
STAT	signal transducer and activator of transcription
STING	stimulator of IFN genes
T1D	type I diabetes
T21	trisomy 21
Th	T helper
TK	tyrosine kinase
TNF-α	tumor necrosis factor-α
TRAIL	TNF-related apoptosis inducing ligand
TRIF	Toll-IL-1 receptor domain-containing adaptor-inducing IFN
Ub	ubiquitin
UC	ulcerative colitis
USP	ubiquitin specific protease
VPS	vacuolar protein sorting-associated protein
VSV	vesicular stomatitis virus
WT	wild-type
βTrCP	beta transducing repeat-containing protein

LIST OF FIGURES IN THE INTRODUCTION

Figure 1. Sequence alignment of the N-terminal region (FERM-SH2 domains) of the four human JAKs 14

Figure 2. Sequence alignment of the SH2-KL linker and the two kinase domains of the four human JAKs 15

Figure 3. Overview of the crystal structure of the JAK1 TK domain 16

Figure 4. Diagram of known interactions between the protein kinase catalytic core, ATP and a substrate 17

Figure 5. Structure of the JAK1 pseudokinase domain 23

Figure 6. Crystal structure of the tandem TYK2 pseudokinase-TK domain 24

Figure 7. The structure of the TYK2 FERM-SH2 receptor-binding module in complex with IFNAR1 26

Figure 8. Comparison of JAK FERM-SH2 domains 27

Figure 9. Views of the interactions between TYK2-IFNAR1 box2 and JAK1-IFNLR1 box1 in detail 29

Figure10. Alignment of box1 and box2 motifs from Janus kinase (JAK)-interacting cytokine receptors 29

Figure 11. Schematic representation of the IFN-triggered JAK/STAT pathway 32

Figure 12. Schematic illustration of the IL-12 and IL-23 receptor complexes 35

Figure 13. Schematic representation of IL-10, IL-22, IFN-λ (IL-28) signaling 38

Figure 14. Schematic representation of IL-6 cytokine family and their receptors 39

Figure 15. Schematic representation of the effects of IL-6 family cytokines on immune cells 40

Figure 16. Schematic representation of IL-4 and IL-13 signaling 41

Figure 17. Cytosolic receptors-mediated IFN induction pathways 53

Figure 18. Targets for interferon (IFN)-stimulated proteins within viral life cycles 55

Figure 19. IFN controls innate and adaptive immunity and intracellular antimicrobial programmes 56

Figure 20. Role of type I interferons in T cell immunity in acute and chronic infections 58

Figure 21. Monogenic disorders (blue boxes) considered as interferonopathies 59

Figure 22. Schematic representation of different pathways leading to ubiquitination-dependent downregulation of IFNAR1 62

Figure 23. Sequence alignment of ISG15s from mouse, human and other species, along with ubiquitin 64

RÉSUMÉ

In recent years, the pervasive action of type I IFN (IFN-α/β, here IFN-I) in human physiology and pathology has become evident. Actors of the immediate defence against viruses, IFN-I contribute to immune cell functions by orchestrating innate and adaptive immune responses. However, if the IFN-I system is dysregulated, altered immune responses and damaging processes can ensue as in the rare mendelian interferonopathies, several inflammatory and auto-immune diseases (AID) and some chronic viral infections. The evolution from beneficial to pathogenic IFN, which promotes persistent inflammation, immune cell dysfunction and tissue injury, remains poorly defined. On this basis, my thesis work has focused on the study of three elements of the IFN response pathway, with the view that their fine functional analyses could bring light onto how dysregulation may occur.

TYK2 belongs to the Janus protein tyrosine kinase family and is involved in signaling of several immunoregulatory cytokines, such as type I IFN (IFN-α/β) and type III IFNs, IL-6, IL-10, IL-12 and IL-23. Depending on the specific receptor complex, TYK2 is co-activated with either JAK1 or JAK2. A detailed molecular characterization of the interplay between the two juxtaposed enzymes is missing. In my study, I characterized TYK2 I684S and TYK2 P1104A, two rare human variants that have been associated with susceptibility to autoimmune diseases. I found that both variants are catalytically impaired but rescue signaling in response to IFN-I in fibroblasts. My results, coupled with additional functional study of JAK1-P1084A, support a model of non-hierarchical activation of Janus kinases where one catalytically competent JAK is sufficient for signaling provided that its partner, even if inactive, behaves as scaffold. Given the multitude of TYK2-activating cytokines, the cell type-specific dependence for TYK2 and the catalytic defect of the two disease-associated variants, I proposed that these two natural variants are relevant in complex immune disorders. Indeed, in addition to be associated with AID, a strong enrichment of TYK2 P1104A homozygosity was recently recorded in a cohort of patients with infection-predisposing primary immunodeficiency. My signaling studies showed that EBV-B cells homozygous for this variant exhibit mildly decreased IFN-I and IL-10 response, but abolished IL-23 signaling.

I studied two additional TYK2 variants (rs12720270, rs2304256) that have been associated with AID. Interestingly, from public eQTL datasets it appears that the rs2304256 minor allele correlates with elevated *TYK2* mRNA expression in many tissues. I found that both minor alleles promote retention of Exon8 and that an engineered TYK2 mutant lacking the Exon8-encoded segment is unable to bind the receptor subunit IFNAR1, though it retains catalytic

activity. I propose that this partial loss of function is due to loss of integrity of the FERM-SH2 domain and/or an alteration of a potential lipid-binding surface.

In the second part of my thesis work I contributed to dissecting the molecular mechanism that tunes down IFN-I response in primary cells derived from rare USP18- and ISG15-deficient patients that suffered of severe and mild interferonopathy, respectively. This work substantiated the role of USP18 as the essential negative feedback regulator of IFN-I particularly in the central nervous system. It also highlighted a novel function of the ubiquitin-like protein ISG15 in restraining IFN-I response in humans, but not in mice. Molecular analysis showed that USP18 tunes down IFN signaling by modulating IFNAR1 recruitment or altering the dynamics of receptor dimerization.

INTRODUCTION

My main research work has been on the protein tyrosine kinase TYK2. I have also actively contributed to projects addressing key questions on the mechanism of type I IFN signaling regulation. Therefore, I have subdivided the Introduction of my thesis into two major parts. Part I will be focused on JAK proteins with emphasis on structural studies aimed at understanding their functioning. TYK2 is involved in signaling of many cytokines, and these will be briefly described. I will also introduce natural TYK2 variants that have been associated with autoimmune diseases. Part II will be focused on type I IFN function and its signaling pathway, with particular attention to two negative feedback regulators, USP18 and ISG15.

Part I - TYK2, from structure-function to diseases

1. Structural studies of the four JAK family members The Janus kinases (JAK) form a small family of non-receptor protein tyrosine kinases comprising four members in vertebrates: TYK2, JAK1, JAK2 and JAK3. By binding to the intracellular regions of Class I and Class II cytokine receptors, these enzymes are utilized by several dozens of helical-bundle cytokines playing essential roles in ontogeny, homeostasis, differentiation, proliferation, survival and function of many cell lineages. Cytokine-induced catalytic activation of JAKs translates into gene expression programs induced by STAT (signal transducer and activator of transcription) family members, via the so-called JAK/STAT pathway. Tyrosine phosphorylated STATs often operate in combination with basal or induced, cell-specific or developmental transcription factors to fine-tune gene expression. By mediating cytokine signaling, JAKs are directly implicated in a variety of biological process ranging from hematopoiesis to the immune response to microbial pathogens and represent excellent targets for therapeutic intervention in human diseases. Since the description in the early nineties of the involvement of TYK2 in type I interferon signaling (1), an enormous effort has been made to elucidate the role of JAK enzymes in physiology and in pathogenic processes.

JAKs are relatively large proteins of 120-140 kDa containing at the N-terminus a FERM (acronym for band 4.1, ezrin, radixin, moesin) domain, followed by an SH2 (Src homology 2)-like domain and two tandem kinase domains, from which originated the name Janus (the roman god with two faces) given to the family. The pseudokinase domain (also called kinase-like or JH2 for JAK homology 2) is centrally located and has critical regulatory functions.

The tyrosine kinase (TK or JH1) domain is at the carboxyl end and exerts the catalytic phospho-transfer activity. These four domains are connected by flexible regions or linkers.

Below I will survey structural studies of the different JAK domains, starting from the TK domain, and provide an overview of our current understanding of the functioning of these proteins. The aligned sequences of the four human JAK paralogues are shown in Fig. 1 (FERM plus SH2-like domains) (2) and Fig. 2 (kinase domains) (3).

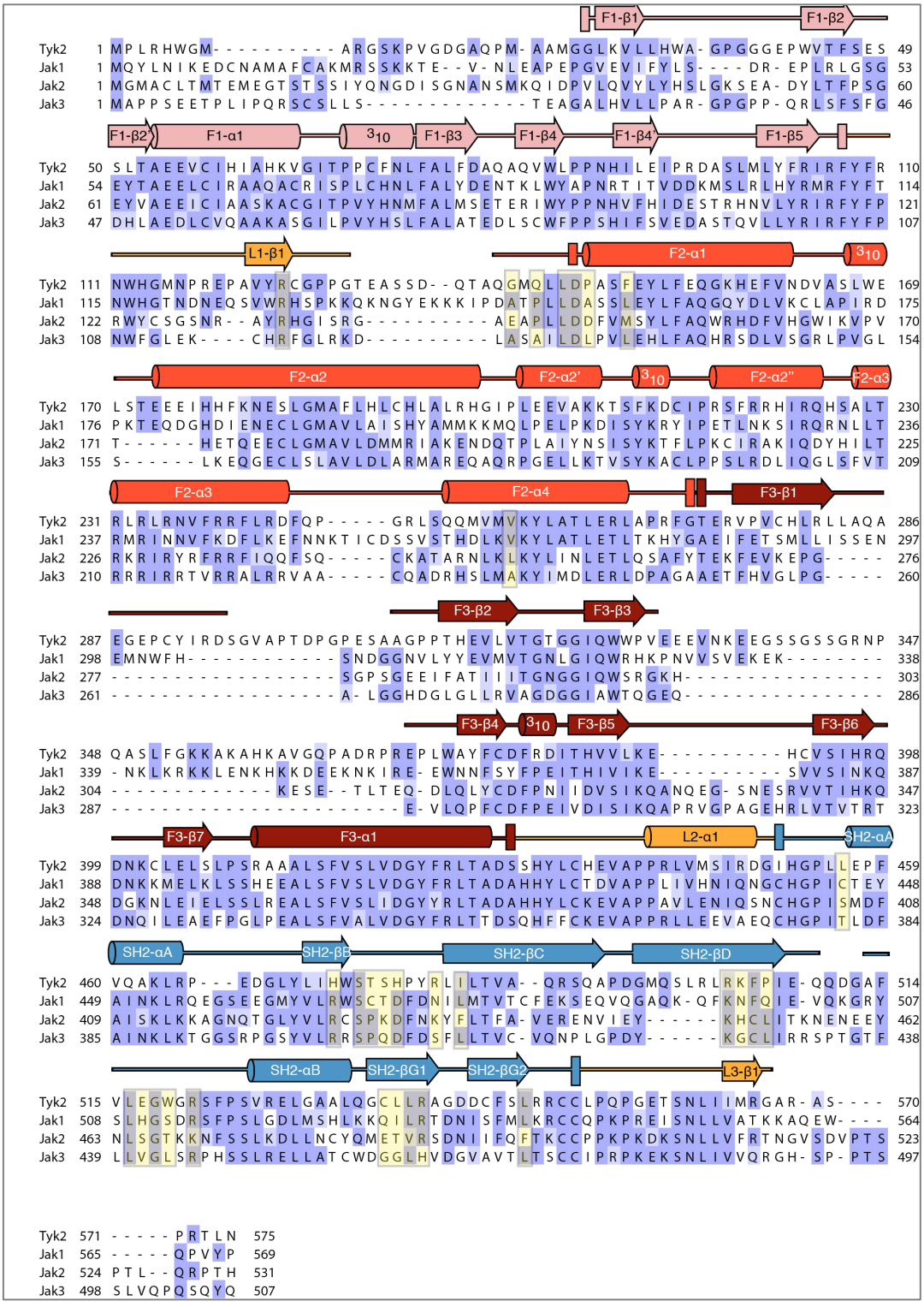

Figure 1. Sequence alignment of the N-terminal region (FERM-SH2 domains) of the four human JAKs, reproduced from (2). Secondary structure elements above the alignments are labeled as established for the FAK FERM domain and the SH2 domain of Lck, with α-helices as cylinders, β-strands as rectangular arrows, and loops displayed as lines. Shaded in yellow are residues contacting IFNAR1 in the crystal of the complex of TYK2 N-terminal region and a segment of its cognate receptor IFNAR1 (see (2) and text).

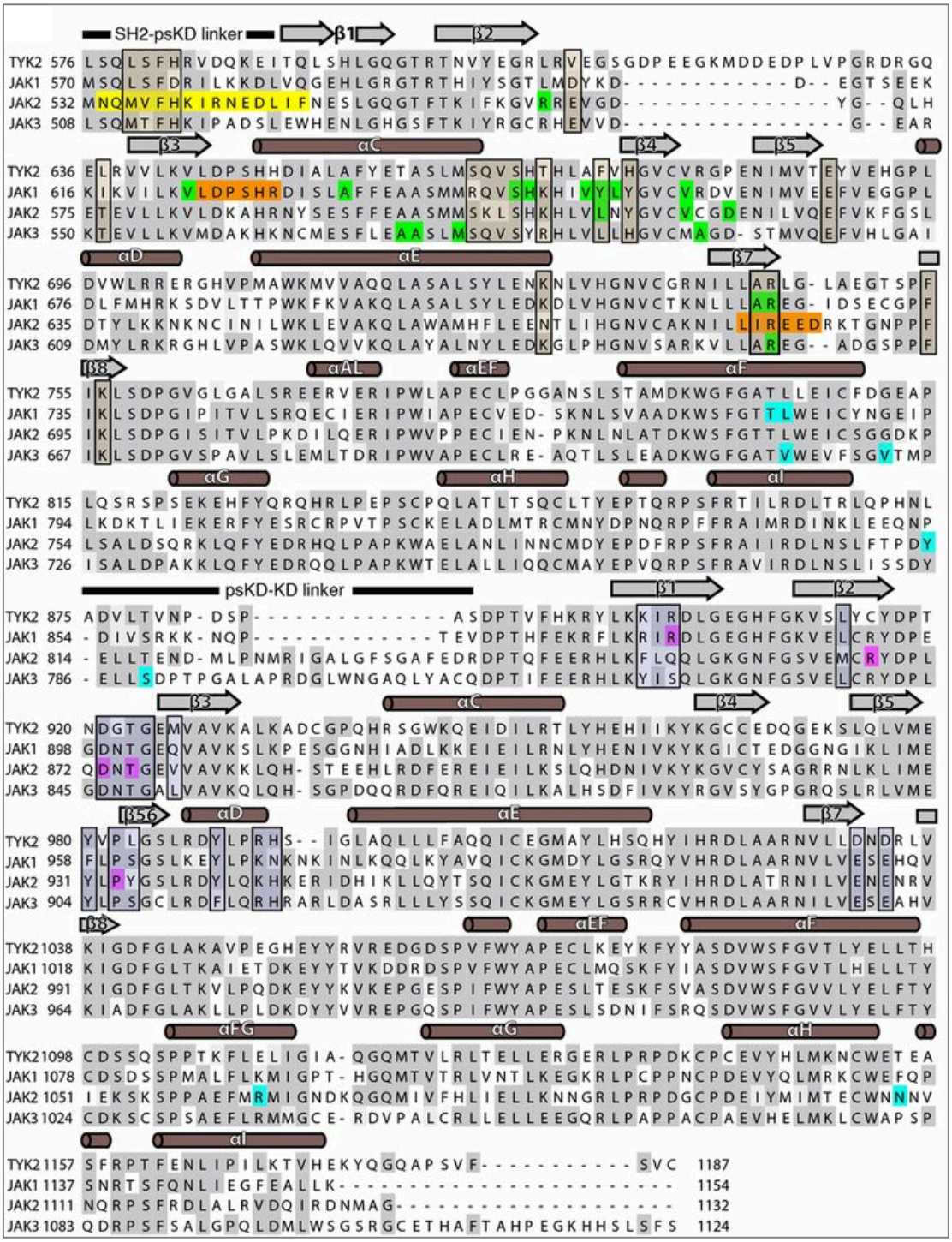

Figure 2. Sequence alignment of the SH2-KL linker and the two kinase domains of the four human JAKs, reproduced from (3). Secondary structural elements are shown above the sequences, with α-helices shown as cylinders and β-strands as rectangular arrows. Residues found within the pseudokinase and kinase interface are boxed and shaded in tan and blue, respectively. Cancer-associated JAK mutations are colored as follows: for the pseudokinase, point mutants are shown in green, deletions in orange, and the exon 12 segment in yellow. Point mutations in the TK domains are shown in magenta. Mutations outside the N-lobes of the pseudokinase or TK are shown in cyan.

1.1 The TK domain The crystal structure of the TK domain has been determined for the four JAKs (4-7) (8; 9). These domains exhibit the classical bi-lobed (small N-lobe and large C-lobe) architecture of a protein kinase domain. The N-lobe consists of five antiparallel β strands (β1 to β5) and one α-helix (αC helix) involved in catalytic regulation (Fig. 3 and cartoon in Fig. 4).

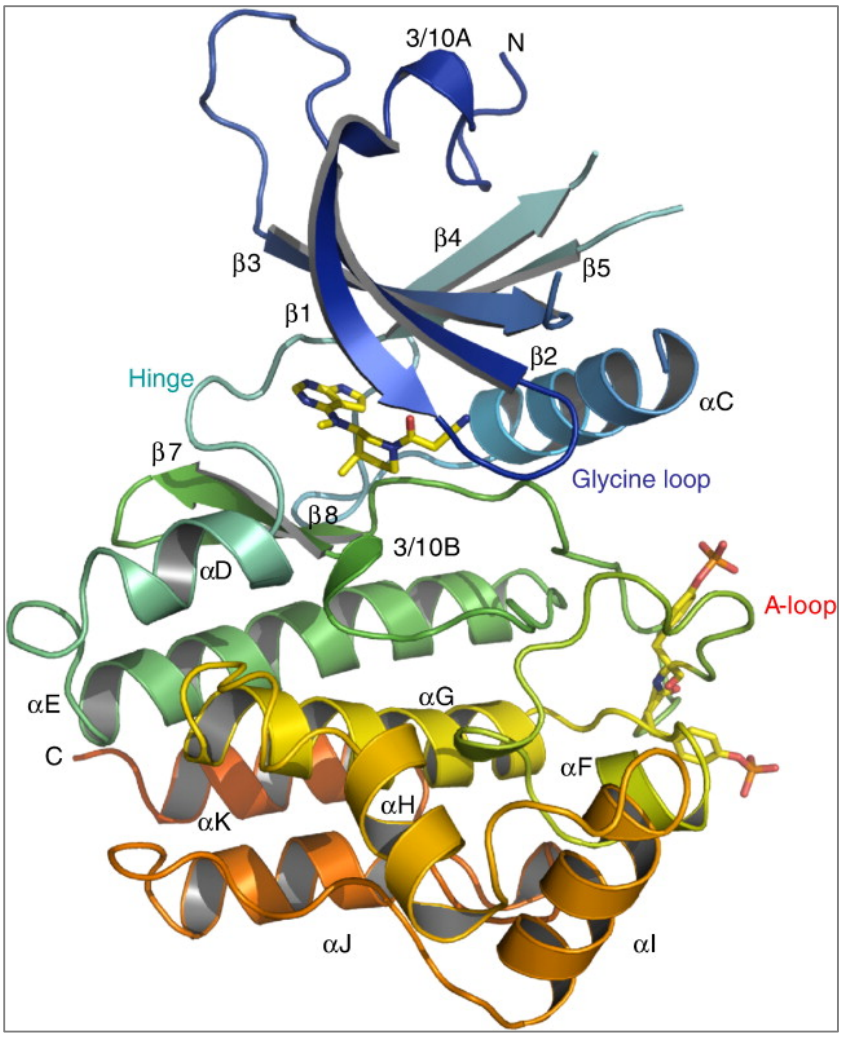

3

Figure 3. Overview of the crystal structure of the JAK1 TK domain in complex with CP-690,550, reproduced from (7). The N-lobe (residues 865-958) comprises a five-stranded antiparallel β-sheet (β1 to β5) and one α-helix (αC). The C-lobe (residues 995-1154) is predominantly helical with eight α-helices (αD to αK) and three 3/10 helices (3/10B, 3/10C and 3/10D), with one main pair of antiparallel β-strands (β7-β8). Locations of the hinge region, G-loop and A-loop are indicated. The bound inhibitor and phosphorylated Tyr1034 and Tyr1035 are presented in a ball-and-stick representation with carbon atoms in yellow, oxygen atoms in red, nitrogen atoms in blue and phosphorus atoms in orange.

The highly conserved structures and residues in this lobe are briefly described hereafter. Between the β1 and β2 strands is the glycine-rich loop (GxGxxG) called the G-loop or the phosphate-binding loop (P-loop), one of the most flexible elements of the catalytic core which participates in the phosphoryl transfer reaction and its regulation. A lysine residue in the β3 strand, called the ATP-binding Lys, establishes crucial contacts with the α- and β-phosphate groups, positioning them for catalysis (Fig. 4). In the active configuration, this Lys makes a salt bridge with a Glu residue of the αC helix (see below). Substitution of this conserved Lys with Arg or Glu abolishes catalytic activity, which can be measured *in vitro* as auto-phosphorylation or substrate phosphorylation.

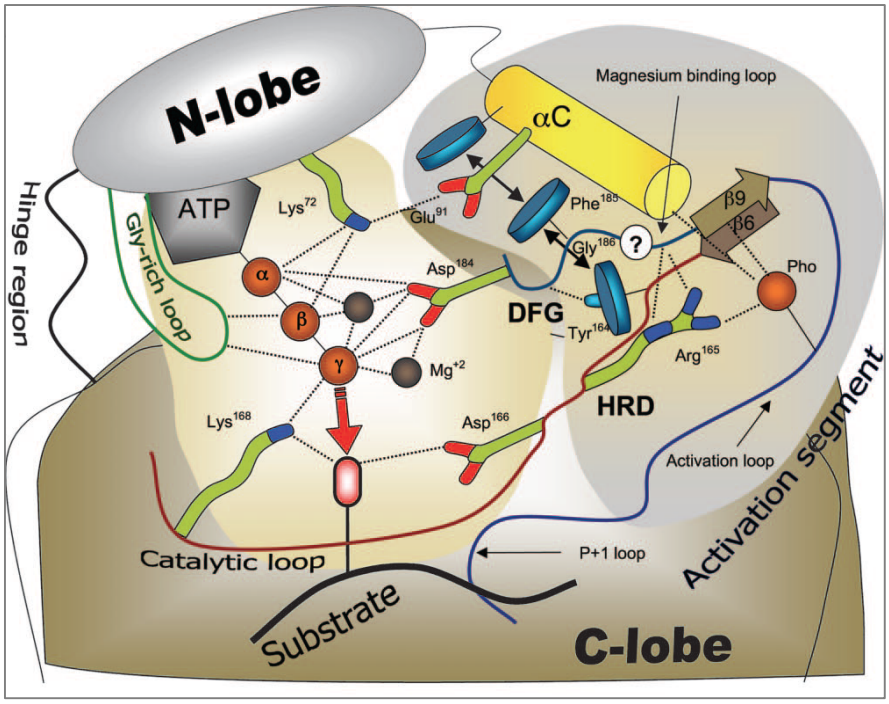

Figure 4. Diagram of known interactions between the protein kinase catalytic core, ATP and a substrate, reproduced from (10). Numbering of the serine-threonine kinase PKA is used. The red arrow indicates catalyzed transfer of the ATP γ-phosphate to a hydroxyl group of a protein substrate. Catalytically important residues which are in contact with ATP and/or substrate are shaded yellow. Secondary structures and residues which are known to be involved in regulation of the catalytic activity are shaded gray. Hydrophobic interactions between the HRD motif, the DFG motif and the αC helix are shown by black arrows. The important polar contacts are shown by dashed lines.

The αC helix is the only conserved helix in the N-lobe. It makes direct contacts with residues in the C-lobe, notably the Phe of the DFG motif of the A-loop. Together with the His of the HRD motif in the catalytic loop (Fig. 4), and with a residue in the β4 strand, these interactions contribute to form a hydrophobic "regulatory spine" in the active form of the kinase (10).

Thus, changes in the conformation of the αC helix will affect these interactions and modulate activity (11). A flexible hinge region connects the N-lobe to the C-lobe. The nucleotide (ATP)-binding site is located between the two lobes, bordering the hinge. Binding of ATP induces conformational changes by assembling a stack of nonlinear hydrophobic residues that span the two lobes, thus forming a "catalytic spine", which mediates phosphate transfer (Fig. 4) (12).

The large C-lobe is characterized by a high helical content (helices αD to αK) and two short β-strands (β7 and β8) preceding a flexible loop of 20 to 30 residues, called the activation or A-loop (Fig. 3). The highly conserved HRD motif is required for catalysis and forms the catalytic loop at the base of the active site (Fig. 4). The DFG motif is located at the N-terminus of the A-loop and, together with the following two residues, forms the Mg-binding loop. The Asp establishes polar contacts with all three ATP phosphates, directly or *via* coordinating atoms of Mg. The APE motif at the C-terminus of the A-loop is critical for organizing the substrate-binding network (12). Located in the A-loop of JAKs are two tyrosine residues (YY motif), whose phosphorylation is critical for kinase activity. In a general model of protein kinase activation, the phosphorylation of the tyrosine(s) of the A-loop causes a rearrangement of the DFG loop (from a 'DFG-out' to a 'DFG-in' position), positioning the Asp for interaction with ATP and the Phe for building the hydrophobic "regulatory spine" (Fig. 4). The αC helix in the N-lobe flips to complete the formation of the spine, securing it with the β3 Lys-Glu salt bridge (10). The substrate binds in an extended conformation across the front end of the nucleotide binding pocket, close to the γ-phosphate of ATP. The exposed phosphorylated A-loop provides a binding platform for the peptide substrate (11).

The TK domains of the four JAKs have all been co-crystallized with ATP-competitive inhibitors (type I inhibitor) and were all found to adopt an active 'DFG-in' conformation, with an exposed A-loop, either phosphorylated or not (Table 1). The JAK2 TK domain was also crystallized in complex with a type II inhibitor (NVP-BBT594) occupying a hydrophobic pocket adjacent to the ATP-binding site (9). Here, the TK domain was found to be in an inactive or 'DFG-out' conformation (Table 1). The first structure was reported by Boggon et al in 2005 (4). The TK domain of JAK3 was found to be in an activated state, *i.e.* with the two tyrosines of the A-loop phosphorylated. It was shown that the phosphate group on Tyr981 is in part coordinated by an Arg residue of the αC helix, suggesting a direct mechanism by which the active position of the αC helix is induced upon phosphorylation of the A-loop. A

direct coupling was also observed in the JAK2 TK structure, where the two phosphorylated tyrosines interact by hydrogen bonding with residues in the N lobe (αC helix), the C lobe and the A-loop, confirming their critical role in JAK activation (5).

In their study, Boggon *et al.* pointed at a unique insertion of about 20 residues located in the C-lobe between the αF and αG helices and thus named helix FG (4). Previously noticed in primary sequence alignments, the insertion was highlighted in the TK structures of the other JAKs and was called αH helix (as in Fig. 3), JAK-specific insertion or lip (5; 8; 13). This insertion may be relatively mobile and consists of a helix of about 8-10 residues followed by a short loop. One TYK2 natural variant (TYK2 P1104A) has been reported to be protective against many autoimmune diseases. TYK2 Pro1104 is located at the first turn of this JAK-specific αH (αFG) helix. Thus, this region is particularly interesting to me.

The αH (αFG) lines the substrate-binding site and is in close proximity to the catalytic cleft. Mutational study in JAK2 has clearly demonstrated an impact of this unique helix on catalytic activity (13). Adjacent to it is an evolutionally conserved GQM motif (Fig. 2) that was identified as a SOCS3-binding site in JAK1, JAK2 and TYK2, but not JAK3. Mutation of the GQM motif in JAK2 did not affect ATP hydrolysis but disturbed phosphate transfer to tyrosine substrate and prevented inhibition by SOCS3 (14). SOCS3 belongs to the family of SOCS (suppressors of cytokine signaling) proteins, which are induced *via* cytokine-JAK-STAT pathways. SOCS proteins suppress cytokine signaling cascade by inducing degradation of the target molecules (receptors or JAKs) *via* ubiquitination (15) or by directly inhibiting JAK kinase activity (16; 17). A 12-aa region at the N-terminus of SOCS1 and SOCS3, called kinase inhibitory region or KIR, was proposed to function as a pseudosubstrate essential for suppression of JAK-mediated cytokine signaling (17). The solved crystal structure of murine SOCS3 complexed with the JAK2 TK domain and a gp130-derived phoshorylated fragment showed that SOCS3 binding is centered on the JAK2 GQM motif and that the KIR of SOCS3 partially occludes the substrate-binding site of JAK2, inhibiting downstream signaling (18). These studies suggested that the JAK-specific insertion participates in the regulation of kinase activity, most likely by modulating substrate binding.

Table 1 Solved kinase domains of human JAK proteins

Reference	JAK	Domain	Inhibitor PDB code	Phosphorylation	Conformation
Boggon et al, Blood 2005 (4)	JAK3	TK 814-1103	AFN941 (stauro-based inhib) PDB: 1YVJ	doubly-P: Y980/981 one monomer	Active: DFG in, A-loop exposed
Lucet et al, Blood 2006 (5)	JAK2	TK	CMP6 PDB: 2B7A	doubly-P: Y1007/1008 two monomers	Active: DFG-in, A-loop exposed Salt bridge between K882 (β3) and E898 (αC)
Williams et al, JMB 2009 (7)	JAK1	TK 865-1154	CMP6 PDB: 3EYH CP690,550 PDB: 3EYG	doubly-P: Y1034/1035 one monomer	Active: A-loop exposed
	JAK2	TK 843-1132	CP690,550 PDB: 3FUP	similar to Lucet et al, Blood 2006 two monomers	
Chrencik et al, JMB 2010 (6)	TYK2 with mutations*	TK 888-1178	CMP6 PDB: 3LXP CP690,550 PDB: 3LXN	mono-P one monomer	Active: DFG-in, exposed A-loop Salt bridge between K930 (β3) and E947 (αC)
	JAK3 C1048S	TK 812-1124	CMP6 PDB: 3LXL CP690,550 PDB: 3LXK	unphosphorylated but enzymatically active	Active: A-loop exposed
Tsui et al, Proteins 2011 (8)	TYK2 D1023N in HRD motif	TK 889-1176 888-1178	Cmpd1 (TYK2 specific) PDB: 3NYX	unphosphorylated (active-site mutant)	Active-like conformation: DFG-in, A-loop exposed No K930-E947 salt bridge; αC is shifted outward
			CMP6 PDB: 3NZ0		Similar to Chrencik et al, JMB 2010
Andraos et al, Cancer Discovery 2012 (9)	JAK2	TK 840-1132	NVP-BBT594 (type II inhibitor) PDB: 3UGC	unphosphorylated (A-loop not accessible)	Inactive conformation: DFG-out, A-loop is missing
Bandaranayake et al, NSMB 2012 (27)	JAK2 WT V617F	KL 536-827	Apo WT PDB: 4FVP ATP WT PDB:4FVQ ATP V617F PDB:4FVR	unphosphorylated	Non-canonical ATP binding mode
Toms et al, NSMB 2013 (30)	JAK1 WT V658F	KL+SH2-KL linker 561-852	Apo WT PDB:4L00 Apo V658F PDB:4L01	unphosphorylated	Superimposes well with JAK2 KL by Bandaranayake et al, NSMB 2012
Lupardus et al, PNAS 2015 (3)	TYK2 D1023N	TK+KL 566-1187	Comp7012 (TYK2 specific) PDB: 4OLI	unphosphorylated	Active-like conformation: TK

* C936A, C1142A, Q969A, E971A, K972A

1.2 The kinase-like domain This domain has been called kinase-like (KL), pseudokinase or JH2 and is the most characteristic feature of JAK proteins and has been deeply investigated. As mentioned above, kinase activation requires 'optimization' of the C-lobe, which is achieved by phosphorylation of the A-loop. The N-lobe needs to be reorganized as well, in order to bind ATP and transfer the γ-phosphate to the substrate. The key residues that mediate these changes are missing in the pseudokinase domains of JAKs (Fig. 2). Notably, a threonine residue is found in place of the third glycine in the G-loop (GxGxxT). The glutamic acid in the αC helix is replaced by alanine or threonine, both unable to make a salt bridge with the ATP-binding lysine of the β3 strand. The catalytic HRD motif is replaced by HGN and the DFG motif by DPG. Finally, the activation loop is seven residues shorter than the A-loop in the TK domain and lacks tyrosine residues (Fig. 2). In spite of these differences, the pseudokinase domain of JAK2 was shown to possess a weak Ser/Thr kinase activity targeting two residues (Ser523 and Thr570) in the pseudokinase domain itself (19). Phosphorylation of these residues has an auto-inhibitory effect on the TK activity. Such mechanism does not operate in the other three JAKs, which lack the two target residues. The regulatory layer unique to JAK2 may relate to the fact that this latter is the only member of the JAK family that pairs with homodimeric-type cytokine receptors, and may thus need to be differently controlled.

The deletion of the pseudokinase domain can have variable functional consequences: in TYK2 it abrogates catalytic activity (20), but in JAK2 and JAK3 it leads to a catalytic gain of function (21). Importantly, in all cases the deletion of the pseudokinase domain abrogates cytokine-induced signaling. Loss-of-function point mutations in the pseudokinase of JAK3 cause severe combined immunodeficiency (22). Single mutations in the pseudokinase domain of TYK2 abrogate catalytic activity (23). The well-studied V617F substitution in the pseudokinase domain of JAK2 causes constitutive catalytic activation and is the predominant somatic mutation found in patients with myeloproliferative disorders (24). The corresponding substitutions in JAK1 (V658F) and TYK2 (V678F), but not JAK3, are also activating mutations (25; 26). The crystal structures of the JAK2 WT and the JAK2 V617F pseudokinase domains (Table 1) have been solved without and with Mg-ATP (27). These domains adopt a prototypical kinase fold and bind ATP and a single Mg^{2+} ion with high affinity but in a non-canonical mode. The F617 residue stabilizes the αC helix *via* an aromatic stacking interaction with two phenylalanines (F594, F595) of the αC helix. These data

supported previous biochemical studies showing that the gain of function of JAK2-V617F requires an aromatic amino acid at residue 595 (28; 29).

The JAK1 V658F mutation was found in T-cell acute lymphoblastic leukemia. The crystal structures (Table 1) of the WT and V658F JAK1 pseudokinase domains have been solved and their overall architecture closely resembles a typical TK domain (30) (Fig. 5). However, the region corresponding to the A-loop adopts a well-defined conformation that is predicted to preclude substrate binding. Importantly, in these two structures the linker connecting the SH2 to the pseudokinase domains (SH2-KL linker) is retained and adopts a partially α-helical conformation, extending along the N-lobe perpendicular to the C lobe. As shown in Fig. 5, V658 is located in a small loop at the end of β4. In the V658F structure, the β4-β5 loop rearranges and F658 occupies a position that in the WT structure is occupied by a residue in the linker (F575). Thus, F658 packs with F636 of the αC helix in an aromatic stacking interaction. In the WT protein, activation is thought to occur through rearrangements of the linker and the KL domain *via* a F-F-V triad (F575 in the linker, F636 in the αC helix, and V658 from the β4-β5 loop). These results suggest that the linker region is prone to movement and may be stabilized by the oncogenic F617. While this rearrangement may occur in all JAK family members, the question of how it leads to activation of the adjacent TK domain remains unanswered. The importance of the SH2-KL linker is further underlined by the fact that many JAK2-activating mutations found in patients lacking the V617F mutation cluster in the linker region (exon 12 mutations) (Fig. 2) (31).

The TYK2 variant rs12720356 (TYK2 I684S) that has been associated to autoimmune diseases is distant only six amino acid from Val678 (Val617 in JAK2) and is located on β5, proximal to the C-terminal end of the β4-β5 loop. The functional impact of this substitution on TYK2 function will be described in Results Part I.

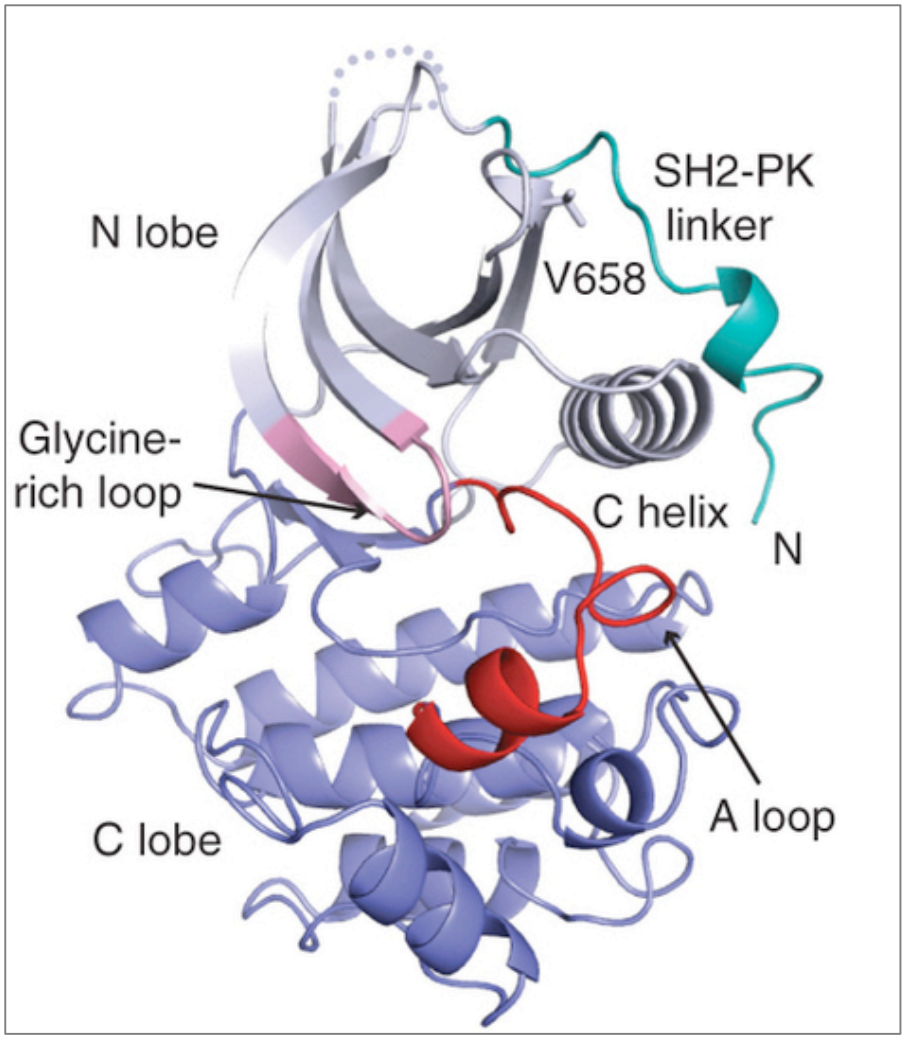

Figure 5. Structure of the JAK1 pseudokinase domain, reproduced from (30). Key structural motifs, and the Val658 residue at the end of the β4 (see text) are indicated. At the N-terminus of the domain, the SH2-KL linker adopts a partially α-helical conformation and extends across the N-lobe roughly perpendicular to the C helix. This domain superimposes well with the JAK2 pseudokinase domain structure reported in (27), where however the SH2-KL linker was missing.

The crystal structure of the pseudokinase and TK domains of TYK2, including the SH2-KL linker, was recently reported (3). The two kinase domains are in contact through their N-lobes (Fig. 6). The interface is generated by the back side of the pseudokinase N-lobe (the αC, the β4 strand and the extended β7-β8 loop), the SH2-KL linker, and the loop between β2 and β3 of the TK domain. Mutation of residues located near the interface resulted in increased *in vitro* kinase activity. The presence of an active-like conformation in this structure suggests that the pseudokinase domain regulates the TK domain by steric inhibition of ATP binding and/or by reducing the flexibility of the TK active site required for catalysis. Overall, these findings support an *in cis* autoinhibitory model (3), which is also proposed for JAK2 in a study based on molecular dynamics simulations of protein docking (32). Using different

approaches, a *trans* (inter-molecular) configuration model of JAK2 associated to the homodimeric growth hormone receptor has also been proposed (33; 34).

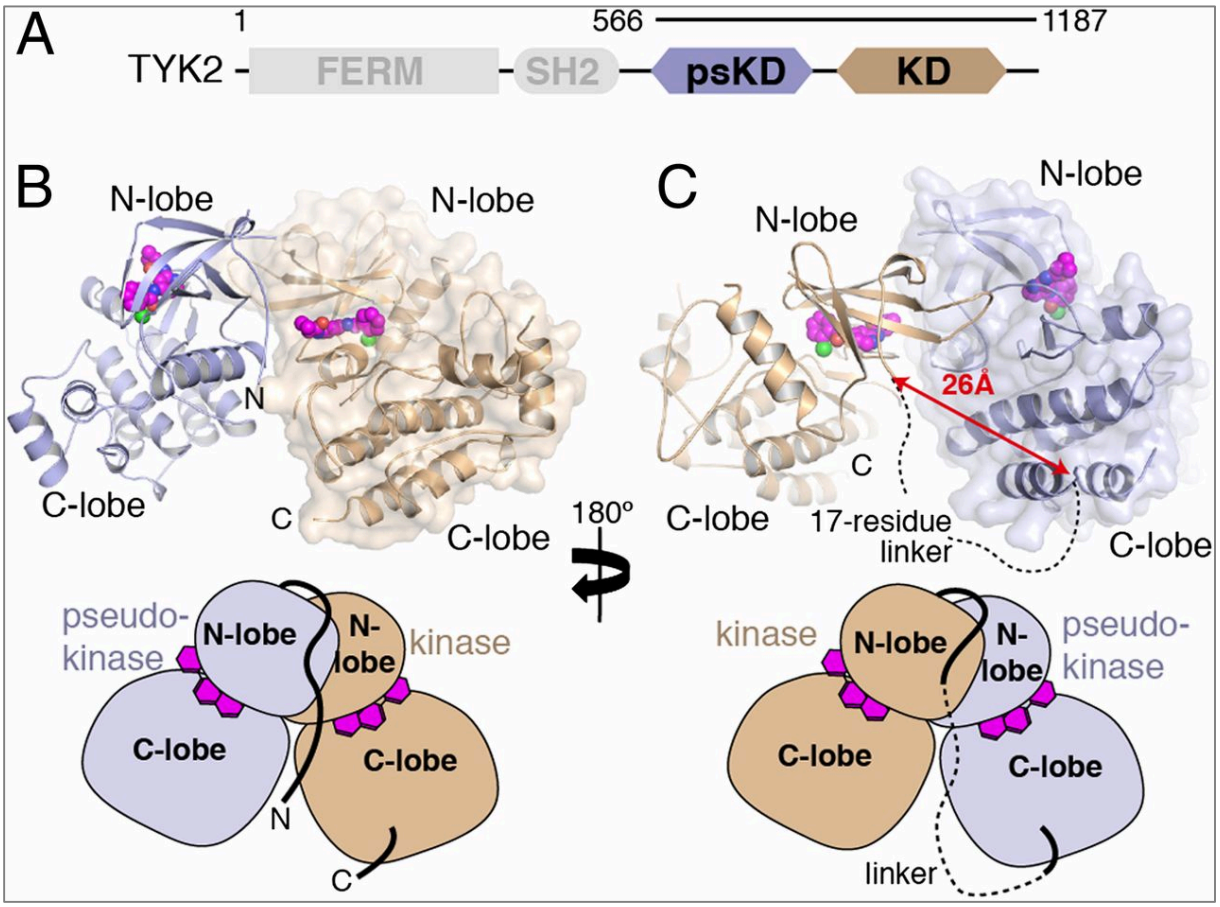

Figure 6. Crystal structure of the tandem TYK2 pseudokinase-TK domain, reproduced from (3). (*A*) Simplified domain structure of TYK2 indicating the boundaries of the pseudokinase-kinase construct used. (*B*) Diagram of the pseudokinase (blue) and kinase (tan) complex. From this view, the N and C termini of the crystallized construct are visible. The protein backbone is shown with the all-atom surface of the kinase domain displayed to AID consideration of the interaction interface. The kinase inhibitor molecule compound 7012 is shown in the active site as spheres (carbon atoms colored purple). (*C*) The diagram from *B* is rotated 180°, with pseudokinase and kinase represented in the same color, but the surface of the pseudokinase is shown. In this view, the region of the interdomain linker between the pseudokinase and kinase are visible, with a distance measurement and a dashed line shown to illustrate the connection made by the unobserved peptide linkage. Simplified diagrams are shown beneath each panel for orientation.

1.3 The N-terminal region. JAK proteins mediate cytokine signaling through direct and specific noncovalent interaction with receptors of the cytokine receptor superfamily. This interaction is highly selective, *i.e.* each JAK binds a defined subset of receptors. JAK3 binds only to the common γc, and JAK2 is the only member of the family that binds to

homodimeric-type receptor complexes. A major question in the field concerns the molecular definition of JAK/receptor binding specificity. No unique motif or structural determinant in cytokine receptor components solely specifies JAK binding, though a membrane-proximal region appears critical. This region contains a proline-rich box1 and a hydrophobic motif or box2, located 10 to 40 residues downstream (Fig. 10) (35).

On the JAK side, the FERM and SH2-like domains contain the structural determinants for receptor binding. In 2014, the first structure of the N-terminal region of a JAK protein was determined (2). The region encompassing the FERM and SH2 domains of TYK2 was crystallized in complex with a box2-containing segment of IFNAR1, one of the two subunits of the type I IFN receptor. Following this pioneer structure (Fig 7, Fig. 8B) (2), crystal structures of the human JAK1 FERM-SH2 fragments complexed with IFNLR (Fig. 8C) (36; 37) and JAK2 FERM-SH2 domains (Fig. 8D) (38) were resolved in 2016. The elucidation of FERM-SH2 structures from three of the four JAK family members enables the comparison of receptor-binding surfaces of each JAK and gives us novel clues to the molecular basis of the JAK-receptor specific interaction (see next section).

In the solved complex of TYK2 FERM-SH2 and IFNAR1*cyt*, the FERM domain displays the three lobed or clover leaf architecture (Fig. 7) which characterizes other FERM domains (39). The F1 lobe exhibits a ubiquitin-like fold with an insertion (L1) that interacts with the C-terminus of the SH2 domain and the IFNAR1 peptide. The F2 lobe is entirely helical and exhibits homology to an acyl-CoA-binding protein fold. Compared to canonical FERM domains, the structure of the F2 subdomain in JAKs is particular in at least two features: one is the prolonged F2-α2 helix and F2-α3 helix, forming an interface to bind the box1 region of cytokine receptors. The other feature of the F2 lobe is a basic patch (Fig.7 B, C) made of three helices (α2', α2", α3) containing 9 (15 in TYK2) conserved surface-exposed basic residues. The positive surface charge of F2 may direct this region in proximity to the phosphatidyl lipid head groups of the membrane Interestingly, in the protein FAK - a tyrosine kinase with a FERM domain - the positively charged region in the F2 lobe was shown to bind to PI(4,5)P2, inducing clustering of the kinase on the lipid bilayer, an important step in FAK activation (40). This patch was also shown to be involved in nuclear localization of FAK (41). The Pellegrini's lab showed that ectopically expressed TYK2 is diffusely localized in the cell including in the nucleus (42). While the role, if any, of this nuclear pool of TYK2 is unknown, it was shown that alanine substitution of three basic residues of the F2 lobe abrogated nuclear localization (42). The analogy with the study of FAK is thus inspiring. My study on the role of the positively charged region on the TYK2 F2 lobe will be described in Results, Part1-3.

The F3 lobe of the FERM domain (Fig. 7A) retains the topology of pleckstrin-homology (PH) domains, known to bind phospholipids and to target proteins to membranous structures. The core structure of the F3 subdomain of TYK2, JAK1, JAK2 is identical and highly similar to that of canonical FERM domains. Yet, the F3 subdomain of TYK2 deviates from those of JAK1 and JAK2 in two loop structures (Fig 1): TYK2 has a longer F3-β1/β2 loop (30, 19, 8 aa in TYK2, JAK1, JAK2, respectively) and F3-β3/β4 loop (44, 32, 12 aa in TYK2, JAK1, JAK2, respectively). In addition, these two F3 loops are highly conserved in different species. Remarkably, there is a specific basic motif (KKAKAHK) in the β3-β4 loop in TYK2 (Fig. 1), which may favor lipid interaction. My study on the role of these two loops of the F3 lobe will be described in Results, Part1-3.

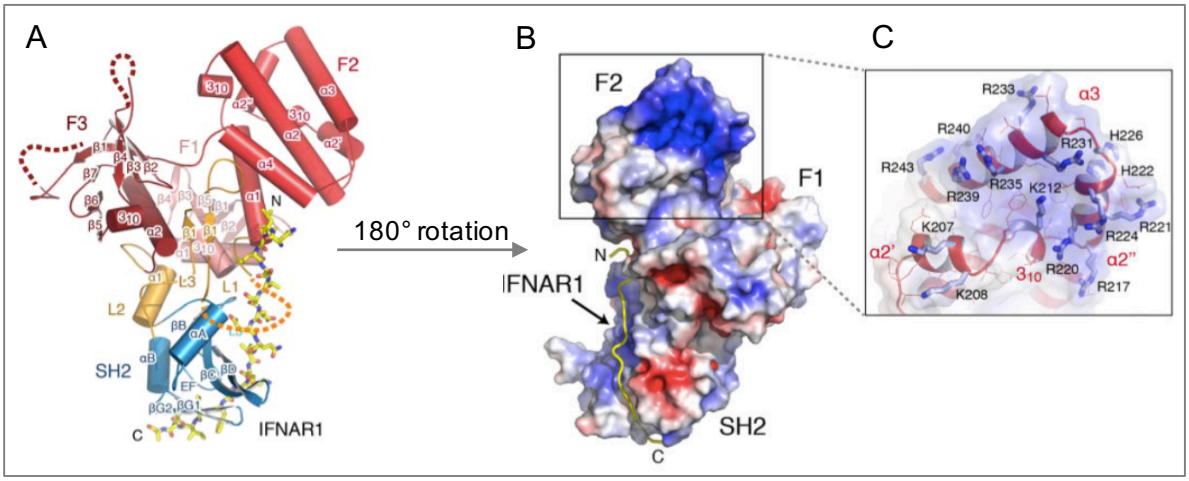

Figure 7. The structure of the TYK2 FERM-SH2 receptor-binding module in complex with IFNAR1, reproduced from (2). (A) A cartoon representation shows the interaction between TYK2 and IFNAR1. The FERM domain is colored in red, with the F1, F2, and F3 subdomains labeled. The SH2 domain is colored in blue, and IFNAR1 is colored in yellow. N- and C-termini are labeled N and C, respectively. (B) Electrostatic surface for the TYK2 FERM–SH2 structure. (C) The inset box shows a detailed view of the α2′, α2″, and α3 helices of the F2 subdomain, with basic side chains shown as sticks and colored in light blue.

In this pioneer structure, the SH2 domain adopts a characteristic SH2 fold and is intimately connected with the FERM domain (2). The C-terminus of the SH2 domain forms a linker which, together with the F1/F2 linker, holds the SH2 domain in place. Thus, the FERM and SH2 domains form a Y-shaped receptor-binding module that interacts with the receptor peptide (19 residues) *via* a composite interface formed by the F2 lobe and the SH2 domain, mimicking a SH2-phosphopeptide interaction. The degree of conservation of the FERM-SH2 and linker sequences in the JAK family suggests conservation of the overall domain (Fig. 1). Taken together, the pioneer TYK2 structure highlights the critical scaffolding function of the

SH2 domain in mediating receptor interaction and provides a hint of how receptor-JAK specificity can be achieved. Considering the described role of the SH2-KL linker in the interface between the two kinase domains and its impact on ATP binding affinity and catalytic activity (see above and (43)), it is plausible that this linker 'transfers' to the kinase the information regarding the conformational changes of the receptor induced by ligand binding. In line with these recent findings, early mutational studies of JAK1 and JAK3 implicated the FERM domain in the regulation of JAK activity (44; 45) and, reciprocally, inactivating mutations in the TK domain were shown to affect receptor function (46; 47).

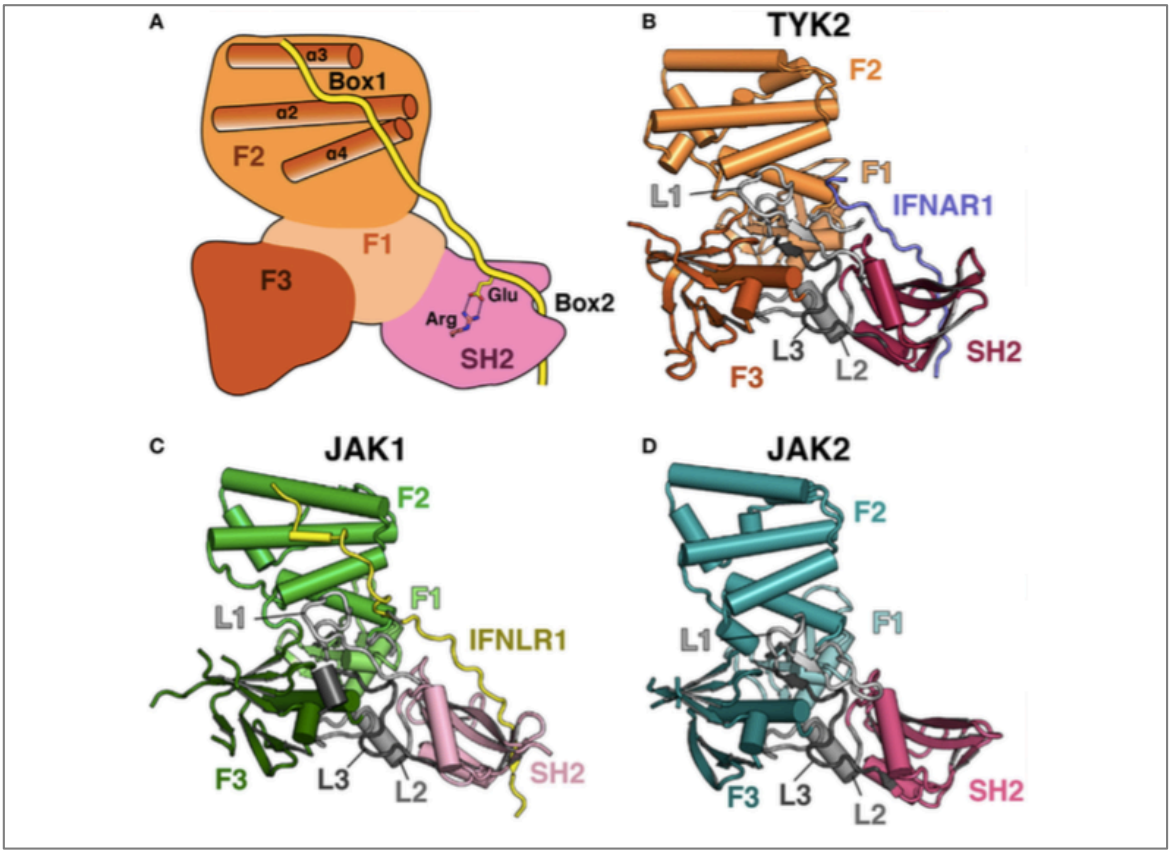

Figure 8. Comparison of JAK FERM-SH2 domains, reproduced from (35). (A) Cartoon depiction of a JAK FERM and SH2 module bound to a receptor, illustrating receptor recognition principles discovered in recent crystal structures, followed by representations of crystal structures solved for (B) TYK2 (C) JAK1 and (D) JAK2. The F1, F2, and F3 FERM subdomains are colored in various shades of orange, green, and blue, respectively. SH2 domains are colored in various shades of pink. Linkers L1, L2, and L3 are colored in various shades of gray. The IFNAR1 receptor peptide is colored blue, and the IFNLR1 is in yellow.

1.4 The JAK-receptor interaction. JAK family members engage specific cytokine receptors. Identifying the molecular determinants of this specificity has been an important goal in the

field. Below I will describe some details of the interface of JAK and receptor in the above structures and discuss the molecular basis of specific JAK-receptor interactions.

To overcome the poor expression and solubility of JAKs and inspired by the finding that TYK2 stabilizes IFNAR1 in cells (48), a protein containing the TYK2 FERM-SH2 domains fused to a juxta-membrane peptide of IFNAR1 enabled the pioneer crystallization of TYK2 FERM-SH2 domain with IFNAR1 Box2 (residues 478-512). In this structure (2), three interaction sections can be seen. The first section includes the interaction between three Leu (490, 491, 492) of box2 and a hydrophobic groove formed between F2, Linker 1 (F1/F2) and F1 (Fig. 9A, top panel). The middle section is a mimic of a pTyr-SH2 interaction, where the highly conserved glutamate residue (E497) of box2 (instead of pTyr) interacts with Ser476 and Thr477 from TYK2-SH2 domain by hydrogen bonds (Fig. 9A, middle panel). The third section involves hydrophobic interaction between box2 (C502, I504, +5 and +7 positions relative to E497) and a short β sheet of the TYK2 SH2 (Fig. 9A, bottom panel). By aligning the intracellular regions (Fig. 10) of cytokine receptors, the authors identified conserved box2-SH2 interaction motifs and other surrounding motifs, which may secure a tight JAK-receptor interface. Taken together, this interaction is primarily mediated by backbone H-bond (middle section) and non-polar interactions, therefore revealing how JAK SH2 domains can bind a range of weakly conserved box2 sequences that contain aliphatic residues in the first and third interaction sections.

IFNLR1 and IL-10R1 were found to bind JAK1 tightly enough to allow purification of a complex and crystallization. Importantly, these structures revealed an interaction between box1 of these class II cytokine receptors and the F2 of the JAK1 FERM (36). This interaction comprises two sites. The first interaction site lying on IFNLR box1 is a 3/10 helix consisting of Pro256, Trp257, and Phe258 (PWF motif). The Trp257 inserts into a deep groove formed by the F2-α2 and α3 helices (Fig. 9B, top panel). The second interaction site lying on IFNLR box1 is another 3/10 helix consisting of Pro264, Leu267, and Phe269 (motif PxxLxF), forming a hydrophobic ridge that interacts with a groove formed by the F2-α2, α3, and α4 helices in the JAK1 FERM F2 domain (Fig. 9B, bottom panel). The proline and leucine residues found in this PxxLxF motif are conserved in all class II cytokine receptors (Fig. 10). Interestingly, IL-10R1 lacking the PWF motif could not be co-crystallized with JAK1. The structure of a hybrid receptor formed by an N-terminal fusion of IFNLR1 PWF motif with the IL-10R1 box1 PxxLxF and box2 motifs display the identical interaction with JAK1 as IFNLR.

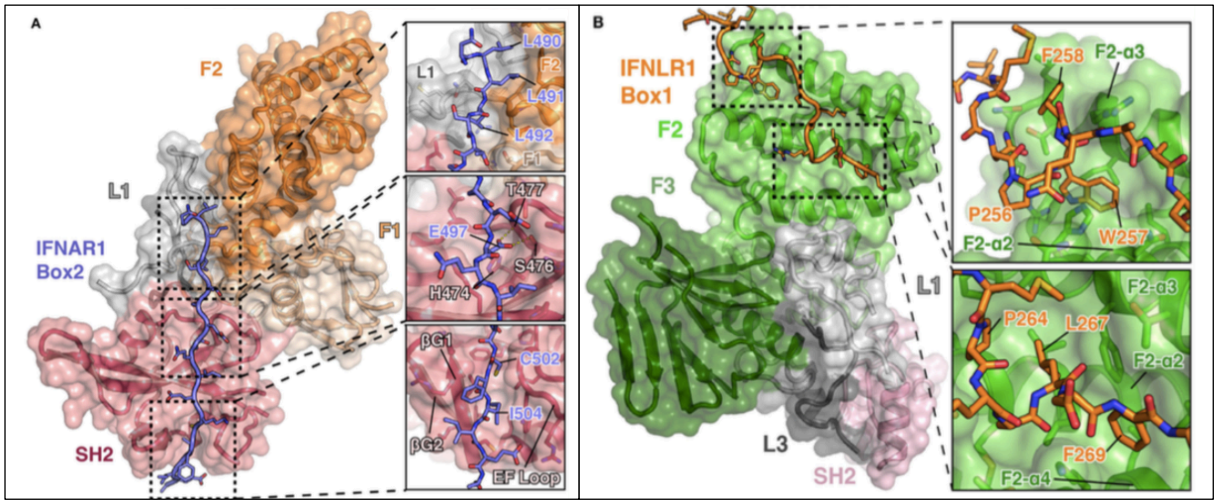

Figure 9. Views of the interactions between TYK2-IFNAR1 box2 and JAK1-IFNLR1 box1 in detail, reproduced from (35). (A) Overview of the interaction between TYK2 FERM and SH2 domains in complex with the IFNAR1 box2 region. Detailed interactions are shown for three regions of the TYK2–IFNAR1 complex (right panels). (B) Overview of the bipartite interaction between JAK1 FERM and SH2 domains in complex with the IFNLR1 box1 region. Detailed interactions are shown for two regions of the JAK1-IFNLR1 complex.

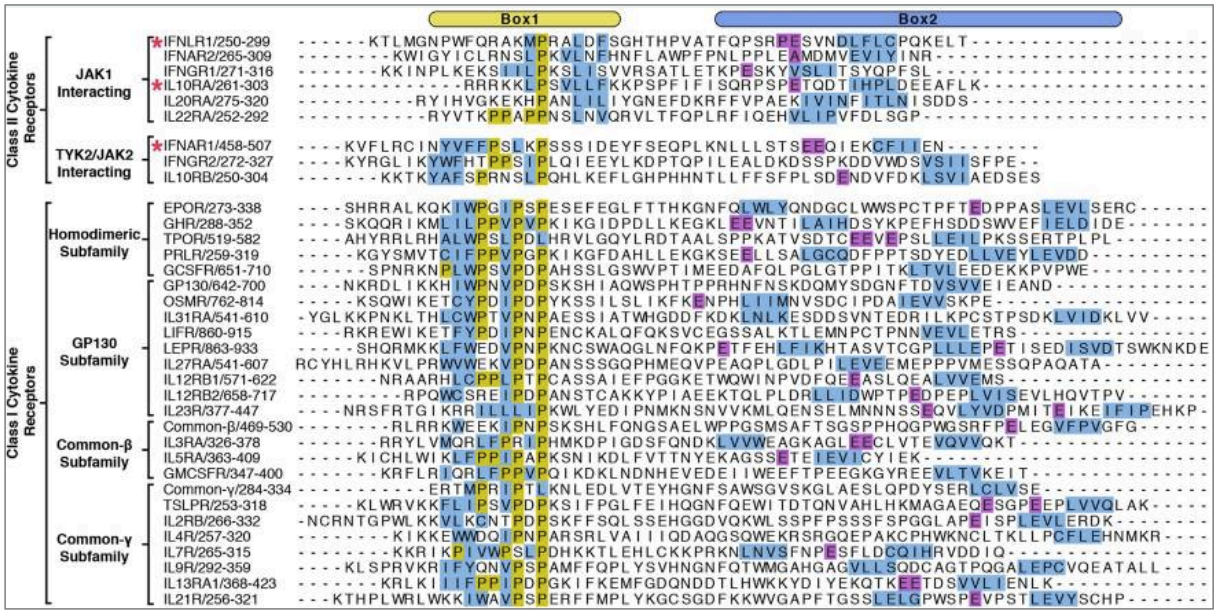

Figure 10. Alignment of box1 and box2 motifs from Janus kinase (JAK)-interacting cytokine receptors, reproduced from (35). The juxtamembrane intracellular sequences from all known signaling receptors that interact with JAKs were aligned by their box1 proline motifs. Hydrophobic residues within the box1 region are colored in blue and prolines in yellow. For the box2 region, putative four-residue hydrophobic motifs (aliphatic-X-aliphatic-X) are colored in blue, with glutamate residues three to seven residues N-terminal to these motifs are colored in purple. Receptors with known structures (IFNAR1, IFNLR1, and IL-10RA) are marked with a star.

A second crystal structure of the JAK1 FERM-SH2/IFNLR1 box1-box2 complex

demonstrated the simultaneous binding of box1 and box2 to a single JAK monomer (37). Here, a fusion of JAK1 FERM-SH2 to the IFNLR1 peptide was used (Fig. 8C). In this structure, box1 of IFNLR interacts with the FERM-F2 of JAK1 identically as described above. Box2 of IFNLR interacts with the JAK1 SH2 domain in a similar mode as in the IFNAR1/TYK2 complex. The first and third interaction sections are mediated by hydrophobic bonds in the same orientation. The major difference lies in the middle section where, instead of the hydrogen bond interaction, the salt bridge formed by the highly conserved glutamate (E285) of the IFNLR box2 and Arg466 (His474 in TYK2) of the SH2 of JAK1 closely mimics the interaction between a phosphate group and the SH2 arginine present in a canonical SH2-pTyr interaction.

Analysis of the conservation of the receptor-binding interfaces on the FERM F2 and SH2 domains indicates a significant level of conservation among JAK family members, suggesting that all JAKs interact with receptors with two common interfaces (Fig. 8A) (35). However, there are several differences in the JAK FERM F2 subdomains that may create incompatibility with certain box1 sequences. For example, the cleft accommodating the W257 of PWF motif in JAK1 is in a closed status in JAK2, the JAK2 F2-α2 helix is one turn shorter than in TYK2 and JAK1, the difference in the linker 1 and side chain variations within the peptide binding F2-α2/α3 interface between JAK1, TYK2, and JAK2. All these differences suggest that box1 PxxLxF is a specific binding motif for JAK1 (35).

With regards to the SH2 domain, the two structures (TYK2-IFNAR1 and JAK1-IFNLR1) show a remarkable similarity in their interaction mode, especially given the low sequence homology in the two receptors. The specificity for box2 binding in the SH2 of JAKs may be determined by certain residues at the interface (38).

Single-particle electron microscopy has been used to obtain molecular snapshots of full-length JAK1 purified from mammalian cells (49). Images indicated a highly flexible particle consisting of three main lobes ranging from an extended to a more compact conformation. In the 3D model, the pseudokinase and TK domains are always in close proximity, the FERM domain is more loosely connected and the SH2 domain seems to project out. Interestingly, the entire IL-6 signaling complex (gp130/IL-6/IL-6Rα and two JAK1) was greatly stabilized when reconstituted in a nanodisc that provides a native-like membrane environment. Thus, the authors speculated that JAK1 may contact the membrane, likely through the FERM domain, and this would enhance gp130 binding.

Among the many questions that remain to be answered is whether JAKs interact with lipids at the cell membrane and/or intracellular membranes? During my studies on TYK2, I have been brought to address this question (Results Part1-3).

2. TYK2-activating cytokines

TYK2 was discovered as the first JAK family member to mediate cytokine signaling (1). It was functionally identified by genetic complementation of the IFN-α unresponsive human fibroblastic cell line 11.1 (1; 50). These TYK2-null cells, called 11.1 or U1A, have been extensively used for structure/function analysis of TYK2 and for studying its implication in cytokine signaling, notably of type I IFNs. Interestingly, 11.1 cells display low residual sensitivity to IFN-β (1). In addition to its tyrosine kinase activity, TYK2 is required for optimal IFN binding to the receptor (20) and for scaffolding IFNAR1 at cell surface (46; 48).

Studies in the last 10-15 years have shown that TYK2 is also activated by members of the IL-12, IL-10 and IL-6 families. Several Tyk2 KO, KI and conditional mouse models have been generated for *in vivo* studies. However, it was only the recent identification of rare TYK2-deficient patients that allow to delineate the indispensable functions of TYK2 in humans.

Hereafter, I will describe succinctly type I IFN and other cytokines that activate TYK2.

2.1 Type I IFN

Type I IFNs (IFN-I, mainly IFNα/β here) are the first cytokines discovered. It is a large family that comprises many subtypes: IFN-β, IFN-ε, IFN-κ, IFN-ω and IFN-ν each encoded by an intron-less gene on chromosome 9, and 13 subtypes of IFN-α (51). With different binding affinities, all subtypes of IFN signal through the IFN heterodimeric receptor complex comprising IFNα receptor 1 (IFNAR1) and IFNAR2 subunits, which are ubiquitously expressed in all nucleated cells.

Type I IFNs signal via the JAK-STAT pathway**.** The JAK-STAT pathway was discovered in the early nineties in the context of IFN studies and was later found to be broadly used by all class I and class II cytokines. Type I IFNs act on cells in an autocrine and paracrine manner by binding and inducing the assembly of IFNAR1 and IFNAR2 subunits at the cell surface (52). It was proposed that IFN-I first bind to the high-affinity IFNAR2, followed by IFNAR1

recruitment in the binary complex. Upon ternary complex assembly, the pre-associated Janus family kinases (JAK) TYK2 on IFNAR1 and JAK1 on IFNAR2 are activated by transphosphorylation. Subsequently they phosphorylate tyrosine residues on the receptors, which serve as docking sites for STAT proteins. STATs in turn are phosphorylated by the JAKs on a specific tyrosine residue. Phosphorylated STATs (P-STAT) form homo- or heterodimers through intermolecular interaction of the phosphorylated tyrosine residue and Src homology 2 (SH2) domains and subsequently translocate into the nucleus and directly regulate interferon-stimulated-gene (ISG) transcription.

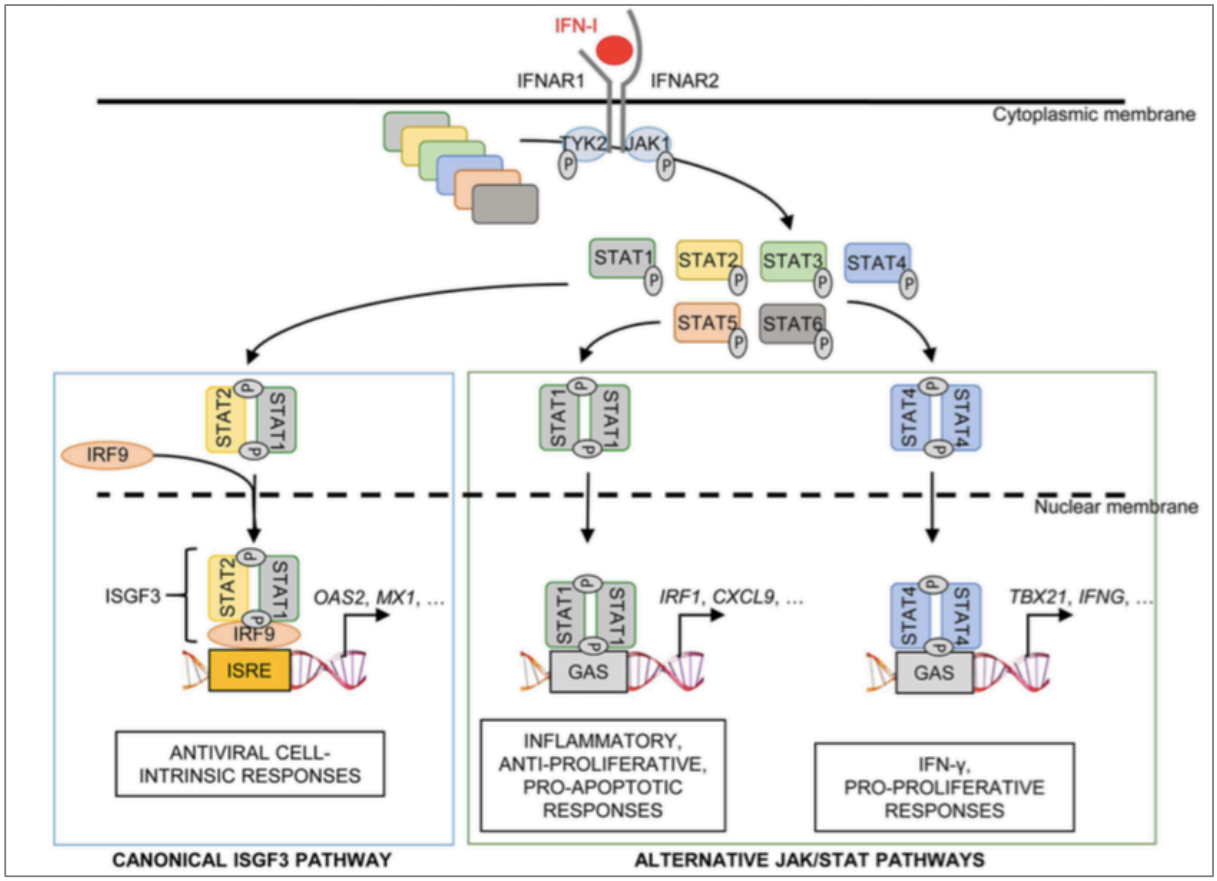

Figure 11. Schematic representation of the type I IFN-triggered JAK/STAT pathway, from (53)

IFN have the unique ability to activate all seven known STATs (STAT1, 2, 3, 4, 5α, 5β, 6), and to induce the formation of many different STAT homodimeric or heterodimeric complexes. The transcription factor ISGF3, formed by the p-STAT1/p-STAT2 heterodimer and IRF9, is the hallmark of type I IFN signaling. ISGF3 binds IFN-stimulated response elements (ISREs) within the promoter of ISGs. Other P-STAT dimers bind the IFN-γ activation sequence (GAS) elements present in ISG promoters (Fig. 11). The combination of

different dimers of phosphorylated STATs with different affinity to specific GAS elements will lead to distinct transcription programs and determine different biological functions. Signaling through STAT1 is known to be pro-inflammatory, anti-proliferative and pro-apoptotic, as opposed to signaling through STAT3, STAT4 and STAT5, which induce genes that promote cell survival, proliferation and differentiation (Fig. 11). Thus, the intracellular competition between STAT1 and STAT3, STAT4 and STAT5 determines the transcriptional and functional consequences of type I IFN signaling (53; 54). For example, in quiescent NK cells where there is more STAT4 than STAT1, IFN-I activate STAT4 and induce pSTAT4 homodimer-mediated NK cell activation, including IFNγ production and T-bet-driven proliferation. In activated NK cells with increased STAT1 level, IFN-I promote a STAT1-mediated anti-proliferative effect (55). In TCR-activated T cells maintaining a low level of STAT1 compared to other STATs, IFN-I signal is transduced by other STATs than STAT1, leading to T cell survival and proliferation, CD8+ T cells differentiation and Th1 cell polarization (54). However, for naïve T cells or in the situation of sustained IFN exposure (for example, chronic infection), type I IFNs exert anti-proliferative and pro-apoptotic effects mediated by STAT1 (54). In addition to the canonical JAK/STAT pathway, IFN have been reported to activate other pathways, such as PI3K signaling. My work has focused on the JAK/STAT pathway.

Type I IFNs play an essential role in host defense against viruses by its direct antiviral activity in infected and neighbouring cells and by activating immune cells. However, if the IFN-I system is dysregulated, altered immune responses and damaging processes can occur, such as in the rare mendelian interferonopathies, auto-immune diseases and some chronic viral and bacterial infections. The evolution from beneficial to pathogenic IFN-I, which promotes persistent inflammation, immune cell dysfunction and tissue injury, remains poorly defined. Aspects of the physiopathological role of IFN-I and negative regulation of signaling will be discussed extensively in Part II of the Introduction.

2.2 IL-12 and IL-23

The IL-12 cytokine family is composed of IL-12, IL-23 and IL-35. TYK2 is involved in IL-12 and IL-23 signaling through its association with the shared receptor IL-12Rβ1 (Fig. 12). Both cytokines play important role in controlling innate and adaptive immune responses.

IL-12 (Fig. 12) is a heterodimer composed of a 35kDa α-chain (p35 subunit) and a 40kDa β-chain (p40 subunit), which are linked via disulphide bonds. The p35 and p40 subunits bind to the receptor IL-12Rβ2 and IL-12Rβ1, respectively. Both receptors are required for high affinity binding of IL-12. TYK2 associates to the intracellular domain of IL-12Rβ1 and JAK2 to IL-12Rβ2. There is no tyrosine residue in the intracellular domain (ICD) of IL-12Rβ1, so that STATs are recruited to IL-12Rβ2 for activation. STAT4 plays a central non-redundant role in the IL-12 signaling cascade, although other STATS, STAT1, STAT3 and STAT5 can be activated by IL-12. Upon pathogenic infection, IL-12 is produced and secreted by macrophages, monocytes, dendritic cells (DCs), granulocytes and B cells. Secreted IL-12 binds to its receptor, mainly expressed on T cells and NK cells, and triggers the JAK-STAT pathway. Phospho-STAT4 binds to the promoter of the IFN-γ gene and rapidly induces IFN-γ production. IFN-γ in turn acts on macrophages enhancing their phagocytic function and local inflammation by inducing NO synthase and the subsequent release of reactive nitrogen species. IFN-γ also acts on T cells in an autocrine manner to maintain IL-12Rβ2 expression which is inhibited by IL-4. Through these auto- and paracrine positive feedback loops, IL-12 plays a central role in the amplification and expansion of Th1 cells. IL-12 also promotes NK cell and CD8+ cytotoxic T lymphocyte (CTL) proliferation and cytotoxic activities (granzyme and perforin production) (56). Patients with genetic deficiencies in the IL-12p40, IL-12Rβ1, IL-12Rβ2, IFN-γR1, and IFN-γR2 genes are more susceptible to mycobacterial infections and display enhanced atopic disease (57).

IL-23 is a heterodimer of p19 and p40 (Fig. 12), the latter being shared with IL-12. The receptor complex is composed of IL-23R and IL-12Rβ1, expressed in Th17 and other immune cells, such as natural killer T (NKT) cells and innate lymphoid cells (ILCs). IL-23 signaling is mediated primarily by the JAK/STAT pathway. IL-23 binding to the receptor leads to activation of TYK2 and JAK2, which mediate receptor phosphorylation and STATs activation. STAT3 is believed to be the major signal transducer, although IL-23 activates STAT1, STAT4 and STAT5 as well. STAT binding sites are located in the IL-23R but not in the IL-12Rβ1 chain.

The main function of IL-23 is to promote Th17 and Th22 cell differentiation and thus production of IL-17 and IL-22. Via broadly expressed IL-17 receptors (on fibroblasts, epithelial cells, keratinocytes, endothelial cells, myeloid cells), IL-17 contributes to the host defense against extracellular bacterial and fungal infections. IL-17 activity also inhibits matrix

production, and can lead to tissue damage and defective tissue repair during chronic inflammation (58).

IL-23 and IL-17 are considered pathogenic in many autoimmune diseases (59), such as rheumatoid arthritis (RA), psoriasis, inflammatory bowel disease (IBD), type I diabetes (T1D), ankylosing spondylitis (AS) and multiple sclerosis (MS). Single-nucleotide polymorphisms (SNPs) in genes involved in IL-23 signaling (*IL-23A, IL-23R, and IL-12B*) have been associated with psoriasis. In addition, an IL-23R variant (R381Q), which leads to decreased receptor expression (60), confers strong protection against many autoimmune diseases, such as AS and Crohn's disease.

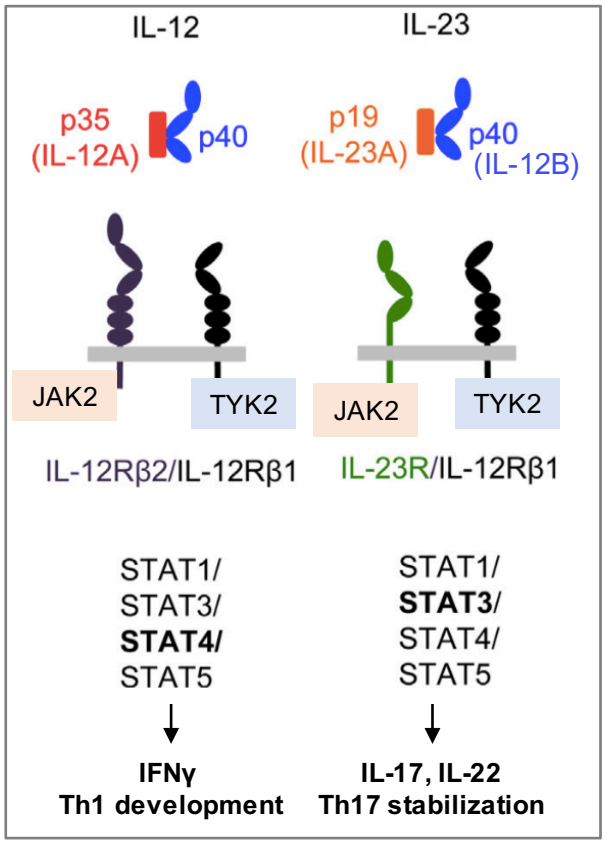

Figure 12. Schematic illustration of the IL-12 and IL-23 receptor complexes. IL-12 mainly induces STAT4 phosphorylation, whereas IL-23 mainly induces STAT3 phosphorylation. Adapted from (61)

2.3 IL-10, IL-22, IL-26 and IFN-λ

IL-10, IL-22, IL-26 and IFN-λ are members of the IL-10 cytokine family, which includes additional members such as IL-19, IL-20, IL-24. TYK2 is involved in signaling of IL-10, IL-22, IL-26 and IFN-λ by associating to the shared receptor IL-10Rβ2. There is no tyrosine residue in the ICD of IL-10Rβ2, so that STATs are recruited to their JAK1-associated

cytokine-specific receptor chain (Fig. 13). The different signaling properties and functions of these cytokines are summarized in Table 2.

IL-10 is considered as a critical anti-inflammatory cytokine regulating innate and adaptive immunity. It is secreted by a variety of cells and has pleiotropic effects on T, B and myeloid cells, and other cell types. In particular, IL-10 inhibits the secretion of pro-inflammatory cytokines, such as tumor necrosis factor α (TNF-α), IL-12, IL-23 and IFN-γ. Thus, IL-10 prevents excessive inflammation and tissue damage during the recovering phase of infections. STAT3 is the key transcription factor. Lack of STAT3 completely abolishes the suppressive effects of IL-10 on production of pro-inflammatory cytokines by macrophages and neutrophils. The protective role of IL-10 in IBD in humans has been corroborated through identification of patients with early-onset IBD that are deficient in IL-10R1 or IL-10R2 (62).

Table 2. Cytokines sharing IL-10R2, adapted from (63)

<table>
<tr><th>Cytokine</th><th>JAK1-associated receptor chain</th><th>STAT</th><th>Major cellular sources</th><th>Cellular targets</th><th>Key functions</th><th>Structure</th></tr>
<tr><td>IL-10</td><td>IL-10R1</td><td>STAT3
STAT1
STAT5</td><td>Leukocytes</td><td>Leukocytes</td><td>Immune repression</td><td>Dimer</td></tr>
<tr><td>IL-22</td><td>IL-22R</td><td rowspan="2">STAT3
STAT1</td><td rowspan="2">Th22, Th1, Th17, others (CD8 T, NK, NKT)</td><td>Epithelial cells</td><td rowspan="2">Antibacterial response, tissue remodeling, wound healing</td><td>Monomer</td></tr>
<tr><td>IL-26</td><td>IL-20R1</td><td>Epithelial cells and immune cells</td><td>Dimer?</td></tr>
<tr><td>IFNλ</td><td>IFNLR1 (IL-28R)</td><td>Same as type I IFN</td><td>Leukocytes, Epithelial cells</td><td>Epithelial cells Leukocytes?</td><td>Antiviral responses</td><td>Monomer</td></tr>
</table>

Unlike IL-10 that targets immune cells, IL-22 and IL-26 primarily target epithelial cells in various organs, protect them from pathogens (bacteria/yeast) invasion and enhance tissue remodeling and wound-healing. Thus, IL-22 and IL-26 help to maintain tissue integrity and restore homeostasis of epithelial layers during infection and inflammatory responses (63). Not expressed in immune cells, IL-22R is expressed in many organs (kidney, the digestive system, lung, trachea) with the highest expression in skin and pancreas) (64). IL-22 activates STAT3, induces antimicrobial peptides and inhibits apoptosis. Impairment of these functions contribute to atopic dermatitis, Staphylococcal skin abscesses and muco-cutaneous candidiasis (63). In a study performed in human cells, IL-22 produced by NK cells was shown to inhibit growth of *M. tuberculosis* by enhancing phagolysosomal fusion in macrophages

(65). Tyk2 knockout mice were shown to have an altered composition of the gut microbiota and an aggravated inflammatory bowel disease in a colitis model (66). Intestinal epithelial cell-specific depletion of Tyk2 exacerbates colitis which can be rescued by excess administration of exogenous IL-22, pointing to the protective role of IL-22 in acute colitis. In autoimmune diseases, IL-22 seems to play a protective role against IBD but a pathogenic role in psoriasis and RA (64). Notably, IL-23 is essential in promoting IL-22 production from many immune cell types (63).

Our understanding of IL-26 signaling and function is sparse (67). IL-26 was initially identified as produced by human T cells infected with Herpes virus *saimiri* (HVS). IL-26 plays a pro-inflammatory role by promoting the secretion of IL-1β, IL-8, TNF-α and neutrophil migration. Experiments in human primary cells suggest a protective role of IL-26 against Gram-negative bacteria, *M. tuberculosis* and virus infections in macrophages, monocytes and NK cells, respectively (67). IL-26 may be an important player in host defense but is also a pathogenic factor in chronic inflammatory disorders of humans.

The type III IFN or the IFNλ family comprises IFN-λ1 (IL-29), IFN-λ2 (IL-28A), IFN-λ3(IL-28B), and IFN-λ4. These cytokines (Fig. 13) signal through the broadly distributed low-affinity receptor subunit IL-10R2 and the specific high-affinity IFN-λ receptor 1 (IFNLR1, formerly IL-28R), which is expressed restrictively in epithelial cells (especially in lung, intestine, and liver tissues). A few other immune cells (e.g. B cells, macrophages and plasmacytoid DCs) may express IFNLR1 (68). Both epithelial cells and myeloid-lineage cells produce IFN-λ. These cytokines exert antiviral activity similar to type I IFNs but they act primarily on epithelial cells. Several SNPs of IFNLR1 have been associated with autoimmune diseases (68).

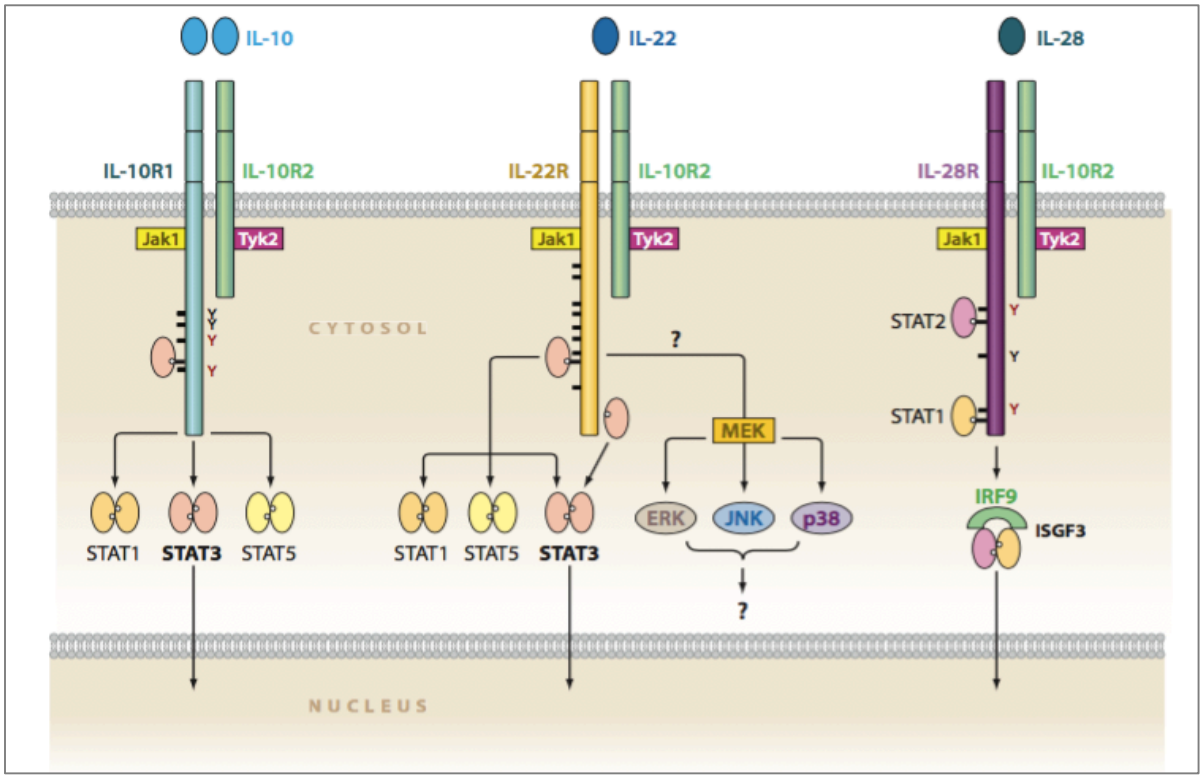

Figure 13. Schematic representation of IL-10, IL-22, IFN-λ (IL-28) signaling, from (63)

2.4 The IL-6 family

The IL-6 cytokine family comprises IL-6, IL-11, IL-27, leukemia inhibitory factor (LIF), oncostatin M (OSM), ciliary neurotrophic factor (CNTF), cardiotrophin-1, cardiotrophin-like cytokine, and neuropoietin. These cytokines share the common signal-transducing receptor protein, glycoprotein 130 (gp130), which is ubiquitously expressed. The cellular responsiveness to these cytokines depends on tightly regulated expression of a specific cytokine receptor subunit, i.e. IL-6R, IL-11R, LIFR, and OSMR (Fig. 14). Binding of these cytokines to their receptor complex leads to phosphorylation and activation of JAK1, JAK2, and Tyk2, which results in the recruitment and activation of STATs, especially STAT1, STAT3, and STAT5. Notably, JAK1, JAK2, and TYK2 are all phosphorylated upon stimulation with these cytokines, but only JAK1 is indispensable for signaling (69). The role of JAK2 and TYK2 is not clear. Several members of the IL-6 cytokine family induce SOCS1 and SOCS3 so that they negatively regulate the JAK/STAT pathway. Most members of this family have neuroprotective effects. Moreover, IL-6, LIF, OSM, and IL-11, play critical immuno-regulatory roles (70; 71). These cytokines have different biological effects despite of similar intracellular signaling. These diverse bioactivities may due to "temporal and spatial receptor activation, higher affinity binding, or activation of negative regulators" (71).

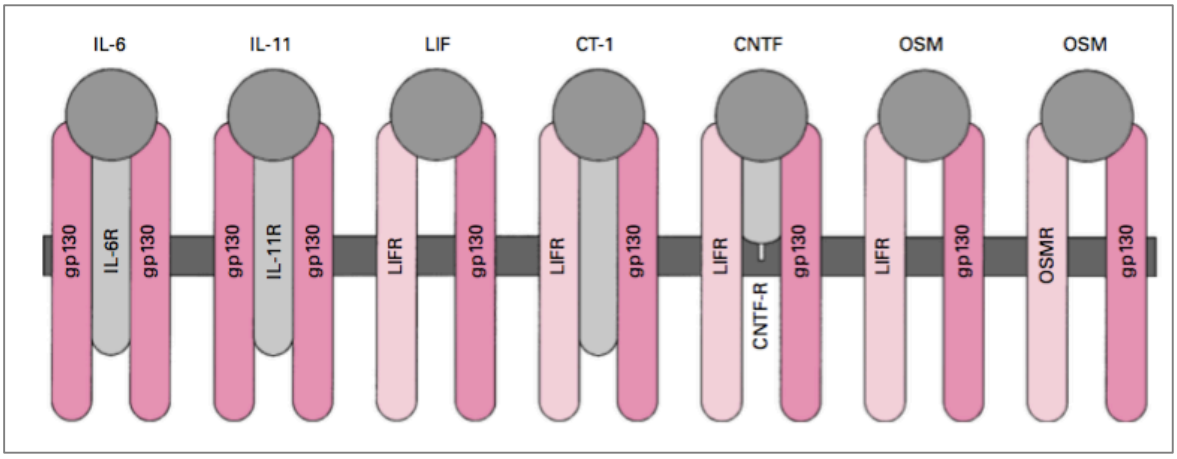

Figure 14. Schematic representation of IL-6 cytokine family and their receptors, from (70)

IL-6 interferes with IFN-γ signaling by upregulating SOCS1 and thus inhibiting Th1 differentiation. Moreover, IL-6 promotes IL-4 production so as to enhance Th2 cell polarization. IL-6 promotes as well T follicular helper cells differentiation and plasma cell development and antibody production. IL-6 supports Th17 cells differentiation but it completely blocks the TGF-β-induced generation of FoxP3+ Treg cells. Conversely, LIF inhibits the development of Th17 cells and promotes expansion of Treg cells (Fig. 15).

IL-11 induces Th2 polarization and inhibits Th1 polarization. In contrast, OSM induces IL-12 in dendritic cells, therefore, enhancing Th1 proliferation and IFN-γ production.

Although IL-6, LIF, OSM, and IL-11 exert diverse impacts on T cell subsets, they all induce an anti-inflammatory effect in macrophages. IL-6 enhances IL-4, IL-10 production and decreases IL-1β secretion in macrophages. LIF reduces the release of pro-inflammatory mediators, such as oxygen radicals and TNF-α by macrophages. IL-11 inhibits production of TNF-α , IL-1β , IL-12, and NO by macrophages. Moreover, IL-6, LIF, and OSM skew human monocytes into an anti-inflammatory M2 subset, which produces high levels of IL-10 and TGF-β, low levels of IL-12, and has poor T cell costimulatory properties.

IL-27 also signals through gp130 chains. It is often functionally classified in the IL-12 family. IL-27 is produced mainly by DC and macrophages upon microbial infection. This cytokine displays pro- and anti-inflammatory functions depending on the activation of STAT1 and STAT3, respectively. On the one hand, IL-27 promotes T-bet and IL-12Rβ2 expression and exerts pro-inflammatory effects, and on the other hand, IL-27 has been shown to prevent tissue damage during excessive inflammation (72)

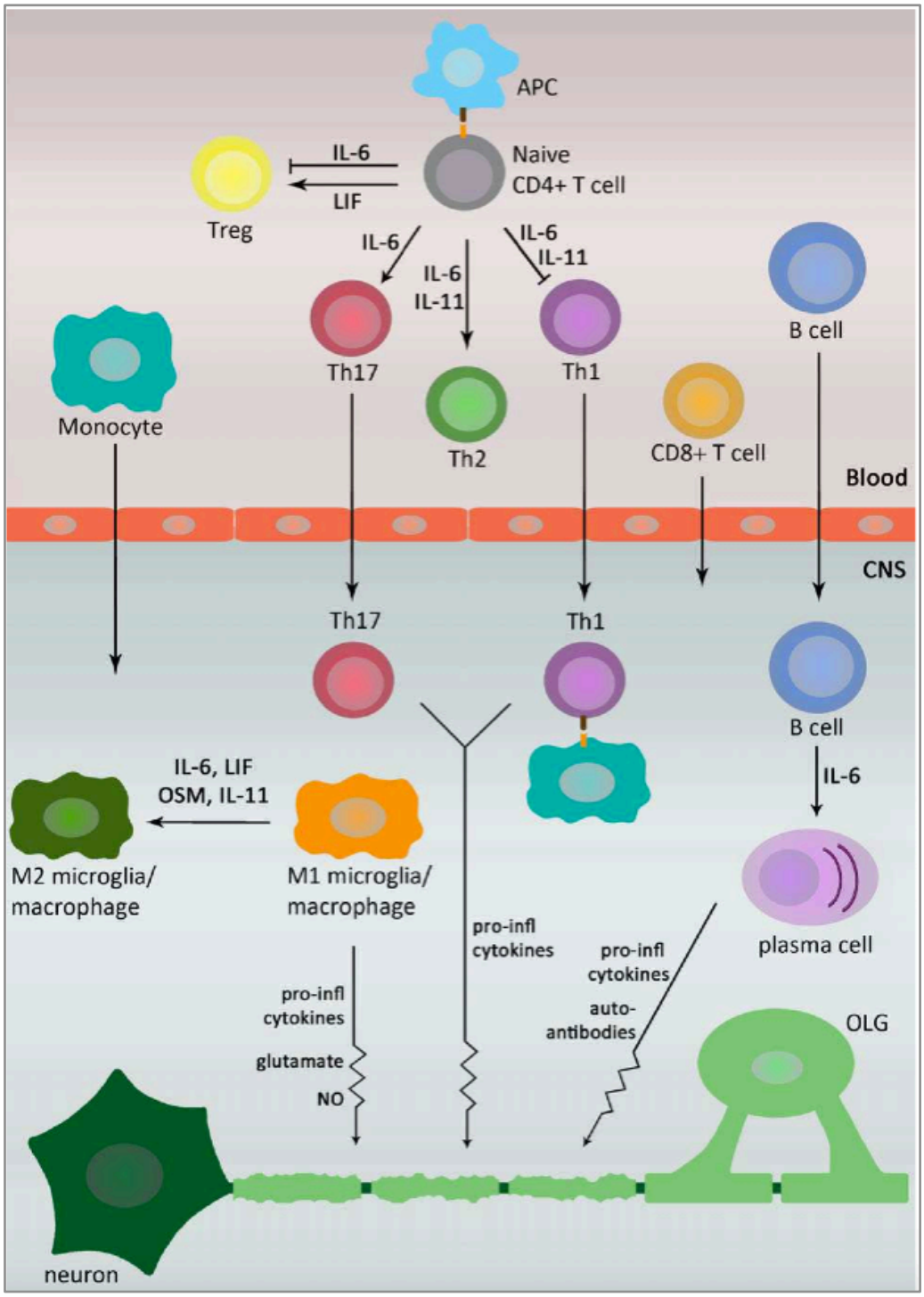

Figure 15. Schematic representation of the effects of IL-6 family cytokines on immune cells (involved in the pathogenesis of MS) , from (71)

2.5 IL-4 and IL-13. TYK2 associates to the IL13Rα chain, shared by IL-13 and IL-4 (Fig. 16). These two cytokines are mainly produced by Th2 cells, granulocytes, monocytes/macrophages and other innate immune cells, and mediate Th2 cell differentiation, M2 macrophage polarization, MHC II expression, B cell and plasma cell differentiation and antibody isotype switch. Originally discovered as a B-cell-stimulating factor, IL-4 promotes

antibody class switch recombination and the production of IgG1 and IgE, which is strongly implicated in atopic and allergic disease (73). Many SNPs in components of the IL-4 and IL-13 signaling pathway have been associated with immune diseases. For example, SNPs leading to increased IL-4 expression are positively correlated with RA, multiple sclerosis (MS) and asthma. Three SNPs in the IL-4RA have been associated with hyper-IgE and atopy. The two cytokines activate mainly STAT6. The precise role of TYK2 in IL-13 and IL-4 signaling remains to be determined.

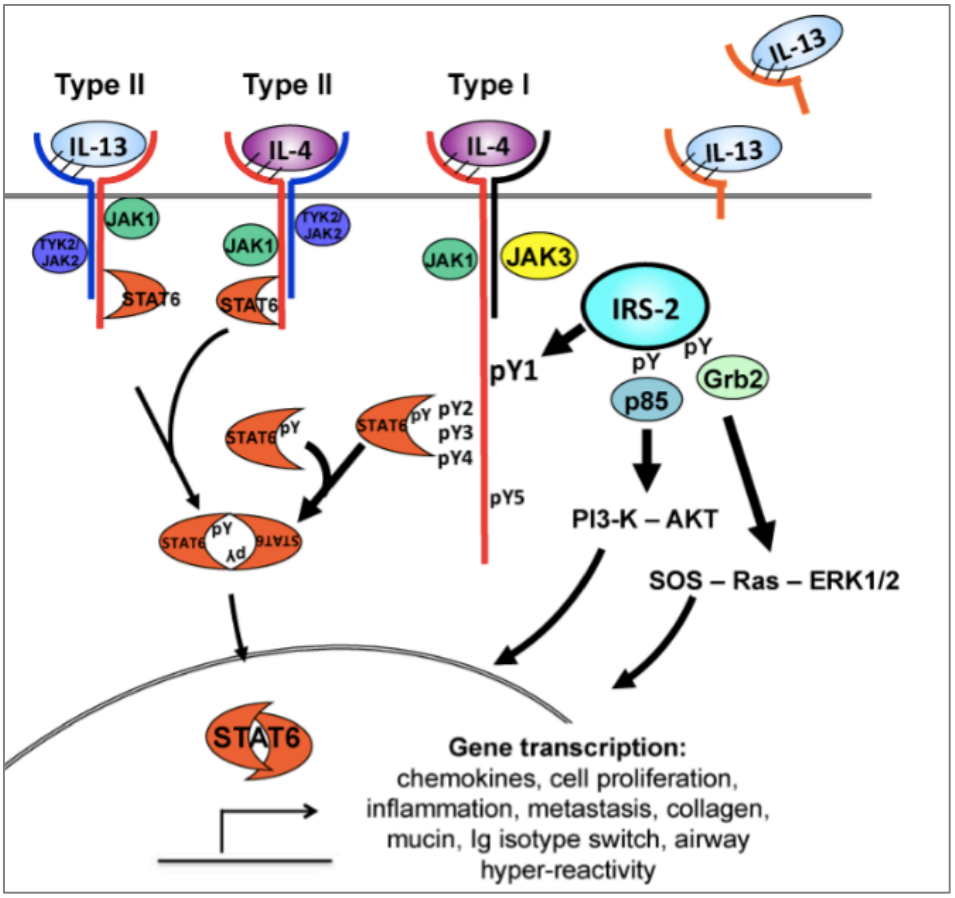

Figure 16. Schematic representation of IL-4 and IL-13 signaling, from (73). The type I receptor composed of the IL-4Rα and common gamma chain (γC), and the type II receptor composed of the IL-4Rα and IL-13Rα1.

3. Tyk2 mouse models

Hereafter, murine *genes* and proteins will be in lower-case (e.g. Tyk2, Isg15).

In 2000 two groups reported on Tyk2-deficient mouse models (74; 75). Viable and fertile, these mice display a mild susceptibility to VSV infection, which is mainly controlled by IFN-

induced antiviral activity. These mice are more susceptible to some other viruses (*e.g.* LCMV) and many bacterial, such as *Listeria monocytogenes*. Surprisingly, MEF or bone marrow macrophages (BMM) derived from Tyk2-/- mice exhibit impaired responsiveness to a low dose of IFN-α, but can fully respond to a high concentration of IFN-α. Notably, unlike in human cell lines, the level of cell surface Ifnar1 was found to be comparable in Tyk2-deficient cells and wt cells, as measured by Western blot (WB). This was later confirmed by flow cytometry for a third Tyk2-/- mouse (76). Thus, these data firmly established that in mice Tyk2 does not sustain Ifnar1, as is the case in humans (see below). Importantly, the level of Stat1 protein was reduced in Tyk2-/- BMM, and this may variably affect signaling by Stat1-activating cytokines (74). T cells from Tyk2-/- mice display a strong impairment of IL-12 response with abrogated IFN-γ production and Th1 cells differentiation (75). Cells from these mice appear to respond normally to IL-10 and IL-6. Notably, Stat3 activation is completely abolished in response to IFN-α and IL-12, suggesting a special relationship between TYK2 and STAT3. Remarkably, the requirement of TYK2 appears cell-type specific. For example, TYK2 is required for LPS-induced IL-12 production in DCs but not in T cells.

Further characterization of TYK2-/- mice revealed that TYK2 plays important protective role in tumor surveillance (77) and allergic asthma (78), while lack of TYK2 leads to resistance against autoimmune and inflammatory diseases (EAE, RA) (79; 80). Interestingly, the B.10Q/J mouse strain was found more resistant to collagen-induced arthritis and extremely susceptible to infection by *Toxoplasma gondii*. This phenotype is due to poor IFN-γ responses to autoantigen priming or parasite challenge, resulting from impaired IL-12 response in lymph node cells from these mice. A point mutation in the Tyk2 gene (E775K) was found to be responsible for the phenotype of the B.10Q/J mouse strain. The E775K substitution results in a kinase inactive form of TYK2 (79).

TYK2-/- mice are more susceptible to Th2-mediated allergic airway inflammation and display increased Th2 development, IgE production and decreased goblet cell, suggesting a potential role of TYK2 in IL-4 and IL-13 signaling (81).

Interestingly, TYK2-/- mice develop obesity due to abnormal brown adipose tissue (BAT) differentiation (82). BAT is not only critical for maintaining body temperature in hibernating animals and human infants but also play an important role in regulating energy expenditure in human adults. The mass of brown fat is inversely correlated with body weight. Reduced TYK2 mRNA and protein level are associated with obesity in both mice and human (82). In addition, Tyk2 is also involved in mitochondrial respiration (83).

4. TYK2-deficient patients

Nine TYK2-deficient patients have been reported so far. They presented with autosomal recessive homozygous mutations, insertions or deletions in the *TYK2* gene, generating nonsense mutations or frameshifts leading to premature stop codons. No full-length or deleted forms of TYK2 protein were detected in patients' cells (84-86).

The first TYK2-deficient patient was reported in 2006. A 22-year-old Japanese patient manifested hyper-IgE syndrome (HIES) - characterized by recurrent skin abscesses, pneumonia, and elevated IgE level - with high susceptibility to intra-macrophage bacteria (BCG, *Salmonella*), and suffered of atopic dermatitis and recurrent viral and fungal infections. Primary T cells and macrophages from this patient were used to investigate the implication of TYK2 in various cytokine pathways and exhibited impaired response to IFN-α, IL-12, IL-23, IL-10 and IL-6 (84).

In 2015 seven TYK2-deficient patients from five families of four ethnic groups (Turkey, Moracco, Iran, Argentina) were reported and analyzed together with the Japanese patient described above (85)

More recently, Fuchs et al reported an additional TYK2-deficient patient of Kurdish origin presenting with eczema, skin abscesses, respiratory infections and elevated IgE level without viral or mycobacterial infection. He was not vaccinated with BCG and tolerated MMR and varicella vaccines (86).

Overall, four of the nine patients suffered from bacterial infection (BCG or *M. tuberculosis*) without altered viral susceptibility, three suffered from both bacterial infection (BCG-osis, *Samonella, Brucella*) and viral infection (HSV, VZV), one suffered only from viral infection (HSV). All had favorable outcomes. Of the two patients with high serum level of IgE and HIES-like disorders, one also displayed susceptibility to mycobacterial and viral infection. Below I will summarize the results obtained by the three laboratories on cytokine signaling in cells derived from TYK2-deficient patients.

4.1 TYK2, cognate cytokine receptors and cytokine signaling

In T cells and EBV-B cells from TYK2-deficient patients, the cell surface levels of IFNAR1 (84; 85), IL-10R2 (85; 86) and IL-12Rβ1 (85) were found to be significantly lower than in control cells. These data corroborated the scaffolding role of TYK2 in sustaining cognate receptors that had been first reported by the Pellegrini's lab (48).

IFN signaling. In patients' T cells the phosphorylation of JAK1, STAT1, STAT2 and STAT3 by IFN-α or IFN-β was undetectable (84; 85). Yet, in patients' EBV-B cells, weak phospho-STAT1 was detected after stimulation with high doses of IFN-α (25nM) or IFN-β (8nM). STAT2 phosphorylation was not reported. Interestingly, STAT3 phosphorylation was not detectable, suggesting strong dependency of STAT3 on TYK2 (85). By EMSA, ISGF3 and GAF binding to target DNA elements in response to high IFN-α or IFN-β stimulation were very low in EBV-B and fibroblasts of patients, and undetectable in HVS-T cells. This suggested that, in IFN signaling, TYK2 may be more critically required in T cells than in B cells or fibroblasts (85).

To study the downstream response, the induction of *ISG15* and *MX1* was measured by qPCR. Normal induction was observed in fibroblasts and EBV-B treated with IFN-α/β for 2 to 6 hours (85). Interestingly, the basal level of the two transcripts was lower in patient's cells than in control cells, suggesting that TYK2 is required for tonic signaling. STAT3-dependent *SOCS3* induction by IFN-α/β was undetectable in patient's cells.

Viral titers were determined in VSV- or HSV-infected EBV-B, HVS-T and fibroblasts pretreated with IFN-α. The antiviral response, measured at 24 or 48 hr after infection, was impaired (84; 85). Interestingly, in the first 6 hr of infection, patient's fibroblasts showed a reduction in viral replication comparable to control cells, suggesting an early TYK2-independent antiviral effect of IFN at least in these cells (85).

The level of STAT1 protein, but not of STAT2 or STAT3, was reduced in patient's T and EBV-B cells compared to control cells (84; 85). This may be due to defective tonic signaling. Interestingly, JAK1 and JAK2 levels were also reduced in TYK2-deficient patient cells (85).

IL-12 signaling. STAT4 phosphorylation was undetectable by western blot in patient's primary T cells or HVS-T cells treated with IL-12 (84; 85). However, in microarray analysis some residual IL-12-induced gene expression was measured, which was not the case for cells from IL-12Rβ1-deficient patient who showed a complete loss of response. Accordingly, BCG+IL-12-induced IFN-γ production in TYK2-deficient patient's PBMCs, T cells, NK cells, was impaired but not abolished (85). Conversely, Fuchs et al reported that IL-12-induced NK cell activation was unaffected (86). Patient's NK cells showed normal degranulation and IFN-γ production in response to IL12/IL18. Cytotoxicity was also normal.

IL-23 signaling. In four of six patients studied IL-23-induced STAT3 phosphorylation was undetectable and in two patients it was very weak (85). It should be noted that in EBV-B cells

from healthy controls a considerable inter-individual variation exists in the level of IL-23-induced STAT3 phosphorylation measured by western blot ((85), my observation). STAT4 phosphorylation was undetectable in patient's primary T cells stimulated with IL-23 (84). In patient's HVS-T cells IL-23 induced-gene expression (microarray analysis) was impaired but not abolished (85).

IL-23 is thought to be important in Th17 differentiation. The proportion of IL-17+ cells in patients' blood was found to be normal (85), suggesting a TYK2-independent pathway for Th17 cell differentiation in vivo. However, the production of IL-17A/F, measured by a cytometric beads assay, was impaired in patient's naïve T cells cultured ex vivo for 5 days in the presence of IL-23.

IL-10 signaling In patient's EBV-B cells the IL-10 response was impaired but not abolished, as shown by EMSA, phospho-STAT3 blot and SOCS3 induction. The inhibition of LPS-induced TNFα production by IL-10 was also partially impaired in patient's macrophages (84-86).

IFN-λ signaling IFN-λ shares with IL-10 the IL-10R2 receptor chain that binds TYK2. In patient's EBV-B cells a sub-optimal IFN-λ response was measured as IFIT1 expression 2-4 hr after IFN-λ (20ng/ml) stimulation. Basal IFIT1 expression was lower inpatient cells (85), again possibly indicating a role of TYK2 in tonic induction of IFIT1.

Interestingly, Fuchs et al measured the IFN-λ response in the leukemic haploid cell line HAP1 with a TYK2 gene deleted by the CRISPR/Cas9 approach (87). The authors concluded that TYK2 is not required for IFN-λ signaling (86). By FACS, TYK2-deficient HAP1 cells showed no phospho-STAT1 in response to IFN-α but normal phospho-STAT1 in response to IFN-λ or IFN-γ. The antiviral response to IFN-λ, but not to IFNα, was normal measured as VSV-GFP replication by FACS.

IL-6, IFN-γ, IL-27, LIF, IL-21 signaling In the TYK2-deficient Japanese patient studied by Minegishi et al the IL-6 response was found to be impaired, as shown by IL-6-induced SOCS3 in PBMCs and by EBV+IL-6-induced IgM production in B cells (84).Yet, the IL-6 response was found to be normal in EBV-B and fibroblasts from the other eight TYK2-deficient patients (phospho- STAT3, EMSA and SOCS3). Of note, the re-expression of TYK2 in EBV-B cells of the Japanese patient failed to rescue IL-6 signaling, which led the authors to conclude that TYK2 is not required for IL-6 response (85). Kreins et al showed that IFN-γ, IL-27, IL-21 signaling in EBV-B cells, LIF signaling in SV40 and primary fibroblasts of

TYK2-deficient patients were not affected, indicating TYK2 is not required for signaling by these cytokines (85).

TYK2 and T cell differentiation IL-12 and IFN-γ promote Th1 differentiation. T cells of TYK2-deficient patients are skewed towards Th2 (84; 85). Naïve and memory T cells purified from three patients and controls were stimulated with anti-CD2/CD3/CD28 for 5 days. While in both patients and controls cytokine production from naïve T cells was extremely low. Compared to controls, patients' memory T cells showed a lower production of cytokines (IL-6, IL-10, IL-17A/F, IL-22) and to some extent of IFN-γ. IL-9 and TNF-α were comparable. Conversely, the production of IL-4, IL-5 and IL-13 was increased, this suggesting a bias towards Th2 differentiation (85).

Concluding remarks In humans TYK2 deficiency leads to mild and curable BCG and/or viral infections. The impaired IL-12-induced IFN-γ production in T cells may account for the mycobacterial infection, while the residual IFN signaling may explain the absence of life-threatening viral infection. Moreover, the intact NK cell function and/or TYK2-independent IFN-λ signaling may compensate the defect in IFN signaling. Two of the nine TYK2-deficient patients developed HIES-like clinical features, which may result from a Th2 bias. One possibility is that in the other patients without HIES an early exposure to Th1-inducing BCG or viruses have re-directed the immune responses and hence the phenotype. From a mechanistic viewpoint, TYK2 is required for responses to IFN-α/β, IL-12, IL-23 and IL-10. However, the degree of requirement varies greatly depending on several factors.

- TYK2 requirement can be cell type-specific. For example, TYK2 is absolutely required for IFN signaling in T cells but less so in EBV-B and fibroblasts. TYK2 may be critical for BCG/IL-12-induced IFN-γ production in T cells but less so for IL-12/IL-18-induced IFN-γ in NK cells.

- TYK2 can be required for activation of a specific STAT. For instance, TYK2 appears to be indispensable for STAT3 phosphorylation in response to IFN, although the mechanistic basis of this is not known.

- The degree of TYK2 requirement may depend on ligand concentration, *i.e*. TYK2 is essential at low ligand concentration (tonic signaling), as shown by the low basal level of *MX1*, *ISG15*, *STAT1*, *IFIT1* transcripts in EBV-B cells from TYK2-deficient patients. A study in the mouse supports this concept (88). The mouse strain B10.Q/J expresses an inactive Tyk2

point mutant (E775K) and display same cytokine signaling and same phenotype as Tyk2 knockout mice. ISGs induction in splenic B cells and macrophages was compared in B10.Q/J and wt mice by microarray analysis at baseline and 2 h after in vivo subcutaneous injection of IFN-α. The ISGs that were unaltered were called "Tyk2-independent". The ISGs that were affected at either baseline or stimulated condition were called "Tyk2-dependent". For example, *isg15, cxcl10, stat2, socs1, tlr3, il18, il-15, cd69, cd274, cd86, jun, oas3* in B cells and *il6, il-10ra, IL-15ra* in macrophages were less induced in B10.Q/J than wt mice, and thus belong to the "Tyk2-dependent" subset. Interestingly, some "Tyk2-independent" ISGs (u*sp18, irf7, irf9, tlr7, ifit1, stat1*) exhibited comparable expression and apparent higher fold changes in response to IFN in B10.Q/J than wt mice. This may indicate that the lower tonic expression of these "Tyk2-dependent" ISGs at baseline can be compensated at high dose of IFN, when they in fact become "Tyk2-independent" ISGs. Accordingly, "Tyk2-independent" ISGs were found to be more sensitive to low IFN doses (lower ED50) as compared to the tonic-sensitive ISGs. Thus, the degree of Tyk2 dependency varies with the target ISG and with the context (basal condition or IFN).

TYK2 appears to contribute to maintain constitutive/tonic expression of some tonic-sensitive ISGs and promotes tonic-insensitive ISGs induction in the presence of high IFN, such as during viral infection. Interestingly, human ISG15 is a TYK2-dependent ISG in the tonic situation, but not at high dose of IFN, while murine Isg15 is a tonic-insensitive and a Tyk2-dependent ISG at high dose of IFN. This difference may indicate a species-specific function of ISG15, which I have studied (Result Part II). Further studies by microarray or RNAseq in TYK2-deficient patients' cells may help to define the TYK2 dependency of various genes in response to other cytokines (IL-12 family, IL-10 family, gp130 family).

- TYK2 is required in a cytokine-specific manner. For example, TYK2 appears more critical for IL-12 than IL-10 signaling. The role of TYK2 in IFN-λ signaling is unclear as the conclusions from two studies are discordant (85; 86). This may be due to the different read-outs (IFIT1 induction, phospho-STAT1, antiviral protection) and the use of different cells (patient's EBV-B vs HAP1 cells).

IL-10R2 is the receptor subunit not only for IFN-λ and IL-10, but also for IL-22 and IL-26. The response of patient's cells to these cytokines was not studied, but it is conceivable that the impact of TYK2 deficiency differs among these cytokines due to unique JAK/receptor arrangement.

TYK2 binds to the ubiquitously expressed gp130 receptor, which is shared by the many cytokines of the IL-6 family. TYK2 is activated in response to IL-6 but does not seem to be required for IL-6 signaling. The role of TYK2 in signaling of IL-22, IL-26 and of other IL-6 family cytokines, such as IL-11, remains to be investigated.

Lastly, it is important to emphasize that it is difficult to define how much the requirement of TYK2 relates to its receptor scaffolding function and how much to its tyrosine kinase activity or other function(s). In mice Tyk2 has no impact on Ifnar1 expression, hence the signaling defects recorded in Tyk2-/- mice could be considered as loss of function of Tyk2 *per se*. In human TYK2-deficiency the issue is more intricate, since signaling impairment may relate to receptor abundance and/or to loss of TYK2 activity. Several natural TYK2 variants have been associated with autoimmune diseases, and the close analysis of these experiments of nature may help to answer this question (Results Part I).

5. TYK2 and diseases Overexpression of TYK2 has been found in many cancer cell lines and in malignant cells in human tumors (81). By RNA interference (RNAi) screening, Tyk2 was found critical for cell survival in T-cell acute lymphoblastic leukemia (T-ALL). Five TYK2 mutant have been identified (G36D, S47N, V731I, E957D, and R1027H) from T-ALL cells (cell lines and patients' cells) and found hyperactive in terms of auto-phosphorylation or STAT phosphorylation upon overexpression in 293T cells. This TYK2-promoted continued leukemic cell survival is shown to be dependent on the TYK2–STAT1–BCL2 pathway (89). Recently, two other TYK2 germline mutations (P760L and G761V) were reported in two ALL patients. Both mutations are in the DPG motif of the KL domain and were found constitutively activated (90). These findings suggest a therapeutic potential of molecular targeting TYK2 in these patients. A rare TYK2 natural variant TYK2-P1104A (rs34536443) was found in different tumor tissues (91) and was detected in 7% of acute myeloid leukemia (AML) patient samples. Another TYK2 natural variant TYK2-V362F (rs2304256) has also been proposed to have tumor-promoting effect (81). Here I will focus on the TYK2 natural variants associated with autoimmune diseases.

5.1 TYK2 variants associated with autoimmune diseases Autoimmune diseases (AID) are chronic inflammatory and destructive diseases arising from attacks by inappropriate or hyperactive immune response against self-tissue. Today, over 80 distinguished autoimmune diseases have been identified, targeting different organs. Etiology of AID is still far from elucidated but known to arise from multiple factors, including genetic, epigenetic and

environmental factors (microbiota, virus, climate etc.). The combination of these factors dictates AID susceptibility by impacting on the immune response, such as cytokine signaling, antigen presentation.

Our knowledge of the pathogenic mechanisms of AID has been augmented by the recently advances in genome-wide association studies (GWAS) across autoimmune and immune-mediated diseases (92). Genetic association studies, such as GWAS, have led to an explosion of genetic loci associated to diseases. Today the new challenge is to biologically interpret these genetic association data, i.e. identify the causal gene(s) and the causal SNPs (single nucleotide polymorphisms) from a cluster of SNPs (haplotype) in linkage disequilibrium (LD), and determine the functional impact of the variant. When a causal gene is involved in multiple pathways, as is the case for TYK2, another challenge is to determine which signaling pathway and in which context (cell type, tissue, cytokine environment etc.) the variant impacts disease pathogenesis.

SNPs are localized in both coding and non-coding regions. Coding SNPs can be silent (synonymous), missense/non-synonymous that lead to altered amino acid, or nonsense that introduce a premature stop codon. Nonsense and some missense SNPs can alter protein expression and function, thus impacting the individual susceptibility to diseases.

Both coding and non-coding SNPs may change gene expression by affecting transcription factor binding, mRNA stability or splicing (skipping of the exon, retention of the intron or generation of a new splice site, *etc*). The complexity of the splicing process, which selects the coding sequences or exons from the more abundant non-coding sequences or introns, has revealed the existence of new splicing regulatory elements. These elements, located in both coding and non-coding regions, are difficult to identify exclusively by sequence inspection. Genetic variations in these elements may result in unexpected deleterious effects on precursor (pre) mRNA splicing (93) and the disruption of exonic splicing signals can be significant in the etiology of genetic diseases (94). Hence, investigating the functional consequence of disease-associated genetic variations in new splicing regulatory elements can be informative to clinical practice (95; 96). My analysis of TYK2 variants is in line with this view (Result Part I-2).

By interacting with receptor subunits, such as IFNAR1, IL-10R2 and IL-112Rβ1, TYK2 mediates signaling by several cytokines that regulate the immune response: type I IFNs (α/β), type III IFNs (λ), IL-10, IL-12, IL-22, IL-23 and IL-26. Thus, natural TYK2 variants are

likely to have a role in disease susceptibility.

In human populations, the *TYK2* gene presents a high level of genetic variation with thousands of SNPs, of which 532 cause nonsynonymous changes, suggesting TYK2 may be a source of inter-individual variation for diseases susceptibility. Indeed, a few of TYK2 SNPs have been associated with autoimmune disease susceptibility. I summarized the information of these SNPs in Table 2 (97-114; 115). Notably these SNPs have different minor allele frequency (MAF) in different populations and most of these SNPs are protective for AID.

Rs55762744, rs2304256, rs12720356, rs35018800 and rs34536443 correspond to the following aa changes in TYK2: A53T, V362F, I684S, A928V and P1104A respectively. Except for Val362, the other residues Ala53, Ile684, Ala928 and Pro1104 are all conserved in JAK proteins. Those nonsynonymous natural TYK2 variants lead to amino acid changes scattered in different functional domains of TYK2 so that they could impact any of the described TYK2 functions: receptor binding, kinase activity and its regulation.

Rs12720270, rs280518, rs280519 are localized proximal to intron/exon junctions and may result in alternative splicing or affect TYK2 expression.

Table 3. Autoimmune disease-associated Tyk2 variants a (-) strand nucleotide. b Minor allele frequency, average

Rs	Ancestral > Derived [a]	MAF [b] (%)				aa residue	Location	Disease association (odds ratio)	Risk allele
		Afr	Amr	Eur	Asn				
55762744	C > T	0	1	1	0	A53T	FERM	Multiple sclerosis MS	T
12720270	G > A	4	18	17	46	Affect Exon 8?	36nt upstream of junction intron 7/exon8	Systemic lupus erythematosus (SLE) (1.57)	G
2304256	C > A	12	23	28	47	V362F	FERM 75nt downstream of junction intron7/ exon8	SLE (0.625 Sweden/Finnish; 0.808 overall populations) Crohn's disease (0.57) Type I diabetes (0.86) Idiopathic inflammatory myopathies	C C C C
280519	G > A	38	59	44	50	affects Exon12?	intron 11 (7nt downstream of exon11)	SLE (1.14) Psoriasis (1.13) Crohn's disease (1.749)	A A A
280518	C > G	13	2	0	0	affects Exon13?	Intron 12 (4nt upstream of exon 13	Ankylosing Spondylitis (AS) (7.7) But not confirmed by Taqman (Parkes, 2013)	G G
12720356	A > C	1	5	10	0	I684S	kinase-like	Rheumatoid arthritis (RA) (0.87) SLE Psoriasis (1.4) Crohn's disease (1.12) IBD (1.2) AS	A A A C C
35018800	G > A	0	0.2	0.6	0	A928V	TK	RA (0.42) SLE (0.4) IBD (0.65)	G G G
34536443	G > C	0	2	3	0	P1104A	TK	MS Primary biliary cirrhosis (1.91) Systemic sclerosis (Ssc) Endometriosis-related infertility RA (0.62) SLE (0.5) IBD (0.67)	G G G G G G G

Part II Type I IFN and its physiopathological role

Historically, the term interferon (IFN) refers to an activity 'interfering' with viral replication and secreted by cells infected with virus (Isaacs and Lindenmann in 1957) (116). Today, three types of IFN are known: type I IFNs, type II IFN (IFN-γ) and type III IFNs (IFN-λ). Each type of IFN binds to a specific receptor.

My study has focused on type I IFNs (mainly IFN-α2 and -β), referred thereafter as IFN.

1. IFN induction

1.1 Constitutive IFN Under steady-state, IFN is not easy to measure using classical methods, like RT-PCR or ELISA. However, many studies substantiated a constitutive low basal level of IFN produced in physiological conditions, probably due to commensal microorganisms (88). Notably, the low constitutive IFN-β induction is NF-κB- and AP-1-dependent and independent of IRF3 and IRF7 (117). From studies in mice, the "tonic" activity of the constitutively secreted IFN is critical for the maintenance of hematopoietic stem cell niche and bone remodeling. It has a perceptible influence on immune cell homeostasis and activity by priming immune cells to subsequent response to IFN and other cytokines, likely via sustaining expression of key transducers (*e.g.* Stat1) and other signaling proteins (117).

Microarray analysis showed that at baseline a set of ISGs is under-expressed in B cells from *ifnar1*-/- compared to wt mice. These ISGs were called tonic-sensitive (*stat1, usp18, irf1, tlr7, mx1/2, ifit1/2/3, oas2*). Another set of ISGs were instead named tonic-insensitive (*isg15, stat2, cxcl10, socs1, tlr3, il-2ra, il18, il-15, cd69, cd274, cd86, tnfsf10*) (88). A trend was noticed toward higher dependence on tonic IFN for the most highly responsive ISGs (fold changes), but this was not uniform. For instance, the highly responsive *cxcl10* was considered tonic-insensitive. Most of the tonic-sensitive ISGs showed an ED50 lower than 5U/ml (1.25pM). Exceptions were noted, suggesting that ISG expression relying on constitutive IFN does not simply reflect the most sensitive end of the IFN signaling spectrum.

The profile of this tonic activity of IFN is not well documented in humans. Interestingly, I noticed that in published western blot datasets the level of STAT1 protein is lower in IFNAR2-deficient (118) or STAT2-deficient (119) patients' fibroblast cells, suggesting defective tonic IFN signaling.

1.2 Pathogen-induced IFN. Almost every cell is capable of producing IFN-α/β. Virus-encoded nucleic acids and other pathogen components in infected or uninfected cells are

recognized as non-self-pathogen-associated molecular patterns (PAMPs) by the pattern-recognition receptors (PRRs), including cytosolic receptors (Fig. 17), such as RIG-I and MDA5 and Toll-like receptors (TLRs). Sensing of PAMPs by the PRRs initiates signaling cascades that act through adaptors such as TRIF, MAVS, STING, and MyD88, leading to activation of transcription factors: IRF3, IRF7, and NF-kB, AP1 for the induction of type I IFN genes and other pro-inflammatory cytokines, such as IL-6. Many factors involved in these signaling cascades, such as RIG-I, MDA5 and IRF7, are encoded by ISGs (Fig. 17). Some ISG products enhance PAMP sensing or stabilize IFN mRNA. This positive feedback regulation of IFN production leads to rapid secretion of high level of the cytokines for an efficient antiviral activity (120; 121).

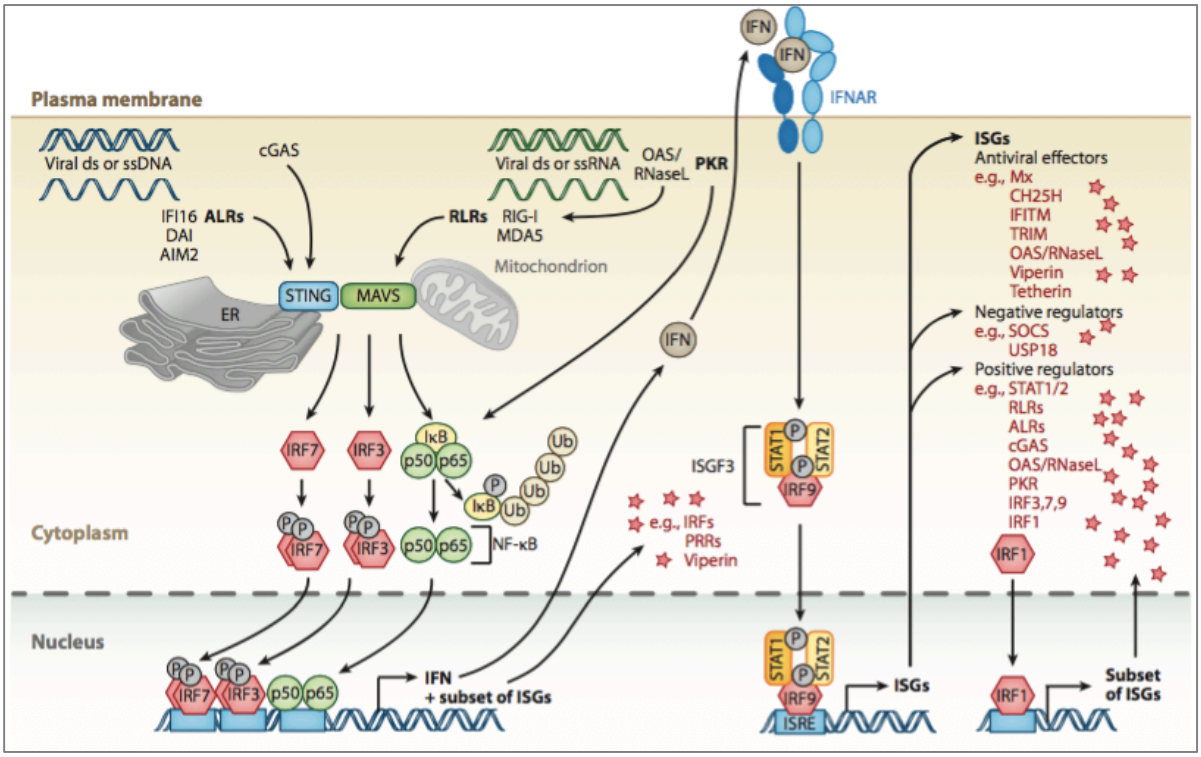

Figure 17. Cytosolic receptor-mediated IFN induction pathways, from (121)

2. IFN activities through ISGs: a double-edged sword

IFNs exert a multitude of effects on cells by upregulating or downregulating thousands of gene that are coding or non-coding. ISGs encode proteins involved in a broad spectrum of biological functions: antiviral, immune modulation, antigen processing, antigen presentation, chemokines, metabolism, transcription, growth modulation and apoptosis (122). A common core of the ISGs is induced in essentially all cell types, but some ISGs are induced only in specific cells (88).

2.1 Direct antiviral activity. ISGs encode a wide variety of direct antiviral effectors interfering with various phases of viral life cycle. To complete their life cycle, viruses must enter cells, translate and replicate their genomes, and exit to infect new cells. Each stage of infection is a potential target for ISG intervention (Fig. 18). For example, Mx1 is one of the first described broad virus inhibitor acting at an early post-entry step of the virus life cycle. Mx1 mediates the inhibition by preventing virus from reaching their cellular destination and promoting virus degradation (121). IFN-induced antiviral activity blocks viral replication as a first line of defense. When this fails, the infection may become systemic, with pDCs producing a large amount of IFN that act on immune cells to prevent systemic dissemination of the virus (see below).

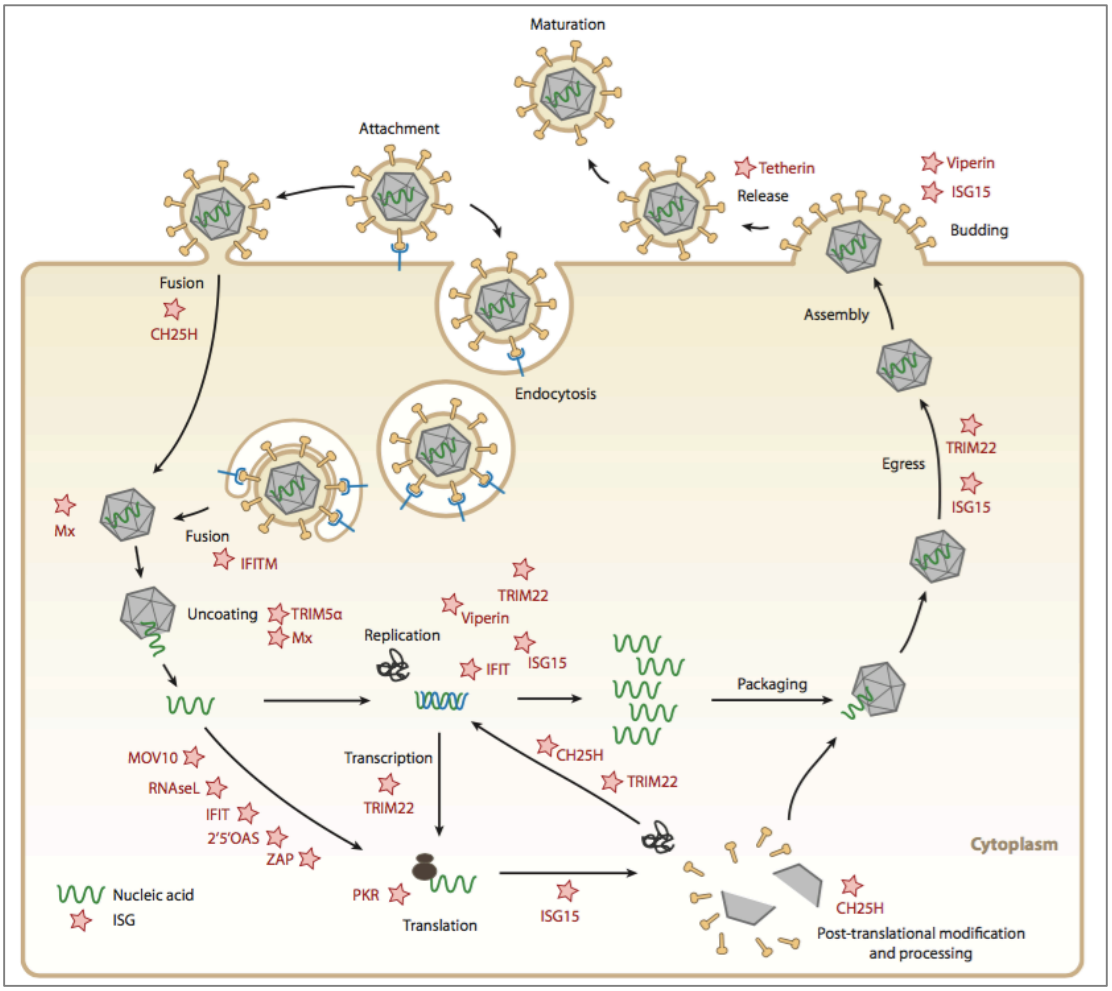

Figure 18. Targets for interferon (IFN)-stimulated proteins within viral life cycles, from (121)

2.2 Orchestrators of innate and adaptive immunity. IFNs act on both innate and adaptive immune cells, inducing expression of various ISGs that orchestrate systemic immune responses (Fig. 19). These ISG products include receptors, cytokines, chemokines, transcription factors (IL-2Rα, IL-12Rβ2, IL-15, CSF1, TNFα, CXCL10, STAT1). Firstly, IFN promote antigen presentation and chemokine production in innate immune cells. For example, IFN promote dendritic cell (DC) maturation: IFNs upregulate MHC-I expression and enhance DC capacity to cross-present antigen to CD8 T cells, which are critical for pathogens clearance. The co-factor CD80/CD86 (B7) binding to the co-stimulatory molecules CD28 or CD27 on T cells are also upregulated by IFN. IFNs induce as well the expression of CC-chemokine receptor 5 (CCR5) and CCR7 and the adhesion molecule lymphocyte function-associated antigen 1 (LFA1), which facilitate DC migration to draining lymph nodes. IFNs promote production the chemoattractants, such as CXC-chemokine ligand 9 (CXCL9) and CXCL10, facilitating T cells activation. IFNs stimulate NK cells cytotoxicity by inducing

granzyme B. IL-15 induced by IFN is critical for NK cell proliferation. Depending on the differentiation state of T cells, IFN can promote activated T cell survival and proliferation or inhibit T cell survival by inducing programmed death ligand 1 (PDL1) (54; 123).

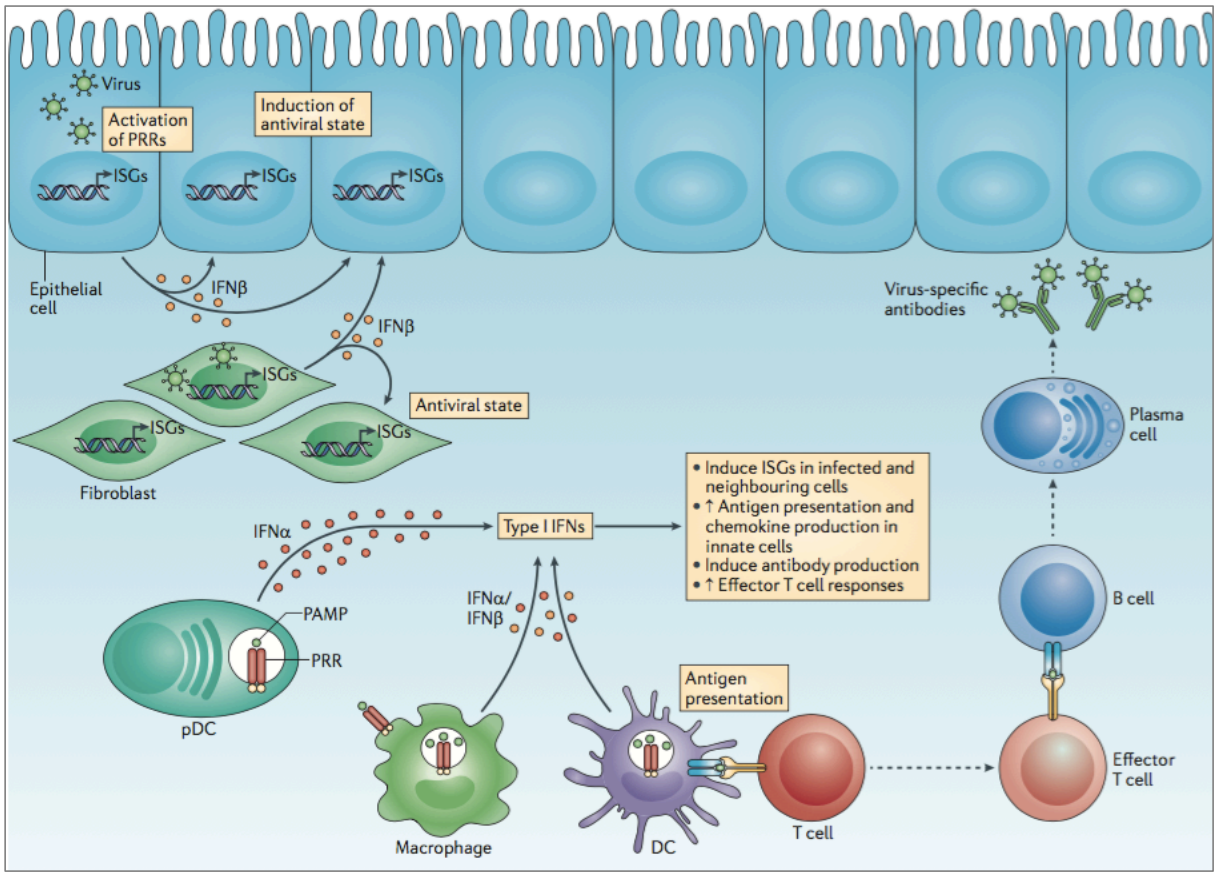

Figure 19. IFN controls innate and adaptive immunity and intracellular antimicrobial programmes, from (123)

2.3 Anti-proliferative activity. Soon after the discovery of IFN, it was recognized that the proliferation of many cell types is inhibited in culture with prolonged exposure to IFN. This anti-proliferative activity of IFN has been attributed to many ISGs including genes involved in apoptosis (TRAIL, FasL) and cell cycle regulation. IFN can delay the cell cycle by inducing different factors in different cell types. For example, IFN inhibit cell division in human colon cancer cells by inducing p21 protein (124), a cyclin-dependent kinase (CDK) inhibitors.

2.4 Detrimental effects of ISGs. Today, there is increasing awareness of the potential detrimental effect of IFN. ISGs are found elevated in blood cells in a range of autoimmune, auto-inflammatory diseases and microbial infections. It is uncertain whether these high ISGs

are causative to the disease or the downstream consequence of inflammation. Yet, it is clear that excessive and persistent exposure to IFN contributes to tissue damage, chronic infection and autoimmune disease.

2.4.1 IFN and infectious diseases During viral infection, appropriate concentration of IFN will lead to induction of antiviral ISGs in infected cells and in immune cells for viral clearance. However, persistent and high IFN signaling may result in tissue damage due to excessive inflammation and apoptosis or block of proliferation of tissue cells (125). Moreover, in chronic virus infection, IFN play an immunosuppressive role (Fig. 20) (54). During chronic LCMV infection, IFN signaling promotes IL-10 production and PDL1 expression and is responsible for the lymphoid tissue disorganization in persistently infected mice, so that inhibiting the IFN response with IFNAR1 neutralizing antibody restores T cell function and helps to cure the persistent infection (126).

IFNs also play a detrimental role in some bacterial infections. For example, compared to wt mice, Ifnar1-deficient mice are more resistant to several bacterial infections (e.g. *Listeria, Mycobacterium tuberculosis*). Several mechanisms have been proposed to explain the action of IFN. IFN was shown to downregulate of IFN-γR1 in myeloid cells, induce the immunosuppressive IL-10 or/and suppress the production of the antibacterial IL-1α/β. IFN also contribute to secondary bacterial co-infection following viral infection, probably via reducing both Th1 and Th17 responses and therefore impair responses to both intracellular and extracellular bacteria (125).

2.4.2 IFN and autoimmune disease With the exception of multiple sclerosis, where IFN-β is used as therapy, in many autoimmune diseases (AID) IFN can have a pathogenic role by promoting antigen presentation and lymphocyte responses and inducing chemokine expression (Fig. 19, Fig. 20). The apparent induction or exacerbation of a preexisting autoimmune disease is relatively frequent in patients treated with recombinant IFN (127). Numerous reports have described the occurrence of features of systemic lupus erythematosus (SLE) and cutaneous lupus erythematosus in IFN-treated patients. The symptoms usually resolve after discontinuation of IFN treatment, suggesting a pathological role of IFN. Moreover, SNPs of IRF5 and TYK2 - involved in IFN induction and IFN cellular response respectively - have been associated with susceptibility to SLE. Today, many TYK2 SNPs have been associated with autoimmune diseases. This is the first topic of my thesis work.

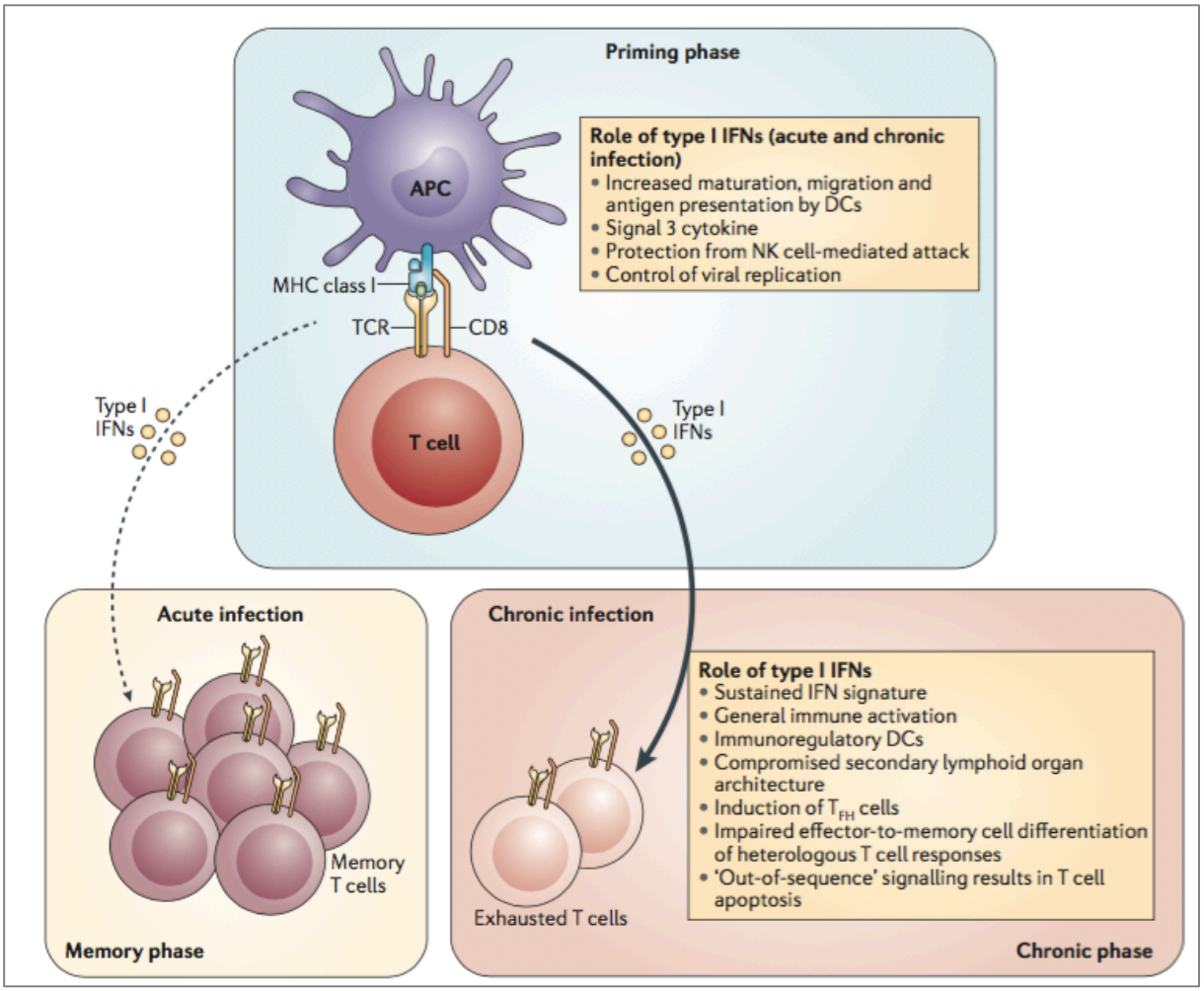

Figure 20. Role of type I interferons in T cell immunity in acute and chronic infections, from (54)

2.4.3 Interferonopathies

Aicardi-Goutières syndrome (AGS) was originally defined as an early-onset progressive inflammatory brain disease. Infants with AGS suffer from epileptic seizures, intracerebral calcifications and leukodystrophy, associated with high numbers of white blood cells in the cerebrospinal fluid. Over time, other features have been associated with AGS, such as skin lesions or chilblains, glaucoma and, in some cases, SLE-like symptoms. Dissection of the genetic basis of AGS has highlighted a connection between nucleic acid metabolism, PRRs and IFN induction. These studies led to define in 2011 human interferonopathies as a broad set of mendelian disorders whose key pathology is a constitutive upregulation of IFN activity (128). This latter can be assessed by measuring the level of ISG transcripts in blood cells (IFN signature). As summarized by Rodero and Crow (129), many monogenic disorders have been considered associated with enhanced IFN induction (Fig. 21). Eleven such genes are involved

in nucleic acid metabolism/signaling. Loss-of-function mutations of these genes disturb endogenous nucleic acid pathways, resulting in accumulation of unusual endogenous nucleic acid products which lead to abnormal sense of self-nucleic acids as "non-self" by PRRs. Gain-of-function mutations in MDA5, RIG-I and STING lead to increased sensitivity to cytosolic nucleic acid ligands or constitutive activation of cytosolic interferon induction pathways.

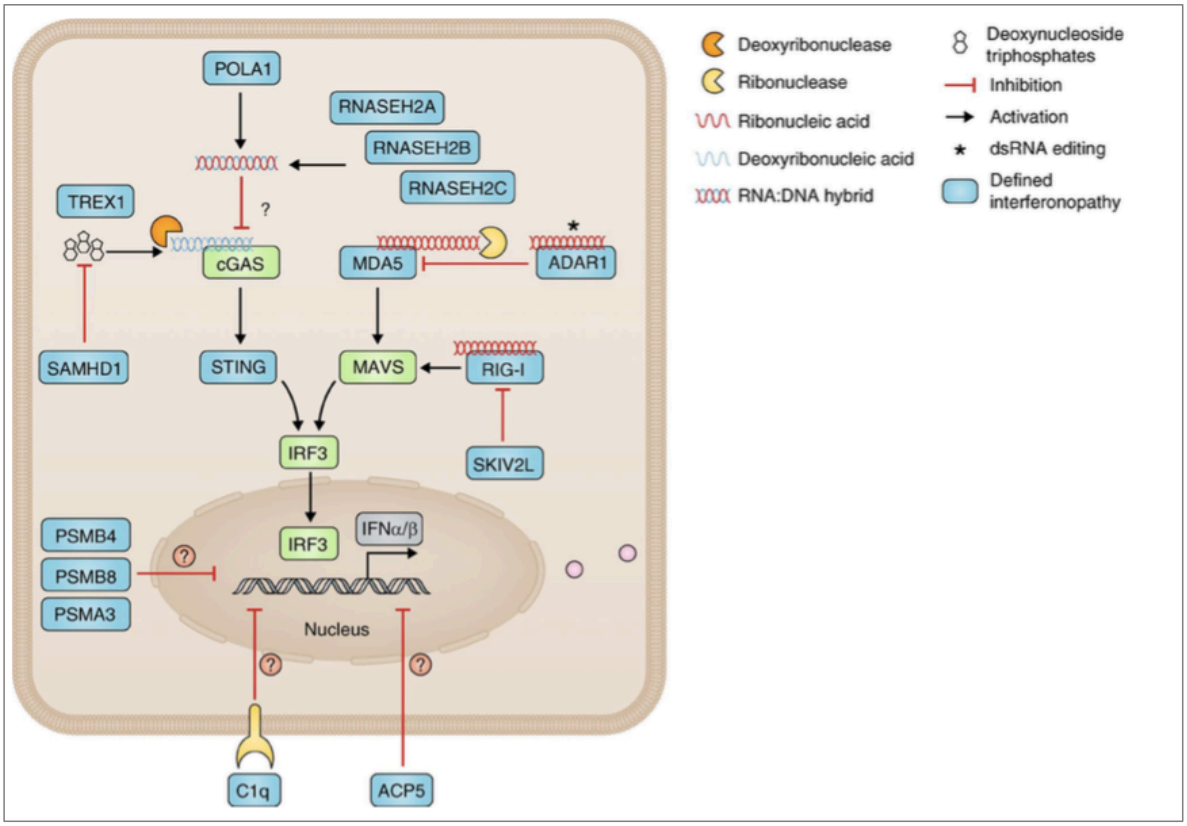

Figure 21. Monogenic disorders (blue boxes) considered as interferonopathies, from (129).

Interestingly, the Down syndrome caused by trisomy 21 (T21) was recently proposed to belong to the interferonopathies (130). T21 is the most common human chromosomal disorder, occurring in about 1 in 700 live births. The extra copy of chromosome 21 affects the development of all major organs, causing neurological problems and stunted growth. Intriguingly, T21 patients are more susceptible to certain diseases, such as autoimmune disorders, but are protected from others, including solid tumors. Sullivan *et al* reported a persistent high constitutive ISG expression in fibroblasts and circulating blood cells from T21 individuals. Of note, in addition to IFNAR1 and IFNAR2, IFNGR2 and IL-10RB, two receptor subunits used by IFN-γ and IFN-λ, are located on chromosome 21, which makes the situation more complicated. In another study, a patient presenting a partial T21 phenotype

was reported to carry a *de novo* 2.78-Mb duplication of chromosome 21q22.11. This duplication contains 16 genes and includes IFNAR1, IFNAR2 but not IFNGR2 and IL-10RB (131). This finding supports the concept that a persistent upregulation of the type I IFN response plays an important pathological role in the Down syndrome.

3 Negative regulation of IFN signaling

As Gresser and colleagues noted in 1980, IFN is "a potent substance" (132). Too much IFN, for too long or at the wrong time or location may be detrimental. Therefore, the induction of IFN and the IFN response are tightly regulated. Transient IFN production and controlled signaling outputs in response to infection promote pathogen clearance and facilitate return to homeostasis limiting detrimental effects. The IFN response is fine-tuned by integrated negative regulators operating at multiple levels in both cell-intrinsic and ISG-mediated manners. As for other cytokines systems, receptor endocytosis and turnover play important roles in rapidly reducing the level of JAK-STAT signaling (133). Signaling can be decreased by the action of phosphatases including SHP1/2 and PTPN1/2 that negatively regulate phosphorylation events associated with IFN signaling. STAT activity can be as well altered by the protein inhibitors of activated STAT (PIAS) family of proteins. Increasing evidence suggests that the IFN response can also be regulated by noncoding RNA including miRNAs and long ncRNAs (lncRNAs). Regulation may become very sophisticated since SOCS proteins themselves are negatively regulated by miRNAs (134). Compared to SOCS proteins, USP18 is a delayed and dedicated negative regulator of IFN. The next chapter is devoted to USP18 and its substrate ISG15. Below I will focus on the internalization of IFNAR1, which has been well dissected and where TYK2 plays a role.

3.1 Internalization, ubiquitination and degradation of IFNAR1 Upon IFN binding, IFNAR1 undergoes rapid turnover (135). This ligand-dependent degradation of IFNAR1 in human and murine cells is mediated by the E3 ubiquitin ligase complex, SCF-βTrCP (Skp1-Cullin1-F-box protein transducing repeat-containing protein), in a phosphorylation-dependent manner (136). It was shown that within 30 min of IFN stimulation, Ser535 and Ser539 of the conserved DSGNYS motif (degron motif) at the distal cytoplasmic tail of IFNAR1 are phosphorylated. This dual phosphorylation is required for recruiting βTrCP, which ubiquitinates IFNAR1 on various lysine residues. Ubiquitin tagging enables efficient IFNAR1 internalization and endosomal sorting towards the lysosome for degradation. The catalytic activity of TYK2 was found to be dispensable for internalization, but to be required for IFN-

induced Ser535 phosphorylation and ubiquitination of IFNAR1 (137). The IFN-dependent phosphorylation of the degron motif is mediated by the serine/threonine protein kinase D2 (PKD2) which is recruited to IFNAR1 after IFN stimulation. TYK2 activity is required for PKD2 activation but not for its recruitment to the receptor (138).

Three of six lysine residues in the cytoplasmic region of IFNAR1 were identified as ubiquitination sites (Lys501, Lys525, Lys526) essential for IFNAR1 degradation (139). It was further noticed that the rapid and maximal internalization of IFNAR1 depends on the interaction of a Tyr-based endocytic motif (Y_{466}VFF) on IFNAR1 and AP2, an adaptor for clathrin-dependent endocytosis. As such, it was proposed that ligand-induced IFNAR1 ubiquitination, *via* conformational changes, promotes the binding of AP2 to this endocytic motif. In the absence of ligand, IFNAR1 would be protected from basal endocytosis by a hypothetical complex (140). Later, TYK2 was identified as the masking protein (141), in agreement with the previous finding that TYK2 controls IFNAR1 cell surface level (48). It is notable that the Tyr residue in the Y_{466}VFF motif and two of the three lysines are absent in the murine Ifnar1, suggesting a species-specific regulatory mechanism.

Interestingly, Ser535 phosphorylation-dependent ubiquitination and degradation of IFNAR1 can be triggered by the unfolded protein response (UPR)/ER stress or by PRR activation (142). These ligand- and TYK2-independent pathways are mediated by the kinase PERK (pancreatic endoplasmic reticulum kinase) or/and p38. The kinase phosphorylates Ser532, which serves as priming site for subsequent Ser535 phosphorylation by CK1α within the degron (143). These different pathways are schematized in Figure 22.

Thus, virus infection or activation of PRR in cells prior to IFN production may trigger downregulation of the IFNAR1 level and may limit cell responses to these cytokines. This may be important for shielding IFN-producing cells (*e.g.* DCs) from the anti-proliferative effect of autocrine/paracrine IFN. Restraining IFN signaling in specialized cells may also allow viral replication to supply enough antigen to stimulate adaptive immunity. (See another example in the chapter on USP18)

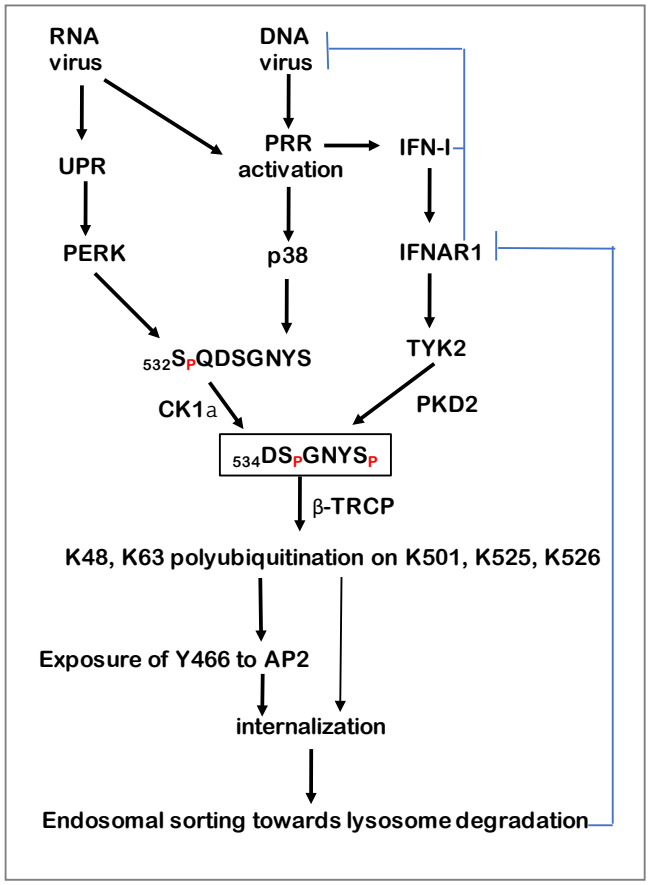

Figure 22. Schematic representation of different pathways leading to ubiquitination-dependent downregulation of IFNAR1. Blue blunt arrows indicate inhibition.

4. ISG15 and USP18

4.1 The ubiquitin-like ISG15. Interferon-stimulated gene 15 (ISG15) is a 15 kDa protein made of two ubiquitin-like (Ubl) domains separated by a hinge. As in ubiquitin the C-terminal sequence LRLRGG is essential for recognition by a processing protease and for conjugation to substrates. Unlike the high evolutionary conservation of ubiquitin, ISG15 conservation is poor (Fig. 21). In addition, ISG15 is only present in vertebrates. Thus, ISG15 is not a housekeeping gene and may carry diverse evolutional functions in different species.

4.1.1 ISGylation. The post-translational modification of protein substrates by covalent linkage of ISG15 (ISGylation) is similar to ubiquitination and is mediated by the consecutive action of enzymes analogous to those for ubiquitin conjugation: an E1 enzyme (UBE1L), an E2 enzyme (UbcH8), and one of several E3 ligases (*e.g.* EFP and HERC5). On the other hand, ubiquitin-specific protease 18 (USP18) is the de-conjugating enzyme to remove ISG15 from its conjugated proteins (de-ISGylation) (144). All the enzymes involved in ISGylation and de-ISGylation, together with ISG15 can be induced by IFN or other stimuli, such as virus and LPS. The functional impact of ISG15 conjugation on protein function is very diverse and specific for each protein.

4.1.2 Extracellular ISG15. ISG15 has been detected as an extracellular protein functioning as a cytokine. ISG15 was found to be secreted from monocytes, lymphocytes and monocyte-derived THP-1 cells stimulated with IFN-α/β. Human recISG15 purified from *E. coli* can induce the production of IFN-γ by PBMCs and promote NK cell proliferation (145; 146). ISG15 has been described as a neutrophil chemotactic factor in *Plasmodium yoelii* (causing malaria)-infected red blood cells (147). The critical role of secreted ISG15 in anti-mycobacterial immunity was recently emphasized when three unrelated patients with susceptibility to the *Mycobacterium bovis* BCG vaccine and inherited ISG15 deficiency were identified (148). The high susceptibility to BCG was ascribed to the failure of PBMC from these patients to produce sufficient IFN-γ, an absolute requirement to control mycobacterial infection (149). Secreted primarily by granulocytes (neutrophils), ISG15 was shown to synergize with IL-12 towards IFN-γ secretion in NK cells and to a lesser extent T cells. Clinically, these patients did not present with viral illnesses and, accordingly, their fibroblasts mounted an efficient antiviral response *in vitro* (148). However, the mode of secretion of ISG15, its receptor and mode of action on target cells remain unknown.

4.1.3 Antiviral role of ISG15. In human cultured cells, many experimental results indicate that ISG15 inhibits infection and replication of various viruses (150). For example, overexpression of ISG15 inhibits HIV-1 replication and co-expression with UBE1L causes a complete inhibition of HIV-1 replication (151). Specifically, ISG15 expression prevents assembly and release of virions from infected cells by inhibiting the ubiquitination of Gag and Tsg101 and disrupts their interaction. Further studies demonstrated that ISGylation and free ISG15 inhibit HIV budding (152).

A number of *in vivo* studies have shown that ISG15 mediates protection in different viral infection models dependent or independent of ISGylation. Both ISG15-/- mice and UBE1L-/- mice are fertile and display no obvious abnormalities. They exhibit an identical increased susceptibility to viral infections, such as influenza B virus. However, ISG15-/- mice, but not UBE1L-/- mice, are more susceptible to chikungunya virus infection, suggesting a conjugation-independent antiviral function of ISG15. Both ISG15-/- mice and UBE1L-/- mice display normal antiviral responses against VSV and LCMV infection.

During the study of cells from ISG15-deficient patients I was brought to address the following question: is ISG15 an essential antiviral protein *in natura*? What is the essential role of ISG15 in humans?

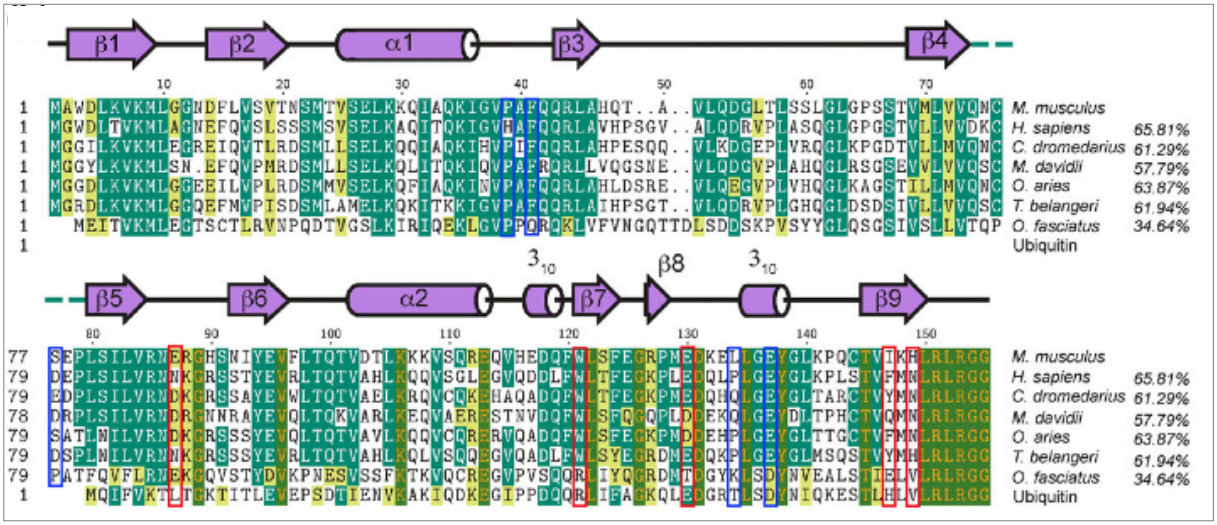

Figure 23. Sequence alignment of ISG15s from mouse, human and other species, along with ubiquitin. The sequence numbering ruler is based on mouse ISG15 (mISG15). Secondary structure of mISG15 is denoted in purple. The hinge region between β4 and β5 is denoted using a dashed line in teal. Percentages indicate sequence identity relative to mISG15. Residue positions form key interactions with Coronavirus Papain-Like Proteases are boxed in red. Key residue positions implicated in driving the specific tertiary fold features of mouse and human ISG15 are boxed in blue. *Reproduced from* (153).

4.2 USP18 Ubiquitin-specific peptidase 18 (USP18, formerly UBP43) is a member of the ubiquitin-specific proteases family removing ubiquitin (Ub) or ubiquitin-like (Ubl) proteins from conjugated substrates. Usp18 specifically removes Isg15 from ISGylated proteins (144). The isopeptidase active site of USP18 lies on three functional domains, including a cysteine box with a Cys residue (C64 in human, C61 in mice), a histidine box as well as an adjacent asparagine (154). The three residues Cys-His-Asp, constitute the catalytic triad. Mutation of the active site cysteine within the Cys box of USP18 protein abolishes its isopeptidase activity (C64S in human, C61S or C61A in mouse).

USP18 is a canonical ISG that can also be induced by type III IFNs, viral infection, LPS, TNF-α, and genotoxic stress (155). The protein is subject to proteasomal degradation mediated by the SCF-Skp2 E3 ubiquitin ligase complex (156). Usp18 is expressed at different levels in several tissues (155). For instance, Usp18 is expressed in liver, spleen, and thymus at high level, while at low but detectable level in bone marrow, adipose tissue, and lung tissue. Usp18 is highly expressed in CD169+ macrophages, bone marrow-derived DCs, peritoneal macrophages, monocyte-derived macrophages.

The USP18 protein is expressed from the same mRNA as two isoforms differing at the N-terminal region due to alternative start codons. USP18 is mainly found in the cytoplasm, but the shorter isoform distributes in cytoplasm and nucleus. Both proteins possess enzymatic and IFNAR2 binding activities (157). The specific role of each isoform is unclear. I observed that the presence of 25 nucleotides in the 5'UTR of *USP18* promotes the expression of the shorter isoform. USP18 exerts two functions, which are considered to be distinct. Originally identified as an isopeptidase, USP18 was later found to inhibit IFN signaling.

4.2.1 Usp18-deficient mice. All Usp18-/- mice present a high level of free and conjugated ISG15, indicating that Usp18 is the dominant de-ISGylation enzyme *in vivo*. However, Usp18-/- mice show a strain-specific phenotype. On a mixed Sv129-C57BL/6 background, Usp18-/- mice are viable at birth, but gradually display neurological disorders associated with hydrocephalus because of necrosis of ependymal cells from 2 to 19 weeks after birth. On a C57BL/6 background, absence of Usp18 leads to fetal death due to "Isg15 dependent-embryonic development disorder". Interestingly, knockout mice generated on the FVB/N background do not display severe neurological symptoms and have a normal life span (155). The different phenotype suggests that the effect of absence of Usp18 on neurological disorders and lethality may depend on unknown strain-specific modifiers. However, the neurological disorders in Usp18-/- mice are not related to high Isg15 or ISGylation, since

hydrocephalus also develops in mice knockout for both Usp18 and Isg15 (158).

Remarkably Usp18-/- mice are so hypersensitive to IFN that they die within 72 h after treatment with the potent IFN inducer poly I:C, whereas wt mice survive. A dramatic decrease of peripheral white blood cell number due to IFN-induced apoptosis, was observed in the Usp18-/- mice but not wt mice after poly I:C treatment (159). Why and how the absence of Usp18 leads to hypersensitivity to IFN?

4.2.2 USP18 as inhibitor of IFN signaling. Using molecular, biochemical, and genetic approaches, Zhang's group demonstrated that Usp18 specifically binds to the IFNAR2 receptor subunit and interferes with JAK1 binding to IFNAR2 (160). Thus, USP18 was found to be a specific inhibitor of IFN signaling. Interestingly, *USP18* expression is negatively correlated to the therapeutic efficacy of IFN-α in patients with chronic hepatitis C (161). Liver cells from mice repeatedly injected with murine IFN-α become refractory to further IFN-α stimulation. However, this desensitized state was not observed in Usp18-/- mice, indicating that Usp18 is essential for IFN-α desensitization (162).

Through finely designed experiments, François-Newton et al (163) found that both type I and type III IFNs induce a long-term desensitization state in cells of different lineages, including human primary hepatocytes. Remarkably, the refractory state is targeted to the IFN- α and IFN-ω subtypes, leaving nearly intact the cells' responsiveness to IFN-β and IFN-λ. Importantly, François-Newton *et al.* demonstrated that USP18 is necessary and sufficient to desensitize cells to IFN by disturbing the assembly of IFN/receptor ternary complex to different extent depending on the binding affinity of the ligand for the receptors. Furthermore, they clarified the critical role of USP18 in establishing transcriptional and anti-proliferative IFN-α/β differential effects, where IFN-β induces a prolonged activation of both STATs and ISGs, including two pro-apoptotic genes (*TRAIL, FAS*) (164) .

4.2.3 USP18 and virus infection in mice

Usp18-/- mice are hypersensitive to IFN and were described to be resistant to fatal viral infections following intracerebral inoculation with lymphochoriomeningitis virus (LCMV) or vesicular stomatitis virus (VSV) (165). However, Usp18-/- mice exhibit increased mortality to intravenous VSV infection. Lang's group showed that, after intravenous infection with VSV, Usp18-/- mice showed typical VSV-mediated paralysis and died 1 week after infection whereas wild-type mice survived (166). These observations suggest that USP18 mediates pro-viral activity in local infection but antiviral activity in systemic infection. Honk et al found

that in specialized macrophages (CD169+ metallophilic macrophages) located in the spleen and LNs, a high basal level of Usp18 is important to reduce their sensitivity to IFN. This facilitates locally restricted viral replication, which is essential to activate the adaptive immune system and to prevent the fatal outcome of intravenous VSV infection in mice. In this study, *Usp18* deficiency in antigen-presenting cells but not in T cells leads to reduced expansion of VSV-specific CD8+ T, CD4+ T cells, delayed IgM response, delayed and reduced VSV-neutralizing IgG antibodies (166). The same mechanism can lead to virus-induced autoimmune diabetes as seen in a mouse model. DCs express more Usp18 than do other cell types and their reduced response to IFN leads to augmented viral replication and a sufficient amount of autoantigen to promote expansion of autoreactive CD8+ T cells. Knocking down Usp18 expression in DCs allows IFN-mediated inhibition of viral replication and consequently prevents autoimmune diabetes in the mouse model (167).

Taken together, the basal expression level of USP18 in different specialized cell types shapes their responsiveness to type I IFN and contributes to orchestrate innate and adaptive antiviral immunity.

OBJECTIVES

Part I Functional characterization of TYK2 natural variants associated with AID

Many SNPs in JAK-encoding loci have been associated with risk or protection to immune-mediated diseases (168-171) (172). The TYK2 SNPs that have been reported so far are noncoding or nonsynonymous, *i.e.* cause a change in amino acid. Instead, for the other JAKs, most AID-associated SNPs are of the noncoding type. This observation hints to a more relaxed and tuning role of TYK2, which may be a source of inter-individual variability in cytokine-regulated functions and in susceptibility to autoimmune diseases (114).

As of today, eight nonsynonymous TYK2 SNPs have been associated with AID by genetic association studies (Introduction Table 2). The main objective of this work was to biologically interpret genetic association data and determine the impact of some disease-associated TYK2 variants on the expression and/or activities of the protein. A second aim was to better define the implication of these variants in disease pathogenesis by determining which signaling pathway(s) is most impacted and in what context (cell type, tissue, cytokine environment).

In Li et al (173), we reported on the properties of two TYK2 variants studied in cells from genotyped individuals. Signaling studies performed in cells reconstituted with these variants allowed me to ask basic mechanistic questions on the specific role of TYK2 *vs* JAK1 in the IFN response pathway.

In an ongoing collaboration with S. Boisson-Dupuis (Rockefeller University, NYC), we have analyzed signaling in response to IFN and other immune cytokines in cells from patients homozygous for one of the two variants.

I have also characterized two additional TYK2 variants. Based on my findings and assisted by the recently published crystal structure of TYK2 FERM-SH2, I sought to analyze in more detail specific regions of the FERM domain. I will present some unpublished results on the study of two loops unique to the FERM domain of TYK2 and potentially involved in lipid binding.

Part II Negative regulation of IFN signaling, from patients to mechanism

II-1 USP18-deficient patients, ISG15-deficient patients and species-specific role of ISG15

In collaboration, we sought to analyze IFN signaling in cells derived from rare USP18-deficient infants and we confirmed a dysregulated IFN response (174). I also contributed to the study of rare ISG15-deficient patients, which revealed an unexpected but essential role of

ISG15 in human (175). I will summarize these two studies in Part II-1, detailing my specific contribution.

The different phenotypes of ISG15-deficient humans and mice led us to address further questions on the species-specific role of ISG15 in the control of IFN signaling. I am the second author in this published work (176).

II-2 Mechanistic studies on USP18 function in IFN signaling

As discussed in the Introduction, USP18 down-regulates IFN signaling in a fine-tuned manner so that its impact varies for IFN subtypes possessing different receptor binding affinity. In a collaboration with the group of Jacob Piehler (Osnabrück University, Germany), we sought to study how USP18 regulates the plasticity of the IFN receptor (177). More recently, I also contributed to a collaborative study demonstrating that the recruitment of USP18 to the IFN receptor is enhanced by STAT2 (178).

MATERIALS AND METHODS

Plasmid constructs

TYK2 WT has been described as pRc-TYK2 (179). TYK2 P1104A and TYK2 I684S, in pRc-CMV and pIRES vectors respectively, were generated by standard PCR technique. To obtain TYK2 V678F/P1104A, a 1kb SgrAI/XbaI fragment spanning the P1104A mutation was prepared from TYK2 P1104A in the pRc-CMV vector and swapped into pRc-TYK2 V678F (25). The human JAK1 P1084A and K908E mutants were generated by site-directed mutagenesis in pBS-JAK1 and recloned into pRc/CMV-JAK1 (180) with AfeI/XbaI. TYK2-ΔE8, TYK2-4K4A, TYK2-Δβ1β2, TYK2-Δβ3β4 were generated by site-directed mutagenesis using QuikChange XL site-directed mutagenesis kit (Aligent Technologies) in pRc-TYK2 or pQE-His-N(180). All new plasmids were verified by sequencing. All expression constructs, except Tyk2 I684S and pQE-His-N, have a C-terminal vesicular stomatitis virus glycoprotein (VSV-G) epitope tag.

Cells and transfection

EBV-transformed B cell lines were obtained from Coriell Cell Repositories (Camden, NJ), the Centre de Ressources Biologiques of the Reseau Français d'Étude Génétique sur la Sclérose en Plaques or from S. Boisson-Dupuis (Rockefeller university). Genotyping for rs12720356, rs34536443, rs12720270, rs2304256 confirmed the presence of the specific polymorphism in the EBV-B lines. Cells were cultured in RPMI 1640 and 10% heat-inactivated FCS. Before cytokine stimulation and protein analysis, cells were serum starved for 2 h. The IFNα–unresponsive human fibrosarcoma 11,1 (U1A, TYK2-deficient) cells and U4C (JAK1-deficient) cells were cultured in DMEM and 10% heat-inactivated FCS. Transfections were performed with FuGENE6 (Roche Applied Science). The 11,1 cells were transfected with pRc-CMV–based plasmids for stable expression of Tyk2 WT or mutants, and clones were selected in 400 μg/ml G418. U4C cells were cotransfected with pSV2-puro and pRc-CMV-JAK1 WT, JAK1 P1084A, and JAK1 K908E. PuroR clones were selected in 400 ng/ml puromycin. IFN-α2 was a gift from D. Gewert (Wellcome Research Laboratories). Recombinant human IL-10 was from PeproTech France. IL-6 was a gift from Merck Serono. IL-23 was from R&D system.

Western blot analysis and Abs

Cells were lysed in modified RIPA buffer (50 mM Tris-HCl pH 8, 200 mM NaCl, 1% NP40, 0.5% DOC, 0.05% SDS, 2mM EDTA) with 1 mM Na_3VO_4 and a cocktail of antiproteases

(Roche). A total of 30 μg proteins was separated by SDS-PAGE and analyzed by western blot. Membranes were cut horizontally according to molecular size markers, and stripes were incubated with different Abs. Immunoblots were analyzed by ECL with the ECL Western blotting Reagent (Pierce) or the more sensitive Western Lightning Chemiluminescence Reagent Plus (PerkinElmer) and bands were quantified with Fuji LAS-4000. For reprobing, blots were stripped in 0.2 M glycine (pH 2.5) for 30 min at room temperature. The following Abs were used, unless otherwise indicated in figure legends: TYK2 mAb T10-2 (Hybridolab, Institut Pasteur); anti-JAK1–phospho-YY1022/23 (BioSource International, Invitrogen); anti-STAT2–phospho-Y689 (R&D); anti-STAT1, anti-STAT2, , anti-STAT3, anti-JAK1, and anti phosphotyrosine mAb 4G10 (Millipore); and anti-STAT1–phospho-Y701, anti-STAT3–phospho-Y705, and anti-TYK2–phospho-YY1054/55 (Cell SignalingTechnology, Beverly, MA).

***In vitro* kinase assay**

Cells were lysed in 50 mM Tris (pH 6.8), 0.5% Nonidet P-40, 200 mM NaCl, 10% glycerol, 1 mM EDTA, 1 mM sodium vanadate, 1 mM sodium fluoride,10 mM PMSF, cocktail of antiproteases (Roche Applied Science). TYK2 and JAK1 were immunoprecipitated from 2 mg lysate using noncommercial R5-17 polyclonal Abs or affinity-purified anti–VSV-G polyclonal Abs (a gift from M. Arpin, Institut Curie) or anti-VSV-G agarose (Sigma). Immunocomplexes were washed three times in buffer 1 (50 mM Tris [pH 6.8], 400 mM NaCl, 0.5% Triton X-100, and 1 mM EDTA), once in buffer 2 (50 mM Tris [pH 6.8] and 200 mM NaCl), and once in kinase buffer (50 mM HEPES [pH 7.6] and 10 mM $MgCl_2$). The kinase reaction was carried out in 50 mM HEPES [pH 7.6], 10 mM $MgCl_2$, 0.6 mg recombinant STAT3 or STAT1 (SignalChem or OriGene Technologies), and with or without 30 μM ATP at 30°C for 5 min in a total volume of 30 μl. The reaction was terminated by boiling in Laemmli buffer. Half of the sample was loaded for SDS-PAGE, transferred to a nitrocellulose membrane, and phosphorylated products were analyzed by Western blotting with anti-phosphotyrosine 4G10mAb or activation loop phospho-specific Abs. After stripping, membranes were reblotted with anti-TYK2 mAb, anti-JAK1, or anti–VSV-G Abs and revealed using ECL detection reagents (Western Lightning; PerkinElmer).

Minigene assays

TYK2 minigene constructs were made in plasmid pI-12, using a ~1.2 kb genomic region comprising rs12720270 and rs2304256, spanning the region from exon 7 to 9. Site-directed

mutagenesis was performed to introduce the different allelic combinations. RNA was isolated from HEK 293T cells using the RNeasy Micro Kit (Qiagen) and cDNA was synthesized. Minigene splicing was analyzed by PCR amplification of cDNA using T7 and SP6 primers that specific to the minigene. All resulting amplification products were sequenced.

Protein purification and *in vitro* pull-down assay

Histidine-tagged proteins were expressed in bacteria, purified on Ni-NTA agarose beads according to the manufacturer's protocol (Qiagen), eluted, and dialyzed against 20 mM Tris-HCl, pH 7.5, 100 mM NaCl, 10% glycerol, and 2mM EDTA, 1mM dithiothreitol (DTT). Proteins were concentrated by vivaspin concentrator (Vivascience) and stored at 80 °C. GST fusion proteins were affinity-purified on glutathione-Sepharose (GE Healthcare). For *in vitro* pull-down assay, same quantity of His-tagged purified recombinant proteins were incubated with glutathione-Sepharose containing about 2μg of bound GST fusion protein in 100 μl of binding buffer (0.1% Nonidet P-40, 10% glycerol, 50 mM NaCl, 50 mM Tris-HCl, pH 8, and 1 mM DTT) with 0.5% bovine serum albumin and protease inhibitors for 60 min at 4 °C. Beads were pelleted and washed three times in binding buffer. Bound proteins were eluted and boiled in 20 μl of Laemmli buffer, separated by SDS-PAGE, and analyzed by immunoblotting with the appropriate antibody.

Lipid binding assay

PIP strips were obtained from Echelon Biosciences (Cat n° P-6001). The PIP Strip contains 15 lipids at 100 pmol per spot (Fig. 3A in part I-3 of Results). The strip was blocked with 1% non-fat dry milk in TBS-T (0.1% v/v Tween-20) for 1 h at room temperature and then incubated with purified His-tagged proteins (around 1 μg in 3 ml TBS-T) for 1 h at room temperature followed by incubation with primary antibody (anti-TYK2 antibody). After washing 5 times with TBS-T , the strip was incubated with HRP-conjugated secondary antibody for 1 h and then visualized with the ECL reagent.

RESULTS

This chapter is divided into two parts.

In Part I, I will summarize published data and additional results concerning the study of four TYK2 variants as well as some recent molecular studies of the FERM domain of TYK2.

In Part II, I will summarize collaborative studies on IFN signaling in cells from rare patients. These studies have been instrumental to reveal the essential roles of USP18 and ISG15 in negative regulation of the IFN response.

Part I

Functional study of natural TYK2 variants associated with AID

Part I-1. Functional impact of Rs12720356 (I684S) and rs34536443 (P1104A)

We characterized two rare TYK2 variants, I684S and P1104A, which have been associated with AID. Specifically, I measured their *in vitro* catalytic activity and their ability to mediate STAT activation in fibroblasts and genotyped B cell lines. Both variants were found catalytically impaired but able to rescue signaling in response to IFN-α/β, IL-6, and IL-10. These data, coupled with the functional study of an engineered JAK1-P1084A, support a model of non-hierarchical activation of juxtaposed JAKs, in which one catalytically competent JAK is sufficient for signaling provided that its partner, even if inactive, behaves as proper scaffold. Through the analysis of IFN-α and IFN-γ signaling in cells with different JAK1-P1084A levels, I also illustrate a context in which a hypomorphic JAK hampers signaling in a cytokine-specific manner. Given the multitude of TYK2-activating cytokines, the cell context-dependent requirement for TYK2 and the catalytic defect of the two disease-associated variants, we predicted that these alleles are functionally significant in complex immune disorders. These results have been published (see article Li et al, J. Immunol 2013, attached below).

In the European population, the frequency of homozygosity of these two variants is rather low (1% for TYK2-I684S and 0.1-0.2 % for TYK2-P1104A). To study the functional impact of TYK2-I684S on cytokine signaling, I used homozygous EBV-B cells from two healthy donors and from a multiple sclerosis patient. The impact of TYK2-P1104A *homozygosity* was studied in patient-derived EBV-B cells in collaboration with S. Boisson-Dupuis (Rockefeller University, NYC). This group recently found a strong enrichment of P1104A homozygosity in a cohort of patients with infection-predisposing primary immunodeficiency. Studies in EBV-B cells showed that TYK2-I684S has no impact on signaling by various cytokines, while P1104A homozygosity mildly decreases IFN and IL-10 signaling, and interestingly abolishes IL-23 signaling. These unpublished results are described below (Additional results part I-1).

Two Rare Disease-Associated Tyk2 Variants Are Catalytically Impaired but Signaling Competent

Zhi Li,*,† Milica Gakovic,*,† Josiane Ragimbeau,*,† Maija-Leena Eloranta,‡ Lars Rönnblom,‡ Frédérique Michel,*,† and Sandra Pellegrini*,†

Tyk2 belongs to the Janus protein tyrosine kinase family and is involved in signaling of immunoregulatory cytokines (type I and III IFNs, IL-6, IL-10, and IL-12 families) via its interaction with shared receptor subunits. Depending on the receptor complex, Tyk2 is coactivated with either Jak1 or Jak2, but a detailed molecular characterization of the interplay between the two enzymes is missing. In human populations, the *Tyk2* gene presents high levels of genetic diversity with >100 nonsynonymous variants being detected. In this study, we characterized two rare *Tyk2* variants, I684S and P1104A, which have been associated with susceptibility to autoimmune disease. Specifically, we measured their in vitro catalytic activity and their ability to mediate Stat activation in fibroblasts and genotyped B cell lines. Both variants were found to be catalytically impaired but rescued signaling in response to IFN-α/β, IL-6, and IL-10. These data, coupled with functional study of an engineered Jak1 P1084A, support a model of nonhierarchical activation of Janus kinases in which one catalytically competent Jak is sufficient for signaling provided that its partner behaves as proper scaffold, even if inactive. Through the analysis of IFN-α and IFN-γ signaling in cells with different Jak1 P1084A levels, we also illustrate a context in which a hypomorphic Jak can hamper signaling in a cytokine-specific manner. Given the multitude of Tyk2-activating cytokines, the cell context–dependent requirement for Tyk2 and the catalytic defect of the two disease-associated variants studied in this paper, we predict that these alleles are functionally significant in complex immune disorders. ***The Journal of Immunology*****, 2013, 190: 2335–2344.**

Tyk2 is one of the four Janus (Jak) tyrosine kinases and is involved in signaling of cytokines, such as type I and type III IFN, proinflammatory cytokines IL-6, -12, -22, -23, and -26, and the anti-inflammatory IL-10. Thus, Tyk2 is an essential enzyme centralizing inputs from cytokines that shape the immune response. Signaling defects to some of these cytokines have been documented in human and murine Tyk2-deficient cells (1–4). To date, Tyk2 deficiency in two patients has been associated with different clinical pictures, one more complex with features of hyper-IgE syndrome, skewed Th2 lymphocyte polarization, and susceptibility to numerous pathogens and the second with disseminated bacillus Calmette-Guérin infection, neurobrucellosis, and herpes zoster infection (4, 5). A role of Tyk2 in the pathogenesis of autoimmune and inflammatory diseases was suggested from the phenotype of the B10.Q/J strain of mice with a Tyk2 missense mutation (6–8). Studies in null murine models showed that the impact of Tyk2 in cytokine responses and defense to pathogens varies among cell types and infectious contexts (reviewed in Ref. 9). Tyk2 participates in the protective antitumor response, and Tyk2 null mice were shown to have increased predisposition to tumor formation due to a compromised immune surveillance (10).

The survey of sequence databases from International Consortia (dbSNP, 1000 Genomes) reveals a high number of single nucleotide polymorphisms (SNPs) in the *Tyk2* gene. Many SNPs are in the coding region, and >100 nonsynonymous variants have been annotated. Genome-wide association studies and more targeted candidate approaches have shown strong linkage of Tyk2 haplotypes or individual SNPs to systemic and organ-specific autoimmune diseases, namely systemic lupus erythematosus (SLE) (11–14), multiple sclerosis (MS) (15–19), Crohn's disease (20–22), psoriasis (23), type 1 diabetes (24), endometriosis-related infertility (25), and primary biliary cirrhosis (26) (Table I). Interestingly, one rare MS-associated variant (rs34536443) is considered to be protective, whereas another (rs55762744) was recently identified as a risk allele (17). rs12720356, initially reported to be protective in SLE (13), was not confirmed in a replication study (12) and instead found to be a risk allele in Crohn's disease (20, 22). A frequent variant (rs2304256) has been shown to be protective in SLE, Crohn's, and type 1 diabetes in European populations (Table I). Tyk2 allelic variants may predispose to tumor formation. Using a computational approach to distinguish polymorphisms from cancer-associated mutations, Kaminker et al. (27) identified the Tyk2 rs34536443 variant as associated to increased cancer risk. rs34536443 was also identified in a high-throughput sequencing approach used to find tyrosine kinase–encoding gene variants potentially relevant in de novo acute myeloid leukemia (28). Altogether, these studies point to Tyk2 as one of the genetic determinants in some complex diseases.

The activation of Tyk2 by immunoregulatory cytokines relies upon its ability to bind specifically to one of the two components of heterodimeric receptors. Whether coactivated with Jak1 or Jak2, Tyk2 is always found associated to the low-affinity receptor subunit (i.e., IFNAR1, IL-12Rβ1, and IL-10R2), which is devoid of essential phospho-Tyr–based Stat recruitment motifs. Early studies of the type I IFN (IFN-α/β) receptor (IFNAR1 and IFNAR2) demonstrated that the structural integrity of the receptor/Tyk2/

*Unit of Cytokine Signaling, Institut Pasteur, Paris 75724, France; †Centre National de la Recherche Scientifique, Unité de Recherche Associée 1961, Paris 75015, France; and ‡Department of Medical Sciences, Rheumatology, Uppsala University, Uppsala 75105, Sweden

Received for publication November 9, 2012. Accepted for publication December 20, 2012.

This work was supported by the Institut Pasteur, Centre National de la Recherche Scientifique, INSERM, and a grant from the French Multiple Sclerosis Research Society (Fondation pour l'Aide à la Recherche sur la Sclérose en Plaques to F.M.). Work in Uppsala, Sweden, was supported by the Alliance for Lupus Research, the Swedish Research Council, and the King Gustaf V's 80-Year Foundation.

Address correspondence and reprint requests to Dr. Sandra Pellegrini, Institut Pasteur, 25 Rue du Docteur Roux, Paris 75724, France. E-mail address: sandra.pellegrini@pasteur.fr

Abbreviations used in this article: MS, multiple sclerosis; SLE, systemic lupus erythematosus; SNP, single nucleotide polymorphism; VF/PA, V678F/P1104A double mutant; VSV-G, vesicular stomatitis virus glycoprotein; WT, wild-type.

Jak1 complex is essential for signaling, because cells lacking either of the two Jaks or expressing only the receptor-binding domain are unresponsive to IFN. The large N-terminal region of Tyk2 (FERM and Src homology 2-like domains) interacts with the membrane-proximal portion of IFNAR1. Phospho-transfer activity requires the regulatory JH2 (kinase-like, pseudokinase) domain and the catalytic tyrosine kinase JH1 domain (29–31). In addition, Tyk2 has a noncatalytic scaffolding function that ensures plasma membrane stability of IFNAR1 (32). As is the case for the other Jaks, little is known of the connectivity and interplay between the various domains of Tyk2 in the basal state. Also, the molecular details that allow cytokine-induced activation of the receptor-associated kinases are not well defined. It is unclear whether heterodimerizing Jaks play equivalent roles or whether one exerts a dominant catalytic (initiator) role and the other a subordinate role that may be essential in some cellular contexts. Related to this is the question of whether each Jak activates unique signaling steps, or both are equally needed to downstream signals. These issues are of clear relevance to the development of specific inhibitors as therapeutics and are addressed in this study.

We studied the functional impact of two Tyk2 disease-associated variants. We demonstrate that Tyk2 I684S (rs12720356) and Tyk2 P1104A (rs34536443) variants are catalytically impaired. However, in contrast to the canonical ATP-binding mutant Tyk2 K930R, these variants were as competent as Tyk2 wild-type (WT) in reconstituting IFN-α–induced Stat signaling in Tyk2-null cells. These data were corroborated by analyses of IFN-α, IL-6, and IL-10 signaling in EBV-B lymphocytes from genotyped individuals. Thus, these two rare Tyk2 variants are hypomorphic alleles for which catalytic deficiency can be compensated by the Jak partner, at least in some cellular contexts and for some cytokines.

Materials and Methods

Plasmid constructs

Tyk2 WT has been described as pRc-Tyk2 (30). Tyk2 P1104A and Tyk2 I684S, in pRc-CMV and pIRES vectors respectively, were generated by standard PCR technique. To obtain Tyk2 V678F/P1104A, a 1-kb SgrAI-XbaI fragment spanning the P1104A mutation was prepared from Tyk2 P1104A in the pRc-CMV vector and swapped into pRc-Tyk2 (33). The human Jak1 P1084A and K908E mutants were generated by site-directed mutagenesis in pBS-Jak1 and recloned into pRc/CMV-Jak1 (31) with AfeI/XbaI. All new plasmids were verified by sequencing. All expression constructs, except Tyk2 I684S, have a C-ter vesicular stomatitis virus glycoprotein (VSV-G) epitope tag.

Cells and transfection

EBV-transformed B cell lines were obtained from Coriell Cell Repositories (Camden, NJ) and the Centre de Ressources Biologiques of Réseau Français d'Étude Génétique sur la Sclérose en Plaques. Genotyping for rs12720356 and rs34536443 confirmed the presence of the specific polymorphism in the EBV-B lines. Cells were cultured in RPMI 1640 and 10% heat-inactivated FCS, and before cytokine stimulation and protein analysis, cells were serum starved for 2 h. The IFN-α–unresponsive human fibrosarcoma 11,1 (U1A, Tyk2-deficient) cells and U4C (Jak1-deficient) cells were cultured in DMEM and 10% heat-inactivated FCS. Transfections were performed with FuGENE6 (Roche Applied Science). The 11,1 cells were transfected with pRc-CMV–based plasmids for stable expression of Tyk2 WT or mutants, and clones were selected in 400 μg/ml G418. U4C cells were cotransfected with pSV2-puro and pRc-CMV-Jak1 WT, Jak1 P1084A, and Jak1 K908E. PuroR clones were selected in 400 ng/ml puromycin. IFN-α2 was a gift from D. Gewert (Wellcome Research Laboratories). Recombinant human IL-10 was from PeproTech France. IL-6 was a gift from Merck Serono.

Western blot analysis and Abs

Cells were lysed in modified RIPA buffer (34). A total of 30 μg proteins was separated by 7% SDS-PAGE and analyzed by Western blot. Membranes were cut horizontally according to molecular size markers, and stripes were incubated with different Abs. Immunoblots were analyzed by ECL with the ECL Western blotting Reagent (Pierce) or the more sensitive Western Lightning Chemiluminescence Reagent Plus (PerkinElmer). For reprobing, blots were stripped in 0.2 M glycine (pH 2.5) for 30 min at room temperature. The following Abs were used, unless otherwise indicated in figure legends: Tyk2 mAb T10-2 (Hybridolab, Institut Pasteur); anti-Jak1–phospho-YY1022/23 (BioSource International, Invitrogen); anti-Stat1, anti-Stat2, anti-Stat2–phospho-Y689, anti-STAT3, anti-Jak1, and anti-phosphotyrosine mAb 4G10 (Millipore); and anti-Stat1–phospho-Y701, anti-Stat3–phospho-Y705, and anti-Tyk2–phospho-YY1054/55 (Cell Signaling Technology, Beverly, MA).

In vitro kinase assay

Cells were lysed in 50 mM Tris (pH 6.8), 0.5% Nonidet P-40, 200 mM NaCl, 10% glycerol, 1 mM EDTA, 1 mM sodium vanadate, 1 mM sodium fluoride, 10 mM PMSF, 3 μg/ml aprotinin, 3 μg/ml leupeptin, and 3 μg/ml pepstatin. Tyk2 and Jak1 were immunoprecipitated from 2 mg lysate using noncommercial R5-17 polyclonal Abs or affinity-purified anti–VSV-G polyclonal Abs (a gift from M. Arpin, Institut Curie). Immunocomplexes were washed three times in buffer 1 (50 mM Tris [pH 6.8], 400 mM NaCl, 0.5% Triton X-100, and 1 mM EDTA), once in buffer 2 (50 mM Tris [pH 6.8] and 200 mM NaCl), and once in kinase buffer (50 mM HEPES [pH 7.6] and 10 mM $MgCl_2$). The kinase reaction was carried out in 50 mM HEPES [pH 7.6], 10 mM $MgCl_2$, 0.6 μg recombinant Stat3 (SignalChem), and with or without 30 μM ATP at 30°C for 5 min in a total volume of 30 μl. The reaction was terminated by boiling in Laemmli buffer. Half of the sample was loaded for SDS-PAGE, transferred to a nitrocellulose membrane, and phosphorylated products were analyzed by Western blotting with anti-phosphotyrosine 4G10 mAb or activation loop phospho-specific Abs. After stripping, membranes were reblotted with anti-Tyk2 mAb, anti-Jak1, or anti–VSV-G Abs and revealed using ECL detection reagents (Western Lightning; PerkinElmer).

Results

Tyk2 I684S is catalytically impaired but relays cytokine signaling

rs12720356 refers to a rare-occurring nonsynonymous variant that maps in exon 15 of the *Tyk2* gene and causes replacement of the amino acid Ile at position 684 with a serine (I684S) (Table I). The

Table I. Disease-associated nonsynonymous Tyk2 variants

Rs	Ancestral > Derived[a]	MAF[b]	Residue (Domain)	Disease Association	Risk Allele	Reference
2304256	C > A	0.29	V362F (FERM)	SLE	C	11–14, 54[c], 55[c]
				Crohn's disease	C	21
				Type 1 diabetes	C	24
12720356	A > C	0.045	I684S (JH2)	SLE	A	11[c], 12[c], 13
				Crohn's disease	C	20, 22
				Psoriasis	A	23
34536443	G > C	0.014	P1104A (JH1)	MS	G	15, 16, 18, 19
				Endometriosis-related infertility	G	25
				Primary biliary cirrhosis	G	26
55762744	C > T	0.004	A53T (FERM)	MS	T	17

[a]Refers to the (−) strand nucleotide.
[b]From the dbSNP database.
[c]Association was not replicated.

Ile residue is located in the JH2 domain and is conserved across species in Tyk2, Jak1, and Jak2 (Fig. 1A, 1B). A threonine residue is present in Jak3 orthologs and *Drosophila* Hopscotch. To functionally analyze this allelic form, we studied EBV-B–transformed lines established from individuals genotyped for rs12720356. Two lines (referred as AA1 and AA2 in this paper) are homozygote for the ancestral A allele, two are homozygote for the derived C allele (CC1 and CC2), and four are heterozygote (AC1 to AC4). The comparable level of Tyk2 expression in the eight cell lines excluded an effect of the mutation on stability (Fig. 2A). First, we compared the autophosphorylation ability of the AA (Tyk2 I684) and the CC variants (Tyk2 S684). For this, the protein was immunoprecipitated from homozygote cells and subjected to in vitro kinase assay in the presence or absence of added ATP. The reaction product was analyzed by immunoblotting to phospho-tyrosine 4G10 mAb and phospho-Tyk2 Abs specific to Tyr$^{1054–1055}$ in the activation loop. As shown in Fig. 2B (*left panel*), in the absence of ATP, a weak phospho-Tyk2 band was detected with 4G10 in both samples, suggesting comparable basal phosphorylation in cells. When ATP was added to the reaction, the intensity of the phospho-Tyk2 reactive band strongly increased in the AA sample (Tyk2 I684), indicating activity. No activity, however, was detected in the CC sample (Tyk2 S684).

We then assessed the in vitro activity of Tyk2 immunopurified from cells stimulated with IFN-α. AA2 and CC2 lines were used as they express comparable surface levels of IFNAR1 and IFNAR2 (data not shown). Upon ATP addition, a 3- to 4-fold increase in phospho-Tyk2 was observed for IFN-α–treated AA2 cells but not for CC2 (Fig. 2B, *right panel*). Overall, these data indicate that, in vitro, Tyk2 S684 has impaired basal and IFN-α–induced autophosphorylation activity. Nonetheless, in cells, the variant is phosphorylated to the same extent as the ancestral form.

Next, we compared the activation of Stat proteins in the EBV-B lines stimulated with cytokines that activate Tyk2. As shown in Fig. 2C, the extent of phosphorylation of Tyk2, Stat1, and Stat2 was comparable in AA2 and CC2 cells stimulated with nonsaturating doses of IFN-α. Activation of Stat3 by IL-6 and IL-10 was measured in two AA lines and two CC lines and found to be roughly comparable (Fig. 2D, 2E). Of note, the low constitutive level of phospho-Stat3 in these cells may be due to secreted autocrine-acting cytokine(s) (35).

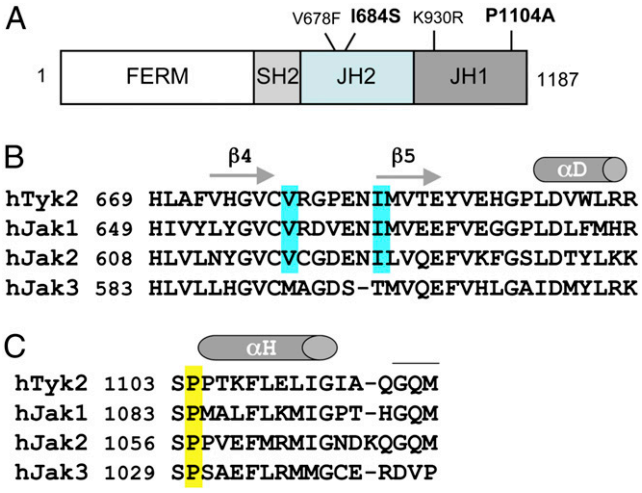

FIGURE 1. (**A**) Schematic representation of the domains of Tyk2 and position of the variants and engineered mutants analyzed in this study. (**B**) Alignment of the sequences of the four human Jak proteins in the region containing the valine and the isoleucine (Tyk2 Val^{678}Ile^{684}) shown in blue. Secondary structure characteristics are indicated above the alignment. (**C**) Alignment of the sequences of the four human Jak proteins in the region containing the proline residue (Tyk2 Pro^{1104}). Secondary helical structure of the unique Jak insertion, in this figure called αH, is indicated above. The adjacent Gly-Gln-Met motif is overlined (see *Discussion*).

To exclude potential effects from other Tyk2 polymorphisms, we engineered the I684S substitution in the *Tyk2* cDNA and derived stable transfectants in Tyk2-deficient 11,1 cells. The in vitro catalytic activity of immunopurified Tyk2 WT and Tyk2 I684S was compared as described above. rStat3 was added to the reaction as exogenous substrate, and the reaction products were immunoblotted with 4G10 mAb to reveal phosphotyrosines. Fig. 3A shows that ATP-dependent autophosphorylation and substrate phosphorylation are impaired in the case of Tyk2 I684S. Of note, when immunopurified from IFN-α–stimulated cells, Tyk2 I684S was phosphorylated on the activation loop to the same extent as the WT protein (Fig. 3A, *lanes 3* and *7*). Next, we compared IFN-α–induced Stat1/2/3 phosphorylation in WT and I684S-expressing cells. No consistent differences were found in the extent of Stat activation, even in the context of a clone expressing a lower level of Tyk2 I684S (cl.2, Fig. 3B). These results reinforce the conclusions drawn from the analysis of EBV-B cell lines that replacement of Ile684 with a serine abrogates Tyk2 kinase activity without affecting cytokine-induced signaling.

Tyk2 P1104A is catalytically impaired but relays Stat signaling

rs34536443 refers to a rare nonsynonymous Tyk2 variant that maps in exon 23 of the *Tyk2* gene and is found only in heterozygote state (Table I). At the protein level, this polymorphism causes alanine substitution of a highly conserved proline residue (Pro^{1104}), which is located in a small Jak-specific insertion in the JH1 domain (Fig. 1A, 1C). To analyze whether this substitution affects Tyk2 function, we engineered the Pro to Ala mutation in *Tyk2* cDNA. Stable WT and P1104A-expressing clones were derived from Tyk2-deficient cells to assess in vitro activity in the presence of rStat3 as exogenous substrate (Fig. 4A). The reaction products were immunoblotted with phospho-Tyk2–specific Abs and 4G10 mAb. Addition of ATP to the WT sample led to rec-Stat3 phosphorylation and Tyk2 autophosphorylation (Fig. 4A, *lanes 1–4*). On the contrary, Tyk2 P1104A was totally impaired in exogenous substrate phosphorylation (*lanes 5–8*). In IFN-stimulated cells, the mutant was phosphorylated and possessed in vitro a weak autophosphorylation activity targeted to tyrosines other than Tyr$^{1054–55}$ in the activation loop (Fig. 4A, *lanes 7* and *8*, 4G10 detection). In comparison, Tyk2 K930R, mutated in the conserved lysine of the ATP binding pocket, was not phosphorylated neither in cells nor in vitro (Fig. 4B). Next, we compared Stat activation in cells expressing Tyk2 WT, P1104A, and K930R that were stimulated with IFN-α. As shown in Fig. 4C, the phosphorylation profiles were comparable in WT and P1104A-expressing cells, whereas signaling was severely hampered in K930R-expressing cells. In accordance with these data, the analysis of EBV-B cells prepared from three heterozygote rs34536443 individuals did not reveal defect in IFN-α signaling (data not shown).

To gain more insight into the impact of the Pro to Ala mutation on enzymatic activity, we asked whether this mutation would perturb the hyperactivity of Tyk2 V678F. This designed mutant is catalytically hyperactive in vitro and basally highly phosphorylated on the activation loop and thus mimics the gain-of-function pathogenic Jak2 V617F (33). We generated the V678F/P1104A double mutant (VF/PA), which was expressed to roughly equivalent level as Tyk2 WT, K930R, P1104A, and V678F in 293T cells (Fig. 5A). As expected, Tyk2 V678F was hyperphosphorylated on the activation loop. Remarkably, the double VF/PA mutant was ~10-fold less phosphorylated than V678F. Moreover, in Tyk2

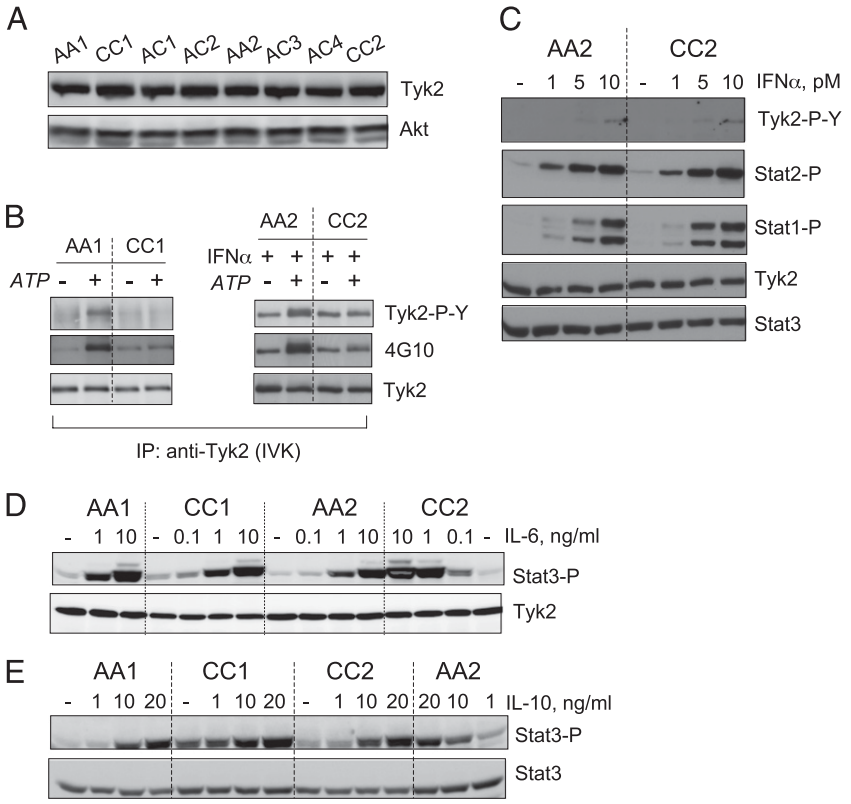

FIGURE 2. Functional analyses of Tyk2 variants in rs12720356 genotyped EBV-B cells. (**A**) Tyk2 expression level in eight EBV-transformed B cell lines from rs12720356 genotyped individuals. Individuals AA1 and AA2 carry two ancestral A alleles; individuals CC1 and CC2 carry two derived C alleles; four individuals, AC1 to AC4, are heterozygotes. Cell lysates (30 μg) were immunoblotted with anti-Tyk2 and anti-Akt as loading control. (**B**) *Left panel*, Basal in vitro kinase (IVK) activity of Tyk2 from unstimulated EBV-B cells of homozygote AA individual (Tyk2 I684) and CC individual (Tyk2 S684). Tyk2 was immunoprecipitated (IP) and subjected to an in vitro kinase reaction for 5 min at 30˚C in the presence (+) or absence (−) of 30 μM ATP. Phosphorylated proteins in the reaction were revealed by successive immunoblotting with 4G10, anti–phospho-Tyr$^{1054–1055}$ specific to the activation loop (Tyk2-P-Y), and anti-Tyk2. *Right panel*, Kinase activity of Tyk2 from the indicated EBV-B cells after stimulation for 15 min with 50 pM of IFN-α. Samples were processed as described above. (**C**) IFN-α–induced Jak/Stat activation in EBV-B cells from one AA individual (Tyk2 I684) and one CC individual (Tyk2 S684). Cells were stimulated with increasing doses of IFN-α for 15 min. The level of tyrosine-phosphorylated Tyk2, Stat1, and Stat2 was analyzed by Western blot with phospho-specific Abs. The membrane was reprobed for Tyk2 and total Stat3 levels. A low level of phospho-Stats was reproducibly detected in nonstimulated cells. (**D**) Stat3 phosphorylation levels in the indicated EBV-B cells stimulated with IL-6 for 15 min. Tyk2 levels shown as loading control. (**E**) Stat3 phosphorylation levels in the indicated EBV-B cells stimulated with IL-10 for 15 min. Stat3 levels shown as loading control.

V678F-expressing cells, endogenous Stat3 was highly phosphorylated (33), but this was not the case in VF/PA-expressing cells (Fig. 5A). Next, we measured the catalytic potential of the double VF/PA mutant in vitro (Fig. 5B). As expected, Tyk2 V678F exhibited a robust activity. Conversely, the VF/PA mutant was impaired in both ATP-dependent autophosphorylation and substrate phosphorylation. Overall, these data showed that the catalytic gain-of-function effect exerted by phenylalanine at position 678 is abrogated by the Pro^{1104}-to-Ala substitution. Thus, the Pro-to-Ala substitution has a strong negative and dominant impact on phospho-transfer activity.

Jak1 P1084A is catalytically impaired but relays Stat signaling

The natural Tyk2 I684S and P1104A variants were found to be functionally impaired in vitro and yet inducibly phosphorylated in cells and competent to rescue signaling. These data supported the view that the kinase activity of Tyk2 is dispensable or subordinate with respect to that of Jak1 (30, 36). To test this model and gain more mechanistic insight on the specific contribution of Tyk2 and Jak1, we engineered the corresponding Jak1 mutant (Jak1 P1084A) and stably expressed it in Jak1-null U4C cells. Clones expressing Jak1 WT and the ATP-binding deficient Jak1 K908E mutant were studied in parallel. In vitro kinase assays were performed on immunopurified Jak1 proteins as described above. Jak1 WT exhibited ATP-dependent (basal and IFN-induced) activity detected with phospho-Tyr$^{1022–1023}$–specific Abs and 4G10 (Fig. 6A, *lanes 1–4*). Conversely, Jak1 P1084A, although phosphorylated in IFN-stimulated cells, failed to autophosphorylate in vitro on the activation loop (Fig. 6A, *lanes 7* and *8*). A weak ATP-dependent phospho-Jak1 P1084A band was detected with 4G10 in IFN-stimulated samples (Fig. 6A, *lanes 7* and *8*; 4G10), similar to that shown for Tyk2 P1104A (Fig. 4A). IFN-induced Stat1/2/3 activation was restored in Jak1 P1084A-expressing cells but not in Jak1 K908E-expressing cells (Fig. 6B).

In conclusion, the Pro-to-Ala substitution in both Tyk2 and Jak1 strongly impacted catalytic activity but did not affect their ability to rescue IFN-α signaling. Thus, these data did not support the notion that Tyk2 is catalytically subordinate with respect to Jak1, but rather suggested a model of catalytic equivalence of the two enzymes and the possibility of their reciprocal compensation.

Pro-to-Ala mutants of Tyk2 and Jak1 are substrates for trans *phosphorylation*

A question raised by the above data concerned the remarkably different behavior between the Pro-to-Ala mutants (Tyk2 P1104A and Jak1 P1084A) and the ATP-binding mutants (Tyk2 K930R and Jak1 K908E). Although all four mutants were inactive in vitro, only the Pro-to-Ala mutants were inducibly phosphorylated on the

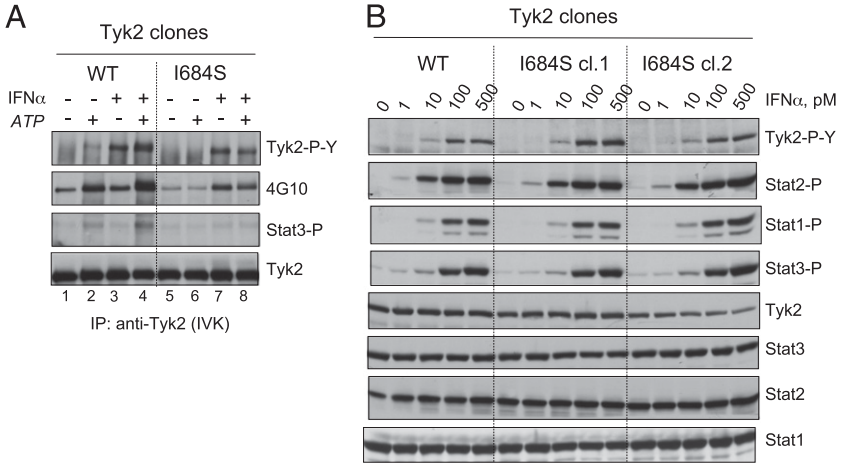

FIGURE 3. Functional analyses of the engineered Tyk2 I684S mutant stably expressed in Tyk2-deficient cells. (**A**) In vitro kinase (IVK) activity of Tyk2 WT and Tyk2 I684S. Tyk2 was immunoprecipitated (IP) from cells nonstimulated or stimulated with IFN-α (500 pM, 15 min) and subjected to an in vitro kinase reaction in the presence or absence of 30 μM ATP for 5 min at 30˚C. rStat3 (0.6 μg) was added to the reaction as exogenous substrate. Phosphorylated proteins in the reaction were revealed by sequential blotting with anti–phospho-Tyr mAb 4G10, anti–phospho-Tyk2, and anti-Tyk2. (**B**) IFN-α–induced Jak/Stat activation in cells expressing Tyk2 WT or Tyk2 I684S. One WT clone and two I684S-expressing clones were stimulated with the indicated doses of IFN-α for 15 min. The phosphorylation level of the indicated proteins was analyzed by immunoblotting with phospho-tyrosine–specific Abs. The membranes were reprobed for total protein level. Total Tyk2, Stat1, Stat2, and Stat3 are shown. Note that IS cl.2 expresses less Tyk2 (~70%) with respect to the other clones.

activation loop in cytokine-stimulated cells and rescued signaling. We reasoned that this may reflect the competence of the protein to be *trans* phosphorylated (i.e., to act as substrate of the Jak partner). To test this, we performed mixed kinase assays in vitro to compare the ability of Tyk2 P1104A and Tyk2 K930R to act as substrates for Jak1. Lysates of Jak1-expressing cells were mixed with lysates of Tyk2 P1104A or Tyk2 K930R-expressing cells. Tagged Jak proteins were coimmunopurified to be assayed in vitro. As shown in Fig. 6C, addition of ATP led to strong phosphorylation of Tyk2 P1104A but not of Tyk2 K930R, indicating that, of the two catalytically impaired mutants, only Tyk2 P1104A is a suitable substrate for Jak1.

In another set of experiments, we assessed whether Jak1 P1084A was a good substrate for Tyk2 WT. For this, Jak1 P1084A-expressing cells were stably transfected with Tyk2 WT or Tyk2 P1104A. Tagged proteins were coimmunopurified and analyzed in vitro. As shown in Fig. 6D, Jak1 P1084A was phosphorylated only when copurified with Tyk2 WT (*lanes 1* and *2*). Conversely, when the two Pro to Ala mutants were copurified, no phosphorylated products were detected (*lanes 3* and *4*). These data con-

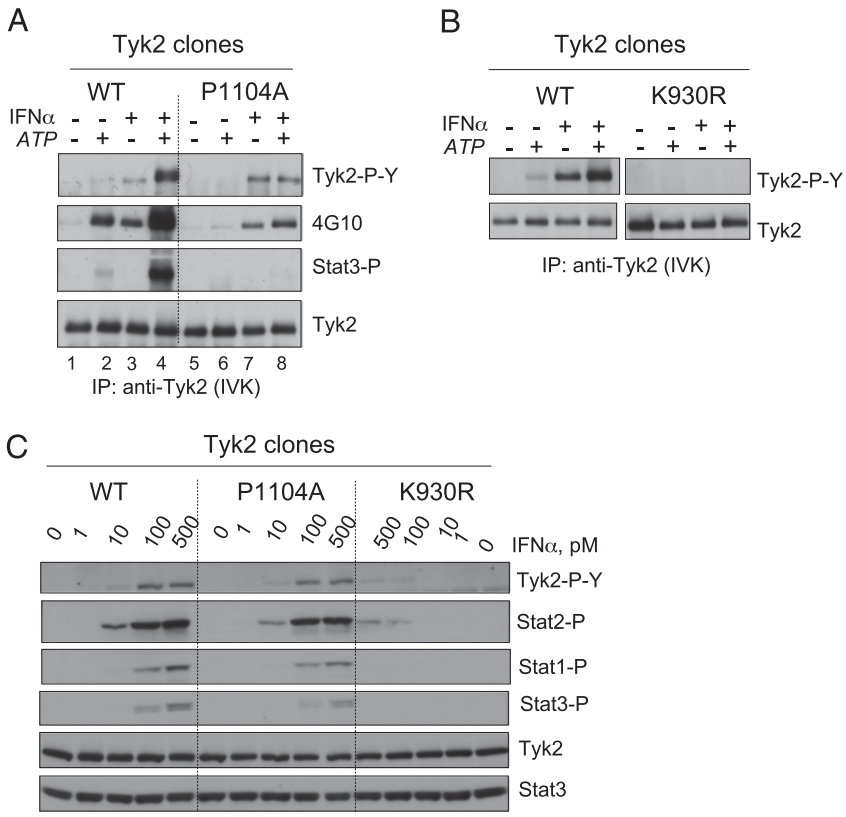

FIGURE 4. Functional analyses of the engineered Tyk2 P1104A mutant. (**A**) In vitro kinase (IVK) activity of Tyk2 WT and Tyk2 P1104A. Neo^R clones were derived from Tyk2-deficient 11,1 cells. Tyk2 was immunoprecipitated (IP) with anti-Tyk2 from nonstimulated or IFN-α–stimulated cells and subjected to in vitro kinase reaction in the presence or absence of 30 μM ATP for 5 min at 30˚C. rStat3 (0.6 μg) was added to the reaction as exogenous substrate. Phosphorylated proteins were revealed by blotting the reaction products with 4G10 and anti–phospho-Tyk2. Total levels of Tyk2 are shown. (**B**) In vitro kinase (IVK) activity of Tyk2 WT and Tyk2 K930R. Analysis as in (A). (**C**) IFN-α–induced Jak/Stat activation. Clones expressing Tyk2 WT, Tyk2 P1104A, or Tyk2 K930R were stimulated with the indicated doses of IFN-α for 15 min. Phosphorylation levels of the indicated proteins were analyzed by Western blot with phospho-tyrosine–specific Abs. The membranes were reprobed for total Tyk2 and Stat3 levels.

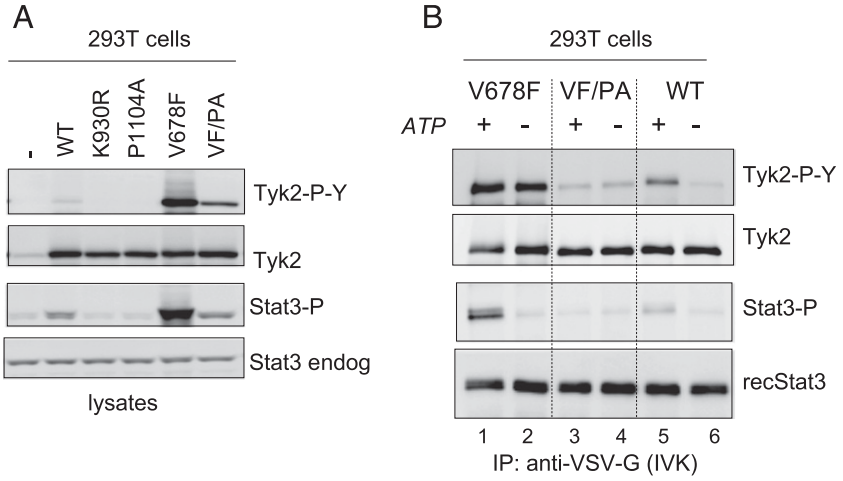

FIGURE 5. Effect of the P1104A substitution on hyperactivity of the Tyk2 V678F mutant. (**A**) Level of autophosphorylation of overexpressed Tyk2 mutants and substrate phosphorylation. 293T cells were transiently transfected with either Tyk2 (WT), the ATP-binding deficient K930R, Tyk2 P1104A, the catalytically hyperactive Tyk2 V678F, and the double mutant V678F/P1104A (VF/PA). Cell lysates were analyzed by Western blot with anti-Tyk2–phospho-Tyr$^{1054-55}$ Abs, anti–P-Stat3, and anti-Tyk2 mAb. Note that in empty vector-transfected cells (−), endogenous Tyk2 is barely detected. (**B**) In vitro kinase (IVK) activity of Tyk2 WT, Tyk2 V678F, and double-mutant V678F/P1104A. Cell lysates were analyzed by Western blot with anti-Tyk2–phospho-Tyr$^{1054-55}$ Abs, anti–P-Stat3, and anti-Tyk2 mAb. IP, Immunoprecipitation.

firmed the catalytic impairment of the Pro-to-Ala mutants and demonstrated that they are suitable substrates for the juxtaposed WT partner.

Impact of Jak1 P1084A in IFN-α and IFN-γ signaling

The studies described above suggested that a Pro-to-Ala mutant, either Tyk2 or Jak1, can be inducibly phosphorylated on the activation loop through the initiating action of the facing WT partner and that this reaction is productive for Stat activation. This model predicts that the WT enzyme may become rate-limiting when the mutant Jak is highly expressed. This possibility was tested by comparing the IFN-α response of cells expressing Jak1 (WT or P1084A) at near-endogenous level (referred as low) or at levels 15–20-fold higher (referred as hi). Jak1 WT^{low} and P1084A^{low} cells responded similarly to IFN-α (Fig. 7A, *lanes 11–20*). In contrast, Jak1^{hi} cells responded differently, with phospho-Stat1 being more abundant in WT^{hi} than in P1084A^{hi} cells (*lanes 1–10*). This suggested that, in the presence of excess Jak1 P1084A mutant, endogenous Tyk2 activity can become limiting.

Jak1 is involved in signaling through the IFN-γ receptor complex, where it is juxtaposed to Jak2. Thus, using the clones described above, we analyzed the rescuing capacity of Jak1 P1084A by measuring IFN-γ–induced Stat1 activation. As shown in Fig. 7B, IFN-γ signaling was comparable in Jak1^{low} WT and P1084A^{low} cells (*lanes 1–8*). Cells reconstituted with the kinase-dead Jak1 K904E mutant, and parental 2C4 cells were monitored

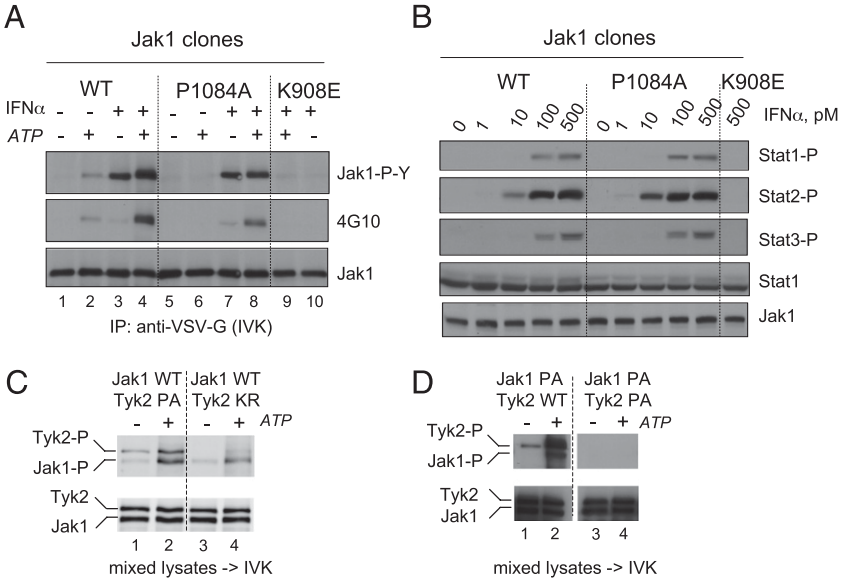

FIGURE 6. Functional analyses of the engineered Jak1 P1084A mutant. (**A**) In vitro kinase (IVK) activity of Jak1 WT, Jak1 P1084A, and the ATP-deficient Jak1 K908E. U4C cell–derived clones reconstituted with the indicated tagged Jak1 form were used. Jak1 was immunoprecipitated (IP) with anti–VSV-G from either nonstimulated cells or IFN-α–stimulated cells and subjected to in vitro kinase reaction. Phosphorylated proteins were revealed by blotting the reaction product with 4G10, anti–phospho-Jak1–Tyr$^{1022-1023}$, and anti-Jak1. (**B**) IFN-α–induced Jak/Stat activation in U4C-derived clones expressing Jak1 WT, Jak1 P1084A, or Jak1 K908E. Cells were treated with increasing doses of IFN-α for 15 min. Phosphorylation levels of the indicated Stat were analyzed by Western blot with phospho-tyrosine specific Abs. Total Jak1 and Stat1 levels are shown. (**C**) In vitro *trans* phosphorylation of Tyk2 P1104A and Tyk2 K930R by Jak1 WT. Lysates were prepared from U4C cells expressing tagged Jak1 WT and from 11,1 cells expressing tagged Tyk2 P1104A (Tyk2 PA) or Tyk2 K930R (Tyk2 KR). Equal amounts (1.75 mg) of the two lysates were mixed. Tagged proteins were coimmunopurified on beads coated with anti–VSV-G and subjected to in vitro kinase (IVK) reaction. Phosphorylated proteins were revealed by blotting the reaction products with 4G10 (*top panel*) and, after stripping, with anti–VSV-G (*bottom panel*). (**D**) In vitro *trans* phosphorylation of Jak1 P1084A by Tyk2 WT or Tyk2 P1104A. U4C cells expressing tagged Jak1 P1084A were engineered to stably coexpress either tagged Tyk2 WT or Tyk2 P1104A. Tagged proteins were coimmunopurified on beads coated with anti–VSV-G and subjected to in vitro kinase reaction. Phosphorylated proteins were revealed by blotting the reaction products with 4G10 (*top panel*) and, after stripping, with anti–VSV-G (*bottom panel*).

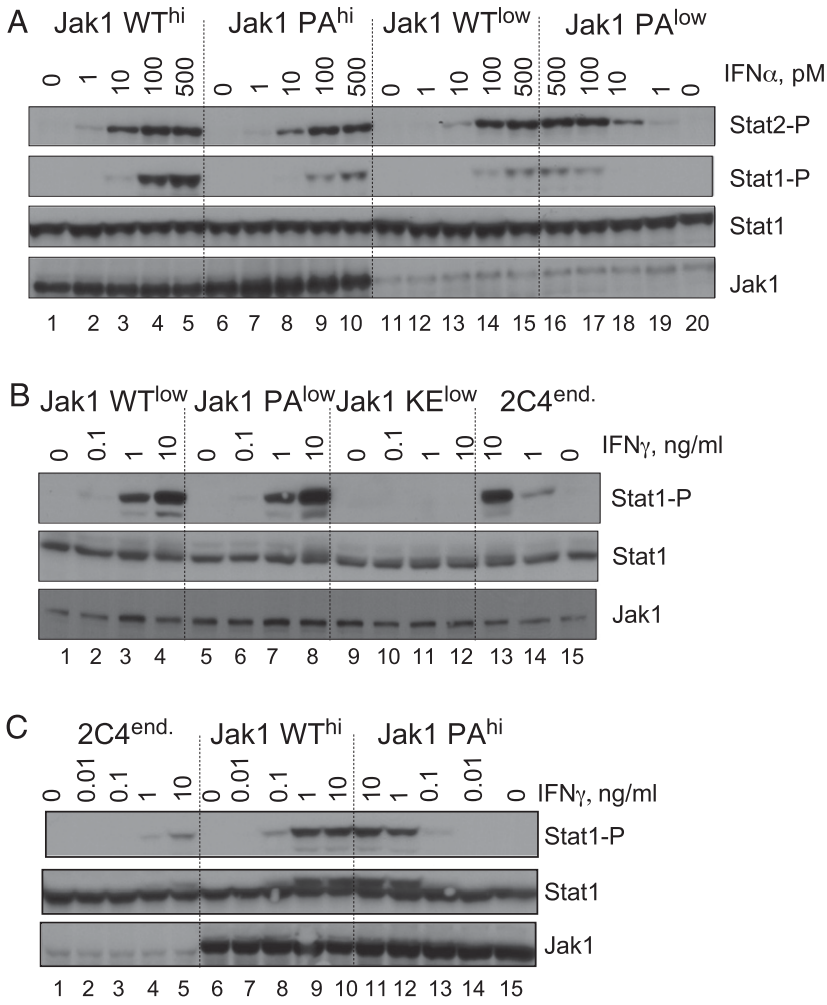

FIGURE 7. Stat1 activation by IFN-α or IFN-γ in cells expressing high or endogenous-like levels of Jak1 P1084A. (**A**) IFN-α–induced Stat1 activation in U4C cells reconstituted with either Jak1 WT or Jak1 P1084A expressed at high (hi) or endogenous-like level (low). Cells were treated with IFN-α for 15 min. Stat1/2 phosphorylation was analyzed by Western blot. Total Jak1 and Stat1 levels are shown. (**B**) IFN-γ–induced Stat1 activation in U4C cells reconstituted with endogenous-like level of Jak1 WT, Jak1 P1084A, or the ATP-binding–deficient Jak1 K908E and in the parental 2C4 cells. Cells were treated with IFN-γ as indicated for 15 min. Stat1 phosphorylation was analyzed with phospho-tyrosine–specific Abs. Total Jak1 and Stat1 levels are shown. (**C**) IFN-γ–induced Stat1 activation in parental 2C4 cells and U4C cells expressing high Jak1 WT or Jak1 P1084A levels. Cells were treated with IFN-γ for 15 min. Stat1 phosphorylation was analyzed with phospho-tyrosine–specific Abs. Total Jak1 and Stat1 levels are shown. Note that the phospho-Stat1 membrane was exposed for shorter time than in (B). 2C4 cells are present in both panels as internal reference.

as controls (Fig. 7B, *lanes 9–15*). Interestingly, Jak1WT^{hi} and P1084A^{hi} cells exhibited a comparable robust IFN-γ signaling (Fig. 7C, *lanes 6–15*). Thus, when overexpressed, Jak1 P1084A is unable to support high signaling from the type I IFN receptor but can do it from the IFN-γ receptor. Overall, these results indicate that the specific role of a Jak, and thus the impact of a variant, can differ in different cytokine receptors.

Discussion

The exact mechanism that controls basal-state and ligand-induced activation of Jak proteins in complex with cytokine receptors remains ill defined. Over the years, this issue has been addressed by measuring the signaling capacity of kinase-dead Jaks mutated in the conserved lysine of the ATP-binding pocket of the JH1 domain. For type I IFN, analysis of Jak1 K907E-expressing cells and Tyk2 K930R cells led to propose a hierarchical asymmetric activation model, with Jak1 playing the initiator role (30, 36). Studies of IFN-γ signaling were performed on cells overexpressing Jak1 or Jak2 lysine mutants and concluded on a hierarchical activation as well, with Jak2 playing the initiator role (36). The question was recently re-examined for IFN-γ with the same mutants expressed at near-endogenous levels, and the data pointed, instead, to Jak1 as the initiator (37). These studies emphasized the impact of Jak expression level and indicated a certain degree of catalytic hierarchy between two juxtaposed Jaks. Interestingly, the Jak1 and Tyk2 lysine mutants were found to have defective interactions with their cognate receptors in the IFN-γ and IFN-α context, respectively (30, 37), suggesting that the alteration of the ATP-binding pocket disturbs the conformational integrity of the enzyme (see below).

In the present work, we describe three mutants (Tyk2 I684S, Tyk2 P1104A, and Jak1 P1084A) that are catalytically impaired and yet indistinguishable in type I IFN signaling potency from the WT proteins. Furthermore, Jak1 P1084A rescues IFN-γ signaling as well. Contrary to the lysine mutants, the Pro-to-Ala mutants are good activation loop phosphorylation substrates, both in cells and in vitro. These data suggest that, at least for these cytokine receptors, one catalytically competent enzyme is sufficient to trigger signaling provided that the juxtaposed partner, although inactive, acts as a proper scaffold and/or phospho-acceptor substrate. This unidirectional activation mode is nonhierarchical and somehow reminiscent of the allosteric mechanism of kinase activation proposed for epidermal growth factor receptor family members (38). Moreover, it is expected to be productive only in cytokine receptors bringing together two different Jaks. Consistent with this, one study showed that a catalytically inactive Jak2 mutant (Jak2 I1065A, Fig. 1C) rescued signaling to IFN-γ but not to erythropoietin, a cytokine that homodimerizes the EpoR/Jak2 complex (39).

The difference in signaling competence between the natural variants and the conventional lysine mutants, all catalytically impaired, is remarkable. As mentioned above, mutants of the lysine in the ATP-binding pocket behave as poor scaffolds and substrates and thus may be constrained in an inhibited conformation, less prone to release the activation loop. As in other protein kinases, ATP binding may prime for critical conformational changes (40, 41). Indeed, structural studies showed that the isolated JH1

domains of the four Jaks complexed with ATP-competitive inhibitors adopt an active conformation with an exposed loop (42–44). With regard to intact Jaks, specific ATP competitive inhibitors that block catalytic function also promote activation loop phosphorylation in cells (45). Moreover, some JH2 mutants of Tyk2 and Jak3 have been described that are catalytically dead but constitutively phosphorylated on the activation loop. Importantly, this phosphorylation was abrogated when the ATP-binding lysine of JH1 was mutated (46, 47). Overall, these data support the concept that scaffolding function, ATP binding- and conformational flexibility of a Jak protein can be more critical than its phospho-transfer activity for signaling through heteromeric receptors.

Although detailed mechanistic understanding of the catalytic defect exhibited by the two Tyk2 variants will require advanced structural knowledge, the positions of each residue in the protein is informative. The isoleucine residue (Tyk2 Ile^{684}) is located in the regulatory JH2 domain, which has negative and positive effects on JH1 (33, 46). As shown in Fig. 8A, the corresponding isoleucine in Jak2 JH2 is located in the N lobe, at the end of the loop connecting the β4 and β5 strands, and is a few residues away from Val^{617} (48). Interestingly, it was shown that the activating V617F mutation rigidifies the JH2 αC helix through π-stacking interactions with two phenylalanines (Phe^{594,595}), confirming previous mutational studies of Jak2 V617F by Constantinescu's group (49). Yet, the mode by which the rigidified αC helix brings about JH1 activation in Jak2 V617F remains unclear. In this study, we show that the V678F and I684S single substitutions in Tyk2 have opposite consequences on catalytic activity and thus may impact in opposite manner on the JH2 αC helix. Indeed, in Jak2 JH2, the isoleucine side chain does not point toward the αC helix, as is the case for the valine, but faces more toward the inner hydrophobic core of the N lobe (Fig. 8A). Thus, substitution of the isoleucine with the small polar serine may disturb the N lobe and compromise productive positioning of the αC helix. Overall, Tyk2 I684S appears to be impaired only in the positive regulatory function of JH2 toward JH1. This contrasts with the more severe loss of function of two point mutants in the C lobe of JH2 (Tyk2 R856G and Tyk2 E782K). These mutants are not only kinase-dead, but also highly phosphorylated on the activation loop and signaling incompetent (6, 46).

Pro1104 is located at the edge of a unique insert (13–15 residues) in the JH1 domain. This insert is conserved in the Jak family with the exception of *Drosophila* Hopscotch, is not found in the JH2 domain nor in other tyrosine kinases, and has been called αH helix, FG helix, Jak-specific insertion, or Lip (43). The insert folds into a short α helix (αH) that is adjacent to the αG helix of the C lobe and close to the catalytic cleft (Fig. 8B). Mutational studies in Jak2 indicated the key role of the αH helix in autophosphorylation (39). Indeed, Jak2 point mutants in conserved residues of αH showed reduced, abrogated, or enhanced phosphorylation in cells. In these studies, the proline corresponding to Tyk2 Pro^{1104} was not analyzed nor was in vitro kinase activity of the Jak2 mutants measured. As discussed above, both Pro-to-Ala Tyk2 and Jak1 mutants that we studied in this paper rescued signaling, indicating no impairment of their respective scaffolding role. In cells, both mutants were inducibly phosphorylated in response to ligand, but failed to auto-*trans* phosphorylate on the activation loop and to phosphorylate an exogenous substrate in vitro.

Several observations suggest that Pro^{1104} and the adjacent αH helix are important in substrate recognition. The catalytic defect of Tyk2 P1104A is dominant in that it could not be rescued by the V678F substitution, which per se causes enzyme hyperactivation. When stimulated by IFN-α in cells and tested in vitro, both Pro-to-Ala mutants exhibited a very weak catalytic activity on tyrosines outside of the activation loop (Figs. 4A, 6A), which may indicate altered substrate recognition. As shown in Fig. 8B, Pro^{1104} appears to pack in a ring-stacking interaction with a tryptophan residue (Trp^{1067}), which is conserved in tyrosine kinases. Interestingly, in place of this tryptophan, Ser/Thr kinases have a tyrosine residue, which, in cAMP-dependent protein kinase studies, was shown to be critical for substrate binding and orienting catalytic residues (50). Moreover, adjacent to the αH helix is the exposed Gly-Gln-Met motif (Figs. 1C, 8B), which is part of a binding surface for the negative regulator suppressor of cytokine signaling 3. Through this

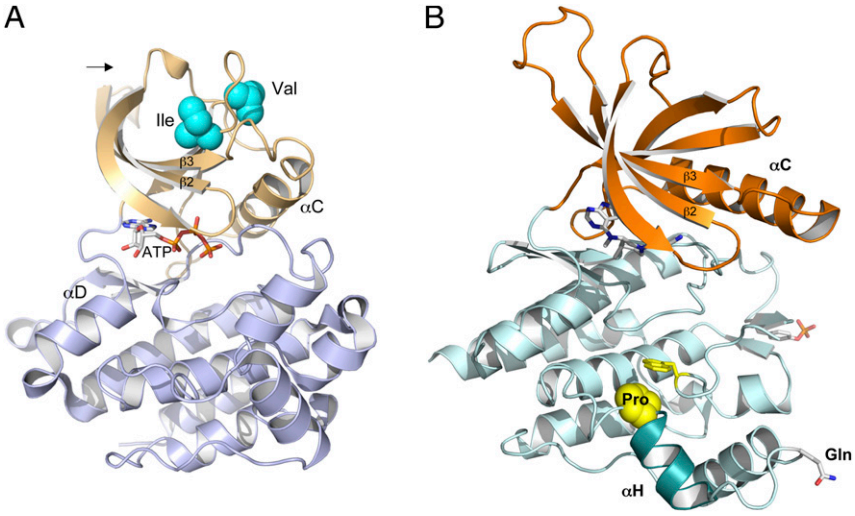

FIGURE 8. (**A**) Location of Jak2 Ile^{623} and Val^{617} residues corresponding to Tyk2 Ile^{684} and Val^{678}. The side chains of Jak2 Ile^{623} and Val^{617}, corresponding to Tyk2 Ile^{684} and Val^{678}, respectively, are highlighted in blue sphere representation on the crystal structure of the active form of the JH2 domain (PDB entry 4FVQ) (48). The N lobe of the kinase domain is in beige and the C lobe in cyan. Note that a unique large insert is present only in Tyk2 between the β2 and β3 strands (arrow). (**B**) Location of Pro^{1104} in the JH1 domain of Tyk2. The side chain of Pro^{1104} is highlighted in yellow sphere representation on the crystal structure of Tyk2 JH1 domain complexed with the Jak inhibitor CP-690550 (PDB entry 3LXN) (42). The N lobe of the kinase domain is in orange, the C lobe in light blue, with the αH helix in darker blue. Facing the proline, a conserved tryptophan residue (Trp1067) is shown in yellow stick representation (see text). The side chain of the glutamine residue of the Gly-Gln-Met motif is depicted (see text) (51). Note that the activation loop, phosphorylated on Tyr^{1054}, is partly disordered.

interaction, suppressor of cytokine signaling 3 was reported to disturb phosphate transfer to the tyrosine substrate without affecting ATP hydrolysis (51).

Tyk2 is an essential element of the tonic signal induced by homeostatic IFN-β and is implicated in signaling networks initiated by a large number of immunoregulatory cytokines (9, 52). As first proposed by Shaw et al. (6) and later supported by human disease genetic-association studies, notably MS, naturally occurring mutations in the *Tyk2* gene may underlie altered susceptibility to autoimmune disorders (Table I). The two rare disease-associated Tyk2 polymorphisms that we studied in this paper have a clear damaging effect, as they give rise to hypomorphic proteins devoid of kinase activity. Yet, the kinase-independent scaffolding function of these proteins appears sufficient for Stat activation by type I IFN, IL-6, and IL-10 in fibroblastic and/or B cell lines. Also, our comparative analysis of IFN-α and IFN-γ signaling in cells expressing different levels of Jak1 P0184A illustrates that a catalytic loss-of-function Jak can hamper signaling in a cytokine-specific manner.

Studies in mice have shown that the requirement for Tyk2 in signaling by type I IFN and other immune cytokines can be cell-context dependent (2, 3, 53). Moreover, it is increasingly clear that the functional impact of many polymorphisms, notably in immune response imbalance, can differ according to cell or tissue types and their particular biological state. A modest reduction of IFN-β signaling has been observed in ex vivo–expanded T cells from heterozygote Tyk2 P1104A carriers (16). As this is not the case in heterozygote B cell lines and reconstituted fibroblasts, it suggests that this Tyk2 variant may have a differential impact depending on cell type. Given the variety of Tyk2-activating cytokines, their intricate effects on the immune response and the lineage complexity of immune and nonimmune target cells, it will be a major challenge to phenotypically assess the beneficial, neutral, or harmful effect of Tyk2 alleles in diverse clinical manifestations (Table I). Yet, the remarkable catalytic impairment of the two Tyk2 variants studied in this paper predicts that they are not neutral but rather functionally significant in complex immune disorders.

Note added in proof. A recent study has also shown that Rs34536443 is associated with rheumatoid arthritis (56).

Acknowledgments

We thank Isabelle Rebeix and Bertrand Fontaine for discussion and providing genotyped EBV-B lines; Pedro Alzari for discussion and making Fig. 8; Gilles Uzé for insightful advice; Béatrice Corre for technical help; Jérémy Manry, Hélène Quach, and Lluis Quintana-Murci for advice and help in genotyping and sequencing; and all of the members of the Cytokine Signaling Unit for discussion. We also thank Vincenzo Di Bartolo, Mark Livingstone, and Gilles Uzé for critical reading of the manuscript.

Disclosures

The authors have no financial conflicts of interest.

References

1. Velazquez, L., M. Fellous, G. R. Stark, and S. Pellegrini. 1992. A protein tyrosine kinase in the interferon α/β signaling pathway. *Cell* 70: 313–322.
2. Karaghiosoff, M., H. Neubauer, C. Lassnig, P. Kovarik, H. Schindler, H. Pircher, B. McCoy, C. Bogdan, T. Decker, G. Brem, et al. 2000. Partial impairment of cytokine responses in Tyk2-deficient mice. *Immunity* 13: 549–560.
3. Shimoda, K., K. Kato, K. Aoki, T. Matsuda, A. Miyamoto, M. Shibamori, M. Yamashita, A. Numata, K. Takase, S. Kobayashi, et al. 2000. Tyk2 plays a restricted role in IFN alpha signaling, although it is required for IL-12-mediated T cell function. *Immunity* 13: 561–571.
4. Minegishi, Y., M. Saito, T. Morio, K. Watanabe, K. Agematsu, S. Tsuchiya, H. Takada, T. Hara, N. Kawamura, T. Ariga, et al. 2006. Human tyrosine kinase 2 deficiency reveals its requisite roles in multiple cytokine signals involved in innate and acquired immunity. *Immunity* 25: 745–755.
5. Kilic, S. S., M. Hacimustafaoglu, S. Boisson-Dupuis, A. Y. Kreins, A. V. Grant, L. Abel, and J. L. Casanova. 2012. A patient with tyrosine kinase 2 deficiency without hyper-IgE syndrome. *J. Pediatr.* 160: 1055–1057.
6. Shaw, M. H., V. Boyartchuk, S. Wong, M. Karaghiosoff, J. Ragimbeau, S. Pellegrini, M. Muller, W. F. Dietrich, and G. S. Yap. 2003. A natural mutation in the Tyk2 pseudokinase domain underlies altered susceptibility of B10.Q/J mice to infection and autoimmunity. *Proc. Natl. Acad. Sci. USA* 100: 11594–11599.
7. Shaw, M. H., G. J. Freeman, M. F. Scott, B. A. Fox, D. J. Bzik, Y. Belkaid, and G. S. Yap. 2006. Tyk2 negatively regulates adaptive Th1 immunity by mediating IL-10 signaling and promoting IFN-gamma-dependent IL-10 reactivation. *J. Immunol.* 176: 7263–7271.
8. Spach, K. M., R. Noubade, B. McElvany, W. F. Hickey, E. P. Blankenhorn, and C. Teuscher. 2009. A single nucleotide polymorphism in Tyk2 controls susceptibility to experimental allergic encephalomyelitis. *J. Immunol.* 182: 7776–7783.
9. Strobl, B., D. Stoiber, V. Sexl, and M. Mueller. 2011. Tyrosine kinase 2 (TYK2) in cytokine signalling and host immunity. *Front. Biosci.* 16: 3214–3232.
10. Stoiber, D., B. Kovacic, C. Schuster, C. Schellack, M. Karaghiosoff, R. Kreibich, E. Weisz, M. Artwohl, O. C. Kleine, M. Muller, et al. 2004. TYK2 is a key regulator of the surveillance of B lymphoid tumors. *J. Clin. Invest.* 114: 1650–1658.
11. Cunninghame Graham, D. S., M. Akil, and T. J. Vyse. 2007. Association of polymorphisms across the tyrosine kinase gene, TYK2 in UK SLE families. *Rheumatology (Oxford)* 46: 927–930.
12. Hellquist, A., T. M. Järvinen, S. Koskenmies, M. Zucchelli, C. Orsmark-Pietras, L. Berglind, J. Panelius, T. Hasan, H. Julkunen, M. D'Amato, et al. 2009. Evidence for genetic association and interaction between the TYK2 and IRF5 genes in systemic lupus erythematosus. *J. Rheumatol.* 36: 1631–1638.
13. Sigurdsson, S., G. Nordmark, H. H. Göring, K. Lindroos, A. C. Wiman, G. Sturfelt, A. Jönsen, S. Rantapää-Dahlqvist, B. Möller, J. Kere, et al. 2005. Polymorphisms in the tyrosine kinase 2 and interferon regulatory factor 5 genes are associated with systemic lupus erythematosus. *Am. J. Hum. Genet.* 76: 528–537.
14. Suarez-Gestal, M., M. Calaza, E. Endreffy, R. Pullmann, J. Ordi-Ros, G. D. Sebastiani, S. Ruzickova, M. Jose Santos, C. Papasteriades, M. Marchini, et al; European Consortium of SLE DNA Collections. 2009. Replication of recently identified systemic lupus erythematosus genetic associations: a case-control study. *Arthritis Res. Ther.* 11: R69.
15. Ban, M., A. Goris, A. R. Lorentzen, A. Baker, T. Mihalova, G. Ingram, D. R. Booth, R. N. Heard, G. J. Stewart, E. Bogaert, et al; Wellcome Trust Case-Control Consortium (WTCCC). 2009. Replication analysis identifies TYK2 as a multiple sclerosis susceptibility factor. *Eur. J. Hum. Genet.* 17: 1309–1313.
16. Couturier, N., F. Bucciarelli, R. N. Nurtdinov, M. Debouverie, C. Lebrun-Frenay, G. Defer, T. Moreau, C. Confavreux, S. Vukusic, I. Cournu-Rebeix, et al. 2011. Tyrosine kinase 2 variant influences T lymphocyte polarization and multiple sclerosis susceptibility. *Brain* 134: 693–703.
17. Dyment, D. A., M. Z. Cader, M. J. Chao, M. R. Lincoln, K. M. Morrison, G. Disanto, J. M. Morahan, G. C. De Luca, A. D. Sadovnick, P. Lepage, et al. 2012. Exome sequencing identifies a novel multiple sclerosis susceptibility variant in the TYK2 gene. *Neurology* 79: 406–411.
18. Johnson, B. A., J. Wang, E. M. Taylor, S. J. Caillier, J. Herbert, O. A. Khan, A. H. Cross, P. L. De Jager, P. A. Gourraud, B. C. Cree, et al. 2010. Multiple sclerosis susceptibility alleles in African Americans. *Genes Immun.* 11: 343–350.
19. Mero, I. L., A. R. Lorentzen, M. Ban, C. Smestad, E. G. Celius, J. H. Aarseth, K. M. Myhr, J. Link, J. Hillert, T. Olsson, et al. 2010. A rare variant of the TYK2 gene is confirmed to be associated with multiple sclerosis. *Eur. J. Hum. Genet.* 18: 502–504.
20. Franke, A., D. P. McGovern, J. C. Barrett, K. Wang, G. L. Radford-Smith, T. Ahmad, C. W. Lees, T. Balschun, J. Lee, R. Roberts, et al. 2010. Genome-wide meta-analysis increases to 71 the number of confirmed Crohn's disease susceptibility loci. *Nat. Genet.* 42: 1118–1125.
21. Sato, K., M. Shiota, S. Fukuda, E. Iwamoto, H. Machida, T. Inamine, S. Kondo, K. Yanagihara, H. Isomoto, Y. Mizuta, et al. 2009. Strong evidence of a combination polymorphism of the tyrosine kinase 2 gene and the signal transducer and activator of transcription 3 gene as a DNA-based biomarker for susceptibility to Crohn's disease in the Japanese population. *J. Clin. Immunol.* 29: 815–825.
22. Wang, K., H. Zhang, S. Kugathasan, V. Annese, J. P. Bradfield, R. K. Russell, P. M. Sleiman, M. Imielinski, J. Glessner, C. Hou, et al. 2009. Diverse genome-wide association studies associate the IL12/IL23 pathway with Crohn Disease. *Am. J. Hum. Genet.* 84: 399–405.
23. Strange, A., F. Capon, C. C. Spencer, J. Knight, M. E. Weale, M. H. Allen, A. Barton, G. Band, C. Bellenguez, J. G. Bergboer, et al; Genetic Analysis of Psoriasis Consortium & the Wellcome Trust Case Control Consortium 2. 2010. A genome-wide association study identifies new psoriasis susceptibility loci and an interaction between HLA-C and ERAP1. *Nat. Genet.* 42: 985–990.
24. Wallace, C., D. J. Smyth, M. Maisuria-Armer, N. M. Walker, J. A. Todd, and D. G. Clayton. 2010. The imprinted DLK1-MEG3 gene region on chromosome 14q32.2 alters susceptibility to type 1 diabetes. *Nat. Genet.* 42: 68–71.
25. Peluso, C., D. M. Christofolini, C. S. Goldman, F. A. Mafra, V. Cavalcanti, C. P. Barbosa, and B. Bianco. 2012. TYK2 rs34536443 polymorphism is associated with a decreased susceptibility to endometriosis-related infertility. *Hum. Immunol.* 74: 93-97.
26. Liu, J. Z., M. A. Almarri, D. J. Gaffney, G. F. Mells, L. Jostins, H. J. Cordell, S. J. Ducker, D. B. Day, M. A. Heneghan, J. M. Neuberger, et al; UK Primary Biliary Cirrhosis (PBC) Consortium; Wellcome Trust Case Control Consortium 3. 2012. Dense fine-mapping study identifies new susceptibility loci for primary biliary cirrhosis. *Nat. Genet.* 44: 1137–1141.

27. Kaminker, J. S., Y. Zhang, A. Waugh, P. M. Haverty, B. Peters, D. Sebisanovic, J. Stinson, W. F. Forrest, J. F. Bazan, S. Seshagiri, and Z. Zhang. 2007. Distinguishing cancer-associated missense mutations from common polymorphisms. *Cancer Res.* 67: 465–473.
28. Tomasson, M. H., Z. Xiang, R. Walgren, Y. Zhao, Y. Kasai, T. Miner, R. E. Ries, O. Lubman, D. H. Fremont, M. D. McLellan, et al. 2008. Somatic mutations and germline sequence variants in the expressed tyrosine kinase genes of patients with de novo acute myeloid leukemia. *Blood* 111: 4797–4808.
29. Velazquez, L., K. E. Mogensen, G. Barbieri, M. Fellous, G. Uzé, and S. Pellegrini. 1995. Distinct domains of the protein tyrosine kinase tyk2 required for binding of interferon-alpha/beta and for signal transduction. *J. Biol. Chem.* 270: 3327–3334.
30. Gauzzi, M. C., L. Velazquez, R. McKendry, K. E. Mogensen, M. Fellous, and S. Pellegrini. 1996. Interferon-alpha-dependent activation of Tyk2 requires phosphorylation of positive regulatory tyrosines by another kinase. *J. Biol. Chem.* 271: 20494–20500.
31. Richter, M. F., G. Duménil, G. Uzé, M. Fellous, and S. Pellegrini. 1998. Specific contribution of Tyk2 JH regions to the binding and the expression of the interferon alpha/beta receptor component IFNAR1. *J. Biol. Chem.* 273: 24723–24729.
32. Ragimbeau, J., E. Dondi, A. Alcover, P. Eid, G. Uzé, and S. Pellegrini. 2003. The tyrosine kinase Tyk2 controls IFNAR1 cell surface expression. *EMBO J.* 22: 537–547.
33. Gakovic, M., J. Ragimbeau, V. Francois, S. N. Constantinescu, and S. Pellegrini. 2008. The Stat3-activating Tyk2 V678F mutant does not up-regulate signaling through the type I interferon receptor but confers ligand hypersensitivity to a homodimeric receptor. *J. Biol. Chem.* 283: 18522–18529.
34. Marijanovic, Z., J. Ragimbeau, K. G. Kumar, S. Y. Fuchs, and S. Pellegrini. 2006. TYK2 activity promotes ligand-induced IFNAR1 proteolysis. *Biochem. J.* 397: 31–38.
35. Miyauchi, K., E. Urano, H. Yoshiyama, and J. Komano. 2011. Cytokine signatures of transformed B cells with distinct Epstein-Barr virus latencies as a potential diagnostic tool for B cell lymphoma. *Cancer Sci.* 102: 1236–1241.
36. Briscoe, J., N. C. Rogers, B. A. Witthuhn, D. Watling, A. G. Harpur, A. F. Wilks, G. R. Stark, J. N. Ihle, and I. M. Kerr. 1996. Kinase-negative mutants of JAK1 can sustain interferon-gamma-inducible gene expression but not an antiviral state. *EMBO J.* 15: 799–809.
37. Haan, S., C. Margue, A. Engrand, C. Rolvering, H. Schmitz-Van de Leur, P. C. Heinrich, I. Behrmann, and C. Haan. 2008. Dual role of the Jak1 FERM and kinase domains in cytokine receptor binding and in stimulation-dependent Jak activation. *J. Immunol.* 180: 998–1007.
38. Zhang, X., J. Gureasko, K. Shen, P. A. Cole, and J. Kuriyan. 2006. An allosteric mechanism for activation of the kinase domain of epidermal growth factor receptor. *Cell* 125: 1137–1149.
39. Haan, C., D. C. Kroy, S. Wüller, U. Sommer, T. Nöcker, C. Rolvering, I. Behrmann, P. C. Heinrich, and S. Haan. 2009. An unusual insertion in Jak2 is crucial for kinase activity and differentially affects cytokine responses. *J. Immunol.* 182: 2969–2977.
40. Cameron, A. J., C. Escribano, A. T. Saurin, B. Kostelecky, and P. J. Parker. 2009. PKC maturation is promoted by nucleotide pocket occupation independently of intrinsic kinase activity. *Nat. Struct. Mol. Biol.* 16: 624–630.
41. Kornev, A. P., S. S. Taylor, and L. F. Ten Eyck. 2008. A helix scaffold for the assembly of active protein kinases. *Proc. Natl. Acad. Sci. USA* 105: 14377–14382.
42. Chrencik, J. E., A. Patny, I. K. Leung, B. Korniski, T. L. Emmons, T. Hall, R. A. Weinberg, J. A. Gormley, J. M. Williams, J. E. Day, et al. 2010. Structural and thermodynamic characterization of the TYK2 and JAK3 kinase domains in complex with CP-690550 and CMP-6. *J. Mol. Biol.* 400: 413–433.
43. Haan, C., I. Behrmann, and S. Haan. 2010. Perspectives for the use of structural information and chemical genetics to develop inhibitors of Janus kinases. *J. Cell. Mol. Med.* 14: 504–527.
44. Tsui, V., P. Gibbons, M. Ultsch, K. Mortara, C. Chang, W. Blair, R. Pulk, M. Stanley, M. Starovasnik, D. Williams, et al. 2011. A new regulatory switch in a JAK protein kinase. *Proteins* 79: 393–401.
45. Andraos, R., Z. Qian, D. Bonenfant, J. Rubert, E. Vangrevelinghe, C. Scheufler, F. Marque, C. H. Régnier, A. De Pover, H. Ryckelynck, et al. 2012. Modulation of activation-loop phosphorylation by JAK inhibitors is binding mode dependent. *Cancer Discov* 2: 512–523.
46. Yeh, T. C., E. Dondi, G. Uze, and S. Pellegrini. 2000. A dual role for the kinase-like domain of the tyrosine kinase Tyk2 in interferon-alpha signaling. *Proc. Natl. Acad. Sci. USA* 97: 8991–8996.
47. Chen, M., A. Cheng, F. Candotti, Y. J. Zhou, A. Hymel, A. Fasth, L. D. Notarangelo, and J. J. O'Shea. 2000. Complex effects of naturally occurring mutations in the JAK3 pseudokinase domain: evidence for interactions between the kinase and pseudokinase domains. *Mol. Cell. Biol.* 20: 947–956.
48. Bandaranayake, R. M., D. Ungureanu, Y. Shan, D. E. Shaw, O. Silvennoinen, and S. R. Hubbard. 2012. Crystal structures of the JAK2 pseudokinase domain and the pathogenic mutant V617F. *Nat. Struct. Mol. Biol.* 19: 754–759.
49. Dusa, A., C. Mouton, C. Pecquet, M. Herman, and S. N. Constantinescu. 2010. JAK2 V617F constitutive activation requires JH2 residue F595: a pseudokinase domain target for specific inhibitors. *PLoS ONE* 5: e11157.
50. Yang, J., L. F. Ten Eyck, N. H. Xuong, and S. S. Taylor. 2004. Crystal structure of a cAMP-dependent protein kinase mutant at 1.26A: new insights into the catalytic mechanism. *J. Mol. Biol.* 336: 473–487.
51. Babon, J. J., N. J. Kershaw, J. M. Murphy, L. N. Varghese, A. Laktyushin, S. N. Young, I. S. Lucet, R. S. Norton, and N. A. Nicola. 2012. Suppression of cytokine signaling by SOCS3: characterization of the mode of inhibition and the basis of its specificity. *Immunity* 36: 239–250.
52. Gough, D. J., N. L. Messina, C. J. Clarke, R. W. Johnstone, and D. E. Levy. 2012. Constitutive type I interferon modulates homeostatic balance through tonic signaling. *Immunity* 36: 166–174.
53. Prchal-Murphy, M., C. Semper, C. Lassnig, B. Wallner, C. Gausterer, I. Teppner-Klymiuk, J. Kobolak, S. Müller, T. Kolbe, M. Karaghiosoff, et al. 2012. TYK2 kinase activity is required for functional type I interferon responses in vivo. *PLoS ONE* 7: e39141.
54. Kyogoku, C., A. Morinobu, K. Nishimura, D. Sugiyama, H. Hashimoto, Y. Tokano, T. Mimori, C. Terao, F. Matsuda, T. Kuno, and S. Kumagai. 2009. Lack of association between tyrosine kinase 2 (TYK2) gene polymorphisms and susceptibility to SLE in a Japanese population. *Mod. Rheumatol.* 19: 401–406.
55. Li, P., Y. K. Chang, K. W. Shek, and Y. L. Lau. 2011. Lack of association of TYK2 gene polymorphisms in Chinese patients with systemic lupus erythematosus. *J. Rheumatol.* 38: 177–178.
56. Eyre, S., J. Bowes, D. Diogo, A. Lee, A. Barton, P. Martin, A. Zhernakova, E. Stahl, S. Viatte, K. McAllister, et al. 2012. High-density genetic mapping identifies new susceptibility loci for rheumatoid arthritis. *Nat. Genet.* 44: 1336–1340.

Additional Results

Part I-1 Additional studies of rs12720356 (I684S) and rs34536443 (P1104A)

TYK2-I684S homozygosity has no impact on IFN, IL-10 and IL-23 signaling The level of activation of STAT proteins was compared in EBV-B cell lines from donors carrying TYK2 WT (TYK2-I684) or TYK2-I684S (TYK2-S684) (Fig. 1, page 83). Cells were stimulated with increasing doses of IFN-α, IL-10, or IL-23. We noticed an inter-individual variability in the basal level of TYK2 and STAT proteins. Taking this into account, we concluded that the levels of STAT1/2/3 phosphorylation in response to IFN-α (Fig. 1A), of STAT3 phosphorylation in response to IL-10 (Fig. 1B) and IL-23 (Fig. 1C) were not consistently different between control and homozygous TYK2-I684S carriers.

TYK2-P1104A homozygosity decreases IFN and IL-10 and abrogates IL-23 signaling. JAK/STAT activation was compared in EBV-B cell lines from two control healthy donors (TYK2-P1104) and two patients with TYK2-P1104A (TYK2-A1104) homozygosity (Fig. 2, page 84). Patients' cells were found to exhibit normal levels of IFNAR1, IL-10R2 and IL-12Rβ1 receptors at the cell surface (S. Boisson-Dupuis, pers. communic). Cells were stimulated with increasing doses of cytokines. In response to IFN-α, TYK2 and STAT1/2 phosphorylation were comparable in control and TYK2-P1104A cells, while STAT3 phosphorylation was modestly reduced in TYK2-P1104A cells (Fig. 2A, D). STAT3 phosphorylation in response to IL-10 was consistently reduced in TYK2-P1104A cells (Fig. 2B) and in response to IL-23 was not detectable (Fig. 2C).

Cytokine signaling in TYK2-/- EBV-B transduced with TYK2-P1104A

To exclude potential effects of other genetic variations on cytokine signaling in patients cells, our collaborator S. Boisson-Dupuis engineered TYK2-/- EBV-B cells retrovirally transduced with TYK2 WT or P1104A. Of note, the level of transduced TYK2-P1104A protein was lower than WT TYK2 (Fig. 3, page 85). Interestingly, in EBV-B cells from patients the level of (endogenous) TYK2-P1104A does not appear to be lower than in controls. When ectopically expressed, the difference in protein level between TYK2 WT and P1104A may be more evident, but the underlying mechanism is unclear. On that line, it was reported that kinase-inactive murine Tyk2-K923E has an extremely shortened half-life due to autophagosomal degradation and that the Tyk2 kinase activity is critical to prevent this degradation (Prchal-Murphy 2012). Compared to WT cells, in TYK2-P1104A cells STAT3 phosphorylation in response to IL-10 was reduced substantially. Remarkably, IL-23-induced STAT3 phosphorylation was abolished in TYK2-P1104A cells (Fig. 3). Of note, in WT cells

the activation of STAT3 in response to IL-23 was about 10 fold higher than in response to IL-10 (Fig. 3). This result suggests a selective impairing effect of TYK2P1104A on the IL-23 response.

Neither STAT3 nor STAT1 can be phosphorylated in vitro by TYK2-P1104A. The extent of phosphorylation of STAT1/2 in response to IFN-α was comparable in TYK2-P1104A- and TYK2 WT-expressing EBV-B cells (Fig. 2A and D). However, the phosphorylation of STAT3 in response to IL-23, and to a lesser extent IL-10 and IFN-α (Fig. 2D, Fig. 3), was strongly impaired in TYK2-P1104A EBV-B cells with respect to control cells. This difference may reflect an altered recognition by the TYK2 variant of STAT3 as substrate. In other words, TYK2-P1104A may be more specifically impaired in phosphorylating STAT3 than STAT1.

To address the above possibility, I compared the ability of TYK2-P1104A to phosphorylate *in vitro* recombinant STAT1 and STAT3 added as exogenous substrates. TYK2 was immunoprecipitated from TYK2-minus cells stably reconstituted with either TYK2 WT or TYK2-P1104A and subjected to *in vitro* kinase assay in the presence or absence of added ATP. RecSTAT1 or recSTAT3 was added to the reaction. The products of the reaction were analyzed by immunoblotting to Abs specific to the two activation loop tyrosines of TYK2 (Tyr1054-1055) and to phospho-STAT1 (Tyr701) or phospho-STAT3 Abs (Tyr705). As shown in Fig. 4 (A and B, lane 1, 2; page 86), when ATP was added to the reaction, the phospho-TYK2 WT band and phospho-STAT1 or STAT3 were detected, demonstrating basal TYK2 catalytic activity. No ATP-induced band was instead detected for TYK2-P1104A, indicating impaired kinase activity as shown in Fig. 4 (A and B, lane 5 and 6).

We similarly assessed cytokine-induced activity of TYK2 by pulsing cells with IFN-β (Fig. 4A, lanes 3, 4 and 7, 8) or IFN-α (Fig. 4B, lanes 3, 4 and 7, 8). Upon addition of ATP to the reaction, a 2 to 4-fold increase in phospho-TYK2 were observed in IFN-treated WT cells (Fig. 4A and B, lanes 3, 4) but not in P1104A cells (Fig. 4A and B, lanes 7, 8). Importantly, ATP-dependent phosphorylation of the two recSTATs substrates was detected with TYK2 WT, but not with TYK2-P1104A. In conclusion, both the basal and the IFNα/β-induced auto-phosphorylation activity of the P1104A variant are impaired. Substrate-phosphorylation activity of the variant is impaired as well, with no difference between STAT1 and STAT3.

Overall, these data suggest that the impaired activation of STAT3 in response to IL-23 in TYK2-P1104A-expressing cells does not relate to an intrinsic defect to phosphorylate STAT3.

Rather, the molecular features of the IL-23 receptor and particularly the precise positioning and role of TYK2 *vs* JAK2 within this receptor/JAK complex may compromise STAT3 phosphorylation in TYK2-P1104A-expressing cells.

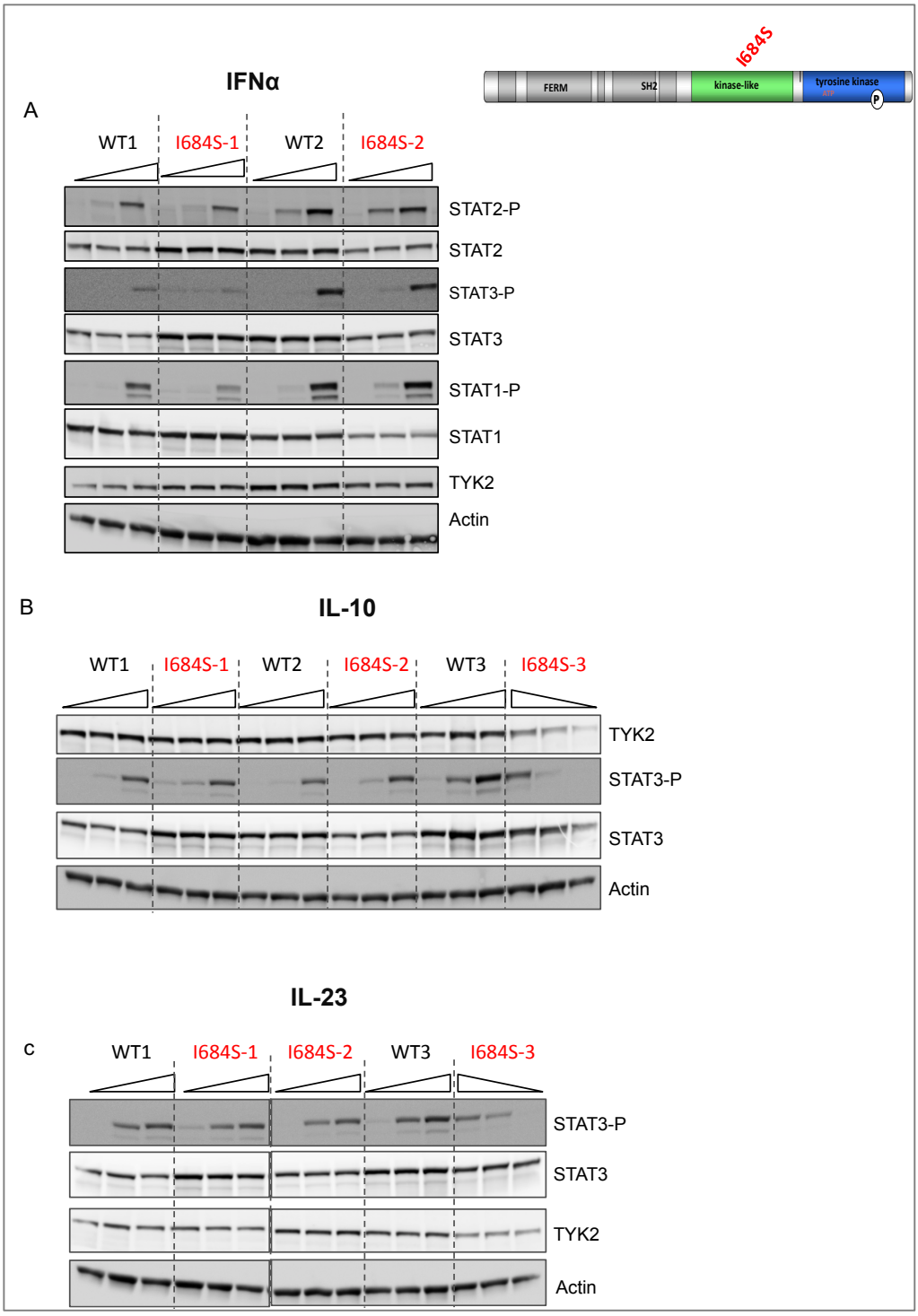

Figure 1. IFN-α, IL-10 and IL-23-induced JAK/STAT activation in EBV-B cells from donors carrying homozygote TYK2 WT or TYK2-I684S. EBV-B cells were treated with increasing doses of (A) IFN-a (0, 10, 100 pM), (B) IL-10 (0, 10, 100 ng/ml) or (C) IL-23 (0, 10, 100 ng/ml) for 15 min**,** (IFN-α**,** IL-10) or 30 min (IL-23). The level of tyrosine-phosphorylated TYK2, STAT1, STAT2 and STAT3 was analyzed by western blot with phospho-specific Abs. The membrane was reprobed for TYK2 and total Stats levels. Actin levels shown as loading control.

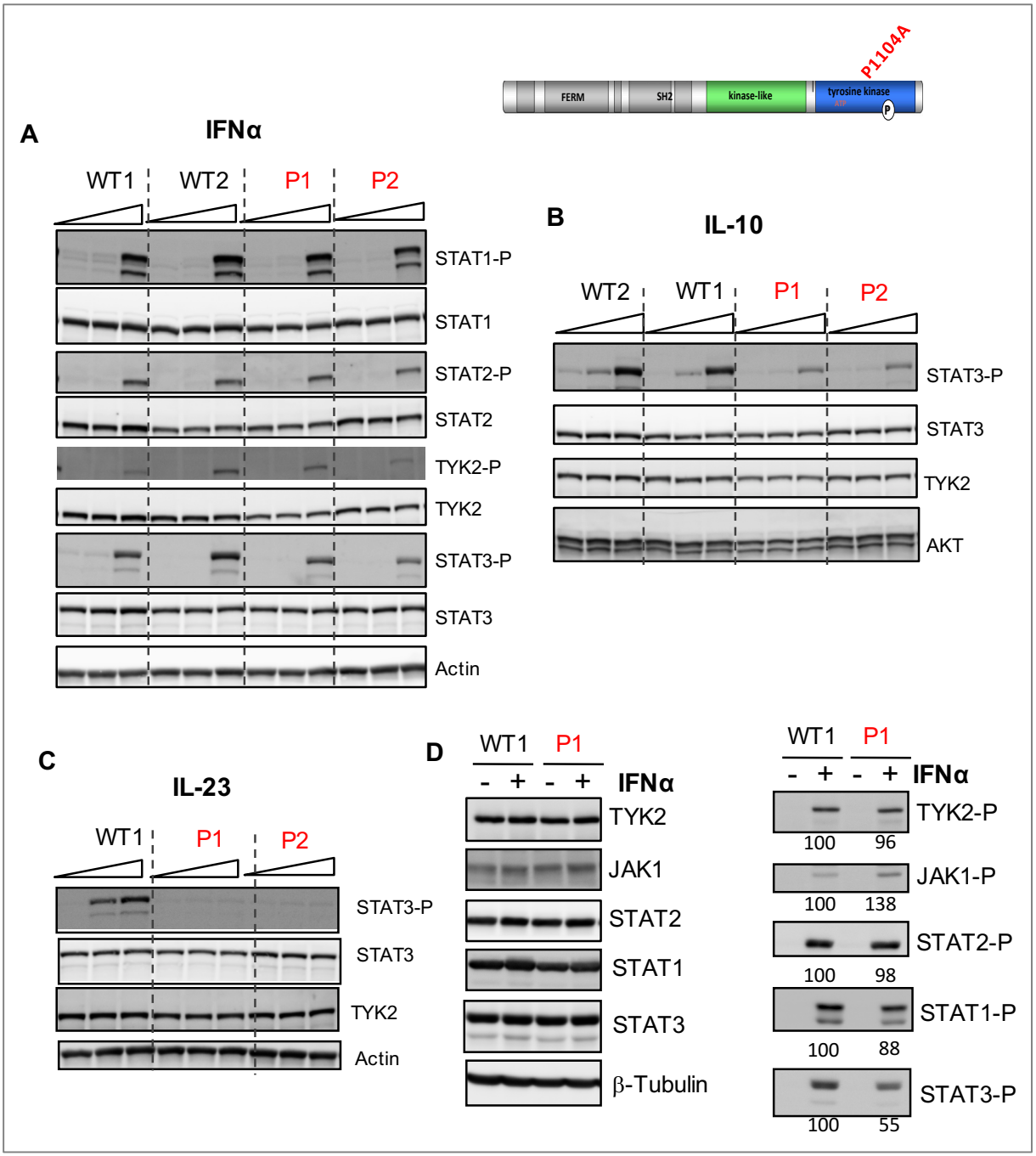

Figure 2. IFN-α, IL-10 and IL-23-induced JAK/STAT activation in EBV-B cells from two healthy donors carrying homozygote TYK2 WT or from two primary immune deficient patients (P1 and P2) carrying TYK2-P1104A. Cells were treated with increasing doses of (A) IFN-α (0, 10, 100 pM) or (B) IL-10 (0, 10, 100 ng/ml) or (C) IL-23 (0, 10, 100 ng/ml) for 15min (IFN-α, IL-10) or 30 min (IL-23). The level of tyrosine-phosphorylated TYK2, STAT1/2/3 was analyzed by western blot with phospho-specific Abs. The membrane was reprobed for TYK2 and total STAT levels. Actin or Akt levels shown as loading control. (D) Quantitative analysis of JAK/STAT activation in response to IFN-α (500 pM, 15min) in EBV-B cells from a healthy donor carrying TYK2 WT or from a patient carrying TYK2-P1104A (P1 in red). Left panels: total protein levels. Right panels: analysis of phosphorylated proteins. The intensity of the phosphorylated band was normalized by the corresponding total protein level and that of WT was taken as 100.

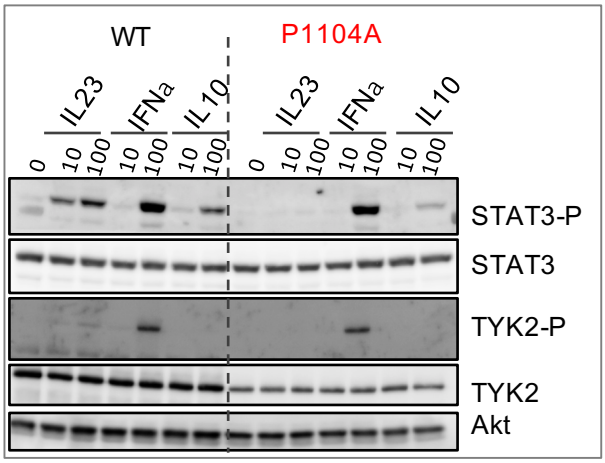

Figure 3. IL-23, IFN and IL-10 signaling in TYK2-/- EBV-B transduced with TYK2 WT or P1104A. EBV-B cells derived from a TYK2-deficient patient were retrovirally transduced with a vector encoding WT or P1104A. Phosphorylation of STAT3 and TYK2 after stimulation with increasing doses of IL-23 (ng/ml), IFN-α (pM) and IL-10 (ng/ml) for 30 min was determined by western blot using specific antibodies recognizing phospho-TYK2 or phospho-STAT3. The membrane was reprobed for TYK2 and STAT levels. Akt level is shown as loading control.

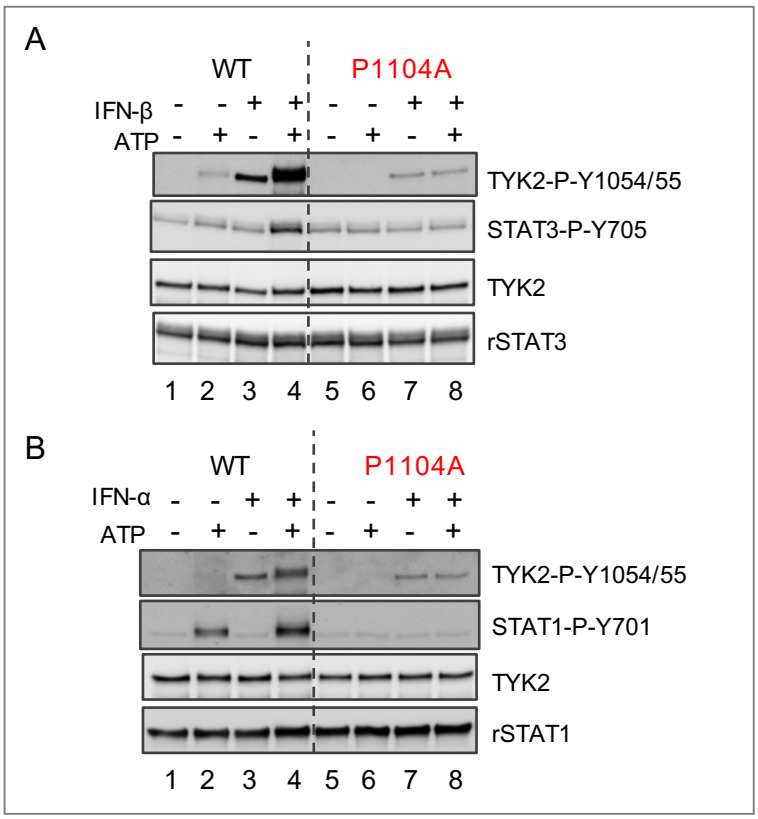

Figure 4. Basal and IFN-induced *in vitro* kinase activity of TYK2-P1104A, using recombinant STAT3 (A) or STAT1(B) as substrate. TYK2 was immunoprecipitated (IP) from 11.1 cells stably expressing TYK2 WT or P1104A and stimulated with IFN (500 pM, 15 min) and subjected to an *in vitro* kinase reaction for 5 min at 30°C in the presence (+) or absence (-) of 30 μM of ATP. Phosphorylated proteins in the reaction were revealed by immunoblotting with anti-phospho-TYK2 and phospho-STAT3 or phospho-STAT1. The membrane was reprobed for TYK2 and STAT levels.

Part I-2. Functional impact of rs2304256 (V362F) and rs12720270

In the European population, the TYK2 variants rs12720270 and rs2304256 are in linkage disequilibrium (r2=0.50, 1000 genomes database). Rs12720270 has been associated with protection from SLE in UK families (98) and in Finnish population (103). As shown in Table 2 (Introduction), its minor allele frequency (MAF) ranges from 4% in Africans to 46% in Asians (1000 genomes Project). Rs12720270 is an intronic SNP, which is located 36 bp upstream of the intron 7/Exon 8 boundary (Fig. 2A) and may therefore influence splicing of Exon 8. Indeed, the analysis of intron 7 with the software HSF (human splicing finder) predicts that the G (ancestral) to A (derived) nucleotide substitution may mildly (-4.78%) decrease the value of a potential branch point (181).

Rs2304256 has been associated to protection against autoimmune diseases, such as SLE, psoriasis and type I diabetes in Caucasian populations (see Table 2 in Introduction). Rs2304256 maps in Exon 8 and causes a valine (V) to phenylalanine (F) substitution at position 362 in the FERM domain of TYK2. This valine residue is *not* conserved in JAK proteins or in TYK2 of other species. Hence, this substitution is unlikely to impact TYK2 function. Accordingly, our functional studies in fibroblasts showed that TYK2 V362F behaves as wild type in terms of stability, catalytic activity and ability to rescue type I IFN signaling (data not shown).

Interestingly, rs2304256 is located 75 bp downstream of the intron 7/Exon 8 boundary (Fig. 2A). Close software-assisted analysis of Exon 8 sequence predicts that the C (ancestral) to A (derived) nucleotide substitution could destroy a putative Exon splice silencer (ESS) or a putative Exon splice enhancer (ESE) recognized by the arginine- and serine-rich protein ASF/SF2 (181), therefore this SNP may impact splicing of Exon 8.

Based on the above data, I hypothesized that rs12720270 and rs2304256, alone or in combination, may influence splicing of Exon 8. My working hypothesis was assessed experimentally as described below.

Results

AA homozygosity at rs2304256 or rs12720270 correlates with absence of the ΔE8 transcript

A survey of the e-Ensembl gene database reveals the existence of a partial *TYK2* transcript lacking Exon 8 (*TYK2 ΔE8*). We succeeded in amplifying from cDNA of EBV-B cells a

partial *TYK2 ΔE8* transcript which is weakly expressed with respect to the full-length transcript. As shown in Fig. 1 (page 91, RT-PCR on EBV-B cells RNA, using primers in Exon 7 and Exon 9, amplified the expected 743nt product and a minor product of 545nt. Sequencing confirmed that the smaller band lacks Exon 8 of 198nt and retains the original open reading frame. The presence of this *ΔE8* transcript was assessed in EBV-B cell lines derived from 30 individuals genotyped for rs12720270 and rs2304256. These cell lines were obtained from Coriell Cell Repositories (n=22) and Genethon (n=8). A perfect correlation was found between absence of the *ΔE8* transcript and AA homozygosity at rs2304256. Cells (n=11) homozygous for the derived A allele (AA) of rs2304256 lacked the *ΔE8* transcript (Table 1, page 91), which indicates that the C to A substitution of rs2304256 promotes retention of Exon 8, possibly due to loss of an exon splice silencer site.

AA homozygosity at rs12720270 (n=3, of which two are combined with AA homozygosity at rs2304256) showed the same tendency, suggesting that G to A substitution of rs12720270 strengthens a potential branch point promoting retention of Exon 8. Overall, these analyses indicated that the derived A allele (AA) of rs2304256 or rs12720270 promotes the retention of Exon 8.

AA homozygosity at rs2304256 or rs12720270 promotes retention of Exon 8 in a minigene assay

To further verify that the two TYK2 allelic variants affect splicing efficiency, we used the minigene assay. One of the advantage of this approach is that it allows to exclude potential influence of other TYK2 polymorphisms on mRNA abundance and/or splicing (95; 96). Usign the pI-12 splicing vector we generated a minigene construct spanning the 1.2kb *TYK2* genomic region from Exon 7 to Exon 9, comprising rs12720270 and rs2304256 (Fig. 2A, page 92). The different alleles combinations were introduced by site-directed mutagenesis (Fig. 2B, page 92). These minigenes were transfected into 293 cells, RNA was isolated and cDNAs synthesized. Splicing events were analysed by PCR using T7 and Sp6 primers specific to the minigene. Three major amplification products were obtained and sequenced (Fig. 2B). The 720nt band contains Exon 7 and Exon 8. The 520nt band contains Exon 7 only. The 210nt band contains splicing donor and acceptor sites only. We then compared the transcripts profiles expressed from the four minigenes. It was evident that, for each SNPs, the presence of the minor allele A led to more abundant levels of the transcript retaining Exon 8

(Exon 8-positive) (Fig. 2B). Moreover, the minigene carrying the minor alleles A for both SNPs was expressed almost exclusively as Exon 8-positive transcript.

Overall, these data indicated that the derived A alleles of rs2304256 and rs12720270 promote the retention of Exon 8 and synergize with each other. It has been described that small changes in the relative abundance of splice variants and the proteins they encode can have a significant biological impact (182). Thus, rs2304256 and rs12720270 appear to affect the fine balance of isoforms produced by alternative Exon 8 splicing.

TYK2-ΔE8 is catalytic competent but unable to rescue signaling or sustain IFNAR1

To study the impact of Exon 8 on protein function, a *TYK2* cDNA lacking Exon 8 (TYK2 ΔE8, lacking aa 338-403) was engineered in the pRc-CMV vector and transfected into TYK2-null human fibrosarcoma cells (11,1). Stable neoR clones were chosen for functional studies. We first compared the auto-phosphorylation activity of TYK2 WT and TYK2 ΔE8. For this, each protein was immunoprecipitated and subjected to *in vitro* kinase assay in the presence or absence of added ATP. The reaction product was analyzed by immunoblotting to phospho-TYK2 Abs specific to Tyr1054-1055 in the activation loop. As shown in Fig. 3A (page 93), when ATP was added to the reaction, the intensity of the phospho-TYK2 reactive band strongly increased in both samples, indicating activity.

Next, we compared the level of STAT activation in cells pulsed with non saturating doses of IFN-β for 15 min. As shown in Fig. 3B, TYK2, STAT1, STAT2 and STAT3 were phosphorylated in a dose-dependent manner in TYK2 WT-expressing clones stimulated with IFN-β. No activation of TYK2 or STATs was detected in ΔE8-expressing clones. Interestingly, the level of IFNAR1 in TYK2-ΔE8 clones was as low as in 11,1 cells (Fig. 3C), indicating that TYK2-ΔE8 is unable to rescue IFNAR1(48). To confirm this finding, we compared the interaction of TYK2 FERM-SH2 (aa 1-591) and a ΔE8 version with IFNAR1cyt *in vitro,* as described in ((180). Bacterially expressed WT and ΔE8 proteins were purified on Ni^2-NTA-agarose beads, eluted and incubated with GST-IFNAR1cyt purified on glutathione-Sepharose beads. The complex retained on Sepharose beads was analyzed by immunoblot with anti-TYK2 and anti-GST Abs. As shown in Fig. 3D, the WT protein, but not the ΔE8 mutant, was retained on GST-IFNAR1cyt. Altogether, these data indicate that the Exon 8-encoded segment is critical for the TYK2/IFNAR1 complex.

The same mutation in TYK2 may have different impact on distinct cytokine receptor complexes, as shown for TYK2-P1104A. We therefore asked whether TYK2-ΔE8 can mediate IL-12 signaling. The WT and ΔE8 constructs were transiently transfected in TYK2-null cells stably expressing the two chains of the IL-12R. As show in Fig. 3E, as opposed to WT TYK2, TYK2-ΔE8 failed to rescue IL-12 signaling. Of note, the WT TYK2-expressing cells responded poorly to IFN, likely due to high ectopic expression of IL-12Rβ1 - another TYK2-binding receptor - and limited TYK2 availability to sustain endogenous IFNAR1 (183).

We also tested whether TYK2-ΔE8 exerts a dominant-negative (DN) effect on IFN signaling. TYK2-ΔE8 and the so-called triple mutant (TYK2 K930R/YYFF1054,55) with known DN effect were overexpressed in parallel in 293T cells and signaling was monitored. As shown in Fig. 3F, compared with an empty vector, the triple mutant led to a decrease in the phosphorylation of endogenous TYK2, STAT1 and STAT2, indicating a DN effect. Overexpressed TYK2-ΔE8 had no such effect, most likely because, not being able to bind to IFNAR1, it cannot compete out endogenous TYK2.

We were unable to detect by western blot endogenous TYK2-ΔE8 in a variety of cell types including PBMCs, suggesting an extremely low level of expression with respect to the full-length TYK2. Interestingly, in a published eQTL loci database (GTEx Consortium, 2015) we found that the minor allele of rs2304256 is associated with increased *TYK2* transcript level in some tissues, such as adrenal gland, adipose, liver, basal ganglia, whole blood cells, skin especially sun-exposed skin, mammary tissues, but not in others (pancreas, spleen, muscle, colon, brain except basal ganglia, EBV-B, transformed fibroblasts etc). Thus, it is tempting to speculate that the increased full-length *TYK2* expression is consequent to more efficient retention of Exon 8 and influences disease pathogenesis. I will discuss this possibility in the last chapter "Discussion and perspectives".

Table 1 Homozygous minor alleles at rs2304256 or rs12720270 and Exon 8 retention

Genotyped EBV-B	550nt band	Rs2304256 (V362F)	Rs12720270 intronic
50044	+	CC	GG
GM07056	+	CC	GG
GM10854	+	CC	GG
GM10846	+	CC	GG
GM10857	+	CC	GG
GM10851	+	CC	GG
GM11830	+	CC	GG
GM12004	+	CC	GG
GM12282	+	CC	GG
GM10836	+	CA	GG
GM10859	+	CA	GG
GM10864	+	CA	GG
51814	+	CA	GG
GM12145	+	CA	GG
GM11918	+	CA	GA
GM10835	+	CA	GA
GM12144	+	CA	GA
52173	+	CA	GA
GM12249	−	CA	AA
34702	−	AA	GG
GM12275	−	AA	GG
50772	−	AA	GG
51464	−	AA	GG
GM11882	−	AA	GG
52279	−	AA	GA
49888	−	AA	GA
GM07037	−	AA	GA
GM12154	−	AA	GA
GM12342	−	AA	AA
GM12234	−	AA	AA

(−) *retention of Exon 8*

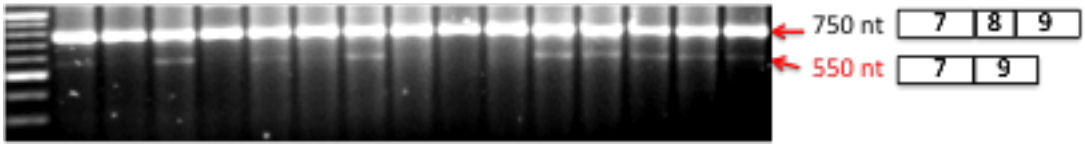

Fig. 1 Detection of *TYK2* transcripts in EBV-B cell lines from genotyped individuals.
RT-PCR (25 cycles) products from 5 ng of RNA from EBV-B cells was loaded on 2% agarose gel, stained by ethidium bromide and visualized under UV light.

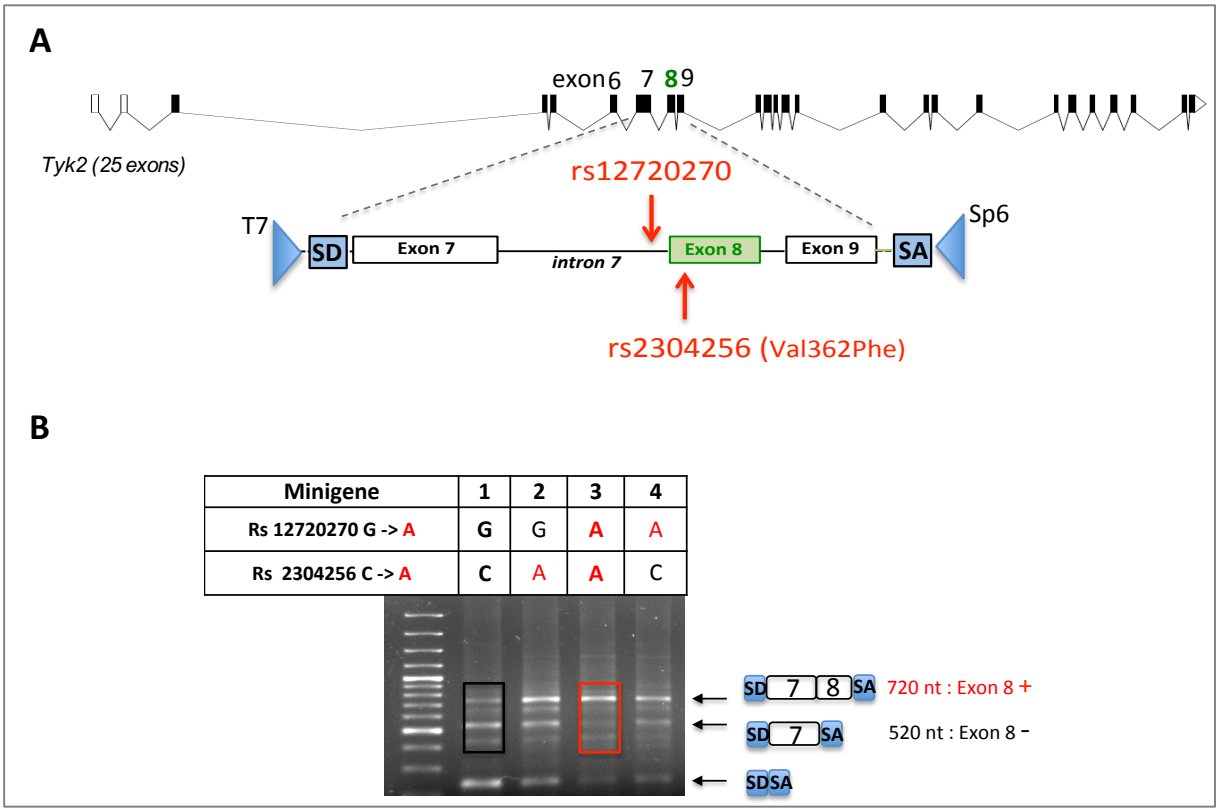

Fig. 2 Rs12720270 and rs2304256 influence Exon 8 splicing

(A) Schematic representation of the *TYK2* gene intron-exon structure and of the sequence inserted in PI-12 vector to obtain the minigene. Splicing donor site (SD) and splicing acceptor site (SA) in the vector are in blue. Exon 8 in green. Position of rs12720270 and rs2304256 are indicated by arrows. (B) Detection of minigene transcripts. the RT-PCR (25 cycles) product from 5 ng of RNA of 293T cells transiently transfected with each minigene was loaded on 2% agarose gel, stained by ethidium bromide and visualized under UV light.

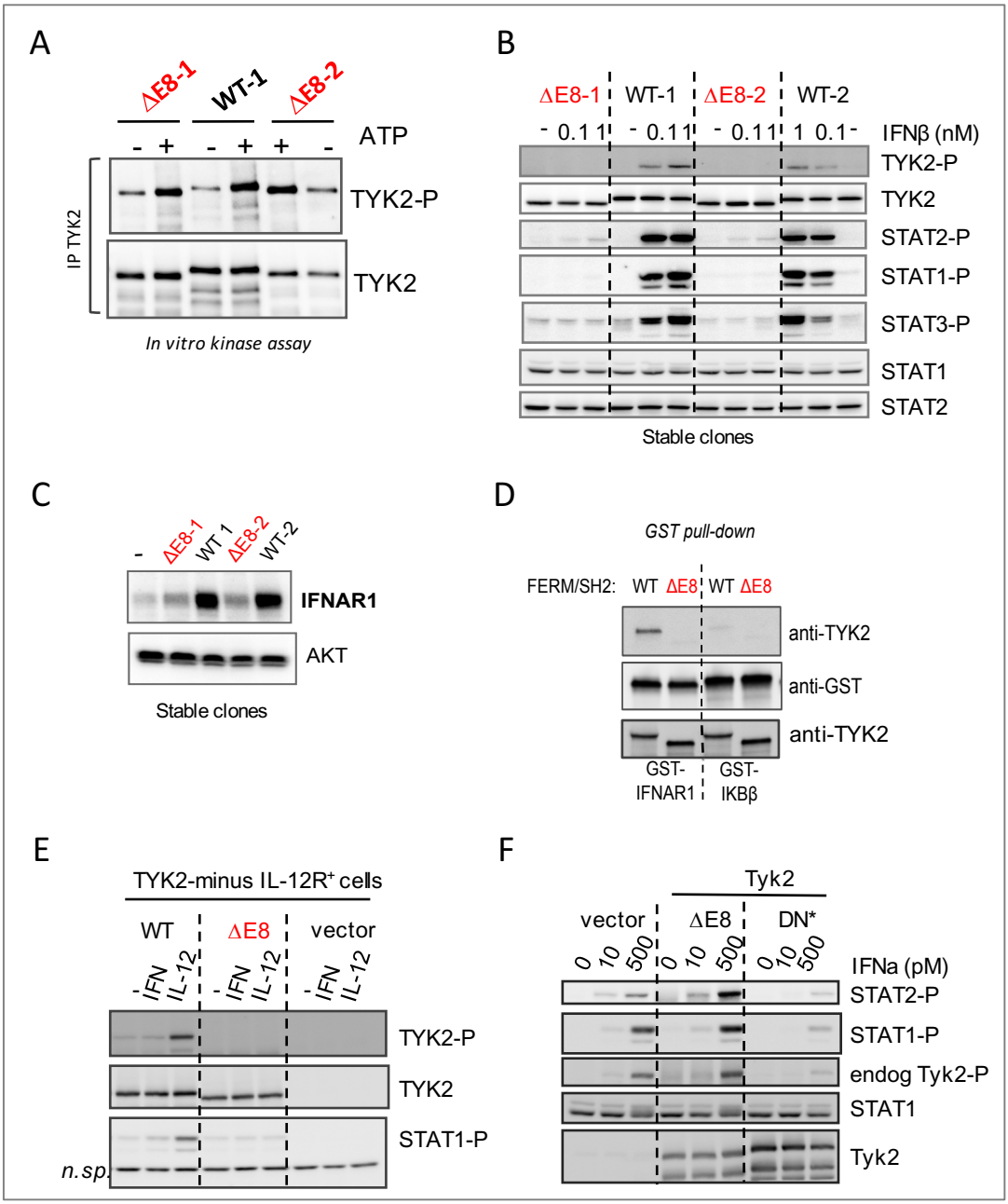

Figure 3. TYK2-ΔE8 is catalytically active but unable to rescue IFN signaling, sustain IFNAR1 or rescue IL-12 signaling.

(A) Basal *in vitro* kinase (IVK) activity of TYK2 from unstimulated 11.1 cells stably expressing TYK2 WT or TYK2-ΔE8. TYK2 was immunoprecipitated and subjected to an in vitro kinase reaction for 5 min at 30°C in the presence (+) or absence (-) of 30 µM ATP. Phosphorylated TYK2 in the reaction was revealed by immunoblotting with anti–phospho-TYK2. The membrane was reprobed for TYK2.

(B) IFN-induced JAK/STAT activation in 11.1 cells stably expressing TYK2 WT or TYK2-ΔE8. Cells were treated with increasing doses of IFN-β (0, 0.1, 1nM) for 15 min. The level of tyrosine-phosphorylated TYK2, STAT1, STAT2 and STAT3 was analyzed by western blot with phospho-specific Abs. The membrane was reprobed for TYK2 and total STATs.

(C) Total IFNAR1 level in 11.1 cells stably expressing TYK2 WT or TYK2-ΔE8.

(D) *In vitro* interaction of His-TYK2-FERM-SH2 with GST-IFNAR1cyt. His-TYK2-FERM-SH2 WT or ΔE8 were incubated with a GST fusion protein containing the cytoplasmic domain of IFNAR1(IFNAR1*cyt*) or IkBβ. Proteins bound to glutathione-Sepharose beads were separated on SDS-PAGE and visualized by anti-TYK2 antibody. 5% input TYK2 protein was shown on the bottom.

(E) IL-12-induced JAK/STAT activation in 11.1 cells stably expressing ectopic IL-12 receptors. Cells were transiently transfected with TYK2 WT or TYK2-ΔE8. Twenty-four hrs later, cells were treated with IFN-β (500 pM) or IL-12 (20 ng/ml) for 15 min. The level of tyrosine-phosphorylated TYK2, STAT1 was analyzed by western blot with phospho-specific Abs. The membrane was reprobed for TYK2 levels. A nonspecific band shown as loading control.

(F) 293T cells were transfected with empty vector, TYK2-ΔE8 or a dominant-negative control mutant TYK2K930R-YYFF1044,55 (DN). Twenty-four hrs later, cells were treated with increasing doses of IFN-a for 15 min. Phosphorylation of STAT1/2 and TYK2 were analyzed by western blot with phospho-specific Abs. The membrane was reprobed for TYK2 and STAT1.

Part I-3. Functional study of the TYK2 FERM domain

The structure of the FERM and SH2 domains of TYK2 complexed with an IFNAR1cyt peptide has been solved (2) (Figure 7 in Introduction). In this structure the Exon 8-encoded segment does not contact IFNAR1. However, as described above, we found that deletion of the Exon 8-encoded segment impairs TYK2 binding to receptors, suggesting that this region is required to maintain proper structural arrangement for receptor binding. Exon 8 encodes a 66 aa-long peptide (aa338-403, Fig.1 in Introduction) which is likely exposed at the surface of the F3 lobe of the FERM and spans from the β3β4 loop to β6 (Fig. 1A, Page 99) (2). The large disordered β3-β4 loop is unique to TYK2 (2). It is a 44 aa-long loop (aa330-364) containing a basic patch (aa354-360, KKAKAHK) which likely forms an interaction surface. Since the F3 lobe has the topology of a pleckstrin homology (PH) domain, this loop with its basic patch may target TYK2 to phospholipid-rich membranes independently of cytokine receptors. Alternatively, the loop may provide contact points to reinforce binding to receptors. Interestingly, another loop between the β1and β2 strands (aa 283-312, Fig.1 in Introduction) is longer in TYK2 than in other JAKs (30aa in TYK2, 19aa in JAK1 and 8aa in JAK2). Recently, I started investigating whether these loops (β3β4 loop and β1β2 loop), play a role in TYK2-mediated cytokine signaling.

Results

The basic patch in the β3-β4 loop of the F3 lobe is required for autophosphorylation but dispensable for cytokine signaling

To study the role of the β3-β4 loop of the F3 lobe, I substituted the KKAKAHK basic patch present in this loop with AAAAAHA and engineered the TYK2-4K4A mutant. I also deleted the unstructured segment (dashed lines in Fig. 1A) of the β1β2 loop and of the β3β4 loop in the F3 lobe (TYK2-Δβ1β2, TYK2-Δβ3β4). I overexpressed these mutants in 293T cells and measured their autophosphorylation and the phosphorylation of endogenous STAT3 (Fig. 1B). TYK2-Δβ1β2 (lacking aa 296-308) behaved as TYK2 WT. Conversely TYK2-ΔE8 (lacking aa 338-403) and TYK2-Δβ3β4 (lacking aa338-370) did not autophosphorylate, while TYK2-4K4A mutant displayed only a modest decrease in autophosphorylation. Of note, the kinase-inactive TYK2-K930R, used as control, was impaired in both autophosphorylation and phosphorylation of endogenous STAT3 (Fig. 1B, page 99). In contrast, the three mutants

(TYK2-4K4A, -Δβ3β4 and -ΔE8) were competent in STAT3 phosphorylation, which suggests that their kinase activity is intact. The autophosphorylation impairment of TYK2-Δβ3β4, TYK2-ΔE8 and TYK2-4K4A may be due to inefficient clustering.

Next, I measured IFN signaling in a 11.1-derived clone stably expressing TYK2-4K4A. Unlike TYK2-ΔE8, TYK2-4K4A rescued IFNAR1 and IFN signaling as well as WT (Fig. 1C). Similar results were obtained in 11.1 cells transiently expressing TYK2-Δβ1β2 or TYK2-Δβ3β4 (data not shown). To analyze IL-12 signaling, I transiently transfected TYK2-Δβ1β2 and TYK2-Δβ3β4 in 11.1 cells stably expressing the two IL-12R chains. Unlike TYK2-ΔE8, TYK2-Δβ1β2 and TYK2-Δβ3β4 rescued IL-12 signaling as well as WT (Fig. 1D). These results suggest that the unstructured fragments (32aa) within the β3β4 loop, including the basic patch (KKAKAHK), is dispensable for receptor binding (shown by rescued cytokine signaling), but mediates TYK2 clustering probably by targeting TYK2 to membrane.

The basic region in the F2 lobe is critical for sustaining receptor level

In parallel, I studied another basic patch comprised of 15 positively charged residues which is on the exposed α2', α2'', α3 helix of the F2 lobe and on the opposite side of the putative Box1 binding site of TYK2 (Fig. 2D). The Pellegrini's group previously reported that Ala substitutions of these basic residues abrogate nuclear localization of ectopically expressed TYK2 (42). These data were revisited in view of recent evidence showing that a corresponding basic patch in the FERM domain of the non-receptor tyrosine kinase FAK is involved in PI(4,5)P binding and in nuclear localization (40). I focused on three mutants: TYK2-3RA (Ala substitution of 3 Arg in the α3 helix, R231/3/5), TYK2-2RA (Ala substitution of 2 Arg in α2'' helix, R220/221) and TYK2 Δ219-240 (deletion of the α2'' helix and half of the α3 helix). The kinase activity of these mutants was considered intact as measured by STAT3 phosphorylation upon their overexpression in 293T cells (data not shown).

TYK2-3RA, -2RA and Δ219-240 were transiently transfected in TYK2-deficient cells stably expressing the two chains of the IL-12 receptors (Fig. 2A, page 101). In response to IL-12, STAT1 phosphorylation was abolished in cells expressing Δ219-240, suggesting no TYK2 binding to the receptor. TYK2-2RA and 3RA mutants mediated STAT1 phosphorylation as well as the WT protein. Surprisingly, phosphorylation of TYK2-3RA was strongly impaired in response to IL-12. Notably, in these cells, the two IL-12R chains are constitutively

expressed. The impaired TYK2 activation and the intact STAT1 activation in TYK2-3RA cells may reflect an impaired but not abolished TYK2/IL-12Rβ1 interaction.

I measured response to IFN in clones stably expressing the TYK2-3RA mutant. These cells exhibited reduced IFN response, as shown by STAT1/2/3 phosphorylation, with TYK2 phosphorylation being most affected (Fig. 2B). This impaired signaling is mostly due to the low level of IFNAR1 in TYK2-3RA cells (Fig. 2C). The three Arg residues are localised on the opposite side of the IFNAR1 binding surface and their Ala substitution is not expected to alter the α3 helix structure. However, the strong impairment of the TYK2-3RA mutant in scaffolding IFNAR1 suggests an interaction via the positively charged patch that could protect IFNAR1 from degradation. I postulate that this positively charged region may target TYK2 to a phospholipid-rich membrane and/or reinforce TYK2/IFNAR1 binding.

The TYK2 FERM domain binds to PI(3)P

Whether TYK2 or other JAKs bind to phospholipids of the plasma membrane or intracellular membranes is not known. To start addressing this question, His tagged FERM-SH2 and FERM-SH2-ΔE8 proteins were purified from *E. coli* and tested for binding to commercial membrane strips spotted with 15 different phospholipids (Fig. 3B, page 103). Binding was revealed by immunoblot with anti-TYK2 Abs. The FERM-SH2 protein, *ie* the entire N-terminal region, showed strong and specific binding to PI(3)P, while the ΔE8 mutant did not bind to any phospholipid (Fig. 3A and C, right stripes).

Interestingly, the FERM domain alone (aa 1-451) was able to bind to PI(3)P (Fig. 3A, left), suggesting that the SH2 domain is not required. Hence, I introduced the Δβ3β4 deletion (including the KKAKAHK basic patch) and the 3RA substitutions in the FERM to study if these basic patches on the F2 and F3 lobes, respectively, play a role in lipid binding. Both the alanine substitution (3RA) in the F2 lobe and the Δβ3β4 deletion in the F3 lobe reduced modestly PI(3)P binding, suggesting the involvement of both positively charged patches in PI(3)P binding.

As stated above, in the Wallweber structure of TYK2 FERM-SH2 complexed with IFNAR1cyt (2), the Exon 8-encoded segment does not contact IFNAR1. However, deletion of this segment impaired binding to receptors (IFNAR1) and to PI(3)P. These data suggest that the Exon 8-encoded segment is critical to the functional integrity of the FERM-SH2. As opposed to Exon 8 deletion, mutations within the Exon 8 segment (4K4A and Δβ3β4) rescued

cytokine signaling, suggesting functional global protein conformation. As shown above, these mutations impaired auto-phosphorylation and PI(3)P binding, suggesting a role of the β3-β4 loop in targeting TYK2 to the membrane.

In the Wallweber structure (2), the F2 lobe does not contact the short IFNAR*cyt* peptide. However, we found that deletion of aa 219-240 abrogates signaling. Thus, the F2 helical fold may be required to bind box1 motifs of cognate receptors, as was shown in the JAK1 FERM-SH2 complexed with IFNLR1cyt (36). Mutations in the Arg-rich patch on the F2 lobe (3RA) partially impairs IFNAR1 scaffolding and IFN signaling, suggesting that this surface contributes to maintain TYK2 in association to cognate receptors and/or binding to membrane lipids.

Although PIP stripe binding is a highly sensitive method, more quantitative approaches, such as surface plasmon resonance or isothermal titration calorimetry, and imaging studies should be used to determine properties and physiological relevance of this lipid binding. I will discuss the possible relevance of TYK2/PI(3)P binding in the "Discussion and perspectives" chapter.

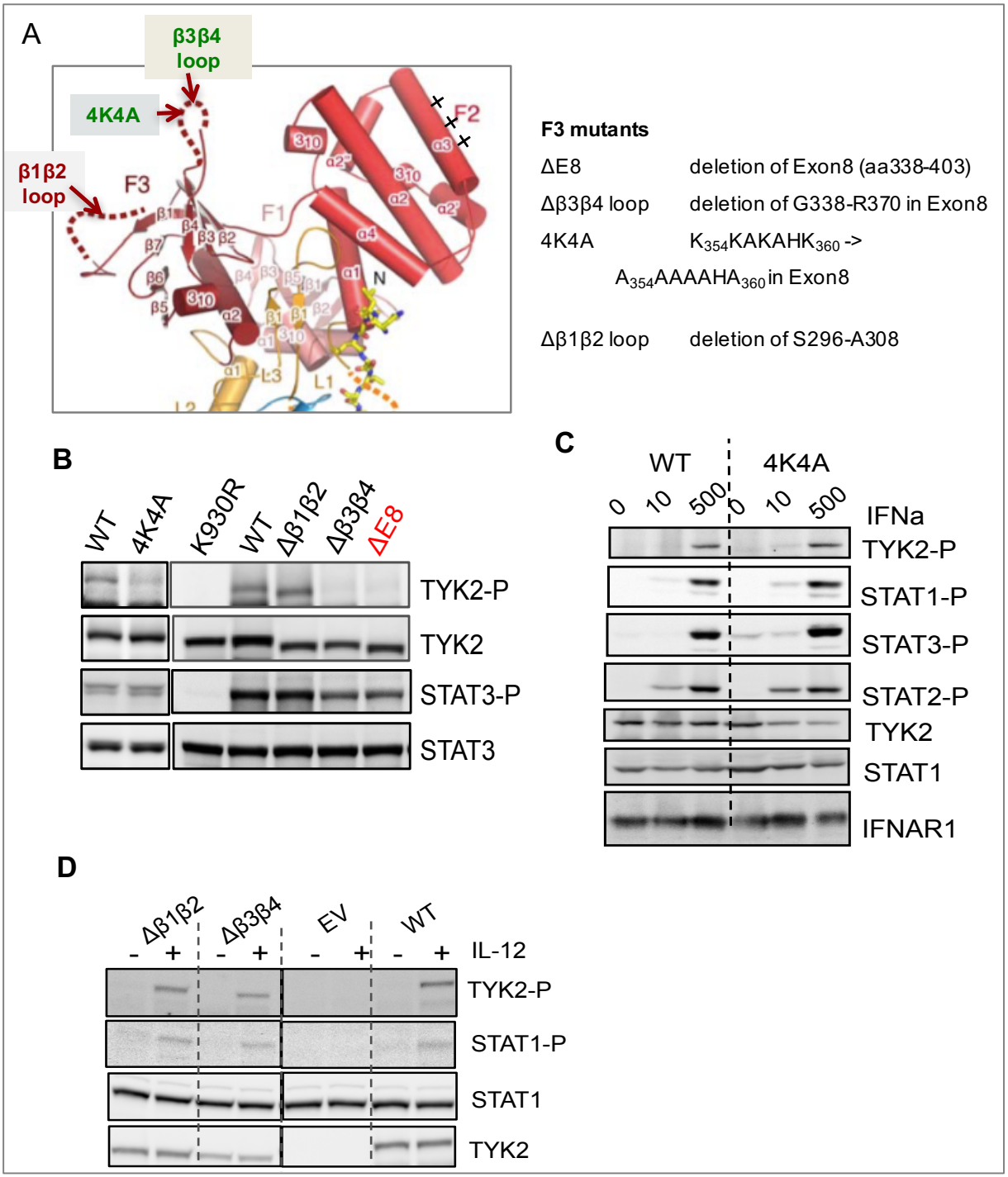

Figure 1. Functional study on the β1-β2 and β3-β4 loops in the F3 lobe.

(A) Localization of the β1-β2 and β3-β4 loops in the F3 lobe of the FERM of TYK2 (adapted from (2). The mutants in F3 lobe studied are detailed on the right panel.

(B) Autophosphorylation of TYK2 and phosphorylation of endogenous STAT3 in 293T cells transiently transfected with the indicated constructs. To note, the first two lanes are from a different blot with different exposure time.

(C) IFN-induced JAK/STAT activation in 11.1 cells stably expressing TYK2 WT or 4K4A. Cells were treated with IFN-α (0, 10, 500 pM) for 15 min. The level of tyrosine-phosphorylated TYK2, and STAT1/2/3 was analyzed by western blot with phospho-specific Abs. The membrane was reprobed for TYK2 and total STAT1 levels. IFNAR1 levels are shown in the bottom stripe.

(D) IL-12 induced TYK2 and STATI phosphorylation in 11.1 cells stably expressing ectopic IL-12 receptors. Cells were transiently transfected with TYK2 Δβ1β2, Δβ3β4, WT or empty vector (EV) and next day cells were treated with IL-12 (20 ng/ml) for 15 min.

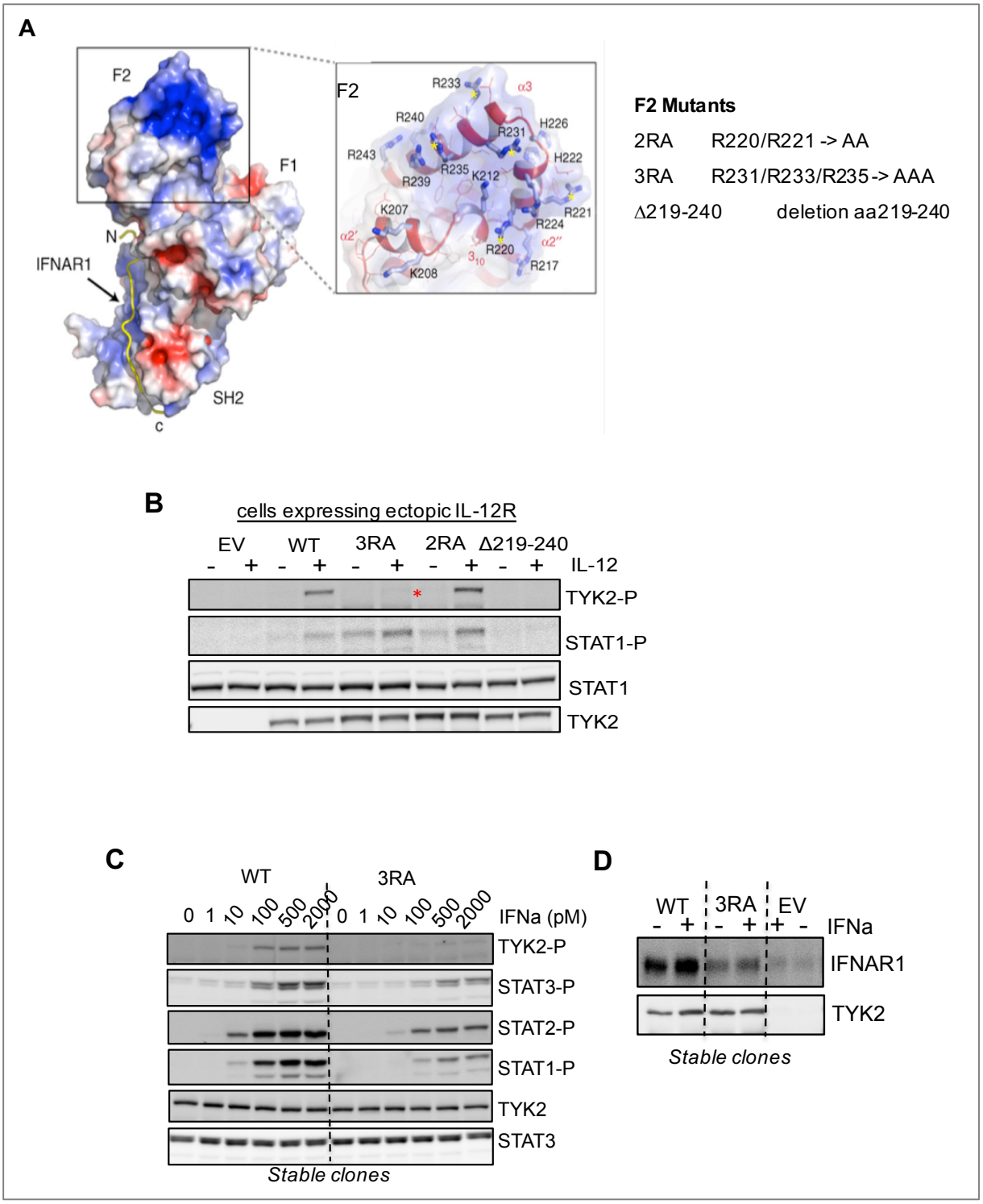

Figure 2. Functional study of the basic region in the F2 lobe.

(A) Localization of the basic region in the F2 lobe of the TYK2 FERM. Fifteen positively charged residues are highlighted in the right box (adapted from (2)). The mutated Arg residues analyzed in this study are indicated by yellow stars. The mutants in F2 lobe studied are detailed on the right panel.

(B) IL-12-induced TYK2 and STAT1 phosphorylation in an 11.1-derived clone stably expressing ectopic IL-12 receptors and transiently transfected with mutants TYK2-3RA (R231A/R233A/R235A), 2RA (R220A/R221A), Δ219-240 or empty vector (EV). Cells were treated with IL-12 (20 ng/ml) for

15 min. The level of phosphorylated TYK2, STAT1 was analyzed with phospho-specific Abs. The membrane was reprobed for TYK2 and STAT1 levels.
(C) IFN-induced TYK2 and STAT1/2/3 phosphorylation in 11.1-derived clones stably expressing TYK2 WT or 3RA. Cells were treated with IFN-a for 15 min and analyzed as above. The membrane was reprobed for TYK2 and STAT3 levels.
(D) IFNAR1 and TYK2 levels in 11.1-derived clones stably expressing TYK2 WT, 3RA or EV.

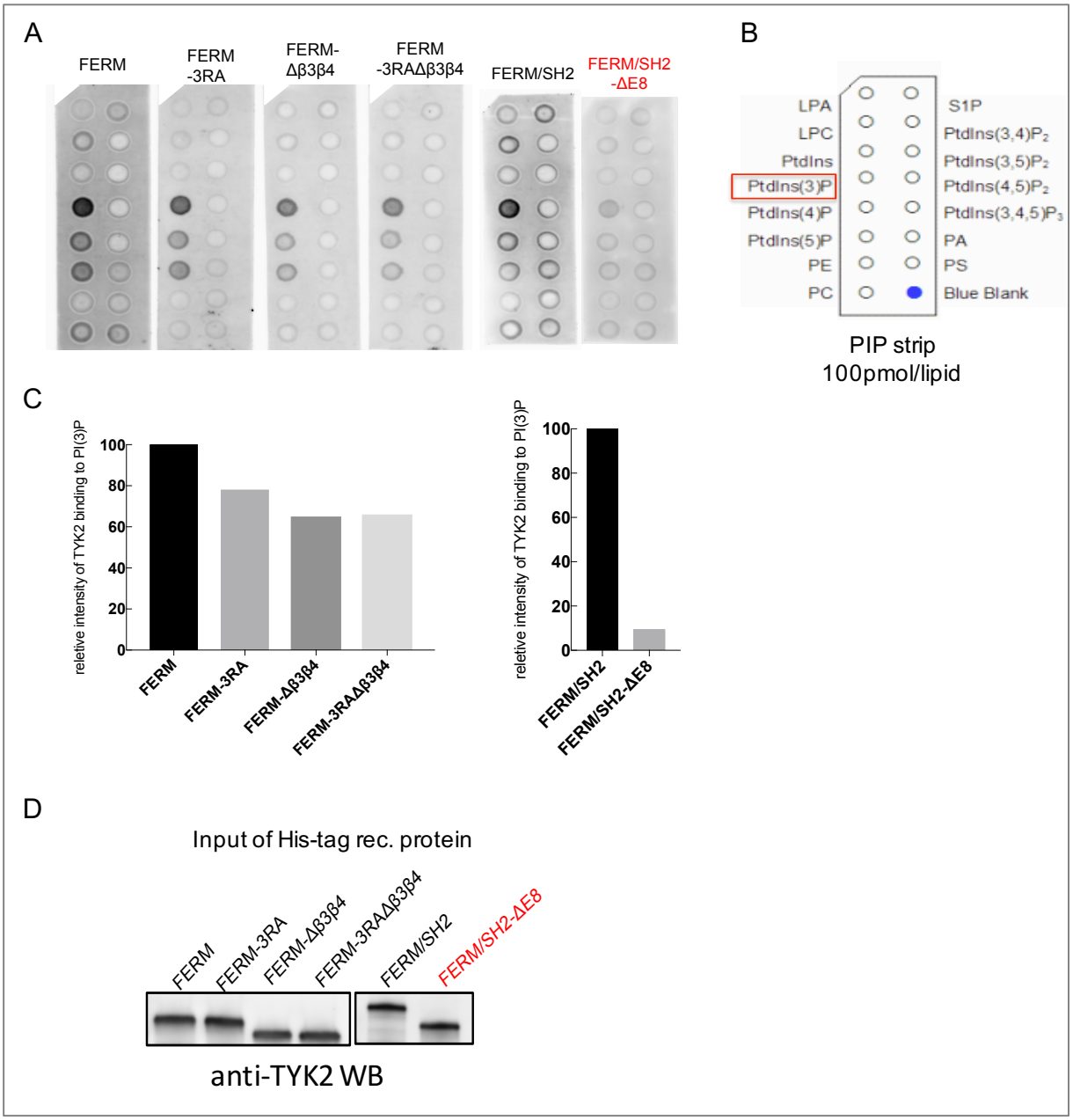

Figure 3. Binding of WT and mutant FERM-SH2 proteins to phospholipids

(A) PIP strips were incubated with various purified His-tagged proteins containing the TYK2 FERM domain (WT, 3RA, Δβ3β4, 3RA/Δβ3β4 double mutant), or the TYK2-FERM-SH2 (WT or ΔE8). Bound proteins were revealed by western blot using anti-TYK2 antibody.

(B) Fifteen different PIP were pre-blotted on the membrane.

(C) Quantitative analysis of the data in (A). Density of the FERM bound to PI(3)P was set at 100.

(D Anti-TYK2 immunoblotting of 0.2% of each sample used in (A).

Part II

Negative regulation of IFN signaling:

from patients to molecular mechanisms

Part II-1 Studies of patients

USP18-deficient patients

Five USP18-deficient patients were identified from two unrelated families (174). These infants presented pseudo-TORCH syndrome (PTS) and perinatal death. PTS is characterized by microcephaly, enlarged ventricles, cerebral calcification, and features at birth resembling the sequelae of congenital infection but in the absence of an infectious agent. *Ex vivo* brain autopsy from one patient demonstrated a strong activation of innate immune cells, as indicated by the robust presence of astrocytes, microglia, and by the up-regulation of MHC class II molecules. Positivity of phospho-STAT1 in the patient *versus* a control brain suggested activation of the IFN pathway. My contribution to this work has been to compare IFN signaling in primary dermal fibroblasts from patients and controls. My results (attached hereafter with the first page of the article) showed that 8 to 36 h post-stimulation with IFN-α, patient fibroblasts displayed enhanced and persistent STAT2 phosphorylation, higher ISG expression and ISGylation (Fig. 1, Fig 2B). Lentiviral transduction of USP18 completely rescued these alterations (Fig. 2A, 2B). Thus, we identified a novel genetic etiology of a type I interferonopathy (174).

Published June 20, 2016

Human USP18 deficiency underlies type 1 interferonopathy leading to severe pseudo-TORCH syndrome

Marije E.C. Meuwissen,[1]* Rachel Schot,[1]* Sofija Buta,[8,9,10] Grétel Oudesluijs,[1] Sigrid Tinschert,[11,12] Scott D. Speer,[8,9,10] Zhi Li,[13] Leontine van Unen,[1] Daphne Heijsman,[2] Tobias Goldmann,[8] Maarten H. Lequin,[3] Johan M. Kros,[4] Wendy Stam,[1] Mark Hermann,[8,9,10] Rob Willemsen,[1] Rutger W.W. Brouwer,[5] Wilfred F.J. Van IJcken,[5] Marta Martin-Fernandez,[8,9,10] Irenaeus de Coo,[6] Jeroen Dudink,[7] Femke A.T. de Vries,[1] Aida Bertoli Avella,[1] Marco Prinz,[14] Yanick J. Crow,[15,16] Frans W. Verheijen,[1]* Sandra Pellegrini,[13]* Dusan Bogunovic,[8,9,10]** and Grazia M.S. Mancini[1]**

[1]Department of Clinical Genetics, [2]Department of Bioinformatics, [3]Department of Radiology, [4]Department of Pathology, [5]Erasmus Center for Biomics, [6]Department of Child Neurology, and [7]Department of Neonatology, Erasmus University Medical Center, 3015 CE Rotterdam, the Netherlands
[8]Department of Microbiology, [9]Department of Pediatrics, and [10]The Mindich Child Health and Development Institute, Icahn School of Medicine at Mount Sinai, New York, NY 10029
[11]Medical Faculty Carl Gustav Carus, Technical University of Dresden, 01069 Dresden, Germany
[12]Division of Human Genetics, Medical University Innsbruck, 6020 Innsbruck, Austria
[13]Institut Pasteur, Cytokine Signaling Unit, Centre National de la Recherche Scientifique URA 1961, INSERM U 1221, 75724, Paris, France
[14]Institute of Neuropathology and BIOSS Center for Biological Signaling Studies, University of Freiburg, 79085 Freiburg, Germany
[15]INSERM UMR 1163, Laboratory of Neurogenetics and Neuroinflammation, Imagine Institute, Necker Hospital, Paris Descartes University, 75015 Paris, France
[16]Manchester Centre for Genomic Medicine and Academic Health Science Centre, University of Manchester, Manchester M13 9PL, England, UK

Pseudo-TORCH syndrome (PTS) is characterized by microcephaly, enlarged ventricles, cerebral calcification, and, occasionally, by systemic features at birth resembling the sequelae of congenital infection but in the absence of an infectious agent. Genetic defects resulting in activation of type 1 interferon (IFN) responses have been documented to cause Aicardi-Goutières syndrome, which is a cause of PTS. Ubiquitin-specific peptidase 18 (USP18) is a key negative regulator of type I IFN signaling. In this study, we identified loss-of-function recessive mutations of *USP18* in five PTS patients from two unrelated families. Ex vivo brain autopsy material demonstrated innate immune inflammation with calcification and polymicrogyria. In vitro, patient fibroblasts displayed severely enhanced IFN-induced inflammation, which was completely rescued by lentiviral transduction of USP18. These findings add *USP18* deficiency to the list of genetic disorders collectively termed type I interferonopathies. Moreover, USP18 deficiency represents the first genetic disorder of PTS caused by dysregulation of the response to type I IFNs. Therapeutically, this places USP18 as a promising target not only for genetic but also acquired IFN-mediated CNS disorders.

Maternal exposure to microbial pathogens can cause severe fetal brain damage that is detectable at birth. The acronym TORCH (toxoplasmosis, other [syphilis, varicella, mumps, parvovirus and HIV], rubella, cytomegalovirus, and herpes simplex) was first coined to highlight the commonality of the observed phenotype secondary to transplacental transmission of such microbes (Shin et al., 1976; Fine and Arndt, 1985; Donley, 1993). Events involved in the control of infections are associated with important immune-mediated collateral damage, with the CNS being more susceptible due to its immune privileged status (Konradt and Hunter, 2015). CNS characteristics of TORCH include microcephaly, white matter disease, cerebral atrophy, and calcifications.

Children are considered to have pseudo-TORCH syndrome (PTS) if they display a clinical phenotype indicative of in utero exposure to infection, but where the disorder has a noninfectious etiology (Reardon et al., 1994; Vivarelli et al., 2001). The high frequency of consanguinity among families with PTS suggests that many cases are genetic, inherited as autosomal recessive traits (Vivarelli et al., 2001).

One known rare Mendelian mimic of congenital infection, overlapping with and falling under the umbrella of PTS, is the Aicardi-Goutières syndrome (AGS; OMIM #225750). AGS is genetically heterogeneous, caused by mutations in any of *TREX1*, *RNASEH2B*, *RNASEH2C*, *RNASEH2A*, *SAMHD1*, *ADAR1*, and *IFIH1* (Crow and Rehwinkel, 2009;

*M.E.C. Meuwissen, R. Schot, F.W. Verheijen, and S. Pellegrini contributed equally to this paper.

**D. Bogunovic and G.M.S. Mancini contributed equally to this paper.

Correspondence to Grazia M.S. Mancini: g.mancini@erasmusmc.nl; or Dusan Bogunovic: Dusan.Bogunovic@mssm.edu

M.E.C. Meuwissen's present address is Dept. of Medical Genetics, Antwerp University Hospital, 2650 Edegen, Belgium.

A. Bertoli Avella's present address is Centogene, 18057 Rostock, Germany

Abbreviations used: AGS, Aicardi-Goutières syndrome; C, control; H&E, hematoxylin and eosin; ISG, IFN-stimulated gene; P, patient; PTS, Pseudo-TORCH syndrome; TORCH, toxoplasmosis, other (infection), rubella, cytomegalovirus, herpes simpex virus.

The Rockefeller University Press $30.00
J. Exp. Med. 2016
www.jem.org/cgi/doi/10.1084/jem.20151529

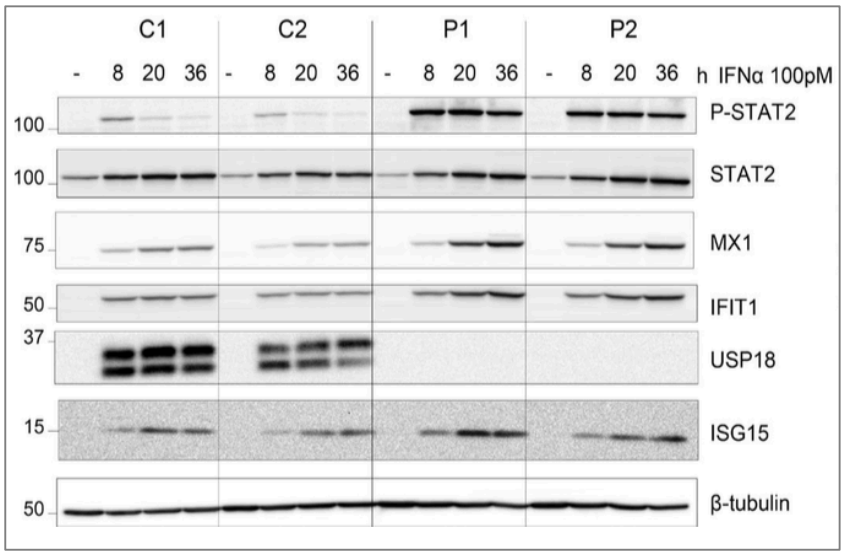

Figure 1. IFN signaling and ISGs protein production in fibroblasts from USP18 deficient patients. Primary fibroblasts from two controls (C1 and C2) and two USP18 deficient patients (P1 and P2) were stimulated with 100 pM IFN-α2 for 8, 20, and 36 h. The levels of phosphorylated STAT2 and of the indicated ISG products were analyzed by western blotting of 20 μg of cell lysate.

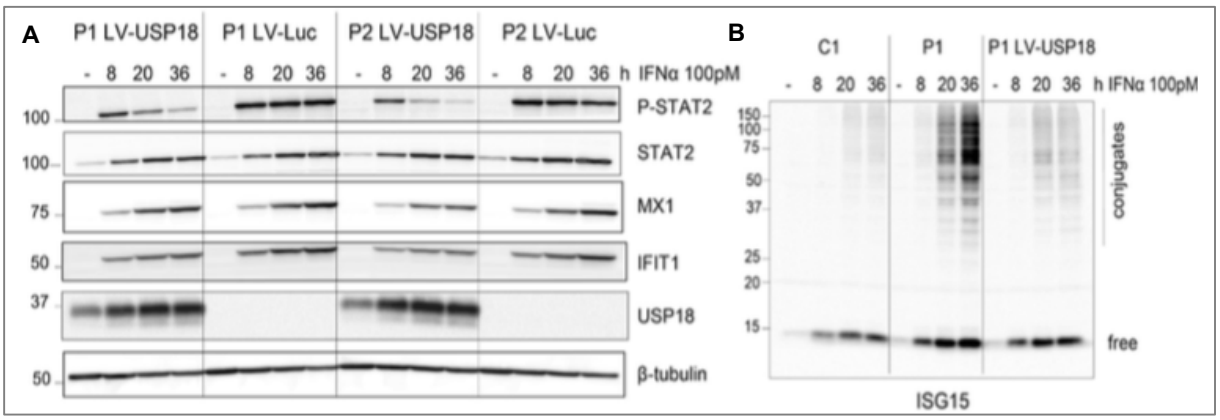

Figure 2. USP18 rescues USP18 deficiency

(A) The levels of the indicated proteins were compared in fibroblasts from P1 and P2, lentiviral transduced with USP18 or with the control Luc LV. Cells were stimulated and processed as in Fig. 1. (B) The levels of free and conjugated ISG15 were analyzed in lysates (40 μg/lane) from a control (C1) and P1 (P1), and USP18-transduced fibroblasts from P1 (P1 LV-USP18), stimulated, and processed as described in Fig. 1.

ISG15-deficient patients

A first report from the Casanova's group described three families with ISG15-deficient individuals suffering from BCG infection (148). Later, a fourth family with three ISG15-deficient patients were identified in China. The Chinese patients, who did not receive BCG vaccine, presented to the clinic with seizures. Calcification in the brain, enhanced ISGs expression in blood cells (IFN signature) and auto-antibodies were found in all patients, suggesting a new interferonophathy. In collaboration with D. Bogunovic, we studied cells from ISG15-deficient individuals and revealed a novel role for ISG15 in suppressing the type I IFN response (175). Indeed, fibroblasts and EBV-B cells derived from these patients exhibited increased and persistent STAT phosphorylation following IFN stimulation. Accordingly, canonical ISGs were more induced. Remarkably, it was noticed that, despite induced mRNA, the level of USP18 protein was lower in patients' cells compared to controls. This observation suggested a role of ISG15 in stabilizing USP18, the known negative regulator of IFN signaling. Indeed, blocking translation with cycloheximide (CHX) resulted in reduced USP18 protein levels in ISG15-deficient fibroblasts than control. In addition, re-expression in patients' fibroblasts of either WT ISG15 or a mutant (ΔGG) unable to conjugate (Introduction 4.1.1), prevented proteolysis in the presence of CHX. These data indicated that ISG15 somehow stabilizes USP18 at a post-translational level and independently of ISGylation. Mechanistically, we could show that, in an overexpression system, ISG15 interferes with the binding of USP18 to SKP2, a ubiquitin E3 ligase involved in cell cycle progression and previously reported to target USP18 to proteasomal degradation (156).

This study demonstrated that ISG15 contributes to the control of the type I IFN response. Thus, in addition to the proposed role of the extracellular form of ISG15 in anti-mycobacterial immunity (148), it is likely that intracellular ISG15 contributes to protective immunity to intracellular bacteria by tuning down type I IFN signaling (Introduction part II-2.4.1 IFN and infectious diseases).

My main contribution to this study was to show that IFN-stimulated fibroblasts and EBV-B cells derived from ISG15-deficient patients exhibit lower USP18, increased and persistent STAT2 phosphorylation and increased levels of canonical ISG-encoded proteins (see Fig. 1 attached hereafter with the first page of the article). This work is described in (175).

LETTER

doi:10.1038/nature13801

Human intracellular ISG15 prevents interferon-α/β over-amplification and auto-inflammation

Xianqin Zhang[1]*, Dusan Bogunovic[2,3]*, Béatrice Payelle-Brogard[4]*, Véronique Francois-Newton[4]*, Scott D. Speer[3,5,6], Chao Yuan[1], Stefano Volpi[7,8], Zhi Li[4], Ozden Sanal[9], Davood Mansouri[10], Ilhan Tezcan[9], Gillian I. Rice[11], Chunyuan Chen[12], Nahal Mansouri[10], Seyed Alireza Mahdaviani[10], Yuval Itan[2], Bertrand Boisson[2], Satoshi Okada[2], Lu Zeng[1], Xing Wang[1], Hui Jiang[13], Wenqiang Liu[1], Tiantian Han[1], Delin Liu[14], Tao Ma[1], Bo Wang[15], Mugen Liu[1], Jing-Yu Liu[1], Qing K. Wang[1,16], Dilek Yalnizoglu[9], Lilliana Radoshevich[17], Gilles Uzé[18], Philippe Gros[19], Flore Rozenberg[20], Shen-Ying Zhang[2], Emmanuelle Jouanguy[21,22], Jacinta Bustamante[21,22,23], Adolfo García-Sastre[3,5,24], Laurent Abel[2,21,22], Pierre Lebon[20], Luigi D. Notarangelo[7], Yanick J. Crow[11,22,25], Stéphanie Boisson-Dupuis[2,21,22], Jean-Laurent Casanova[21,22,26,27]§ & Sandra Pellegrini[4]§

Intracellular ISG15 is an interferon (IFN)-α/β-inducible ubiquitin-like modifier which can covalently bind other proteins in a process called ISGylation; it is an effector of IFN-α/β-dependent antiviral immunity in mice[1–4]. We previously published a study describing humans with inherited ISG15 deficiency but without unusually severe viral diseases[5]. We showed that these patients were prone to mycobacterial disease and that human ISG15 was non-redundant as an extracellular IFN-γ-inducing molecule. We show here that ISG15-deficient patients also display unanticipated cellular, immunological and clinical signs of enhanced IFN-α/β immunity, reminiscent of the Mendelian autoinflammatory interferonopathies Aicardi–Goutières syndrome and spondyloenchondrodysplasia[6–9]. We further show that an absence of intracellular ISG15 in the patients' cells prevents the accumulation of USP18[10,11], a potent negative regulator of IFN-α/β signalling, resulting in the enhancement and amplification of IFN-α/β responses. Human ISG15, therefore, is not only redundant for antiviral immunity, but is a key negative regulator of IFN-α/β immunity. In humans, intracellular ISG15 is IFN-α/β-inducible not to serve as a substrate for ISGylation-dependent antiviral immunity, but to ensure USP18-dependent regulation of IFN-α/β and prevention of IFN-α/β-dependent autoinflammation.

Calcification of the cerebral basal ganglia during childhood is an important radiological sign associated with a range of genetic and non-genetic states[12,13]. In Fahr's disease, also known as idiopathic basal ganglia calcification (IBGC)[14–17], the genetic causes identified are germline mutations of the *SLC20A2*, *PDGFB* and *PDGFRB* genes[15,16]. Intracranial calcification is also a well recognized feature of a group of Mendelian autoinflammatory diseases associated with upregulation of IFN-α/β signalling[8,18], including Aicardi–Goutières syndrome (AGS) and spondyloenchondromatosis (SPENCD), in particular. We investigated three siblings from China with IBGC. The eldest child (P4) died during an episode of epileptic seizures at the age of 13 years (Supplementary Information, case report). The other two siblings, currently aged 11 (P6) and 13 (P5) years, have suffered only occasional seizures. Despite having been exposed to common childhood viruses (Extended Data Table 1), these children have experienced no severe infectious disease. Whole-exome sequencing (WES) of P5 and P6 and their healthy mother identified only one common nonsense homozygous mutation, which had not been reported in public databases or in in-house WES data for 1,500 other individuals (Extended Data Table 2). This variant was in exon 2 of *ISG15*: c.163C>T/163C>T (p.Gln 55*/Gln 55*; asterisks denote stop codons). Familial segregation was consistent with an autosomal recessive mode of inheritance (Fig. 1a, b and Extended Data Fig. 1a).

This observation was surprising, as we recently described three unrelated children from two families from Turkey and Iran who were homozygous for loss-of-function mutations of *ISG15*[5]. These patients (P1, P2 and P3, now aged 17, 14 and 17 years, respectively) displayed clinical disease caused by the BCG vaccine, which, in otherwise healthy individuals, defines Mendelian susceptibility to mycobacterial disease (MSMD), a rare disorder characterized by severe clinical disease following infection with weakly virulent mycobacteria[19,20]. In these patients, MSMD resulted from insufficient ISG15-dependent IFN-γ production[21]. These patients displayed no severe viral disease[2]. Following the identification of *ISG15* mutations in Chinese children with a putative diagnosis of IBGC, we performed computed tomography (CT) scans on the Iranian and Turkish ISG15-deficient MSMD patients. We found that P1 and P2 displayed calcification of the basal ganglia, with CT imaging in P3 also showing calcification along the cerebral falx (Fig. 1c). The ISG15-deficient patients from China were not vaccinated with BCG at birth, consistent with their current lack of an MSMD phenotype. The c.163C>T/163C>T mutant allele showed no ISG15 protein on western blots (Extended Data Fig. 1b). In total, six patients (P4 with inferred genotype) with IBGC

[1]Key Laboratory of Molecular Biophysics of the Ministry of Education, College of Life Science and Technology, Huazhong University of Science and Technology, Wuhan 430074, China. [2]St. Giles Laboratory of Human Genetics of Infectious Diseases, Rockefeller Branch, The Rockefeller University, New York, New York 10065, USA. [3]Department of Microbiology, Icahn School of Medicine at Mount Sinai, New York, New York 10029, USA. [4]Institut Pasteur, Cytokine Signaling Unit, CNRS URA 1961, 75724 Paris, France. [5]Global Health and Emerging Pathogens Institute, Icahn School of Medicine at Mount Sinai, New York, New York 10029, USA. [6]Microbiology Training Area, Graduate School of Biomedical Sciences of Icahn School of Medicine at Mount Sinai, New York, New York 10029, USA. [7]Division of Immunology, Children's Hospital Boston, Boston, Massachusetts 02115, USA. [8]Department of Neuroscience, Rehabilitation, Ophthalmology, Genetics, Maternal and Child Health, University of Genoa, 16132 Genoa, Italy. [9]Immunology Division and Pediatric Neurology Department, Hacettepe University Children's Hospital, 06100 Ankara, Turkey. [10]Division of Infectious Diseases and Clinical Immunology, Pediatric Respiratory Diseases Research Center, National Research Institute of Tuberculosis and Lung Diseases, Shahid Beheshti University of Medical Sciences, 4739 Teheran, Iran. [11]Manchester Academic Health Science Centre, University of Manchester, Genetic Medicine, Manchester, M13 9NT, UK. [12]Department of Pediatrics, Third Xiangya Hospital, Central South University, Changsha 410013, China. [13]BGI-Shenzhen, Shenzhen 518083, China. [14]Sangzhi County People's Hospital, Sangzhi 427100, China. [15]Genetics Laboratory, Hubei Maternal and Child Health Hospital, Wuhan, Hubei 430070, China. [16]Center for Cardiovascular Genetics, Department of Molecular Cardiology, Lerner Research Institute, Cleveland Clinic, Cleveland, Ohio 44195, USA. [17]Institut Pasteur, Bacteria-Cell Interactions Unit, 75724 Paris, France. [18]CNRS UMR5235, Montpellier II University, Place Eugène Bataillon, 34095 Montpellier, France. [19]Department of Biochemistry, McGill University, Montreal, QC H3A 0G4, Canada. [20]Paris Descartes University, 75006 Paris, France. [21]Laboratory of Human Genetics of Infectious Diseases, Necker Branch, INSERM U1163, Necker Hospital for Sick Children, 75015 Paris, France. [22]Paris Descartes University, Imagine Institute, 75015 Paris, France. [23]Center for the Study of Primary Immunodeficiencies, Necker Hospital for Sick Children, 75015 Paris, France. [24]Department of Medicine, Division of Infectious Diseases, Icahn School of Medicine at Mount Sinai, New York, New York 10029, USA. [25]INSERM UMR 1163, Laboratory of Neurogenetics and Neuroinflammation, Imagine Institute, 75006 Paris, France. [26]Howard Hughes Medical Institute, New York, New York 10065, USA. [27]Pediatric Hematology–Immunology Unit, Necker Hospital for Sick Children, 75015 Paris, France.
*These authors contributed equally to this work.
§These authors jointly supervised this work.

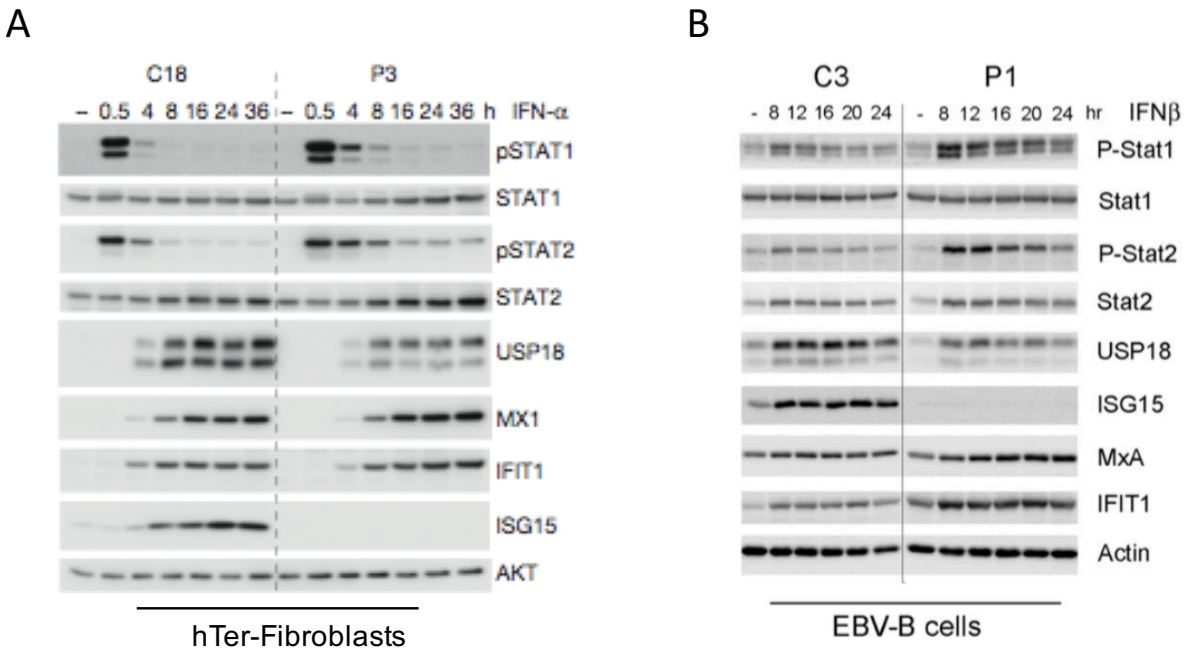

Figure 1. Prolonged IFN signaling, low USP18, and high interferon-stimulated-gene-encoded protein levels in patient-derived cells. hTer-immotalized fibroblasts (A) and EBV-transformed B cells (B) from control (C3) and ISG15-deficient patient P1 were stimulated with 100 pM of IFN-α or IFN-β for 0.5-36h. Cell lysates (30 μg) were analyzed by western blot with the indicated antibodies.

ISG15 deficiency and increased viral resistance in humans but not mice

ISG15 has been shown to be an antiviral effector molecule in murine models of infection and in cultured human cells (Introduction part II-4.1.3). Isg15-/- mice are highly susceptible to many viral infections. Yet, none of the ISG15-deficient patients exhibit signs of viral diseases. The different phenotype of ISG15 deficiency in humans and mice led us to study the mechanism of how lack of ISG15 differently impacts antiviral response in humans and in mice. In this study, we describe that fibroblasts derived from ISG15-deficient patients display enhanced antiviral protection compared to control cells after IFN stimulation and that re-expression of ISG15 in ISG15-/- cells attenuates viral resistance. I contributed to the mechanistic studies. In the 293T overexpression system, I compared human *vs* murine ISG15 for their capacity to stabilize USP18 and to complex with it. I found that only the human ISG15 can stabilize human USP18 and complex with it. Murine orthologues of ISG15 and USP18 do not form a stable complex. Thus, the species-specific gain-of-function in antiviral immunity observed in ISG15 deficiency is explained by the requirement of ISG15 to sustain USP18 levels in humans, a mechanism not operating in mice. This work is described in (176) attached hereafter in which I am the second author.

nature COMMUNICATIONS

ARTICLE

Received 18 Nov 2015 | Accepted 4 Apr 2016 | Published 19 May 2016

DOI: 10.1038/ncomms11496 OPEN

ISG15 deficiency and increased viral resistance in humans but not mice

Scott D. Speer[1], Zhi Li[2], Sofija Buta[1], Béatrice Payelle-Brogard[2], Li Qian[1], Frederic Vigant[1], Erminia Rubino[2], Thomas J. Gardner[1], Tim Wedeking[3], Mark Hermann[1], James Duehr[1], Ozden Sanal[4], Ilhan Tezcan[4], Nahal Mansouri[5], Payam Tabarsi[5], Davood Mansouri[5], Véronique Francois-Newton[2], Coralie F. Daussy[2], Marisela R. Rodriguez[6], Deborah J. Lenschow[6], Alexander N. Freiberg[7], Domenico Tortorella[1], Jacob Piehler[3], Benhur Lee[1], Adolfo García-Sastre[1], Sandra Pellegrini[2,*] & Dusan Bogunovic[1,*]

ISG15 is an interferon (IFN)-α/β-induced ubiquitin-like protein. It exists as a free molecule, intracellularly and extracellularly, and conjugated to target proteins. Studies in mice have demonstrated a role for Isg15 in antiviral immunity. By contrast, human ISG15 was shown to have critical immune functions, but not in antiviral immunity. Namely, free extracellular ISG15 is crucial in IFN-γ-dependent antimycobacterial immunity, while free intracellular ISG15 is crucial for USP18-mediated downregulation of IFN-α/β signalling. Here we describe *ISG15*-deficient patients who display no enhanced susceptibility to viruses *in vivo*, in stark contrast to *Isg15*-deficient mice. Furthermore, fibroblasts derived from *ISG15*-deficient patients display enhanced antiviral protection, and expression of ISG15 attenuates viral resistance to WT control levels. The species-specific gain-of-function in antiviral immunity observed in ISG15 deficiency is explained by the requirement of ISG15 to sustain USP18 levels in humans, a mechanism not operating in mice.

[1] Department of Microbiology, Icahn School of Medicine at Mount Sinai, New York 10029, USA. [2] Institut Pasteur, Cytokine Signalling Unit, CNRS URA 1961, 75724 Paris, France. [3] Department of Biology, University of Osnabrück, 49076 Osnabrück, Germany. [4] Immunology Division, Hacettepe University, Ihsan Dogramaci Children's Hospital, 06100 Ankara, Turkey. [5] Division of Infectious Diseases and Clinical Immunology, Pediatric Respiratory Diseases Research Center, National Research Institute of Tuberculosis and Lung Diseases, Shahid Beheshti University of Medical Sciences, 4739 Teheran, Iran. [6] Department of Medicine and Department of Pathology and Immunology, Washington University School of Medicine, St. Louis, Missouri 63110, USA. [7] Department of Pathology, University of Texas Medical Branch, Galveston, Texas 77555, USA. * These authors contributed equally to this work. Correspondence and requests for materials should be addressed to S.P. (email: Sandra.Pellegrini@pasteur.fr) or to D.B. (email: Dusan.Bogunovic@mssm.edu).

Interferon-stimulated gene 15 (ISG15) is an interferon (IFN)-α/β-inducible ubiquitin-like molecule. It has two ubiquitin-like domains and is synthesized from an immature precursor by cleavage of a C-terminal extension peptide[1]. Mature ISG15 has the LRLRGG sequence, which is also present at the C terminus of mature ubiquitin. ISG15 exists in two distinct states: as a free molecule (intracellular and extracellular) or conjugated to target protein lysine residues (ISGylation)[2–10]. In a process similar to ubiquitin ligation, ISGylation involves a conjugation pathway including E1 (UBE1L), E2 (UBCH8) and E3 (HERC5, EFP, HHARI) enzymes. ISGylation is reversed by the action of the isopeptidase ubiquitin-specific protease 18 (USP18; UBP43)[11,12]. Accordingly, cells deficient in the conjugation machinery exhibit absent or reduced ISGylation, while *Usp18*-deficient cells exhibit high levels of Isg15 conjugates[13]. All of the enzymes involved in ISGylation/de-ISGylation are transcriptionally induced by IFN-α/β.

Numerous *in vivo* and *in vitro* studies have ascribed an antiviral role to ISG15. Mice lacking Isg15 exhibit enhanced susceptibility to challenge with multiple viruses, including murine gammaherpesvirus 68 (ref. 14), influenza A virus (IAV)[14], influenza B virus[14,15], Sindbis virus[14], vaccinia virus[16], herpes simplex virus 1 (HSV-1)[14], Chikungunya virus[17] and murine norovirus[18], yet no enhanced susceptibility to vesicular stomatitis virus (VSV) and lymphocytic choriomeningitis virus[19]. *In vitro* studies in mouse embryonic fibroblasts (MEFs), mouse lung fibroblasts and RAW 264.7 cells have demonstrated an antiviral role for Isg15 during Sindbis virus[20], vaccinia virus[16], Ebola virus[21], Dengue virus and West Nile virus[22] infection, although there are several reports of viruses exhibiting no enhanced replication in the absence of Isg15 (murine gammaherpesvirus 68, HSV-1, Sindbis virus, IAV[14]). ISG15 small interfering RNA (siRNA) knockdown in human cells has also suggested an antiviral role for free and/or conjugated ISG15 during infection with numerous viruses, including IAV[23], human immunodeficiency virus[24–26], Ebola virus[21,27], human papilloma virus[28], VSV[27], Japanese encephalitis virus[15] and Sendai virus (SeV)[29]. While these many studies have suggested an antiviral role for ISG15, others have suggested no role at all; the one clear exception is hepatitis C virus (HCV). *In vitro* studies of HCV infection suggest that ISG15 exhibits proviral activity[30,31]. The silencing of ISG15 in human hepatoma cells was found to lead to an inhibition of HCV replication, increases in cell sensitivity to IFN-α/β and accumulation of IFN-α/β-stimulated gene products (ISGs).

Our studies on *ISG15*-deficient individuals have demonstrated a critical role for free extracellular ISG15 in the induction of IFN-γ and protection against mycobacterial disease. These findings were confirmed in *Isg15*-deficient mice[9]. Intriguingly, there is no evident overlap in viral susceptibility phenotype between mice and humans lacking ISG15. Despite being serologically positive for numerous childhood viruses, such as human cytomegalovirus (HCMV), Epstein Barr virus, measles virus, varicella-zoster virus, HSV-1 and -2, mumps virus, IAV and hepatitis A virus, *ISG15*-deficient individuals exhibit no overt susceptibility to viral disease[9,10]. We recently demonstrated that human free intracellular ISG15 binds USP18, a negative regulator of IFN-α/β signalling. This binding prevents the SKP2-mediated degradation of USP18, and thus is critical for the accumulation of USP18 and the appropriate regulation of IFN-α/β signalling. Indeed, patients lacking ISG15, and consequently having low USP18 levels, display higher steady-state levels of ISG transcripts in whole blood than controls[10,32].

We demonstrate that human cells deficient in ISG15 exhibit a persistent elevation in ISG expression. We find that, not only do humans deficient in ISG15 lack any overt susceptibility to viral infection, but cells derived from these individuals exhibit an enhancement of broad protection against viruses. Complementation of ISG15-deficient cells with the wild-type (WT) or conjugation-deficient ΔGG *ISG15* alleles rescues both WT levels of ISG expression and viral susceptibility. Furthermore, we demonstrate that there is a species-specific interaction between ISG15 and USP18. While humans require ISG15 for USP18 stability and appropriate negative regulation of the IFN response, mice lack this stable interaction and can regulate the IFN response in the absence of Isg15.

Results

Persistent increase of ISG expression in cells lacking ISG15. The *ISG15*-deficient individuals identified to date have been infected with numerous childhood viruses, against which they mounted a humoral immune response[9,10]. No overt viral illnesses were documented in these patients, suggesting that ISG15 may not be essential for immunity to these viruses. *ISG15*-deficient patients may actually have a milder disease course than wild-type individuals. However, this is difficult to demonstrate, as information about subclinical illness is often not transmitted by patients to their doctors or noted by the doctors themselves. We tested this hypothesis *in vitro* using hTert-immortalized dermal fibroblasts derived from *ISG15*-deficient patients and relevant WT controls. Human cells lacking ISG15 also have low USP18 levels (due to the lack of USP18 stabilization by ISG15) and high levels of ISG transcripts, as documented *ex vivo* with leukocytes from *ISG15*-deficient individuals[10]. We carried out *in vitro* studies, monitoring the kinetics and persistence of ISG induction by quantitative real-time PCR in WT and *ISG15*-deficient fibroblasts during and after IFN priming, in which the cells were pulsed with IFN-α2b for 12 h and then allowed to rest for 36 h. We determined mRNA levels for the IFN-induced protein with tetratricopeptide repeats 1 (IFIT1) and myxovirus resistance 1 (MX1), from 12 h to 6 days post-IFN-α/β priming. The expression levels of *IFIT1* and *MX1* transcripts during peak induction and early dampening were similar between *ISG15*-deficient and control cells (Fig. 1a). However, the time taken for *IFIT1* transcript levels to return to baseline after IFN priming differed between control and *ISG15*-deficient cells. Specifically, *IFIT1* transcript levels remained significantly elevated for more than 5 days in *ISG15*-deficient cells, whereas they returned to basal levels within 2 days in control cells (Fig. 1a).

***ISG15*-deficient IFN-primed cells are resistant to viral infection.** *ISG15*-deficient patients had previously been infected with HSV-1, HCMV and IAV, as indicated by the results of serological tests[10], but did not develop severe disease. We, therefore, investigated whether the prolonged increase in ISG levels affected the susceptibility of the patients' cells to viral challenge. When IFN-α/β-primed *ISG15*-deficient fibroblasts were infected with HSV-1 (Fig. 1b), HCMV (Fig. 1c) or IAV (Fig. 1d) levels of viral replication were significantly lower in *ISG15*-deficient cells than in control cells. SeV, a murine paramyxovirus known to be highly sensitive to human ISGs, also replicated significantly less efficiently in IFN-α/β-primed *ISG15*-deficient cells (Fig. 1e). Finally, we investigated whether *ISG15*-deficient cells were also resistant to highly pathogenic viruses affecting humans that our patients would have been unlikely to encounter, by infecting control and *ISG15*-deficient fibroblasts with Rift Valley fever virus (RVFV) and Nipah virus (NiV). Both of these viruses also appeared to replicate less efficiently in IFN-α/β-primed *ISG15*-deficient cells than in control cells (Fig. 1f,g), although neither RVFV nor NiV reached statistical significance. Thus, the prolonged induction of ISGs observed in *ISG15*-deficient human

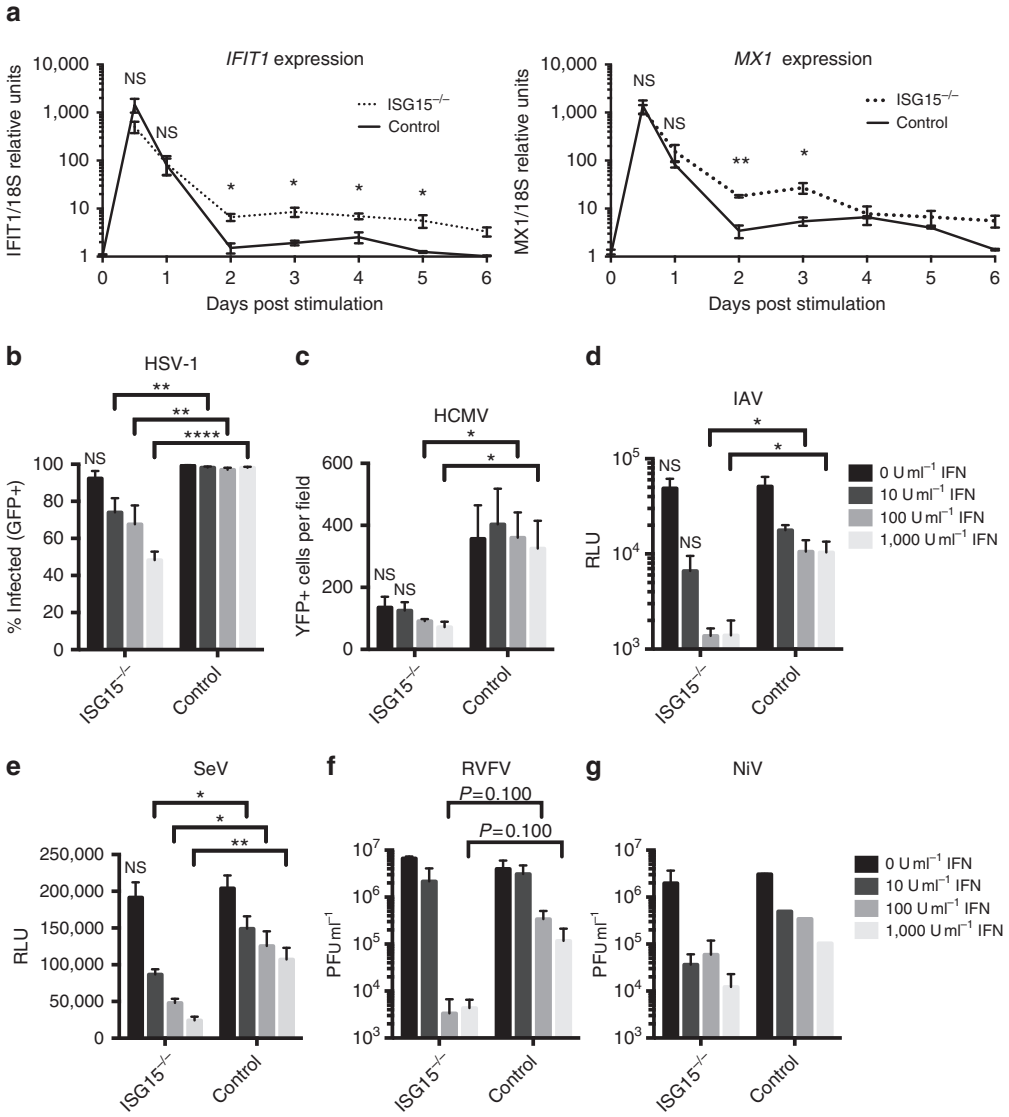

Figure 1 | *ISG15*-deficient cells exhibit prolonged ISG expression and resistance to infection with viruses from multiple families. hTert-immortalized fibroblasts from *ISG15*-deficient patients ($n=3$) or controls ($n=5$) were treated with the indicated concentration of IFN-α2b for 12 h, washed, and allowed to rest for 36 h before infection. (**a**) Relative *IFIT1* (left panel) or *MX1* (right panel) mRNA levels at 12 (time of IFN-α2b removal), 24, 48, 72, 96, 120 and 144 h post-priming with 1,000 IU ml^{-1}. (**b**) Cells were infected with HSV-1-US11-GFP at a multiplicity of infection (MOI) of 1.0 for 24 h, fixed, subjected to Hoechst 33342 nuclear staining, and imaged. Shown are the percentages of cells positive for both GFP and nuclear staining. (**c**) Cells were infected with HCMV-IE2-YFP at an MOI of 2.0 for 24 h, fixed, and imaged. Shown are the numbers of GFP-positive cells field^{-1}. (**d**) Cells were infected with IAV PR8-gLuc-PTV1 at an MOI of 10.0 for 24 h. Lysates were collected and assayed for luciferase activity. Shown are the results in relative luminescence units. (**e**) Cells were infected with SeV-GFP-gLuc at an MOI of 0.1 for 24 h. Supernatants were collected and assayed for luciferase activity. Shown are the results in relative luminescence units. (**f**) Cells were infected with RVFV at an MOI of 0.01 for 48 h. Supernatants were collected and titered by plaque assay. (**g**) Cells were infected with NiV-gLuc-P2A-eGFP at an MOI of 0.01 for 24 h. Supernatants were titered by plaque assay. **a** shows the combined results of two experiments. **b**,**c**, and **e** show a single representative experiments of three performed. **d** shows the combined results of three experiments. **f** and **g** are single experiments performed in the BSL-4. Error bars, s.d. Comparisons made with unpaired *t*-test. *$P<0.05$, **$P<0.01$, ****$P<0.0001$. NS, not significant.

cells protects against viruses from multiple families, having both RNA and DNA genomes, and causing both low and highly pathogenic disease in normal healthy humans. These results further suggest that viral infections in *ISG15*-deficient individuals may follow an attenuated course with milder symptoms. Thus, the *in vivo* clinical follow-up of *ISG15*-deficient individuals, serological testing and the results of *in vitro* studies of patient-derived cells all indicate a greater resistance to viral challenge, consistent with a proviral role of ISG15 in humans.

WT or ΔGG *ISG15* allele restores WT viral susceptibility. We verified that the observed phenotype was due solely to the lack of ISG15 by stably transducing *ISG15*-deficient patient and control fibroblasts with lentiviral particles encoding *ISG15* or control luciferase[10]. The cells were subsequently infected with VSV, another virus known to be sensitive to low levels of IFN-α/β. Control fibroblasts displayed similar levels of VSV replication with and without IFN-α/β priming, suggesting that most of the ISG antiviral activity had declined during the post-priming rest (Fig. 2a). By contrast, IFN-α/β-primed cells deficient in ISG15 displayed significantly lower levels of viral replication (Fig. 2a), indicating a protracted antiviral state, as confirmed with other viral challenges (Fig. 1b-g). The resistance phenotype was confirmed using fibroblasts from the three *ISG15*-deficient

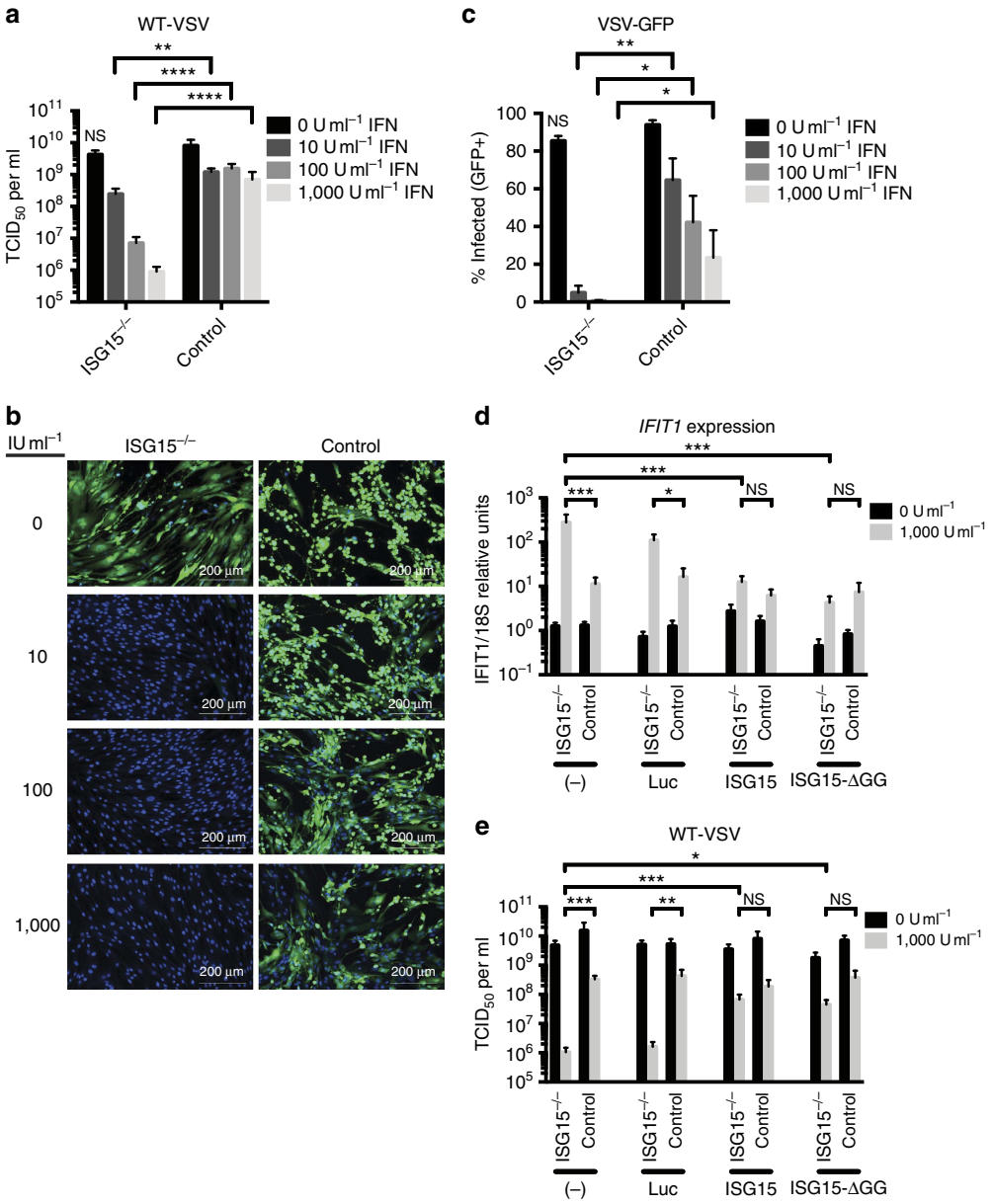

Figure 2 | WT ISG15 and ISG15ΔGG restore VSV infection phenotype in *ISG15*-deficient cells. (**a**–**c**) hTert-immortalized fibroblasts from *ISG15*-deficient patients ($n=3$) or controls ($n=2$ or 3) were treated with the indicated concentration of IFN-α2b for 12 h, washed, and allowed to rest for 36 h before infection. (**a**) Cells were infected with VSV at an MOI of 1.0 for 24 h. Supernatants were titered by $TCID_{50}$. (**b**) Cells were infected with VSV–GFP at an MOI of 1.0 for 24 h, fixed, subjected to nuclear staining, and imaged. Representative images are shown for each treatment group. (**c**) Quantification of panel b. Shown is the percentage of cells positive for both GFP and nuclear staining. (**d**) and (**e**) hTert-immortalized fibroblasts from *ISG15*-deficient patients ($n=3$) or controls ($n=2$), untransduced or stably transduced with luciferase, ISG15 or ISG15ΔGG, were mock-treated or primed with 1,000 IU ml^{-1} IFN-α2b for 12 h, washed, and allowed to rest for 36 h. (**d**) Relative *IFIT1* mRNA levels 48 h post-priming. (**e**) Fibroblasts were infected with VSV at an MOI of 1.0, 48 h post-priming. Supernatants were collected at 24 h post-infection and titered by $TCID_{50}$ in duplicate. **a**,**d** and **e** show the combined results of three experiments. **b** and **c** show single representative experiments of three performed. Error bars, s.d. Comparisons made with unpaired *t*-test. $^{*}P<0.05$, $^{**}P<0.01$, $^{***}P<0.001$, $^{****}P<0.0001$. NS, not significant.

patients and five controls (Supplementary Fig. 1). Similar phenotypic differences in viral replication were observed between control and *ISG15*-deficient fibroblasts infected with VSV-expressing GFP (VSV–GFP), as assessed by fluorescence microscopy (Fig. 2b,c). Complementation of *ISG15*-deficient patient fibroblasts with WT ISG15, but not with control luciferase, restored both ISG expression (Fig. 2d) and viral replication (Fig. 2e) to the levels observed in the control cells. We have previously shown that the conjugation-deficient mutant of ISG15 (ISG15ΔGG) retains the ability to bind and stabilize USP18, and is thus a functional negative regulator of IFN signalling[10]. Accordingly, we used *ISG15*-deficient fibroblasts transduced with ISG15ΔGG, which exhibit fully functional downregulation of IFN signalling but no ISGylation, to determine the relative role of each function during viral infection. As observed with WT ISG15, complementation with ISG15ΔGG rescued both the ISG expression and VSV replication phenotypes in *ISG15*-deficient fibroblasts (Fig. 2d,e). Similar results were obtained in A549 and Hela cells that were silenced with siRNA targeting ISG15 or a non-silencing control. In both

cell lines, knockdown of ISG15 enhanced ISG expression and resistance to viral replication (Supplementary Fig. 2a-f). These data demonstrate the dependence of the *in vitro* phenotype on the *ISG15* allele and suggest that, in human epithelial cells, the dominant role of ISG15 during viral replication is the ISGylation-independent downregulation of IFN-α/β signalling.

***Isg15*-deficient mice do not exhibit elevated ISG expression.** All of our observations, whether from the clinical history of *ISG15*-deficient patients or from *in vitro* studies of *ISG15*-deficient patient-derived cells, point to a lack of overt susceptibility to viruses, and suggest that ISG15 may exhibit a proviral role. We were unable to reconcile these data with the numerous reports ascribing a critical antiviral role to Isg15 during the infection of mice *in vivo* with multiple viruses (for example, chikungunya virus[17], murine gammaherpesvirus 68 (ref. 14), IAV[14], influenza B virus[14,33], Sindbis virus[14], vaccinia[16], HSV-1 (ref. 14) and murine norovirus[18]). We, therefore, analysed whole blood from *Isg15*-deficient mice, to determine whether these mice, like *ISG15*-deficient humans, also displayed elevated levels of steady-state ISG expression in the absence of diagnosable infection[10]. In unstimulated conditions, *Ifit1* mRNA levels of *Isg15*-deficient animals were similar to those of their age-matched WT cagemates (Fig. 3a). This indicates a species-specific difference in ISG regulation in the absence of ISG15. We then hypothesized that, *in natura,* humans are constantly exposed to environmental challenges that induce IFN-α/β, resulting in persistently high levels of ISGs in *ISG15*-deficient individuals, due to a lack of negative regulation. Our mice were not housed in completely sterile conditions, but were nevertheless somewhat shielded from true environmental exposure to microbes. IFN-α/β induction was mimicked by injecting 10,000 U of type-I IFN intraperitoneally into WT control and *Isg15*-deficient mice, followed by analysis of the levels of ISG transcripts in whole blood at multiple timepoints. As expected, the animals receiving IFN injections displayed a robust increase in ISG expression within 8 h that was fully resolved within 24 h. However, no difference in ISG expression levels between *Isg15*-deficient and WT mice was observed at any time point (Fig. 3b–d). For further comparison with our results in human cells, primary MEFs derived from both WT and *Isg15*-deficient mice were primed with type-I IFN for 12 h, allowed to rest for 36 h and the levels of *Ifit1* mRNA were analysed. No differences in *Ifit1* expression levels were observed between WT and *Isg15*-deficient cells at any time point after IFN priming (Fig. 3e). These experiments suggest that the impact of ISG15 on IFN-α/β-induced signalling may indeed differ between humans and mice.

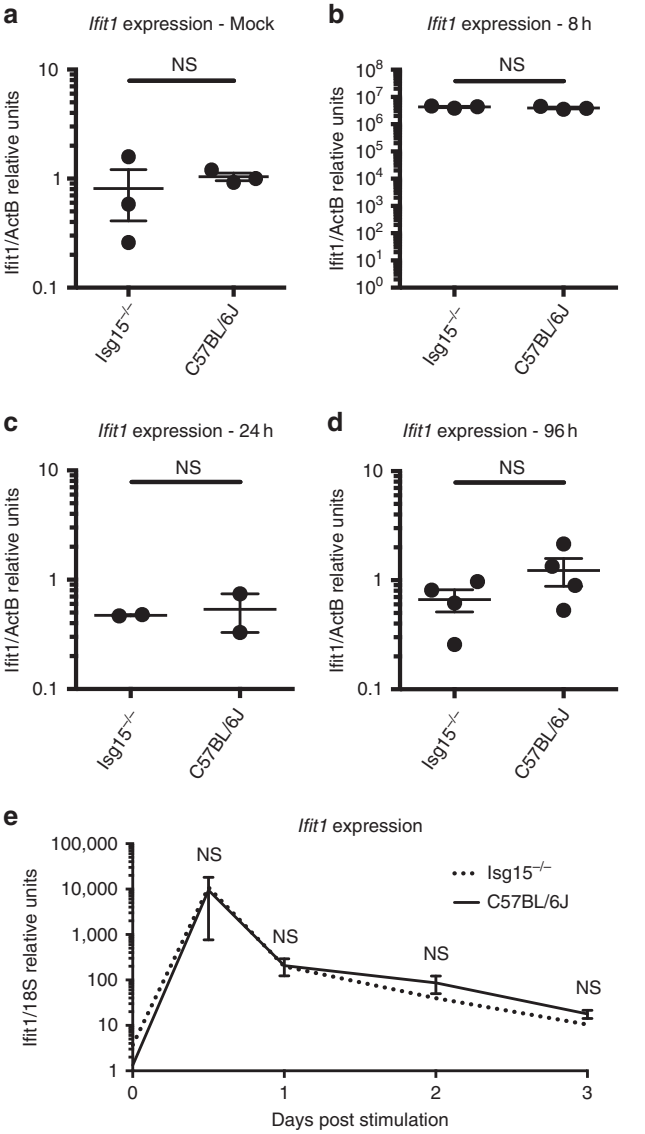

Figure 3 | Murine Isg15 deficiency does not affect the regulation of *Ifit1* transcripts. (**a**–**d**) Age-matched *Isg15*-deficient ($n=2$–4 per group) or WT C57BL6/J ($n=2$-4 group^{-1}) mice received intraperitoneal injections of (**a**) PBS (mock) or (**b**–**d**) 10,000 IU type-I IFN. Animals were sacrificed at the (**b**) 8 h, (**c**) 24 h or (**d**) 96 h post treatment and relative *Ifit1* mRNA levels were determined by qPCR. (**e**) MEFs derived from *Isg15*-deficient or C57BL/6 J mice were mock-treated or primed with 1000 IU ml^{-1} type-I IFN for 12 h, washed and allowed to rest for 36 h. Relative mRNA levels for *Ifit1* were determined by qPCR at the indicated times post-priming. **e** shows the combined results of three experiments. Error bars, s.d. Comparisons made with unpaired *t*-test. NS, not significant.

Isg15 does not sustain Usp18 levels in mice. Due to the suboptimal levels of USP18, IFN-α/β signalling persists and ISG transcripts accumulate in *ISG15*-deficient human cells[10]. We, therefore, investigated whether late IFN-α/β signalling and Usp18 levels were also affected in *Isg15*-deficient murine cells. WT and *Isg15*-deficient MEFs were subjected to prolonged stimulation with IFN-β, and the levels of phosphorylated Stat2 and IFN-stimulated proteins were measured by western blotting. In contrast to what was observed for human fibroblasts, WT and *Isg15*-deficient MEFs accumulated similar levels of phosphorylated Stat2, Ifit2 and Usp18 over the time course of the experiment (Fig. 4a). The IFN-α/β response was also studied in primary bone marrow-derived macrophages (BMM) from WT, *Isg15*-deficient or *Ube1L*-deficient (free Isg15 present, but no ISGylation) mice. No major differences were observed between the three strains, indicating that neither free, nor conjugated Isg15 was required to stabilize Usp18 in mice (Fig. 4b). Similar conclusions were drawn from studies of a murine fibroblast cell line (LL171), in which *Isg15* was silenced with siRNA (Fig. 4c). These results provide strong evidence to suggest that, in the mouse system, Isg15 is not involved in the Usp18-mediated negative feedback loop.

USP18 stabilization by ISG15 is species-specific. The unique properties of the USP18 or ISG15 orthologues, or of both of them, may underlie the observed species-specific functional differences. ISG15 is weakly conserved across species[34], whereas the murine and human USP18 proteins are 70.1% identical and

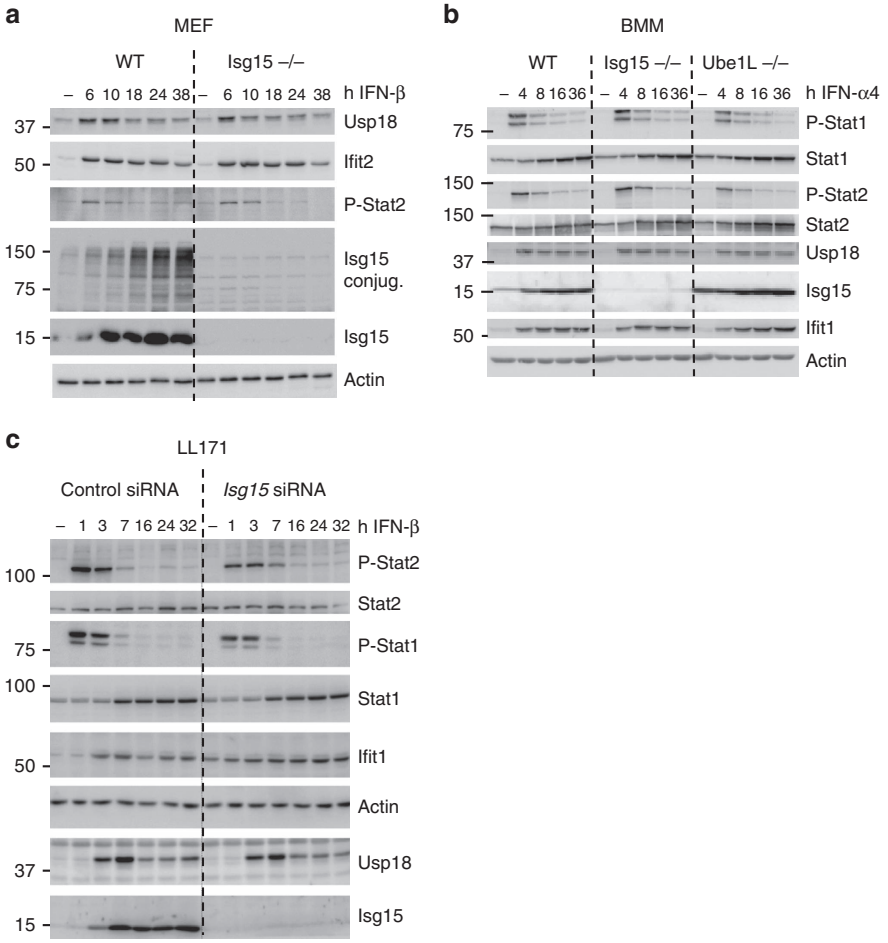

Figure 4 | Murine Isg15 does not control Usp18 accumulation and IFN-α/β signalling. (**a**) Primary MEFs from WT and *Isg15*-deficient mice were primed with murine IFN-β (500 pM) for 6–38 h. Cell lysates (30 μg) were analysed by western blotting with the antibodies indicated. (**b**) BMM from WT, *Isg15*-deficient and *Ube1L*-deficient mice were primed with murine IFN-α4 (250 pM) for 4–36 h. Cell lysates (20 μg) were analysed by western blotting with the antibodies indicated. (**c**) Murine LL171 cells were transfected with non-silencing control or ISG15 siRNA. 24 h post-transfection, the cells were primed for 1–32 h with murine IFN-β (10 pM). Cell lysates (30 μg) were analysed by western blotting with the antibodies indicated.

79.7% similar. We confirmed that human ISG15 stabilizes USP18 through ISGylation-independent binding[10], since the conjugation-deficient ISG15ΔGG mutant was able to stabilize USP18 (Fig. 5a). Furthermore, co-expression of USP18 with an unrelated protein (GFP) did not sustain USP18 levels (Fig. 5b). The ISG15:USP18 complex could be detected by co-immunoprecipitation (co-IP; Fig. 5c, lane 2) and was abolished in the presence of N-ethylmaleimide (NEM), which alkylates cysteine residues (Fig. 5c, lane 3). Yet, the ISG15:USP18 complex retained NEM sensitivity even when we used the USP18-C64S catalytic mutant, suggesting a role for cysteine residues outside of the catalytic core (Fig. 5d).

Next, we tested whether murine Isg15:Usp18 complexes could be detected by co-IP. Weak or completely absent interactions between the two murine proteins was detected in co-IP assays (Fig. 5e). However, USP18 is the cognate deISGylase both in humans and mice. To further examine this interaction we used a micropatterning approach to quantify the stability of the ISG15:USP18 complex in living cells[35]. In this experimental setup, the murine Usp18:Isg15 complex was observed, but it exhibited reduced stability when compared to the human complex (Supplementary Figs 3 and 4, Supplementary Movie 1 and Supplementary Methods). The controls for the micropatterning and fluorescence recovery after photobleaching experiments are outlined in Supplementary Fig. 4. Next, we tested whether transient co-expression of murine Isg15 and Usp18 influenced the levels of murine Usp18. Murine Isg15 failed to sustain the level of murine Usp18 (Fig. 5f–h), in contrast to the phenotype observed with the human orthologues. The inability of overexpressed murine Isg15 to sustain murine Usp18 is consistent with our functional data on the endogenous murine proteins (Fig. 4) and with the comparable downregulation of IFN-α/β responses in WT and *Isg15*-deficient mice *in vivo* (Fig. 3a–d). Altogether, these results indicate that the difference in viral susceptibility between *ISG15*-deficient humans and mice stems from the need for ISG15 to stabilize USP18, and thus downregulate the IFN-α/β response, in humans but not in mice.

Discussion

IFN-α/β signalling and ISG induction are controlled at multiple levels by negative regulators, such as SOCS (suppressor of cytokine signalling), PIAS (protein inhibitor of activated STAT), protein phosphatases (for example, SHP1) and USP18 (refs 36–38). However, we have shown that these regulators are not sufficient, and that ISG15 is required for complete downregulation of IFN-α/β signalling (Fig. 1a). Humans lacking ISG15 consistently display high steady-state levels of ISGs in whole blood, and in patient-derived fibroblasts following priming with IFN-α/β (ref. 10). We hypothesized that this dysregulation

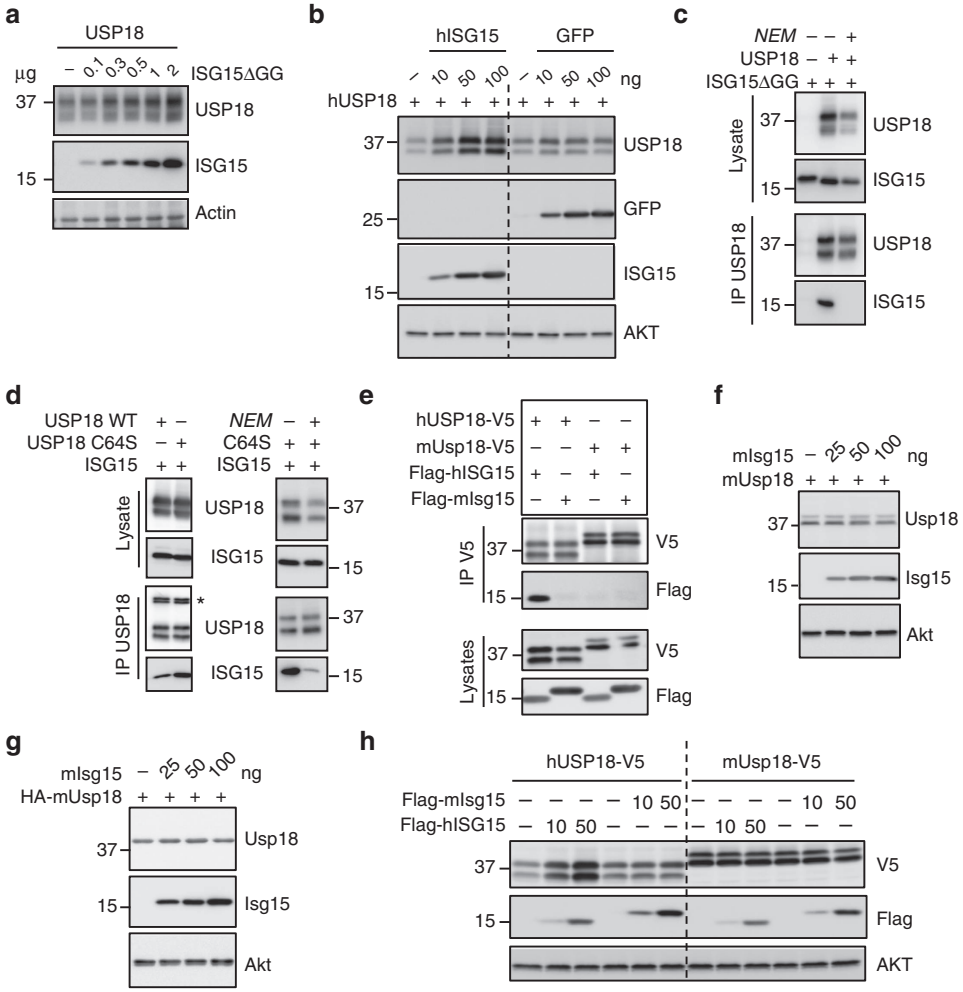

Figure 5 | Murine free Isg15 does not interact stably with Usp18. (**a**) HEK293T cells were transfected with a human USP18 expression vector (0.5 μg) alone or with increasing amounts of the human Flag-ISG15ΔGG construct. 48 h post transfection, cell lysates were analysed by western blot with antibodies against USP18 and Flag. (**b**) Cells were transfected with human USP18 (0.5 μg) alone or with increasing amounts of human ISG15 or GFP expression vectors. 48 h later lysates were analysed with the indicated antibodies. (**c**) Cells were transfected with human Flag-ISG15ΔGG (3 μg) alone or with human USP18, as indicated (1.5 μg). NEM (10 mM) was added to the lysis buffer (lane 3). Lysates were subjected to IP with USP18 antibodies. Lysates and co-IP eluates were analysed with antibodies against USP18 and Flag. (**d**) Left panel: cells were transfected with human Flag-ISG15 (1.5 μg), and either human USP18 WT or USP18 C64S (1.5 μg). 48 h later, lysates were subjected to anti-USP18 IP. Lysates and co-IP eluates were analysed with antibodies against USP18 and Flag. Right panel: cells were cotransfected with Flag-ISG15 (1.5 μg) and USP18 C64S (1.5 μg). NEM (10 mM) was added to the lysis buffer (lane 3). Lysates were subjected to anti-USP18 IP. Lysates and co-IP eluates were analysed with antibodies to USP18 and Flag. (**e**) Cells were cotransfected with human or murine USP18-V5 and human or murine Flag-ISG15. 48 h later, lysates were subjected to co-IP with anti-V5 antibodies. Co-IP eluates (top panels) and total lysates (bottom panels) were analysed with the indicated antibodies. (**f**) Cells were transfected with untagged murine Usp18 (0.5 μg) alone or with increasing amounts of murine Flag-Isg15. Lysates were analysed with antibodies to murine Usp18, Flag and Akt. (**g**) As in **f**, except that HA-tagged murine Usp18 was transfected and detected with HA antibodies. (**h**) Cells were transfected with human USP18-V5 or murine Usp18-V5 Usp18 (500 ng) alone or with the indicated amount of human Flag-ISG15 or murine Flag-Isg15. 48 h later, cell lysates were analysed by western blot.

of IFN-α/β signalling would account for the lack of an overt viral susceptibility in humans, in contrast to what was observed in mice. We show here that, unlike the antiviral activity of Isg15 observed in mice, human ISG15 promotes a proviral state following IFN priming. The persistent ISG expression observed in human *ISG15*-deficient cells imparts a resistance to infection with multiple families of viruses with both RNA and DNA genomes.

These findings contrast from previous reports that have ascribed an antiviral role to ISG15 in human cells. Shi *et al.*[29] reported that, following silencing of ISG15 for 48 h in HEK-293 cells, SeV titres increased by ~0.5 and ~1.0 log at 6 h and 12 h post infection, respectively. Tang *et al.*[23] found that following ISG15 silencing, A549 cells became ~fivefold more susceptible to infection by IAV (A/PR/8/1934). While these studies point to an antiviral role of ISG15 in human cells, our experiments with SeV and IAV do not capture the small observed difference in viral growth when comparing WT and *ISG15*-deficient hTert-immortalized fibroblasts without IFN priming (Fig. 1). These studies focused on early timepoints of the acute IFN response induced by the virus, and did not capture the more powerful role of ISG15 as a negative regulator of IFN signalling. Even if there may be a small antiviral role for ISG15 during the acute IFN response, it is clinically irrelevant *in vivo* and not readily captured *in vitro*.

Interestingly, we observed that the conjugation-deficient ISG15ΔGG was as efficient as WT ISG15 in rescuing viral replication in *ISG15*-deficient patient cells. One could have predicted an even better rescue of both the ISG expression and

infection phenotypes by ISG15ΔGG, since the latter should be more readily accessible to mediate USP18 stability than the conjugation-competent form of ISG15. However, this was not the case, suggesting the possibility that ISG15ΔGG may have lower USP18-binding affinity or that only a small amount of ISG15 is required to stabilize USP18, and the increased availability of ISG15ΔGG has no further effect. An additional possibility, albeit less likely given the depth of work demonstrating the antiviral role of ISGylation, is that ISG15 in the conjugated form may also exhibit some proviral properties.

We have shown that free ISG15 associates with higher affinity to USP18 in humans as compared with mice, although the species-specific structural determinants involved in complex formation have yet to be identified. Another species-restricted complex involving free ISG15 has been described. The NS1 protein of influenza B virus binds non-covalently to human and non-human primate ISG15, but not to murine Isg15 (refs 39–41). Mutational and structural studies of the NS1:ISG15 complex have shown that the molecular determinant of the binding specificity (humans versus mice) lies in the small hinge region of ISG15 (refs 42,43). Further work is required to identify the domain(s) responsible for the human ISG15:USP18 interactions that are required to enhance stability and properly regulate the IFN responses.

Unlike humans, mice can downregulate IFN signalling regardless of ISG15 competency and it is currently unknown whether murine Usp18 is stabilized by another protein, IFN-stimulated or otherwise. Individuals lacking ISG15 exhibit elevated ISG expression, which may confer an enhanced protection against viral infection, but do not exhibit any of the side-effects associated with IFN treatment[10]. As such, the USP18:ISG15 interaction is a potentially attractive target for small molecule-based short-term treatments to boost endogenous IFN activity.

Our findings raise interesting questions about the evolutionary role of ISG15. Given the detrimental effects that inflammation may cause in species with a longer lifespan, gain-of-function binding mutations in ISG15 and/or USP18 may reflect an evolutionary necessity in humans, and likely other mammals, to more stringent tuning of the IFN system. On the other hand, viruses have developed immune evasion strategies in parallel. Indeed, many human viral pathogens were shown to oppose ISGylation (influenza B virus NS1[39] and vaccinia virus E3L[16,44] proteins) or induce de-ISGylation (numerous viral L proteins containing ovarian tumour[45] or papain-like protease[46]). Much of the work characterizing these viral proteins has focused on the inhibition/removal of conjugated ISG15 from viral and host targets. However, in light of our data demonstrating that the primary role of human ISG15 is to stabilize USP18 and downregulate the IFN response, it may be that inhibition of ISGylation and removal of conjugated ISG15 is a novel mode of IFN antagonism. By enhancing the pool of free ISG15, these viral proteins may enhance USP18 levels, dampen IFN signalling and promote viral escape.

Based on current knowledge, murine Isg15 acts in an antiviral manner (largely *via* ISGylation), while murine Usp18 functions in a proviral manner (IFN negative regulation and de-ISGylation). By contrast, human ISG15 and USP18 both appear to function in an anti-inflammatory manner. Consequently, this makes them proviral, although the ISGylation of cellular or viral proteins may play a non-dominant antiviral role. However, if both ISGylation and de-ISGylation are proviral (through provision of the free ISG15 required for USP18 stabilization), this notion becomes somewhat paradoxical. In humans then, this process may serve as a mechanism for the temporal regulation of IFN-α/β-induced signalling. We suggest that one of the roles of ISGylation at early stages of viral infection in humans is to sequester free ISG15, thereby allowing IFN signalling to occur. At later stages, USP18-mediated de-ISGylation releases free ISG15, which in turn stabilizes USP18 and tunes down IFN-α/β signalling and inflammation.

Methods

Cells. Icahn School of Medicine IRB board has approved the use of human subject cell lines. Dermal fibroblasts from *ISG15*-deficient patients ($n=3$) and WT controls ($n=5$) were immortalized by stable transduction with hTert[10]. Patient ($n=3$) and control ($n=2$) cells were stably complemented with ISG15, ISG15ΔGG or luciferase by lentiviral transduction[10]. Transduced fibroblasts were sorted on the basis of RFP expression (BD FACS Aria II). The stable expression of the transduced constructs was periodically checked by western blotting. Murine embryonic fibroblasts from WT C57BL6/J and *Isg15*-deficient mice were derived by disaggregation of day 13.5 embryos from timed matings by trituration of the embryos at 37 °C in trypsin[19]. Mouse bone marrow macrophages (BMM) were generated by isolating bone marrow cells capable of adhering to non-tissue-culture treated plates for 7 days in BMM media (Dulbeco's Modified Eagle Medium, 10% fetal calf serum, 5% horse serum, 2% supernatant derived from CMG14-12 cells)[47]. LL171 cells (clonal isolate of murine L929 fibroblasts; from G. Uzé, CNRS, Montpellier, France), HEK293T (CRL-11268; ATCC), Vero-E6 (CRL-1586; ATCC), Vero (CCL81; ATCC), HeLa (CCL-2; ATCC), A549 (CCL-185; ATCC), murine embryonic fibroblasts and human fibroblasts were cultured in normal growth medium consisting of DMEM supplemented with 10% fetal calf serum. All cells were cultured at 37 °C and 10% CO_2. All cells were tested for mycoplasma contamination using the PlasmoTest kit according to the manufacturer instructions (Invivogen).

Priming. Untransduced, luciferase-, ISG15-, and ISG15ΔGG-transduced fibroblasts (Figs 1–3) were primed by incubation with 0, 10, 100, or 1,000 IU ml^{-1} IFN-α2b (Merck IntronA) in normal growth medium for 12 h. The IFN-α2b was then eliminated by thorough washing with PBS and the cells were allowed to rest for 36 h in normal medium before infection. Murine embryonic fibroblasts were primed with 1,000 U universal type-I IFN (Fig. 3; PBL IFN) or 500 pM murine IFN-β (Fig. 4; PBL IFN). Mouse bone marrow macrophages were primed with 250 pM murine IFN-α4 (Fig. 4; Calbiochem). LL171 cells were primed with 10 pM murine IFN-β (Fig. 4; PBL IFN).

ISG Expression analysis. RNA was extracted from fibroblasts (Qiagen RNeasy) or whole blood (PAXgene Blood RNA Kit) and reverse-transcribed (ABI High Capacity Reverse Transcriptase) according to the instructions provided by the manufacturer. Levels of ISG expression (*IFIT1, MX1*), relative to the *18S* rRNA housekeeper gene, were analysed by Taqman quantitative real-time PCR (TaqMan Universal Master Mix II w/ UNG, Roche LightCycler 480 II). The relative expression levels of the ISGs were calculated by the ΔΔCT method, with comparison with the mean value for mock-treated controls.

Viral infections. All infections were performed 48 h after IFN treatment (12 h priming, 36 h rest) in normal growth medium. The viruses and multiplicities of infection used were as follows: VSV Indiana strain at an MOI of 1.0, rVSV–GFP Indiana strain[48] at an MOI of 10.0, rHSV-1 US11-GFP Patton strain[49] at an MOI of 1.0 (kindly provided by the laboratory of Ian Mohr), rHCMV IE2-YFP strain AD169 (ref. 50) at an MOI of 2.0, rIAV A/PR/8/34 gLuc virus[51] modified by the introduction of a PTV1 2A cleavage site (PR8-gLuc-PTV1; kindly provided by Nick Heaton) at an MOI of 10.0, rSeV-eGFP Fushimi strain[52] modified by the introduction of a gLuc-P2A cleavage site (rSeV-gLuc-P2A-eGFP; same method as for NiV below) at an MOI of 0.1, RVFV strain ZH501 at an MOI of 0.01, and the rNiV-gLuc-P2A-eGFP Malaysian strain[52] at an MOI of 0.01. All work with infectious RVFV and rNiV was carried out under biosafety level 4 (BSL-4) conditions at the Robert E. Shope BSL-4 laboratory at the University of Texas Medical Branch.

Analysis of viral replication. VSV-infected supernatants were removed 24 h.p.i. and titered by determining the 50% tissue culture infectious dose on Vero-E6 cells. RVFV and rNiV-gLuc-P2A-eGFP-infected supernatants were collected at 48 and 24 h.p.i., respectively, and titered by plaque assays on Vero-CCL81 cells. Fibroblasts infected with rVSV–GFP or rHSV-1-US11-GFP were fixed in 4% PFA 24 h.p.i. and stained with 5 μg ml^{-1} Hoechst 33342 in PBS. Cells were imaged and the results were analysed (BioTek Cytation 3; Gen5 software). HCMV-IE2-YFP-infected cells were fixed with 4% PFA 24 h.p.i., and imaging analysis was performed on an Acumen Explorer plate cytometer. Fibroblasts infected with IAV PR8-gLuc-PTV1 were collected and washed with PBS at 24 h.p.i. The cells were lysed and assayed for luciferase activity, according to the manufacturer's instructions (Promega Renilla Luciferase Assay System; BioTek Cytation 3). We collected rSeV-gLuc-P2A-eGFP-infected supernatants were collected at 24 h.p.i. Supernatant samples were inactivated with lysis buffer, and assayed for luciferase activity

according to the manufacturer's instructions (Promega Renilla Luciferase Assay System; BioTek Cytation 3).

Mouse studies. Co-housed 10-week-old female C57BL6/J (Jackson) and *Isg15*-deficient[19] mice received intraperitoneal injections of PBS or 10,000 IU universal type-I IFN (PBL Interferon Source). At the post-treatment times indicated, the mice were sacrificed and exsanguinated for the analysis of ISG levels in whole blood. All procedures were carried out in accordance with National Institutes of Health and Icahn School of Medicine at Mount SinaiInstitutional Animal Care and Use Committee guidelines.

Plasmids and transfection. HEK-293 T cells were transiently transfected with Lipofectamine-2000 (Invitrogen), complexed with the following constructs according to the instructions provided by the manufacturer. Pseudotyped lentiviral particles were produced by transfection of pCAGGS-VSV-G, pCMV-Gag/Pol and pTRIP-hISG15ΔGG-IRES-RFP. The following constructs were used for expression and co-IP assays: pcDNA4b-huUSP18 (ref. 53), pcDNA3-3xFlag-huISG15 (from J. Huibregtse, University of Texas at Austin, TX, USA), pBabe-3xFlag-His6-huISG15ΔGG was derived from the construct above; pBK-CMV-mUsp18, pcDNA3-HA-mUsp18 and pCAGGS-Flag-mIsg15 (Addgene), pEGFP-N1 (Clontech), pcDNA4B-hUSP18-V5, and pcDNA4B-mUsp18-V5.

siRNA-mediated silencing. Murine LL171 cells were silenced by incubation for 24 h with 25 nM Isg15 siRNA (5′-CACAGUGAUGCUAGUGGUACA-3′; Sigma) followed by priming with IFN. HeLa and A549 cells were silenced by incubation for 24 h with 25 nM ISG15 siRNA followed by priming with IFN. siRNA transfections were performed with Lipofectamine RNAi max reagent (Invitrogen) according to the manufacturer's instructions.

Protein analysis. Cells were lysed in radioimmunoprecipitation assay buffer (RIPA buffer; 10 mM Tris-Cl, 1 mM EDTA, 0.5 mM EGTA, 1% Triton X-100, 0.1% sodium deoxycholate, 0.1% SDS, 140 mM NaCl, 150 mM PMSF, protease inhibitor cocktail (Sigma-Aldrich), 1 μg ml^{-1} okadaic acid (Merck), and Halt phosphatase inhibitor (Thermo Scientific)) and analysed by western blot. For co-IP assays, transfected cells were lysed in 50 mM Tris pH 6.8, 0.5% Nonidet P40, 200 mM NaCl, 10% glycerol, 1 mM EDTA and a protease inhibitor cocktail. Sensitivity to NEM (Sigma-Aldrich) was assessed by adding this compound to the lysis buffer at a concentration of 10 mM. USP18 was immunoprecipitated with anti-human USP18 (Cell Signaling Technology D4E7, 1:250) or anti-V5 (Invitrogen R960-25, 1:200) monoclonal antibodies. The following antibodies were used for western blot analysis: human ISG15 (Santa Cruz 3E5, 1:1,000; ABGENT AP1150a, 1:1,000; mAb cl. 2.1, 1:1,000 (a gift from E.C. Borden, Cleveland Clinic, Cleveland OH[54])); human USP18 (Cell Signaling Technology D4E7, 1:5,000); murine Isg15 (rabbit mAb 1551, 1:3,000; or rabbit pAbs, 1:5,000 (a gift from A.L. Haas, LSU Health Sciences Center School of Medicine, New Orleans, LA[55]); murine Usp18 (1:3,000 (a gift from K.P. Knobeloch, University of Freiburg, Freiburg, Germany[56]); V20 (Santa Cruz Biotechnology sc-50019, 1:200); murine Ifit1 (1:5,000) and Ifit2 (1:10,000; gifts from G. Sen (Cleveland Clinic, Cleveland, OH[57]); Stat1 (Millipore 06-501, 1:2,000); phospho-Stat1 (Cell Signaling Technology 9171 L, 1:1,000); murine Stat2 (1:5,000) (a gift from C. Schindler, Columbia University, NY, NY[58]); phospho-Stat2 (Millipore 07224, 1:1000); AKT (Cell Signaling Technology 40D4, 1:1000); actin (Sigma-Aldrich cl. AC-40, 1:10,000); HA (Sigma-Aldrich H9658, 1:2,000); Flag (Sigma-Aldrich F3165, 1:5,000); GFP (Rockland Immunochemicals 600-101-215, 1:1,000); V5 (Sigma-Aldrich V8137, 1:5,000). Antibody binding was detected by enhanced chemiluminescence (Western Lightning, Perkin Elmer). Relative band intensities were determined with a Fuji ImageQuant LAS-4000. Uncropped images for Fig. 4a and b can be found in Supplementary Fig. 5a–b. Uncropped images for Fig. 5a,e,f,h can be found in Supplementary Fig. 6a–d (ref. 59).

References

1. Narasimhan, J. *et al.* Crystal structure of the interferon-induced ubiquitin-like protein ISG15. *J. Biol. Chem.* **280,** 27356–27365 (2005).
2. Farrell, P. J., Broeze, R. J. & Lengyel, P. Accumulation of an mRNA and protein in interferon-treated Ehrlich ascites tumour cells. *Nature* **279,** 523–525 (1979).
3. Korant, B. D., Blomstrom, D. C., Jonak, G. J. & Knight, Jr. E. Interferon-induced proteins. Purification and characterization of a 15,000-dalton protein from human and bovine cells induced by interferon. *J. Biol. Chem.* **259,** 14835–14839 (1984).
4. Blomstrom, D. C., Fahey, D., Kutny, R., Korant, B. D. & Knight, Jr. E. Molecular characterization of the interferon-induced 15-kDa protein. Molecular cloning and nucleotide and amino acid sequence. *J. Biol. Chem.* **261,** 8811–8816 (1986).
5. Reich, N. *et al.* Interferon-induced transcription of a gene encoding a 15-kDa protein depends on an upstream enhancer element. *Proc. Natl Acad. Sci. USA* **84,** 6394–6398 (1987).
6. Kessler, D. S., Levy, D. E. & Darnell, Jr. J. E. Two interferon-induced nuclear factors bind a single promoter element in interferon-stimulated genes. *Proc. Natl Acad. Sci. USA* **85,** 8521–8525 (1988).
7. Knight, Jr. E. *et al.* A 15-kDa interferon-induced protein is derived by COOH-terminal processing of a 17-kDa precursor. *J. Biol. Chem.* **263,** 4520–4522 (1988).
8. Durfee, L. A. & Huibregtse, J. M. Identification and validation of ISG15 target proteins. *Subcell. Biochem.* **54,** 228–237 (2010).
9. Bogunovic, D. *et al.* Mycobacterial disease and impaired IFN-gamma immunity in humans with inherited ISG15 deficiency. *Science* **337,** 1684–1688 (2012).
10. Zhang, X. *et al.* Human intracellular ISG15 prevents interferon-alpha/beta over-amplification and auto-inflammation. *Nature* **517,** 89–93 (2015).
11. Zhang, D. & Zhang, D. E. Interferon-stimulated gene 15 and the protein ISGylation system. *J. Interferon Cytokine Res.* **31,** 119–130 (2011).
12. Basters, A. *et al.* Molecular characterization of ubiquitin-specific protease 18 reveals substrate specificity for interferon-stimulated gene 15. *FEBS J.* **281,** 1918–1928 (2014).
13. Malakhova, O. A. *et al.* UBP43 is a novel regulator of interferon signaling independent of its ISG15 isopeptidase activity. *EMBO J.* **25,** 2358–2367 (2006).
14. Lenschow, D. J. *et al.* IFN-stimulated gene 15 functions as a critical antiviral molecule against influenza, herpes, and Sindbis viruses. *Proc. Natl Acad. Sci. USA* **104,** 1371–1376 (2007).
15. Hsiao, N. W. *et al.* ISG15 over-expression inhibits replication of the Japanese encephalitis virus in human medulloblastoma cells. *Antiviral Res.* **85,** 504–511 (2010).
16. Guerra, S., Caceres, A., Knobeloch, K. P., Horak, I. & Esteban, M. Vaccinia virus E3 protein prevents the antiviral action of ISG15. *PLoS Pathog.* **4,** e1000096 (2008).
17. Werneke, S. W. *et al.* ISG15 is critical in the control of Chikungunya virus infection independent of UbE1L mediated conjugation. *PLoS Pathog.* **7,** e1002322 (2011).
18. Rodriguez, M. R., Monte, K., Thackray, L. B. & Lenschow, D. J. ISG15 functions as an interferon-mediated antiviral effector early in the murine norovirus life cycle. *J. Virol.* **88,** 9277–9286 (2014).
19. Osiak, A., Utermohlen, O., Niendorf, S., Horak, I. & Knobeloch, K. P. ISG15, an interferon-stimulated ubiquitin-like protein, is not essential for STAT1 signaling and responses against vesicular stomatitis and lymphocytic choriomeningitis virus. *Mol. Cell. Biol.* **25,** 6338–6345 (2005).
20. Zhang, Y., Burke, C. W., Ryman, K. D. & Klimstra, W. B. Identification and characterization of interferon-induced proteins that inhibit alphavirus replication. *J. Virol.* **81,** 11246–11255 (2007).
21. Malakhova, O. A. & Zhang, D. E. ISG15 inhibits Nedd4 ubiquitin E3 activity and enhances the innate antiviral response. *J. Biol. Chem.* **283,** 8783–8787 (2008).
22. Dai, J., Pan, W. & Wang, P. ISG15 facilitates cellular antiviral response to dengue and west nile virus infection *in vitro*. *Virol. J.* **8,** 468 (2011).
23. Tang, Y. *et al.* Herc5 attenuates influenza A virus by catalyzing ISGylation of viral NS1 protein. *J. Immunol.* **184,** 5777–5790 (2010).
24. Kuang, Z., Seo, E. J. & Leis, J. Mechanism of inhibition of retrovirus release from cells by interferon-induced gene ISG15. *J. Virol.* **85,** 7153–7161 (2011).
25. Okumura, A., Lu, G., Pitha-Rowe, I. & Pitha, P. M. Innate antiviral response targets HIV-1 release by the induction of ubiquitin-like protein ISG15. *Proc. Natl Acad. Sci. USA* **103,** 1440–1445 (2006).
26. Pincetic, A., Kuang, Z., Seo, E. J. & Leis, J. The interferon-induced gene ISG15 blocks retrovirus release from cells late in the budding process. *J. Virol.* **84,** 4725–4736 (2010).
27. Okumura, A., Pitha, P. M. & Harty, R. N. ISG15 inhibits Ebola VP40 VLP budding in an L-domain-dependent manner by blocking Nedd4 ligase activity. *Proc. Natl Acad. Sci. USA* **105,** 3974–3979 (2008).
28. Durfee, L. A., Lyon, N., Seo, K. & Huibregtse, J. M. The ISG15 conjugation system broadly targets newly synthesized proteins: implications for the antiviral function of ISG15. *Mol. Cell* **38,** 722–732 (2010).
29. Shi, H. X. *et al.* Positive regulation of interferon regulatory factor 3 activation by Herc5 via ISG15 modification. *Mol. Cell. Biol.* **30,** 2424–2436 (2010).
30. Broering, R. *et al.* The interferon stimulated gene 15 functions as a proviral factor for the hepatitis C virus and as a regulator of the IFN response. *Gut* **59,** 1111–1119 (2010).
31. Chua, P. K. *et al.* Modulation of alpha interferon anti-hepatitis C virus activity by ISG15. *J. Gen. Virol.* **90,** 2929–2939 (2009).
32. Francois-Newton, V., Livingstone, M., Payelle-Brogard, B., Uze, G. & Pellegrini, S. USP18 establishes the transcriptional and anti-proliferative interferon alpha/beta differential. *Biochem. J.* **446,** 509–516 (2012).
33. Lai, C. *et al.* Mice lacking the ISG15 E1 enzyme UbE1L demonstrate increased susceptibility to both mouse-adapted and non-mouse-adapted influenza B virus infection. *J. Virol.* **83,** 1147–1151 (2009).
34. Bogunovic, D., Boisson-Dupuis, S. & Casanova, J. L. ISG15: leading a double life as a secreted molecule. *Exp. Mol. Med.* **45,** e18 (2013).

35. Lochte, S., Waichman, S., Beutel, O., You, C. & Piehler, J. Live cell micropatterning reveals the dynamics of signaling complexes at the plasma membrane. *J. Cell Biol.* **207,** 407–418 (2014).
36. Hertzog, P. J. & Williams, B. R. Fine tuning type I interferon responses. *Cytokine Growth Factor Rev.* **24,** 217–225 (2013).
37. Ivashkiv, L. B. & Donlin, L. T. Regulation of type I interferon responses. *Nat. Rev. Immunol.* **14,** 36–49 (2014).
38. Porritt, R. A. & Hertzog, P. J. Dynamic control of type I IFN signalling by an integrated network of negative regulators. *Trends Immunol.* **36,** 150–160 (2015).
39. Yuan, W. & Krug, R. M. Influenza B virus NS1 protein inhibits conjugation of the interferon (IFN)-induced ubiquitin-like ISG15 protein. *EMBO J.* **20,** 362–371 (2001).
40. Zhao, C., Collins, M. N., Hsiang, T. Y. & Krug, R. M. Interferon-induced ISG15 pathway: an ongoing virus-host battle. *Trends Microbiol.* **21,** 181–186 (2013).
41. Versteeg, G. A. *et al.* Species-specific antagonism of host ISGylation by the influenza B virus NS1 protein. *J. Virol.* **84,** 5423–5430 (2010).
42. Guan, R. *et al.* Structural basis for the sequence-specific recognition of human ISG15 by the NS1 protein of influenza B virus. *Proc. Natl Acad. Sci. USA* **108,** 13468–13473 (2011).
43. Sridharan, H., Zhao, C. & Krug, R. M. Species specificity of the NS1 protein of influenza B virus: NS1 binds only human and non-human primate ubiquitin-like ISG15 proteins. *J. Biol. Chem.* **285,** 7852–7856 (2010).
44. Eduardo-Correia, B., Martinez-Romero, C., Garcia-Sastre, A. & Guerra, S. ISG15 is counteracted by vaccinia virus E3 protein and controls the proinflammatory response against viral infection. *J. Virol.* **88,** 2312–2318 (2014).
45. Bailey-Elkin, B. A., van Kasteren, P. B., Snijder, E. J., Kikkert, M. & Mark, B. L. Viral OTU deubiquitinases: a structural and functional comparison. *PLoS Pathog.* **10,** e1003894 (2014).
46. Mielech, A. M., Chen, Y., Mesecar, A. D. & Baker, S. C. Nidovirus papain-like proteases: multifunctional enzymes with protease, deubiquitinating and deISGylating activities. *Virus Res.* **194,** 184–190 (2014).
47. Hwang, S. *et al.* Nondegradative role of Atg5-Atg12/ Atg16L1 autophagy protein complex in antiviral activity of interferon gamma. *Cell Host Microbe* **11,** 397–409 (2012).
48. Stojdl, D. F. *et al.* VSV strains with defects in their ability to shutdown innate immunity are potent systemic anti-cancer agents. *Cancer Cell* **4,** 263–275 (2003).
49. Benboudjema, L., Mulvey, M., Gao, Y., Pimplikar, S. W. & Mohr, I. Association of the herpes simplex virus type 1 Us11 gene product with the cellular kinesin light-chain-related protein PAT1 results in the redistribution of both polypeptides. *J. Virol.* **77,** 9192–9203 (2003).
50. Gardner, T. J. *et al.* Development of a high-throughput assay to measure the neutralization capability of anti-cytomegalovirus antibodies. *Clin. Vaccine Immunol.* **20,** 540–550 (2013).
51. Heaton, N. S. *et al. In vivo* bioluminescent imaging of influenza a virus infection and characterization of novel cross-protective monoclonal antibodies. *J. Virol.* **87,** 8272–8281 (2013).
52. Pernet, O. *et al.* Evidence for henipavirus spillover into human populations in Africa. *Nat. Commun.* **5,** 5342 (2014).
53. Francois-Newton, V. *et al.* USP18-based negative feedback control is induced by type I and type III interferons and specifically inactivates interferon alpha response. *PLoS ONE* **6,** e22200 (2011).
54. D'Cunha, J. *et al. In vitro* and *in vivo* secretion of human ISG15, an IFN-induced immunomodulatory cytokine. *J. Immunol.* **157,** 4100–4108 (1996).
55. Loeb, K. R. & Haas, A. L. The interferon-inducible 15-kDa ubiquitin homolog conjugates to intracellular proteins. *J. Biol. Chem.* **267,** 7806–7813 (1992).
56. Ketscher, L. *et al.* Selective inactivation of USP18 isopeptidase activity *in vivo* enhances ISG15 conjugation and viral resistance. *Proc. Natl Acad. Sci. USA* **112,** 1577–1582 (2015).
57. Terenzi, F., White, C., Pal, S., Williams, B. R. & Sen, G. C. Tissue-specific and inducer-specific differential induction of ISG56 and ISG54 in mice. *J. Virol.* **81,** 8656–8665 (2007).
58. Park, C., Li, S., Cha, E. & Schindler, C. Immune response in Stat2 knockout mice. *Immunity* **13,** 795–804 (2000).
59. Wedeking, T. *et al.* Spatiotemporally controlled reorganization of signaling complexes in the plasma membrane of living cells. *Small* **11,** 5912–5918 (2015).

Acknowledgements

This was supported in part by NIH grant R00 AI106942-02 to D.B., NIH grant R01 AI101820 to D.T., an American Heart Association pre-doctoral fellowship and a USPHS Institutional Research Training Award T32-AI07647 to T.J.G., NRSA T32 AR07279-30 to M.R.R., NIH grant RO1 A1080672 and Pew Scholar Award to D.J.L., funding by the DFG (SFB 944) to J.P., NIH grant R33 AI102267 to A.N.F. and B.L., CRIP (Center for Research on Influenza Pathogenesis), and NIAID funded Center of Excellence for Influenza Research and Surveillance (contract #HHSN272201400008C) to AGS. Experimental support was provided by the Speed Congenics Facility of the Rheumatic Disease Core Center (P30 AR048335). Work in the Cytokine Signaling Unit was supported by Institut Pasteur, CNRS, INSERM and an Amgen Scholarship to E.R.

Author contributions

S.D.S. and B.P.-B. contributed significantly to the acquisition, analysis and interpretation of data, study design and drafting of the manuscript. Z.L., S.B., B.P.-B., L.Q., F.V., E.R., T.J.G., T.W., M.H. and J.D. contributed significantly to the acquisition of data and critical review of the manuscript. O.S., I.T., N.M., P.T., D.M., V.F.-N., C.F.D. and M.R.R. contributed significantly to development of necessary reagents and critical review of the manuscript. D.L., A.N.F., D.T., J.P., B.L., A.G.S., S.P. and D.B. contributed significantly to the interpretation of data, study design, drafting and critical review of the manuscript.

Additional information

Supplementary Information accompanies this paper at http://www.nature.com/naturecommunications

Competing financial interests: The authors declare no competing financial interests.

Reprints and permission information is available online at http://npg.nature.com/reprintsandpermissions/

How to cite this article: Speer, S. D. *et al.* ISG15 deficiency and increased viral resistance in humans but not mice. *Nat. Commun.* 7:11496 doi: 10.1038/ncomms11496 (2016).

Part II-2 Mechanistic studies of USP18 function in negative regulation of IFN signaling

As discussed in the Introduction, USP18 down-regulates the IFN response in a fine-tuned manner by attenuating ligand/receptor binding to different extent depending on the binding affinity of the IFN subtypes (163). Here we have addressed the question of how USP18 regulates this plasticity. By optimizing single-molecule fluorescence imaging techniques, our collaborators (J. Piehler and coll.) were able to measure the assembly of ligand and receptor subunits in live cells at physiological receptors levels. They demonstrated that USP18 downregulates IFN-α2 response by attenuating IFNAR1 recruitment and thus by impairing the formation of a ternary (ligand/IFNAR2/IFNAR1) complex. This work also showed that JAK1 binding to IFNAR2, but not JAK1 catalytic activity, is required for efficient IFNα2-driven receptor dimerization (177).

The IFNα2-M148A mutant binds IFNAR2 with 50-fold reduced affinity compared to IFNα2 so that fluorescently labeled ^{DY647}IFNα2-M148A only binds significantly to cell surface receptors when it interacts simultaneously with IFNAR1 and IFNAR2, and thus it was used as an indirect marker of ternary complex (177). Upon expression of USP18, binding of ^{DY647}IFNα2-M148A to the cell surface was reduced by 80%. USP18 did not interfere with the binding of IFN to IFNAR2, instead it affected the ability to recruit IFNAR1 and to form a ternary complex.

My contribution to these studies have been: 1) to validate the activity of IFNα2-M148A and show that it is able to induce desensitization (Fig. 1) and 2) to demonstrate that mutants of IFNα2 that exhibit reduced affinity to IFNAR1 mimic the USP18 phenotype on dampening IFN response. I performed dose-response assays with different IFNα2 mutants using a stable clone expressing ectopic USP18 (HU13 cells). The dose-response curves of IFNα2 revealed a substantial reduction in the maximum level of pSTAT1 and pSTAT2 upon ectopic expression of USP18 (HU13). Indeed, the maximum amplitudes of pSTAT1 and pSTAT2 were reduced by 75% and 50%, respectively, which is in line with the reduced maximum number of ternary complexes formed in the presence of USP18 and measured by single-molecule fluorescence imaging techniques. For IFNα2-R120A, a mutant with 60-fold reduced IFNAR1 binding affinity, a similar reduction in the maximum amplitude of pSTAT1 and pSTAT2 was already observed in the absence of USP18. In contrast, for IFNα2-M148A, with its 50-fold reduced binding affinity toward IFNAR2, the same maximum level of phospho-STATs as for IFNα2-wt was still obtained, though at higher ligand concentrations (Fig. 2). Thus, the reduction of

the affinity of IFN toward IFNAR1 mimics the phenotype caused by USP18, corroborating the fact that USP18 regulates IFN signaling at the level of IFNAR1 recruitment and receptor dimerization dynamics. This work is described in (177). Fig. 1 and Fig. 2 are attached hereafter with the first page of the article.

Published May 25, 2015

Receptor dimerization dynamics as a regulatory valve for plasticity of type I interferon signaling

Stephan Wilmes,[1] Oliver Beutel,[1] Zhi Li,[2] Véronique Francois-Newton,[2] Christian P. Richter,[1] Dennis Janning,[1] Cindy Kroll,[1] Patrizia Hanhart,[1] Katharina Hötte,[1] Changjiang You,[1] Gilles Uzé,[3] Sandra Pellegrini,[2] and Jacob Piehler[1]

[1]Department of Biology, Division of Biophysics, University of Osnabrück, 49074 Osnabrück, Germany
[2]Institut Pasteur, Cytokine Signaling Unit, Centre National de la Recherche Scientifique URA1961, 75724 Paris, France
[3]Centre National de la Recherche Scientifique Montpellier, 34095 Montpellier, France

Type I interferons (IFNs) activate differential cellular responses through a shared cell surface receptor composed of the two subunits, IFNAR1 and IFNAR2. We propose here a mechanistic model for how IFN receptor plasticity is regulated on the level of receptor dimerization. Quantitative single-molecule imaging of receptor assembly in the plasma membrane of living cells clearly identified IFN-induced dimerization of IFNAR1 and IFNAR2. The negative feedback regulator ubiquitin-specific protease 18 (USP18) potently interferes with the recruitment of IFNAR1 into the ternary complex, probably by impeding complex stabilization related to the associated Janus kinases. Thus, the responsiveness to IFNα2 is potently down-regulated after the first wave of gene induction, while IFNβ, due to its ∼100-fold higher binding affinity, is still able to efficiently recruit IFNAR1. Consistent with functional data, this novel regulatory mechanism at the level of receptor assembly explains how signaling by IFNβ is maintained over longer times compared with IFNα2 as a temporally encoded cause of functional receptor plasticity.

Introduction

Functional plasticity, i.e., the ability to elicit differential cellular responses through the same cell surface receptor by means of different ligands, is a frequently observed feature of cytokine receptor signaling (Moraga et al., 2014), which plays an important role for drug development (Schreiber and Walter, 2010). The molecular mechanisms regulating functional plasticity have so far remained unclear, though some common determinants are emerging (Moraga et al., 2014). A prominent paradigm of cytokine receptor plasticity is the type I interferon (IFN) receptor. All 15 members of the human IFN family recruit a shared cell surface receptor comprising the subunits IFNAR1 and IFNAR2 (Uzé et al., 1992, 2007; Novick et al., 1994; Pestka et al., 2004), through which they activate a broad spectrum of defense mechanisms against pathogen infection and malignancy development (Deonarain et al., 2002; Parmar and Platanias, 2003; Decker et al., 2005; Hertzog and Williams, 2013; Schneider et al., 2014).

Differential cellular responses activated by different IFNs have been reported for numerous instances (Abramovich et al., 1994; Rani et al., 1996; Coelho et al., 2005; Uzé et al., 2007). Although all IFNs induce antiviral activity with very similar potencies, other cellular responses regulating proliferation and differentiation are much more potently induced by IFNβ compared with IFNα subtypes. Detailed mutational studies on the IFN–receptor interaction (Piehler and Schreiber, 1999b; Runkel et al., 2000; Roisman et al., 2001; Cajean-Feroldi et al., 2004; Lamken et al., 2005; Strunk et al., 2008), as well as extensive low- and high-resolution structural data on the binary and ternary complexes (Chill et al., 2003; Quadt-Akabayov et al., 2006; Li et al., 2008; Strunk et al., 2008; Thomas et al., 2011; de Weerd et al., 2013), clearly established that, rather than differences in the structure, the diverse binding affinities of IFNs toward the receptor subunits are responsible for differential signaling (Subramaniam et al., 1995; Russell-Harde et al., 1999; Lamken et al., 2004; Jaks et al., 2007; Lavoie et al., 2011). In particular, the ∼100-fold higher binding affinity toward IFNAR1 observed for IFNβ compared with IFNα subtypes was suggested to be responsible

Correspondence to Jacob Piehler: piehler@uos.de

Abbreviations used in this paper: HBS, Hepes-buffered saline; HTL, HaloTag ligand; IFN, type I interferon; IFNAR, type I interferon receptor; JAK, Janus kinase; MBP, maltose-binding protein; PEG, poly(ethylene glycol); PICCS, particle image cross-correlation spectroscopy; PLL, poly-L-lysine; STAT, signal transducer and activator of transcription; TIRFM, total internal reflection fluorescence microscopy; TMR, tetramethyl rhodamine; USP, ubiquitin-specific protease; wt, wild type.

Supplemental Material can be found at:
http://jcb.rupress.org/content/suppl/2015/05/25/jcb.201412049.DC1.html

The Rockefeller University Press $30.00
J. Cell Biol. Vol. 209 No. 4 579–593
www.jcb.org/cgi/doi/10.1083/jcb.201412049

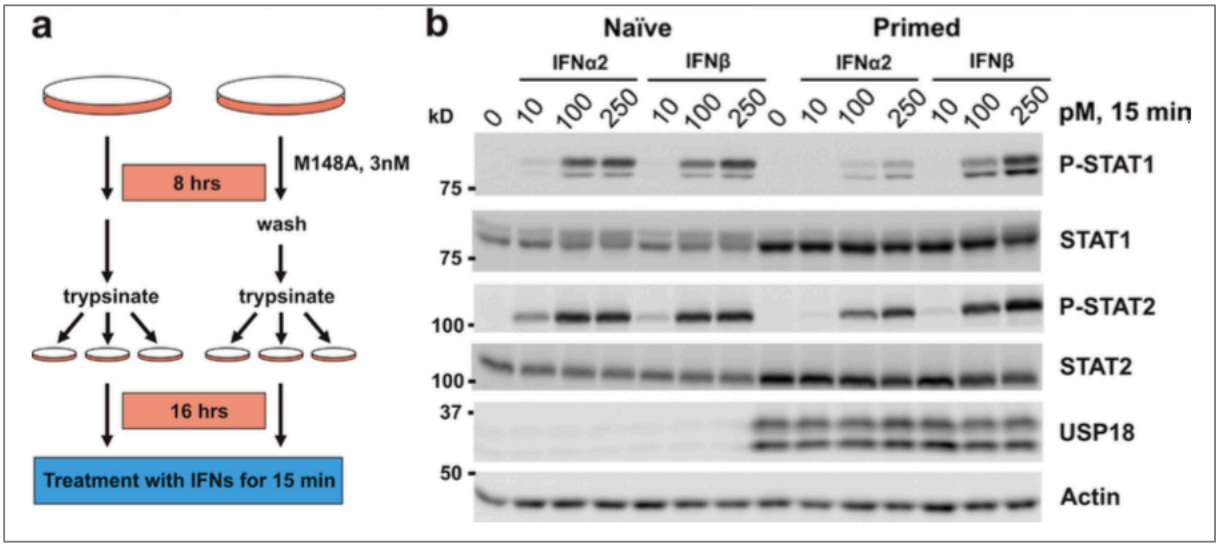

Figure 1. Desensitization of IFN signaling in HeLa cells primed with 3 nM IFNα2-M148A.
(a) Scheme of the treatment of naive and primed cells before western blot analysis.
(b) Analysis of STAT phosphorylation and USP18 expression.

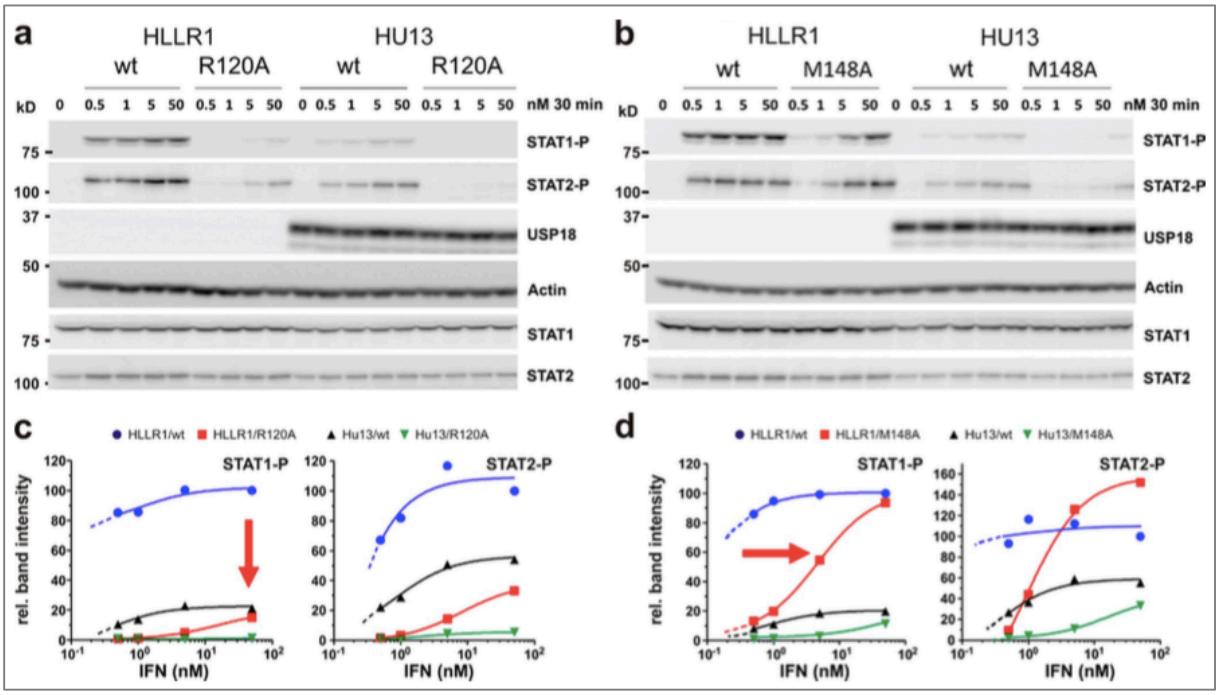

Figure 2. Functional consequences of USP18-mediated interference with ternary complex assembly. (a and b) western blot analysis of STAT1 and STAT2 phosphorylation in parental HLLR1 cells versus cells stably expressing USP18 (HU13) stimulated with IFNα2-wt, -R120A, or -M148A.
(c and d) Dose-response curve for pSTAT normalized to total STAT calculated from the band intensities in the western blot. Values were normalized to those obtained at the highest dose of IFN WT, which was taken as 100%. The broken lines represent the curve extrapolations for lower IFN doses expected from independent experiments.

DISCUSSION and PERSPECTIVES

What have we learned from the AID-associated TYK2 natural variants: TYK2-I684S, TYK2- P1104A?

In humans, TYK2-deficiency leads to reduced levels of cell surface IFNAR1, IL-10R2 and IL-12Rβ1. TYK2-deficient EBV-B cells display impaired response to IFN, IL-10, IL-12 and IL-23, which may reflect lower receptor abundance and/or lack of catalytic activity. Unlike EBV-B cells derived from TYK2-deficient patients, cells from individuals carrying homozygosity of TYK2 I684S or TYK2 P1104A exhibit normal levels of IFNAR1, IL-10R2 and IL-12Rβ1 receptors at the cell surface. Thus, any alteration of cytokine signaling in cells from these individuals is expected to reflect essential role(s) of TYK2 other than receptor scaffolding.

Our results showed that the two AID-associated variants, TYK2 I684S and TYK2 P1104A are both catalytically impaired and yet have different impact on cytokine signaling. TYK2 I684S does not appear to cause detectable alteration in STAT activation by the cytokines tested in fibroblasts or EBV-B cells. TYK2 P1104A leads to impaired signaling but to different extent, depending on the cytokine. This difference may relate to the position of the aa residues, I684 being in the KL domain and P1104 in the TK domain, and suggests that the two mutations impair kinase activity through different mechanisms (see below).

TYK2 I684S may alter the interface between the KL and TK domains without changing the conformation of the TK domain. Ile 684 is in the N lobe of the KL domain and 6 aa downstream of Val 678 (corresponding to Val 617 of JAK2 and V658F of JAK1) (Fig. 5 in Introduction). These two residues are localized at the two ends of the small β4-β5 loop respectively and are not part of the inhibitory interface between KL and TK domains. The crystal of JAK1 V658F is characterized by a rearrangement of the small β4-β5 loop with the F658 stacking with F636 from the αC helix by occupying the position of F575 from the SH2-KL linker. This linker is part of the auto-inhibitory KL-TK interface (Fig. 5 and Fig. 6 in Introduction, KL domain). Ile 684 faces the hydrophobic core of the N lobe. Substitution of Ile 684 by a small polar serine at one end of β4-β5 loop may disturb the flexibility of this loop and hamper JAK activation by altering the layout of the SH2-KL linker with respect to the αC of KL domain via the proposed F-F-V triad (Introduction page 22). Our *in vitro* kinase assay showed that serine substitution of Ile 684 results in a kinase-inactive TYK2 variant, probably due to an enforced *in cis* auto-inhibition. However, activation of JAK proteins in cells is certainly more complex. Considering the critical role of SH2 domain in receptor binding, it is plausible that, upon ligand binding, the conformational change of the receptor

drives a shift of the SH2-KL linker position, loosening the auto-inhibitory interaction between KL and TK domains, leading to JAK activation. It is possible that in cells the shift of the SH2-KL linker induced by ligand binding to receptors may bypass the impact of the I684S substitution and lead to TK domain activation. This may explain the intact cytokine signaling observed in I684S cells.

TYK2 P1104 is localized in the TK domain and this substitution abolishes kinase activity probably due to altered substrate recognition (173). In the crystal of the TK domain of JAK2 P1057A (corresponding to TYK2 P1104A), Dendrou *et al* highlighted a 15 angstrong shift of the αFG (αH, JAK-specific insertion) and αG helices (184). This shift may alter the conformation of the substrate-binding sites. We showed that, in EBV-B cells from patients the catalytically impaired TYK2 P1104A mediates IFN signaling almost as well as in control cells. Moreover, TYK2 P1104A, but not the ATP-binding lysine mutant K930R, rescues IFN signaling in fibroblasts (173) and EBV-B cells (data not shown) from TYK2-deficient patient. The difference between TYK2 K930R and P1104A in mediating cytokine signaling is remarkable and suggests critical structural contributions of the binding of ATP and the phosphorylation of the activation loop to cytokine signaling through heteromeric receptors.

By measuring IFN-α and IFN-γ responses in fibroblasts expressing JAK1-P1084A, we proposed that a catalytic JAK hypomorphe can hamper signaling in a cytokine-specific manner (173). We found that at endogenous expression level JAK1-P1084A rescues both IFN-α and IFN-γ signaling as well as WT JAK1. However, when overexpressed, JAK1-P1084A boosts IFN-γ signaling as well as WT JAK1, but not IFN-α signaling. One interpretation relates to the stoichiometry of the two cytokine receptor/JAK complexes. Unlike IFN-α, which is a monomer and signals through a heterodimeric receptor, IFN-γ is a homodimer and signals through two IFNGR1 subunits and two IFNGR2 subunits, which are likely associated to two JAK1 and two JAK2 molecules, respectively. Thus, in the IFN-γ receptor complex the two WT JAK2 may better compensate for the impairment of JAK1 P1084A than the single WT TYK2 in the IFN-α receptor complex.

Related to this, it is conceivable that such a JAK hypomorphe may have different impact on cytokine signaling depending on expression level of the JAK proteins.

Similarly, we found that the response to IFN-α of EBV-B cells derived from TYK2 P1104A homozygous patients is almost unaffected, while the response to IL-23 is much reduced. Thus, the impaired catalytic activity of TYK2 P1104A can be compensated within the IFNARs/JAK1 complex but not within the IL-23R/JAK2 complex. One possibility is that in

this latter complex TYK2, associated to IL-12Rβ1, operates as the "initiator" kinase. Interestingly, the IL-23R/JAK2 complex was shown to assemble in a non-canonical manner, with JAK2 binding to IL-23R at an unusual distance from the juxtamembrane region (185). Thus, in this particular complex, JAK2 may be unable to properly contact TYK2 P1104A. Alternatively, the recruitment of STAT3 to the TYK2 P1104A-containing multimeric complex may be impaired. The precise molecular mechanism needs to be further studied.

Recently, Dendrou *et al* confirmed that the rs34536443 (P1104A) minor allele is protective for AID (184). Most importantly, rs34536443 homozygosity (C/C, P1104A) was shown to confer more than double protective effect than a single allele (nonadditivity effect). The C/C (TYK2 P1104A) homozygosity was identified as highly protective against autoimmunity (odds ratio, OR= 0.094, 0.095, 0.158, 0.188, 0.307 for CD, AS, psoriasis (Ps), ulcerative colitis (UC), MS respectively). It is noteworthy that for ulcerative colitis, only the C/C homozygosity of rs34536443 but not heterozygosity was found to be protective.

These authors also measured, mostly by flow cytometry, the functional impact of rs34536443 on cytokine signaling in primary immune cells from healthy donors carrying homozygous TYK2 P1104A (Oxford Biobank). TYK2 and cell surface IFNAR1 were normally expressed. The total level of each STAT protein was not reported. The authors concluded that P1104A homozygosity causes a significantly impaired response to IFN (primary B cells, T cells and monocytes) and IL-12, IL-23 (pre-activated T cells), based on phospho-STAT positivity (184). Interestingly, IL-10, IL-6, or IL-13 signaling were shown not to be affected.

However, some inconsistencies make the data inconclusive. I found intriguing that in IFNα-stimulated TYK2 P1104A cells, with the 80% decrease of pSTAT3 positivity, the reported decrease of pSTAT3 MFI appears not significant ($P>0.05$) and the peak shift of pSTAT3 in the histogram presentation is very subtle in both WT and TYK2 P1104A cells. Moreover, in response to IL-12, with 70% decrease of pSTAT4 positivity in PHA-pre-activated T cells, the decrease of IFN-γ production measured by ELISA was only ~2% in IL-12 mediated differentiated CD4+ Th1 derived from TYK2 P1104A individuals compared to WT control.

Interestingly, with such impaired cytokine signaling, the Oxford Biobank C/C (TYK2-P1104A) individuals (European ancestral population) are all self-reported healthy, with normal frequencies of peripheral blood leukocyte subset (184). The authors conclude that TYK2 P1104A homozygosity determines an "optimal" cytokine response, *i.e.* low enough to protect from autoimmune disease but sufficient to fight infections. On the other hand, our

collaborators at the Rockefeller University found an enrichment of TYK2 P1104A homozygosity in primary immunodeficient patients with tuberculosis. Of note, eight of nine patients are from geographic regions outside Europe, where BCG is mandatory and tuberculosis is endemic. Europeans are less exposed to BCG and even less to *M. tuberculosis* than other populations, which could explain the lack of infectious phenotype in the Oxford Biobank individuals with homozygous TYK2 P1104A studied by Dendrou et al.

Overall, homozygosity of the catalytically impaired TYK2 allelic variant (P1104A) which is protective in many AID, represents a risk allele in primary immunodeficiency (S. Boisson-Dupuis, unpublished observation), probably by selective impairment of IL-23 response, which may be particularly dependent on TYK2 catalytic activity (186). In this regard, the potential risk of infection in patients with AID treated with TYK2 specific inhibitors will have to be considered.

Interestingly, TYK2 I684S was reported to be protective for some AID (SLE, RA, psoriasis) and risky for others (AS, IBD). In line with my results in EBV-B cells, Dendrou *et al* showed that rs12720356 (TYK2 I684S) did not affect TYK2 expression nor STAT phosphorylation in various immune cell types stimulated with the various cytokines (184). TYK2 mediates signaling of other cytokines such as IL-22 and IL-11 that may be involved in AID pathogenesis. The impact of TYK2 I684S and TYK2 P1104A on the signaling in response to these cytokines needs to be studied.

JAK is not "just another kinase". We showed that JAK proteins play a critical catalytic - independent structural function for receptor scaffolding, mediating cytokine signaling (173) and stabilizing the ternary complex (177). In heterodimeric cytokine receptors, the specific role (catalytic *vs* scaffolding) of each JAK may differ, being influenced by the properties of the cognate receptor chain and its re-orientation upon ligand binding. Our studies on functional impact of TYK2 mutants, including the two catalytically loss-of-function mutants (P1104A or I684S) and the catalytic gain-of-function TYK2 V658F showed that none of the mutants affected the level of STAT activation (25; 173) in response to IFN. This suggests that the conformational integrity and scaffold function of a JAK can, in some receptor contexts, be more critical than its phospho-transfer activity. This concept may be instrumental for clinical application of JAK inhibitors. For example, one would predict that, due to catalytic redundancy, the therapeutic catalytic inhibition of one JAK may not abrogate certain cytokine signaling (13). On the other hand, the catalytic role of TYK2 appears indispensable in the IL-

12 and IL-23 signaling pathways (186; our results). When the precise contribution of each JAK in signaling through a heterodimeric-type cytokine receptor is known, the choice may be to inhibit the catalytically dominant JAK, or to inhibit both (187).

Our studies on EBV-B cells from patients carrying TYK2 P1104A showed a selective abrogation of the IL-23 signaling. Moreover, in these cells activation of STAT3 by other cytokines (IL-10, IFN-α) appears to be more impaired than that of other STATs. The role of TYK2 in lipid metabolism (82) and mitochondrial respiration (83) is probably linked to STAT3. Expression of a constitutively active Stat3 can compensate the loss of Tyk2 function on the mitochondrial respiration or on the lipid metabolism in Tyk2-null murine cells. Altogether, these scattered observations call for a further investigation of the relationship between TYK2 and STAT3.

Is TYK2 rs2304256 (V362F) causal in AID?

Rs2304256 is located in Exon 8 of *TYK2* and leads to a Val to Phe substitution (V362F) in the FERM domain F3 lobe. Our unpublished data show that this amino acid change has no effect on TYK2 kinase activity or function. However, I found that the rs2304256 minor allele (AA) promotes the retention of Exon 8 and may therefore promote the full length *TYK2* expression. I also showed that TYK2-ΔE8 is a loss-of-function protein that cannot bind to receptors or mediate cytokine signaling (Results, Part I-2). In agreement with this, by analyzing public eQTL datasets (188), I found that the rs2304256 minor allele (A) correlates with increased *TYK2* expression in many tissues (adrenal gland, adipose, liver, whole blood cells, sun-exposed skin, mammary tissues), but not in others (pancreas, spleen, muscle, colon, EBV-B, transformed fibroblasts *etc)*. I hypothesize that the increased retention of Exon 8 by rs2304256 may increase TYK2 level in some cell types and affect disease susceptibility.

A meta-analysis of genome-wide-association datasets showed that TYK2 rs2304256 (V362F) is protective for type 1diabetes (T1D, OR=0.86, $p=4.13x10^{-9}$) in the European population (113). However, the reports on the role of TYK2 in pathogenesis of T1D appear discordant.

Type 1 diabetes (T1D) arises from loss of pancreatic β cells and failure to produce insulin. Destruction of pancreatic β cells could result from autoimmunity caused by an excessive inflammatory response to certain viral infections among susceptible individuals where autoreactive T cells would contribute to β cell killing. Conversely, in the case of fulminant T1D (absence of autoantibody), the β cells could be directly destroyed by the viral infection.

TYK2 may be damaging or protective in the same disease, depending on the pathogenic mechanism. For instance, low antiviral activity due to a TYK2 loss-of-function mutation may trigger virus-induced diabetes (189). At the same time, the mutation can be protective by preventing IFN-induced β cells apoptosis or/and by reducing the recruitment of T cells to the islets or limiting T cell activation (190).

Nagafuchi *et al.* showed that in the Japanese population a TYK2 promoter variant (haplotype) that decreases *TYK2* expression (82% of *WT*, measured in luciferase reporter assay) is associated with higher susceptibility to both type 1 and type 2 diabetes (OR=2.1 and 2.4 for T1D and T2D, respectively), particularly in patients with T1D associated with flu-like syndrome at onset (OR=4.8) (189). In this study of Japanese patients, rs2304256 was not in the promoter haplotype and was considered not to be associated with diabetes. There was no difference in the MAF of rs2304256 (GT+TT) between diabetes patients and healthy controls, as shown in the Suppl. Table 2 (below) taken from the report (189). In this study, rs2304256 (V362F) was also named "SNP at Exon 8, 15597 G/T". "G/T" in the positive strand corresponds to "C/A" in the negative strand of *TYK2* referred in my study. However, I noticed an interesting difference in the frequency of the homozygous minor allele (TT, corresponding to AA in my study) between controls and T1D or T2D patients (9% vs 15.2%, 14.9% respectively).

Table from (189)

Supplementary Table 2. SNP at *TYK2* Exon 8 in patients with T1D, T2D and healthy controls.

SNP at Exon 8 (15597G/T)	Healthy Controls (n=254)	Type 1 DM All (n=244)		Type 1 DM Flu-like syndrome* associated (n=36)		Type 2 DM (n=255)	
	No (%)	No (%)	OR#(95% CI)	No (%)	OR#(95% CI)	No (%)	OR#(95% CI)
GG	115 (45.3%)	103 (42.2)	1.00¶	18 (50.0)	1.00¶	96 (37.6)	1.00¶
GT	116 (45.7%)	104 (42.6)	1.1 (0.8–1.6)	12(33.3)	0.8 (0.4–1.7)	121 (47.5)	1.3 (0.9–1.9)
TT	23 (9.0%)	37 (15.2)		6 (16.7)		38 (14.9)	
P value†		0.49		0.59		0.08	

*Symptoms of flu-like syndrome includes fever, chills, sore throat, muscle and joint aches, poor appetite, diarrhea, cough, and fatigue, suggestive of certain viral infections.

¶referent, #OR, odds ratio; §CI,confidence interval

†Heterozygous and homozygous variant genotypes combined versus homozygous wild genotype.

Taken together, the rs230456 AA homozygosity, which leads to higher level of *TYK2* in blood cells, but not in pancreatic cells, is more frequent in Japanese diabetes patients. Given the involvement of TYK2 in signaling of many pro-inflammatory cytokines, I postulate that a higher activation of immune cells (*e.g.* Th1 or/and autoreactive CD8+ T cells) due to higher level of TYK2 protein, resulting from rs2304256 AA homozygosity (*i.e.* enhanced Exon 8 retention as shown in Result Part I-2), could promote autoimmunity against β cells and increase susceptibility to diabetes in Japanese population.

The etiology of T1D in different ethnic groups may be different. Europeans are more prone to T1D than Japanese. Childhood obesity has been positively correlated with risk of T1D in individuals of European ancestry (191). Decreased levels of TYK2 are associated with obesity in both mice and humans (82). Thus, rs2304256 may protect against T1D in the European population (113), because of a reduced risk of obesity due to higher TYK2 expression resulting from Exon 8 retention.

Rs2304256 has been associated with SLE, Crohn's disease and T1D. In two recent studies, rs2304256 (V362F) was found falsely associated with SLE (114) and multiple sclerosis (115) driven by imperfect linkage disequilibrium to rs34536443 (P1104A) and rs12720356 (I684S). During my studies, I found that most, if not all, P1104A and I684S individuals carry V362F (data not shown). Interestingly, P1104A and I684S have not been associated with T1D to which rs2304256 (V362F) has been instead associated, suggesting an independent role of this SNPs in T1D pathogenesis. Of note, rs34536443 (P1104A), rs12720356 (I684S) are not found in the Asian population and the frequency of rs2304256 (V362F) is higher in the Asian population (47%) than in other populations.

It is conceivable that in case of heterozygosity of P1104A or I684S occurring within the same locus of the minor allele (A) of rs2304256 (V362F), the expression of the full-length protein from this locus will be more abundant than from the WT locus in certain cell types, and therefore more available for receptor binding. This situation may favor the impact of the hypomorphic TYK2 P1104A or I684S on signaling of cytokines for which the catalytic activity of TYK2 is indispensable, such as IL-23. In contrast, rs2304256 may enhance signaling by cytokines for which the catalytic activity of TYK2 is dispensable, such as IFN-α, due to increased level of TYK2. Thus, rs2304256 may have both direct and indirect effects on

susceptibility to different AID depending on the pathogenic role of different cytokines.

In conclusion, I found that the minor allele of rs2304256 (AA) promotes Exon 8 retention, which may lead to increased full-length TYK2 expression. Given the role of TYK2 in mediating signaling of multiple immuno-regulatory cytokines and in metabolism (obesity), I predict that rs2304256 could be a causal SNP in AID, such as type I diabetes. Rs2304256 was found to increase *TYK2* expression in some tissues, such as adrenal gland and whole blood, but not in EBV-B cells or pancreatic cells. It will be interesting to identify the cell type(s) in which rs2304256 impacts TYK2 expression and may influence susceptibility to AID.

Why and how TYK2 FERM domain binds to PI(3)P

The molecular mechanism of IFN-induced receptor dimerization, TYK2/JAK1 activation, receptor complex internalization and sorting start to be elucidated. It will be important to investigate how TYK2 or/and JAK1 are involved in these processes and if they have comparable roles in other cytokine pathways.

In preliminary studies of the potential ability of the TYK2 FERM domain to bind lipids, I found that the TYK2 FERM domain, expressed as a recombinant protein, interacts with PI(3)P, a phosphoinositide (PIP). Different PIPs originate by the attachment of phosphate groups by specific kinases to the 3, 4 or 5 positions of the inositol ring of phosphatidylinositols (PtdIns) (Fig. D1). The majority of PIPs are constitutively expressed on specific organelles (Fig. D2) and specifically recruit a range of peripheral membrane proteins (192). Thus, the temporal and spatial (organelle-specific) distribution of different forms of PIPs mediates specific protein/membrane interaction and plays a critical role in cellular functions, such as signaling transduction, intracellular membrane trafficking and cellular organization (193).

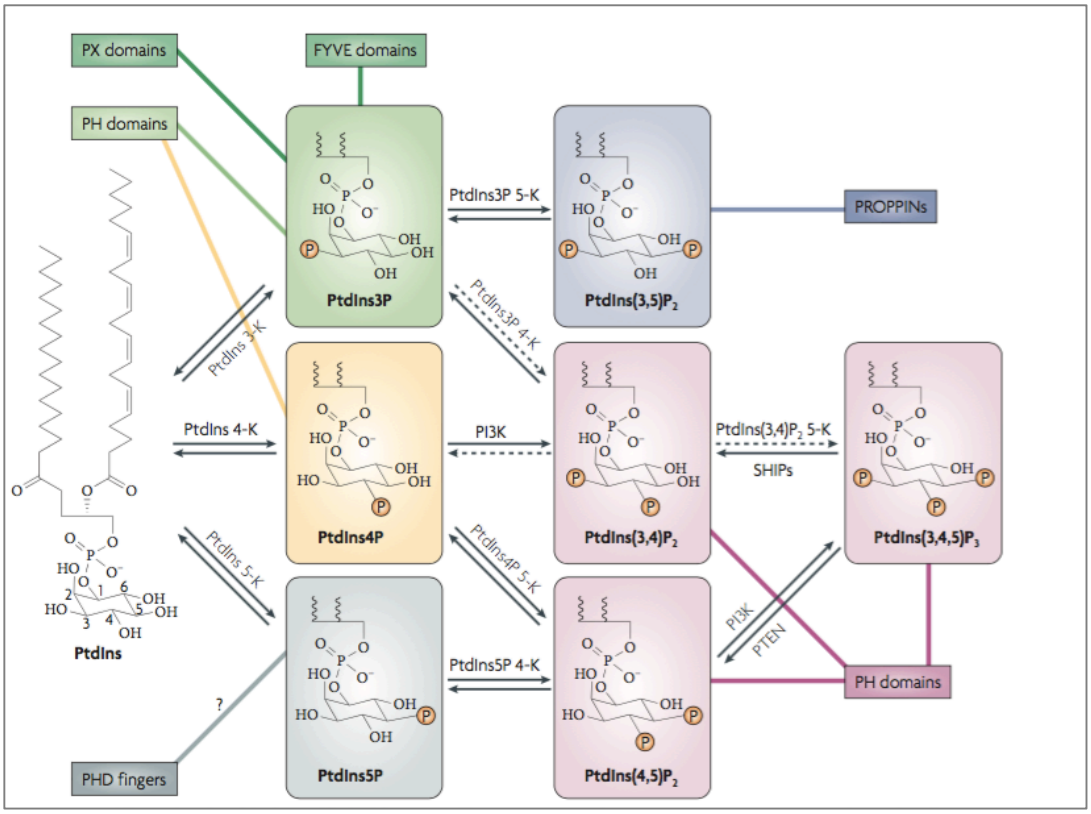

Figure D1. Domains that bind lipid targets. From (193)

PI(3)P is enriched at the surface of early endosomes, intraluminal vesicles of multivesicular endosomes and autophagosomes. It is also found at the site of LC3-associated phagocytosis and at the primary cilium (Fig. D2). Usually, PI(3)P recruits proteins which serve as scaffolds for other proteins regulating membrane remodeling, trafficking or signaling events. For example, PI(3)P is required for efficient recruitment of retromer (Fig. D2) to endosomes, and this facilitates sorting of membrane proteins to the late Golgi or back to the plasma membrane. Retromer is a multi-subunits complex. The mammalian retromer complex is composed of a dimer of sorting nexins (a combination of SNX1, SNX2, SNX5 and SNX6) and a trimer of Vps26–Vps29-Vps35. SNX contains a phox homology (PX) domain which binds to PI(3)P in the membrane of endosomes. The Vps26–Vps29–Vps35 trimer is responsible for recruiting cargo protein by binding to the cytosolic tail of transmembrane receptors (194).

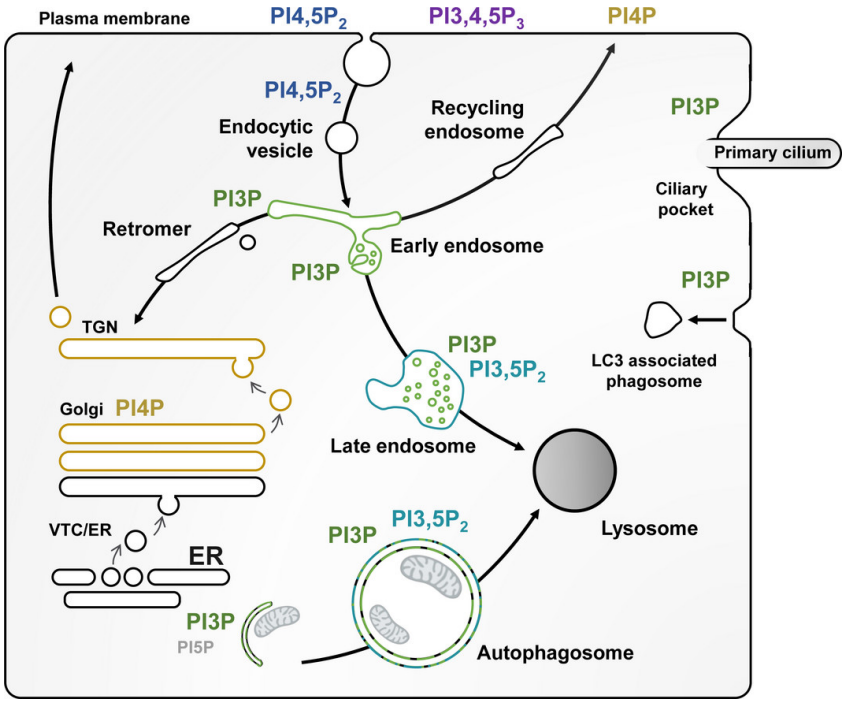

Figure D2. Overview of PIP subcellular localization and endomembrane trafficking in mammalian cells involving endosomes and autophagy-related organelles. Major PIPs are shown in different colors. TGN, trans-Golgi network; VTC, vesiculo-tubular clusters; ER, endoplasmic reticulum. From (195).

Proteins can bind to PI(3)P (193) via FYVE domains (as in EEA1, Hrs, DFCP1), PX domains (as in sorting nexins) or WD40 domains (as in ATG18). PH domains can also mediate PI(3)P binding (as a split PH domain in Vps36).

The Pellegrini's lab found that, shortly after IFN stimulation, ubiquitinated IFNAR1, IFNAR2 and tyrosine-phosphorylated TYK2 and JAK1 can be found in an EEA+ endosomal compartment, which suggested the possibility of persistent signaling (196). Thus, on the one hand internalization may promote immediate signaling by concentrating signaling components on endosomes. This was also suggested by the lower IFNα/β-induced STAT1/2 phosphorylation (about 50% reduction) measured in cells pre-treated with pitstop, a selective inhibitor of clathrin-dependent internalization (Pellegrini's lab, unpubl. obs.). On the other hand, internalization serves to down-regulate IFNAR1, ultimately dampening IFN binding. Interestingly, upon ligand binding, IFNAR2 was shown to be down-regulated by IFN-β but not by IFN-α, suggesting that the strength of ligand binding and/or the lifetime of the ternary complex (ligand/receptor subunits) influence the fate of IFNAR2 (197). A recent study showed that after IFN stimulation, internalized IFNAR1 and IFNAR2 are differentially sorted by the retromer (Fig. D2). IFNAR2 binding to retromer in early endosomes drives the sorting of both receptor chains to distinct pathways: IFNAR1 towards lysosomal degradation and

IFNAR2 back to the cell membrane (198). Since PI(3)P is enriched on the membrane of early endosomes, it is conceivable that TYK2 binding to PI(3)P could play a role in the process of receptor internalization and sorting.

I found that the TYK2 FERM domain binds to PI(3)P *in vitro*, probably via the two basic patches of the F2 and F3 lobes. Deletion of the Exon 8 encoding segment abolished this interaction. In cells, alanine substitution of the two basic patches disturbs TYK2 basal or induced phosphorylation and also the receptor scaffolding function (Results part I-3). In the crystal structure, these two basic patches are not involved in the direct interaction with IFNAR1 and are unlikely to affect IFNAR1 binding. This needs to be confirmed by an *in vitro* pull-down assay. TYK2 sustains IFNAR1 on the cell surface by preventing its internalization (48). TYK2 activity was shown to be required for PDK2-mediated IFNAR1 ubiquitination and turnover (137). TYK2 and JAK1 proteins contribute to the stability of the ligand/receptor ternary complex (20; 177). Thus, I hypothesize that the TYK2-FERM/PI(3)P binding may target TYK2 to cell membrane and/or intracellular membrane and this could ensure an optimal receptor binding, activation of TYK2, ternary complex formation and/or receptor internalization/sorting. Further studies are needed to investigate this hypothesis and the relevance of the FERM/PI(3)P interaction in cells. The subcellular localization of WT and mutated TYK2 should be studied before and after cytokine stimulation (e.g. IFN). We need to study whether other JAKs can bind to PI(3)P and related to this, delimit the PI(3)P binding site(s) and the mode of regulation of the interaction.

A study of knock-in mice expressing a kinase-dead Tyk2 K923E reported that the Tyk2 K923E protein level is substantially reduced compared to the WT TYK2 protein and its level can be restored by an inhibitor of the autophagy-lysosome systems (199). An assay with panJAK inhibitor showed that Tyk2 activity is critical to prevent Tyk2 from autophagosomal degradation. PI(3)P is present on the autophagosome (Fig. D2). Whether the TYK2/PI(3)P interaction plays a role in TYK2 degradation need to be further studied.

USP18, ISG15 and species-specific interaction of USP18/ISG15

Our collaborative studies on USP18 and ISG15-deficient patients have added two new genes to the growing list of genes known to be involved in rare genetic interferonopathies (Fig. D3). USP18 and ISG15 deficiencies are the first identified interferonopathies caused by a dysregulation of the response to type I IFNs and not due to an excess production of these

cytokines.

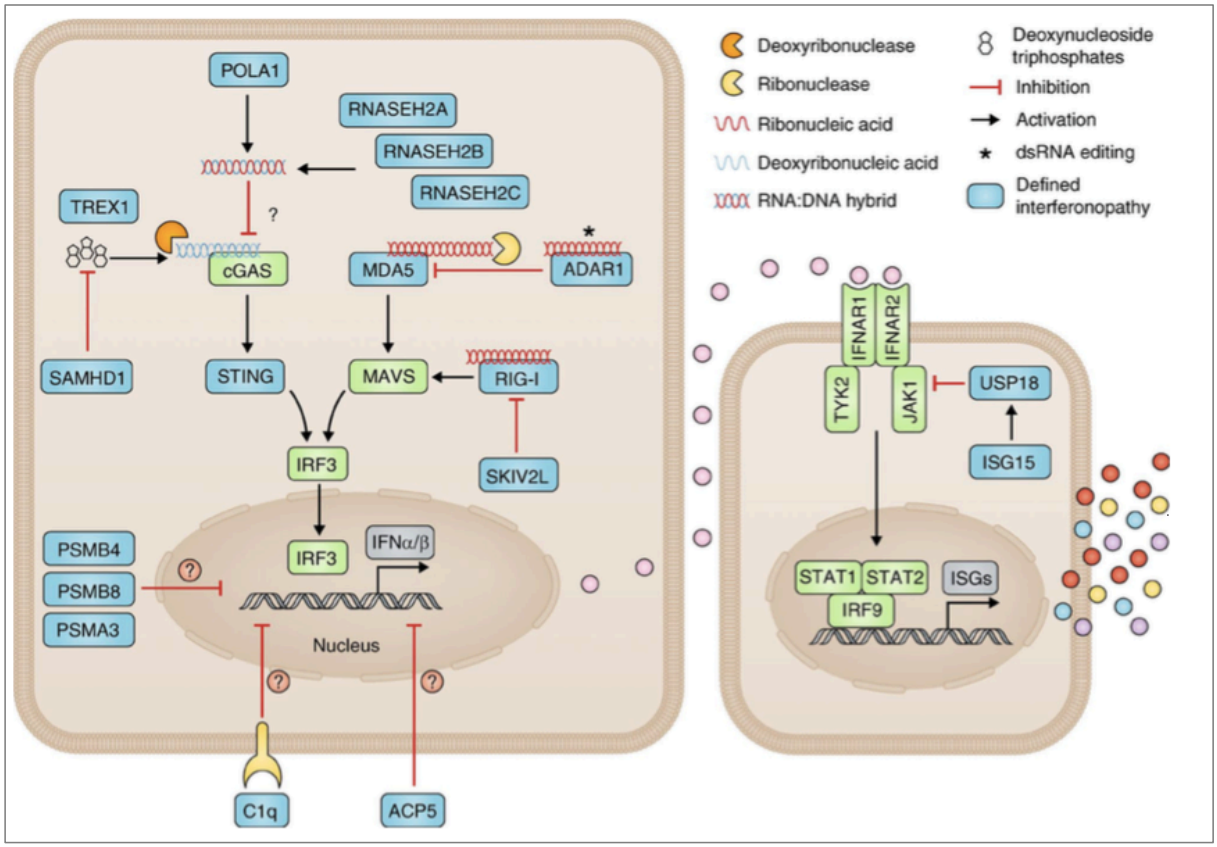

Figure D3 Monogenic disorders (blue boxes) considered as interferonopathies. From (129)

We have described ISG15 as a novel and human-specific negative regulator of IFN-I signaling (175) (Fig. D4). The different phenotypes of ISG15 deficiency in humans and in mice is remarkable and seems to be related to the fact that in human cells, but not in murine cells, ISG15 contributes to the stability of the negative regulator USP18 (176). The mechanism underlying this different behavior is still unclear. Recently, a comparison of the crystal structure of full-length hISG15 and mIsg15 proteins revealed a similar secondary structure in each individual domain of hISG15 and mIsg15 (Fig. 21). However, the overall conformation of their tertiary structures is dramatically different due to a distinct arrangement of the N- and C-terminal domains (153). Precisely, with respect to hISG15, the orientation between the C- and N-terminal domain of mIsg15 is twisted from 43.0° to 66.9° (Fig. D5-a). In addition, hISG15 contains a continuous negatively charged surface across the two domains (Fig. D5-b), which lacks in mIsg15.

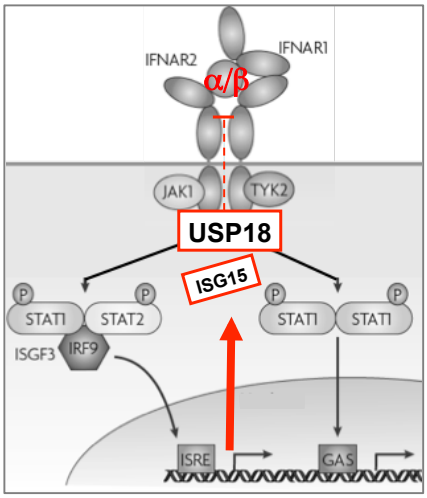

Figure D4. ISG15 is a negative regulator of IFN by protecting USP18 from degradation in humans but not in mice.

We have shown that murine Isg15 cannot form a complex with human USP18 (176). However, we do not know whether the tertiary structure and electrostatic properties unique to hISG15 do account for its ability to interact with USP18. The structure of human USP18 is not available yet, but the crystal structure of the murine Isg15/Usp18 complex has been solved. In this complex, Usp18-devoid of its N-ter and C-ter ends- exhibits the typical fold of the catalytic core of USPs, *i.e.* a "right hand"-like structure comprised of three major domains (finger, palm and thumb), Isg15 interacts with the palm and thumb domain of Usp18 via its C-terminal Ubl domain only. (200). Conversely, In the solved complex of another protease, USP21, and di-Ubiquitin (201), both Ub domains contact the protease. The N-terminal Ub domain is in contact with the finger domain in this USP21-di-Ub complex and the author proposed that ISG15 which contains 2 tandem Ubl domain binds USP18 in a similar manner. A crystal structural of huUSP18/ISG15 will shed light on this species-specific interaction.

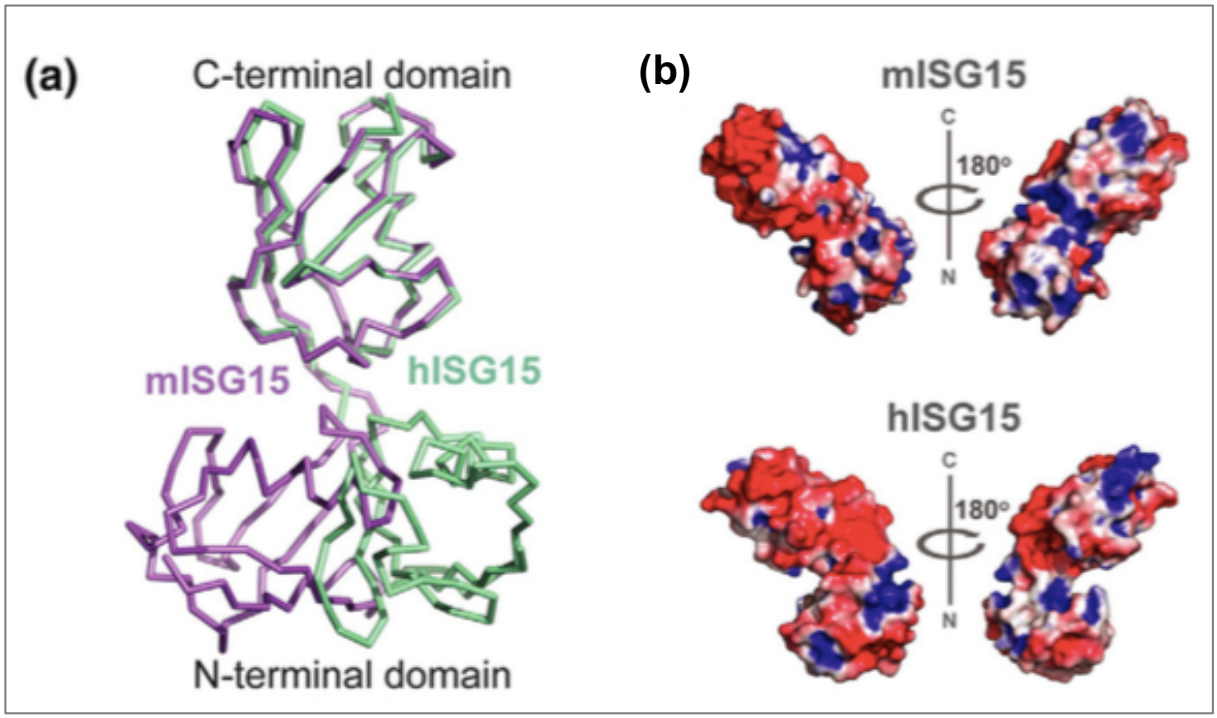

Figure D5. (a) Overlay of mISG15 (purple) and hISG15 (green) shown in ribbons. (b) Electrostatic surface of mISG15 and hISG1. From (153).

A novel negative regulatory role of STAT2

STAT2 is an essential and specific positive effector of type I IFN signaling and it is well known that it constitutively interacts with aa 418–444 of IFNAR2 (Nguyen 2002). We demonstrated that STAT2 is required for USP18 to exert its inhibitory effect on IFN-I (178). Hence, ectopic USP18 was shown not to affect STAT1 phosphorylation in STAT2-deficient U6A cells treated with IFN-α, whereas in parental 2fTGH cells and U2A (IRF9-deficient) cells, USP18 clearly dampened STAT1 phosphorylation. Using a series of STAT2 deletion mutants, aa 138-572, including the coiled-coil (CC) and DNA-binding (DB) domains plus linker region, were found to be required for the USP18 binding and IFN-I signaling inhibition. Interestingly, these domains are also critical for the constitutive interaction of STAT2 with IFNAR2 (Nguyen 2002). On the other hand, USP18 interacts simultaneously with membrane proximal site of IFNAR2 (160) via the N and C-terminal regions (aa 36-51 and aa 313-371) and interacts with STAT2 (178) via the adjacent region (aa 51-112 and aa 303-312).
Our results indicate that the presence of STAT2 is required for USP18-mediated inhibition of IFN-induced receptor assembly as well as JAKs phosphorylation. These observations establish the key role of STAT2 in USP18-mediated inhibition of IFN signaling and moreover suggest that the increased STAT2 levels observed in response to IFN may further enhance

negative feedback regulation.

In addition to ISG15 and STAT2, it is possible that other adaptors could be involved in the USP18-mediated negative regulation. These adaptors might act in species-specific manner, such as ISG15. The molecular details of the interaction between USP18/ISG15 and among USP18/ STAT2/IFNAR2/JAK1 still await further clarification. Another interesting question is whether ISG15 binding (free or conjugation) alters interaction between USP18, STAT2, and IFNAR2.

At present time, our mechanistic studies illustrate that USP18, *via* simultaneous interaction with IFNAR2 and STAT2 (178), hamper JAK1 binding to IFNAR2, and thus blocks the recruitment of IFNAR1 to the ligand receptor complex (177). This model also emphasizes the role of JAK proteins in the formation of the ternary complex (20; 177).

REFERENCES

References

1. Velazquez L, Fellous M, Stark GR, Pellegrini S. 1992. A protein tyrosine kinase in the interferon α/β signaling pathway. *Cell* 70:313-22
2. Wallweber HJ, Tam C, Franke Y, Starovasnik MA, Lupardus PJ. 2014. Structural basis of recognition of interferon-alpha receptor by tyrosine kinase 2. *Nat Struct Mol Biol* 21:443-8
3. Lupardus PJ, Ultsch M, Wallweber H, Bir Kohli P, Johnson AR, Eigenbrot C. 2014. Structure of the pseudokinase-kinase domains from protein kinase TYK2 reveals a mechanism for Janus kinase (JAK) autoinhibition. *Proc Natl Acad Sci USA* 111:8025-30
4. Boggon TJ, Li Y, Manley PW, Eck MJ. 2005. Crystal structure of the Jak3 kinase domain in complex with a staurosporine analog. *Blood* 106:996-1002
5. Lucet IS, Fantino E, Styles M, Bamert R, Patel O, et al. 2006. The structural basis of Janus kinase 2 inhibition by a potent and specific pan-Janus kinase inhibitor. *Blood* 107:176-83
6. Chrencik JE, Patny A, Leung IK, Korniski B, Emmons TL, et al. 2010. Structural and thermodynamic characterization of the TYK2 and JAK3 kinase domains in complex with CP-690550 and CMP-6. *J. Mol. Biol.* 400:413-33
7. Williams NK, Bamert RS, Patel O, Wang C, Walden PM, et al. 2009. Dissecting specificity in the Janus kinases: the structures of JAK-specific inhibitors complexed to the JAK1 and JAK2 protein tyrosine kinase domains. *J Mol Biol* 387:219-32
8. Tsui V, Gibbons P, Ultsch M, Mortara K, Chang C, et al. 2011. A new regulatory switch in a JAK protein kinase. *Proteins* 79:393-401
9. Andraos R, Qian Z, Bonenfant D, Rubert J, Vangrevelinghe E, et al. 2012. Modulation of activation-loop phosphorylation by JAK inhibitors is binding mode dependent. *Cancer Discov* 2:512-23
10. Kornev AP, Haste NM, Taylor SS, Eyck LF. 2006. Surface comparison of active and inactive protein kinases identifies a conserved activation mechanism. *Proc Natl Acad Sci USA* 103:17783-8
11. Huse M, Kuriyan J. 2002. The conformational plasticity of protein kinases. *Cell* 109:275-82
12. Kornev AP, Taylor SS, Ten Eyck LF. 2008. A helix scaffold for the assembly of active protein kinases. *Proc Natl Acad Sci USA* 105:14377-82
13. Haan C, Kroy DC, Wuller S, Sommer U, Nocker T, et al. 2009. An unusual insertion in Jak2 is crucial for kinase activity and differentially affects cytokine responses. *J Immunol* 182:2969-77
14. Babon JJ, Kershaw NJ, Murphy JM, Varghese LN, Laktyushin A, et al. 2012. Suppression of cytokine signaling by SOCS3: characterization of the mode of inhibition and the basis of its specificity. *Immunity* 36:239-50
15. Zhang JG, Farley A, Nicholson SE, Willson TA, Zugaro LM, et al. 1999. The conserved SOCS box motif in suppressors of cytokine signaling binds to elongins B and C and may couple bound proteins to proteasomal degradation. *Proc Natl Acad Sci U S A* 96:2071-6
16. Linossi EM, Chandrashekaran IR, Kolesnik TB, Murphy JM, Webb AI, et al. 2013. Suppressor of Cytokine Signaling (SOCS) 5 utilises distinct domains for regulation of JAK1 and interaction with the adaptor protein Shc-1. *PLoS One* 8:e70536
17. Yasukawa H, Misawa H, Sakamoto H, Masuhara M, Sasaki A, et al. 1999. The JAK-binding protein JAB inhibits Janus tyrosine kinase activity through binding in the activation loop. *EMBO J* 18:1309-20

18. Kershaw NJ, Murphy JM, Liau NP, Varghese LN, Laktyushin A, et al. 2013. SOCS3 binds specific receptor-JAK complexes to control cytokine signaling by direct kinase inhibition. *Nat Struct Mol Biol* 20:469-76
19. Ungureanu D, Wu J, Pekkala T, Niranjan Y, Young C, et al. 2011. The pseudokinase domain of JAK2 is a dual-specificity protein kinase that negatively regulates cytokine signaling. *Nat Struct Mol Biol* 18:971-6
20. Velazquez L, Mogensen KE, Barbieri G, Fellous M, Uze G, Pellegrini S. 1995. Distinct domains of the protein tyrosine kinase tyk2 required for binding of interferon-alpha/beta and for signal transduction. *J Biol Chem* 270:3327-34
21. Saharinen P, Silvennoinen O. 2002. The pseudokinase domain is required for suppression of basal activity of Jak2 and Jak3 tyrosine kinases and for cytokine-inducible activation of signal transduction. *J Biol Chem* 277:47954-63
22. O'Shea JJ, Husa M, Li D, Hofmann SR, Watford W, et al. 2004. Jak3 and the pathogenesis of severe combined immunodeficiency. *Mol Immunol* 41:727-37
23. Yeh TC, Dondi E, Uze G, Pellegrini S. 2000. A dual role for the kinase-like domain of the tyrosine kinase Tyk2 in interferon-alpha signaling. *Proc. Natl. Acad. Sci. USA* 97:8991-6
24. Pasquier F, Cabagnols X, Secardin L, Plo I, Vainchenker W. 2014. Myeloproliferative neoplasms: JAK2 signaling pathway as a central target for therapy. *Clin Lymphoma Myeloma Leuk* 14 Suppl:S23-35
25. Gakovic M, Ragimbeau J, Francois V, Constantinescu SN, Pellegrini S. 2008. The Stat3-activating Tyk2 V678F mutant does not up-regulate signaling through the type I interferon receptor but confers ligand hypersensitivity to a homodimeric receptor. *J Biol Chem* 283:18522-9
26. Staerk J, Kallin A, Demoulin JB, Vainchenker W, Constantinescu SN. 2005. JAK1 and Tyk2 activation by the homologous polycythemia vera JAK2 V617F mutation: cross-talk with IGF1 receptor. *J Biol Chem* 280:41893-9
27. Bandaranayake RM, Ungureanu D, Shan Y, Shaw DE, Silvennoinen O, Hubbard SR. 2012. Crystal structures of the JAK2 pseudokinase domain and the pathogenic mutant V617F. *Nat. Struct. Mol. Biol.* 19:754-9
28. Dusa A, Mouton C, Pecquet C, Herman M, Constantinescu SN. 2010. JAK2 V617F constitutive activation requires JH2 residue F595: a pseudokinase domain target for specific inhibitors. *PLoS One* 5:e11157
29. Silvennoinen O, Hubbard SR. 2015. Molecular insights into regulation of JAK2 in myeloproliferative neoplasms. *Blood* 125:3388-92
30. Toms AV, Deshpande A, McNally R, Jeong Y, Rogers JM, et al. 2013. Structure of a pseudokinase-domain switch that controls oncogenic activation of Jak kinases. *Nat Struct Mol Biol* 20:1221-3
31. Scott LM, Tong W, Levine RL, Scott MA, Beer PA, et al. 2007. JAK2 exon 12 mutations in polycythemia vera and idiopathic erythrocytosis. *N Engl J Med* 356:459-68
32. Shan Y, Gnanasambandan K, Ungureanu D, Kim ET, Hammaren H, et al. 2014. Molecular basis for pseudokinase-dependent autoinhibition of JAK2 tyrosine kinase. *Nat Struct Mol Biol* 21:579-84
33. Brooks AJ, Dai W, O'Mara ML, Abankwa D, Chhabra Y, et al. 2014. Mechanism of activation of protein kinase JAK2 by the growth hormone receptor. *Science* 344:1249783
34. Waters MJ, Brooks AJ, Chhabra Y. 2014. A new mechanism for growth hormone receptor activation of JAK2, and implications for related cytokine receptors. *JAKSTAT* 3:e29569

35. Ferrao R, Lupardus PJ. 2017. The Janus Kinase (JAK) FERM and SH2 Domains: Bringing Specificity to JAK-Receptor Interactions. *Front Endocrinol (Lausanne)* 8:71
36. Ferrao R, Wallweber HJ, Ho H, Tam C, Franke Y, et al. 2016. The Structural Basis for Class II Cytokine Receptor Recognition by JAK1. *Structure* 24:897-905
37. Zhang D, Wlodawer A, Lubkowski J. 2016. Crystal Structure of a Complex of the Intracellular Domain of Interferon lambda Receptor 1 (IFNLR1) and the FERM/SH2 Domains of Human JAK1. *J Mol Biol* 428:4651-68
38. McNally R, Toms AV, Eck MJ. 2016. Crystal Structure of the FERM-SH2 Module of Human Jak2. *PLoS One* 11:e0156218
39. Frame MC, Patel H, Serrels B, Lietha D, Eck MJ. 2010. The FERM domain: organizing the structure and function of FAK. *Nat Rev Mol Cell Biol* 11:802-14
40. Goni GM, Epifano C, Boskovic J, Camacho-Artacho M, Zhou J, et al. 2014. Phosphatidylinositol 4,5-bisphosphate triggers activation of focal adhesion kinase by inducing clustering and conformational changes. *Proc Natl Acad Sci USA* 111:E3177-86
41. Lim ST, Mikolon D, Stupack DG, Schlaepfer DD. 2008. FERM control of FAK function: implications for cancer therapy. *Cell Cycle* 7:2306-14
42. Ragimbeau J, Dondi E, Vasserot A, Romero P, Uze G, Pellegrini S. 2001. The receptor interaction region of Tyk2 contains a motif required for its nuclear localization. *J Biol Chem* 276:30812-8
43. Sanz Sanz A, Niranjan Y, Hammaren H, Ungureanu D, Ruijtenbeek R, et al. 2014. The JH2 domain and SH2-JH2 linker regulate JAK2 activity: A detailed kinetic analysis of wild type and V617F mutant kinase domains. *Biochim Biophys Acta* 1844:1835-41
44. Haan S, Margue C, Engrand A, Rolvering C, Schmitz-Van de Leur H, et al. 2008. Dual role of the Jak1 FERM and kinase domains in cytokine receptor binding and in stimulation-dependent Jak activation. *J Immunol* 180:998-1007
45. Zhou YJ, Chen M, Cusack NA, Kimmel LH, Magnuson KS, et al. 2001. Unexpected effects of FERM domain mutations on catalytic activity of Jak3: structural implication for Janus kinases. *Mol Cell* 8:959-69
46. Gauzzi MC, Barbieri G, Richter MF, Uze G, Ling L, et al. 1997. The amino-terminal region of Tyk2 sustains the level of interferon alpha receptor 1, a component of the interferon alpha/beta receptor. *Proc Natl Acad Sci U S A* 94:11839-44
47. Haan C, Kreis S, Margue C, Behrmann I. 2006. Jaks and cytokine receptors--an intimate relationship. *Biochem Pharmacol* 72:1538-46
48. Ragimbeau J, Dondi E, Alcover A, Eid P, Uze G, Pellegrini S. 2003. The tyrosine kinase Tyk2 controls IFNAR1 cell surface expression. *EMBO J.* 22:537-47
49. Lupardus PJ, Skiniotis G, Rice AJ, Thomas C, Fischer S, et al. 2011. Structural snapshots of full-length Jak1, a transmembrane gp130/IL-6/IL-6Ralpha cytokine receptor complex, and the receptor-Jak1 holocomplex. *Structure* 19:45-55
50. Pellegrini S, John J, Shearer M, Kerr IM, Stark GR. 1989. Use of a selectable marker regulated by alpha interferon to obtain mutations in the signaling pathway. *Mol Cell Biol* 9:4605-12
51. Pestka S. 2007. The interferons: 50 years after their discovery, there is much more to learn. *J Biol Chem* 282:20047-51
52. Uze G, Schreiber G, Piehler J, Pellegrini S. 2007. The receptor of the type I interferon family. *Curr Top Microbiol Immunol* 316:71-95
53. Tomasello E, Pollet E, Vu Manh TP, Uze G, Dalod M. 2014. Harnessing Mechanistic Knowledge on Beneficial Versus Deleterious IFN-I Effects to Design Innovative

Immunotherapies Targeting Cytokine Activity to Specific Cell Types. *Front Immunol* 5:526
54. Crouse J, Kalinke U, Oxenius A. 2015. Regulation of antiviral T cell responses by type I interferons. *Nat Rev Immunol* 15:231-42
55. Miyagi T, Gil MP, Wang X, Louten J, Chu WM, Biron CA. 2007. High basal STAT4 balanced by STAT1 induction to control type 1 interferon effects in natural killer cells. *J Exp Med* 204:2383-96
56. Zundler S, Neurath MF. 2015. Interleukin-12: Functional activities and implications for disease. *Cytokine Growth Factor Rev* 26:559-68
57. Jouanguy E, Doffinger R, Dupuis S, Pallier A, Altare F, Casanova JL. 1999. IL-12 and IFN-gamma in host defense against mycobacteria and salmonella in mice and men. *Curr Opin Immunol* 11:346-51
58. Miossec P, Kolls JK. 2012. Targeting IL-17 and TH17 cells in chronic inflammation. *Nat Rev Drug Discov* 11:763-76
59. Waite JC, Skokos D. 2012. Th17 response and inflammatory autoimmune diseases. *Int J Inflam* 2012:819467
60. Pidasheva S, Trifari S, Phillips A, Hackney JA, Ma Y, et al. 2011. Functional studies on the IBD susceptibility gene IL23R implicate reduced receptor function in the protective genetic variant R381Q. *PLoS One* 6:e25038
61. Floss DM, Schroder J, Franke M, Scheller J. 2015. Insights into IL-23 biology: From structure to function. *Cytokine Growth Factor Rev* 26:569-78
62. Glocker EO, Kotlarz D, Boztug K, Gertz EM, Schaffer AA, et al. 2009. Inflammatory bowel disease and mutations affecting the interleukin-10 receptor. *N Engl J Med* 361:2033-45
63. Ouyang W, Rutz S, Crellin NK, Valdez PA, Hymowitz SG. 2011. Regulation and functions of the IL-10 family of cytokines in inflammation and disease. *Annu Rev Immunol* 29:71-109
64. Wolk K, Witte E, Witte K, Warszawska K, Sabat R. 2010. Biology of interleukin-22. *Semin Immunopathol* 32:17-31
65. Dhiman R, Indramohan M, Barnes PF, Nayak RC, PAIDipally P, et al. 2009. IL-22 produced by human NK cells inhibits growth of Mycobacterium tuberculosis by enhancing phagolysosomal fusion. *J Immunol* 183:6639-45
66. Hainzl E, Stockinger S, Rauch I, Heider S, Berry D, et al. 2015. Intestinal Epithelial Cell Tyrosine Kinase 2 Transduces IL-22 Signals To Protect from Acute Colitis. *J Immunol* 195:5011-24
67. Tengvall S, Che KF, Linden A. 2016. Interleukin-26: An Emerging Player in Host Defense and Inflammation. *J Innate Immun* 8:15-22
68. Egli A, Santer DM, O'Shea D, Tyrrell DL, Houghton M. 2014. The impact of the interferon-lambda family on the innate and adaptive immune response to viral infections. *Emerg Microbes Infect* 3:e51
69. Guschin D, Rogers N, Briscoe J, Witthuhn B, Watling D, et al. 1995. A major role for the protein tyrosine kinase JAK1 in the JAK/STAT signal transduction pathway in response to interleukin-6. *EMBO J* 14:1421-9
70. Heinrich PC, Behrmann I, Muller-Newen G, Schaper F, Graeve L. 1998. Interleukin-6-type cytokine signalling through the gp130/Jak/STAT pathway. *Biochem J* 334 (Pt 2):297-314
71. Janssens K, Slaets H, Hellings N. 2015. Immunomodulatory properties of the IL-6 cytokine family in multiple sclerosis. *Ann N Y Acad Sci* 1351:52-60
72. Zwirner NW, Ziblat A. 2017. Regulation of NK Cell Activation and Effector Functions by the IL-12 Family of Cytokines: The Case of IL-27. *Front Immunol* 8:25

73. McCormick SM, Heller NM. 2015. Commentary: IL-4 and IL-13 receptors and signaling. *Cytokine* 75:38-50
74. Karaghiosoff M, Neubauer H, Lassnig C, Kovarik P, Schindler H, et al. 2000. Partial impairment of cytokine responses in Tyk2-deficient mice. *Immunity* 13:549-60
75. Shimoda K, Kato K, Aoki K, Matsuda T, Miyamoto A, et al. 2000. Tyk2 plays a restricted role in IFN alpha signaling, although it is required for IL-12-mediated T cell function. *Immunity* 13:561-71
76. Sheehan KC, Lai KS, Dunn GP, Bruce AT, Diamond MS, et al. 2006. Blocking monoclonal antibodies specific for mouse IFN-alpha/beta receptor subunit 1 (IFNAR-1) from mice immunized by in vivo hydrodynamic transfection. *J Interferon Cytokine Res* 26:804-19
77. Stoiber D, Kovacic B, Schuster C, Schellack C, Karaghiosoff M, et al. 2004. TYK2 is a key regulator of the surveillance of B lymphoid tumors. *J Clin Invest* 114:1650-8
78. Ubel C, Graser A, Koch S, Rieker RJ, Lehr HA, et al. 2014. Role of Tyk-2 in Th9 and Th17 cells in allergic asthma. *Sci Rep* 4:5865
79. Shaw MH, Boyartchuk V, Wong S, Karaghiosoff M, Ragimbeau J, et al. 2003. A natural mutation in the Tyk2 pseudokinase domain underlies altered susceptibility of B10.Q/J mice to infection and autoimmunity. *Proc Natl Acad Sci U S A* 100:11594-9
80. Oyamada A, Ikebe H, Itsumi M, Saiwai H, Okada S, et al. 2009. Tyrosine kinase 2 plays critical roles in the pathogenic CD4 T cell responses for the development of experimental autoimmune encephalomyelitis. *J Immunol* 183:7539-46
81. Strobl B, Stoiber D, Sexl V, Mueller M. 2011. Tyrosine kinase 2 (TYK2) in cytokine signalling and host immunity. *Front Biosci* 17:3214-32
82. Derecka M, Gornicka A, Koralov SB, Szczepanek K, Morgan M, et al. 2012. Tyk2 and Stat3 regulate brown adipose tissue differentiation and obesity. *Cell Metab* 16:814-24
83. Potla R, Koeck T, Wegrzyn J, Cherukuri S, Shimoda K, et al. 2006. Tyk2 tyrosine kinase expression is required for the maintenance of mitochondrial respiration in primary pro-B lymphocytes. *Mol Cell Biol* 26:8562-71
84. Minegishi Y, Saito M, Morio T, Watanabe K, Agematsu K, et al. 2006. Human tyrosine kinase 2 deficiency reveals its requisite roles in multiple cytokine signals involved in innate and acquired immunity. *Immunity* 25:745-55
85. Kreins AY, Ciancanelli MJ, Okada S, Kong XF, Ramirez-Alejo N, et al. 2015. Human TYK2 deficiency: Mycobacterial and viral infections without hyper-IgE syndrome. *J Exp Med* 212:1641-62
86. Fuchs S, Kaiser-Labusch P, Bank J, Ammann S, Kolb-Kokocinski A, et al. 2016. Tyrosine kinase 2 is not limiting human antiviral type III interferon responses. *Eur J Immunol* 46:2639-49
87. Essletzbichler P, Konopka T, Santoro F, Chen D, Gapp BV, et al. 2014. Megabase-scale deletion using CRISPR/Cas9 to generate a fully haploid human cell line. *Genome Res* 24:2059-65
88. Mostafavi S, Yoshida H, Moodley D, LeBoite H, Rothamel K, et al. 2016. Parsing the Interferon Transcriptional Network and Its Disease Associations. *Cell* 164:564-78
89. Sanda T, Tyner JW, Gutierrez A, Ngo VN, Glover J, et al. 2013. TYK2-STAT1-BCL2 pathway dependence in T-cell acute lymphoblastic leukemia. *Cancer Discov* 3:564-77
90. Waanders E, Scheijen B, Jongmans MC, Venselaar H, van Reijmersdal SV, et al. 2017. Germline activating TYK2 mutations in pediatric patients with two primary acute lymphoblastic leukemia occurrences. *Leukemia* 31:821-8

91. Kaminker JS, Zhang Y, Waugh A, Haverty PM, Peters B, et al. 2007. Distinguishing cancer-associated missense mutations from common polymorphisms. *Cancer Res.* 67:465-73
92. Cho JH, Feldman M. 2015. Heterogeneity of autoimmune diseases: pathophysiologic insights from genetics and implications for new therapies. *Nat Med* 21:730-8
93. Baralle D, Baralle M. 2005. Splicing in action: assessing disease causing sequence changes. *J Med Genet* 42:737-48
94. Cartegni L, Chew SL, Krainer AR. 2002. Listening to silence and understanding nonsense: exonic mutations that affect splicing. *Nat Rev Genet* 3:285-98
95. Gregory AP, Dendrou CA, Attfield KE, Haghikia A, Xifara DK, et al. 2012. TNF receptor 1 genetic risk mirrors outcome of anti-TNF therapy in multiple sclerosis. *Nature* 488:508-11
96. Ng KP, Hillmer AM, Chuah CT, Juan WC, Ko TK, et al. 2012. A common BIM deletion polymorphism mediates intrinsic resistance and inferior responses to tyrosine kinase inhibitors in cancer. *Nat Med* 18:521-8
97. Sigurdsson S, Nordmark G, Goring HH, Lindroos K, Wiman AC, et al. 2005. Polymorphisms in the tyrosine kinase 2 and interferon regulatory factor 5 genes are associated with systemic lupus erythematosus. *Am. J. Hum. Genet.* 76:528-37
98. Graham DS, Akil M, Vyse TJ. 2007. Association of polymorphisms across the tyrosine kinase gene, TYK2 in UK SLE families. *Rheumatology* 46:927-30
99. Cunninghame Graham DS, Morris DL, Bhangale TR, Criswell LA, Syvanen AC, et al. 2011. Association of NCF2, IKZF1, IRF8, IFIH1, and TYK2 with systemic lupus erythematosus. *PLoS Genet* 7:e1002341
100. Eyre S, Bowes J, Diogo D, Lee A, Barton A, et al. 2012. High-density genetic mapping identifies new susceptibility loci for rheumatoid arthritis. *Nat Genet* 44:1336-40
101. Dyment DA, Cader MZ, Chao MJ, Lincoln MR, Morrison KM, et al. 2012. Exome sequencing identifies a novel multiple sclerosis susceptibility variant in the TYK2 gene. *Neurology* 79:406-11
102. Franke A, McGovern DP, Barrett JC, Wang K, Radford-Smith GL, et al. 2010. Genome-wide meta-analysis increases to 71 the number of confirmed Crohn's disease susceptibility loci. *Nat. Genet.* 42:1118-25
103. Hellquist A, Jarvinen TM, Koskenmies S, Zucchelli M, Orsmark-Pietras C, et al. 2009. Evidence for Genetic Association and Interaction Between the TYK2 and IRF5 Genes in Systemic Lupus Erythematosus. *J. Rheumatol.* 36:1631-8
104. Johnson BA, Wang J, Taylor EM, Caillier SJ, Herbert J, et al. 2010. Multiple sclerosis susceptibility alleles in African Americans. *Genes Immun.* 11:343-50
105. Liu JZ, Almarri MA, Gaffney DJ, Mells GF, Jostins L, et al. 2012. Dense fine-mapping study identifies new susceptibility loci for primary biliary cirrhosis. *Nat. Genet.* 44:1137-41
106. Mero IL, Lorentzen AR, Ban M, Smestad C, Celius EG, et al. 2010. A rare variant of the TYK2 gene is confirmed to be associated with multiple sclerosis. *Eur. J. Hum. Genet.* 18:502-4
107. Peluso C, Christofolini DM, Goldman CS, Mafra FA, Cavalcanti V, et al. 2012. TYK2 rs34536443 polymorphism is associated with a decreased susceptibility to endometriosis-related infertility. *Hum. Immunol.*
108. Sato K, Shiota M, Fukuda S, Iwamoto E, Machida H, et al. 2009. Strong evidence of a combination polymorphism of the tyrosine kinase 2 gene and the signal transducer and activator of transcription 3 gene as a DNA-based biomarker for susceptibility to Crohn's disease in the Japanese population. *J Clin Immunol* 29:815-25

109. Ban M, Goris A, Lorentzen AR, Baker A, Mihalova T, et al. 2009. Replication analysis identifies TYK2 as a multiple sclerosis susceptibility factor. *Eur. J. Hum. Genet.*
110. Strange A, Capon F, Spencer CC, Knight J, Weale ME, et al. 2010. A genome-wide association study identifies new psoriasis susceptibility loci and an interaction between HLA-C and ERAP1. *Nat. Genet.* 42:985-90
111. Suarez-Gestal M, Calaza M, Endreffy E, Pullmann R, Ordi-Ros J, et al. 2009. Replication of recently identified systemic lupus erythematosus genetic associations: a case-control study. *Arthritis Res. Ther.* 11:R69
112. Wang K, Zhang H, Kugathasan S, Annese V, Bradfield JP, et al. 2009. Diverse genome-wide association studies associate the IL12/IL23 pathway with Crohn Disease. *Am. J. Hum. Genet.* 84:399-405
113. Wallace C, Smyth DJ, Maisuria-Armer M, Walker NM, Todd JA, Clayton DG. 2010. The imprinted DLK1-MEG3 gene region on chromosome 14q32.2 alters susceptibility to type 1 diabetes. *Nat. Genet.* 42:68-71
114. Diogo D, Bastarache L, Liao KP, Graham RR, Fulton RS, et al. 2015. TYK2 Protein-Coding Variants Protect against Rheumatoid Arthritis and Autoimmunity, with No Evidence of Major Pleiotropic Effects on Non-Autoimmune Complex Traits. *PLoS One* 10:e0122271
115. Lopez-Isac E, Campillo-Davo D, Bossini-Castillo L, Guerra SG, Assassi S, et al. 2016. Influence of TYK2 in systemic sclerosis susceptibility: a new locus in the IL-12 pathway. *Ann Rheum Dis* 75:1521-6
116. Isaacs A, Lindenmann J. 1957. Virus interference. I. The interferon. *Proc R Soc Lond B Biol Sci* 147:258-67
117. Gough DJ, Messina NL, Clarke CJ, Johnstone RW, Levy DE. 2012. Constitutive type I interferon modulates homeostatic balance through tonic signaling. *Immunity* 36:166-74
118. Duncan CJ, Mohamad SM, Young DF, Skelton AJ, Leahy TR, et al. 2015. Human IFNAR2 deficiency: Lessons for antiviral immunity. *Sci Transl Med* 7:307ra154
119. Hambleton S, Goodbourn S, Young DF, Dickinson P, Mohamad SM, et al. 2013. STAT2 deficiency and susceptibility to viral illness in humans. *Proc Natl Acad Sci U S A* 110:3053-8
120. Honda K, Takaoka A, Taniguchi T. 2006. Type I interferon [corrected] gene induction by the interferon regulatory factor family of transcription factors. *Immunity* 25:349-60
121. Schneider WM, Chevillotte MD, Rice CM. 2014. Interferon-stimulated genes: a complex web of host defenses. *Annu Rev Immunol* 32:513-45
122. de Veer MJ, Holko M, Frevel M, Walker E, Der S, et al. 2001. Functional classification of interferon-stimulated genes identified using microarrays. *J Leukoc Biol* 69:912-20
123. Ivashkiv LB, Donlin LT. 2014. Regulation of type I interferon responses. *Nat Rev Immunol* 14:36-49
124. Katayama T, Nakanishi K, Nishihara H, Kamiyama N, Nakagawa T, et al. 2007. Type I interferon prolongs cell cycle progression via p21WAF1/CIP1 induction in human colon cancer cells. *Int J Oncol* 31:613-20
125. Davidson S, Maini MK, Wack A. 2015. Disease-promoting effects of type I interferons in viral, bacterial, and coinfections. *J Interferon Cytokine Res* 35:252-64
126. Teijaro JR, Ng C, Lee AM, Sullivan BM, Sheehan KC, et al. 2013. Persistent LCMV infection is controlled by blockade of type I interferon signaling. *Science* 340:207-11
127. Tovey MG, Lallemand C. 2010. Safety, Tolerability, and Immunogenicity of Interferons. *Pharmaceuticals (Basel)* 3:1162-86

128. Crow YJ. 2011. Type I interferonopathies: a novel set of inborn errors of immunity. *Ann N Y Acad Sci* 1238:91-8
129. Rodero MP, Crow YJ. 2016. Type I interferon-mediated monogenic autoinflammation: The type I interferonopathies, a conceptual overview. *J Exp Med* 213:2527-38
130. Sullivan KD, Lewis HC, Hill AA, Pandey A, Jackson LP, et al. 2016. Trisomy 21 consistently activates the interferon response. *Elife* 5
131. Weisfeld-Adams JD, Tkachuk AK, Maclean KN, Meeks NL, Scott SA. 2016. A de novo 2.78-Mb duplication on chromosome 21q22.11 implicates candidate genes in the partial trisomy 21 phenotype. *NPJ Genom Med* 1
132. Gresser I, Morel-Maroger L, Riviere Y, Guillon JC, Tovey MG, et al. 1980. Interferon-induced disease in mice and rats. *Ann N Y Acad Sci* 350:12-20
133. Coccia EM, Uze, G., Pellegrini, S. 2006. Negative regulation of Type I Interferon Signaling: Facts and Mechanisms. *Cellular and Molecular Biology* 52:77-87
134. Porritt RA, Hertzog PJ. 2015. Dynamic control of type I IFN signalling by an integrated network of negative regulators. *Trends Immunol* 36:150-60
135. Constantinescu SN, Croze E, Wang C, Murti A, Basu L, et al. 1994. Role of interferon alpha/beta receptor chain 1 in the structure and transmembrane signaling of the interferon alpha/beta receptor complex. *Proc Natl Acad Sci U S A* 91:9602-6
136. Kumar KG, Tang W, Ravindranath AK, Clark WA, Croze E, Fuchs SY. 2003. SCF(HOS) ubiquitin ligase mediates the ligand-induced down-regulation of the interferon-alpha receptor. *Embo J* 22:5480-90
137. Marijanovic Z, Ragimbeau J, Kumar KG, Fuchs SY, Pellegrini S. 2006. TYK2 activity promotes ligand-induced IFNAR1 proteolysis. *Biochem. J.* 397:31-8
138. Zheng H, Qian J, Baker DP, Fuchs SY. 2011. Tyrosine phosphorylation of protein kinase D2 mediates ligand-inducible elimination of the Type 1 interferon receptor. *J Biol Chem* 286:35733-41
139. Kumar KG, Krolewski JJ, Fuchs SY. 2004. Phosphorylation and specific ubiquitin acceptor sites are required for ubiquitination and degradation of the IFNAR1 subunit of type I interferon receptor. *J. Biol. Chem.* 279:46614-20
140. Kumar KG, Barriere H, Carbone CJ, Liu J, Swaminathan G, et al. 2007. Site-specific ubiquitination exposes a linear motif to promote interferon-alpha receptor endocytosis. *J Cell Biol* 179:935-50
141. Kumar KG, Varghese B, Banerjee A, Baker DP, Constantinescu SN, et al. 2008. Basal ubiquitin-independent internalization of interferon alpha receptor is prevented by Tyk2-mediated masking of a linear endocytic motif. *J Biol Chem* 283:18566-72
142. Liu J, Carvalho LP, Bhattacharya S, Carbone CJ, Kumar KG, et al. 2009. Mammalian casein kinase 1alpha and its leishmanial ortholog regulate stability of IFNAR1 and type I interferon signaling. *Mol Cell Biol* 29:6401-12
143. Qian J, Zheng H, Huangfu WC, Liu J, Carbone CJ, et al. 2011. Pathogen recognition receptor signaling accelerates phosphorylation-dependent degradation of IFNAR1. *PLoS Pathog* 7:e1002065
144. Malakhov MP, Malakhova OA, Kim KI, Ritchie KJ, Zhang DE. 2002. UBP43 (USP18) specifically removes ISG15 from conjugated proteins. *J Biol Chem* 277:9976-81
145. Recht M, Borden EC, Knight E, Jr. 1991. A human 15-kDa IFN-induced protein induces the secretion of IFN-gamma. *J Immunol* 147:2617-23
146. D'Cunha J, Ramanujam S, Wagner RJ, Witt PL, Knight E, Jr., Borden EC. 1996. In vitro and in vivo secretion of human ISG15, an IFN-induced immunomodulatory cytokine. *J Immunol* 157:4100-8

147. Owhashi M, Taoka Y, Ishii K, Nakazawa S, Uemura H, Kambara H. 2003. Identification of a ubiquitin family protein as a novel neutrophil chemotactic factor. *Biochem Biophys Res Commun* 309:533-9
148. Bogunovic D, Byun M, Durfee LA, Abhyankar A, Sanal O, et al. 2012. Mycobacterial disease and impaired IFN-gamma immunity in humans with inherited ISG15 deficiency. *Science* 337:1684-8
149. Casanova JL. 2015. Severe infectious diseases of childhood as monogenic inborn errors of immunity. *Proc Natl Acad Sci U S A* 112:E7128-37
150. Morales DJ, Lenschow DJ. 2013. The antiviral activities of ISG15. *J Mol Biol* 425:4995-5008
151. Okumura A, Lu G, Pitha-Rowe I, Pitha PM. 2006. Innate antiviral response targets HIV-1 release by the induction of ubiquitin-like protein ISG15. *Proc Natl Acad Sci U S A* 103:1440-5
152. Woods MW, Kelly JN, Hattlmann CJ, Tong JG, Xu LS, et al. 2011. Human HERC5 restricts an early stage of HIV-1 assembly by a mechanism correlating with the ISGylation of Gag. *Retrovirology* 8:95
153. Daczkowski CM, Dzimianski JV, Clasman JR, Goodwin O, Mesecar AD, Pegan SD. 2017. Structural Insights into the Interaction of Coronavirus Papain-Like Proteases and Interferon-Stimulated Gene Product 15 from Different Species. *J Mol Biol* 429:1661-83
154. Ye Y, Scheel H, Hofmann K, Komander D. 2009. Dissection of USP catalytic domains reveals five common insertion points. *Mol Biosyst* 5:1797-808
155. Honke N, Shaabani N, Zhang DE, Hardt C, Lang KS. 2016. Multiple functions of USP18. *Cell Death Dis* 7:e2444
156. Tokarz S, Berset C, La Rue J, Friedman K, Nakayama K, et al. 2004. The ISG15 isopeptidase UBP43 is regulated by proteolysis via the SCFSkp2 ubiquitin ligase. *J Biol Chem* 279:46424-30
157. Burkart C, Fan JB, Zhang DE. 2012. Two independent mechanisms promote expression of an N-terminal truncated USP18 isoform with higher DeISGylation activity in the nucleus. *J Biol Chem* 287:4883-93
158. Knobeloch KP, Utermohlen O, Kisser A, Prinz M, Horak I. 2005. Reexamination of the role of ubiquitin-like modifier ISG15 in the phenotype of UBP43-deficient mice. *Mol Cell Biol* 25:11030-4
159. Malakhova OA, Yan M, Malakhov MP, Yuan Y, Ritchie KJ, et al. 2003. Protein ISGylation modulates the JAK-STAT signaling pathway. *Genes Dev* 17:455-60
160. Malakhova OA, Kim KI, Luo JK, Zou W, Kumar KG, et al. 2006. UBP43 is a novel regulator of interferon signaling independent of its ISG15 isopeptidase activity. *EMBO J* 25:2358-67
161. Sarasin-Filipowicz M, Oakeley EJ, Duong FH, Christen V, Terracciano L, et al. 2008. Interferon signaling and treatment outcome in chronic hepatitis C. *Proc Natl Acad Sci U S A* 105:7034-9
162. Sarasin-Filipowicz M, Wang X, Yan M, Duong FH, Poli V, et al. 2009. Alpha interferon induces long-lasting refractoriness of JAK-STAT signaling in the mouse liver through induction of USP18/UBP43. *Mol Cell Biol* 29:4841-51
163. Francois-Newton V, Magno de Freitas Almeida G, Payelle-Brogard B, Monneron D, Pichard-Garcia L, et al. 2011. USP18-based negative feedback control is induced by type I and type III interferons and specifically inactivates interferon alpha response. *PLoS One* 6:e22200

164. Francois-Newton V, Livingstone M, Payelle-Brogard B, Uze G, Pellegrini S. 2012. USP18 establishes the transcriptional and anti-proliferative interferon alpha/beta differential. *Biochem J* 446:509-16
165. Ritchie KJ, Hahn CS, Kim KI, Yan M, Rosario D, et al. 2004. Role of ISG15 protease UBP43 (USP18) in innate immunity to viral infection. *Nat Med* 10:1374-8
166. Honke N, Shaabani N, Cadeddu G, Sorg UR, Zhang DE, et al. 2011. Enforced viral replication activates adaptive immunity and is essential for the control of a cytopathic virus. *Nat Immunol* 13:51-7
167. Honke N, Shaabani N, Zhang DE, Iliakis G, Xu HC, et al. 2013. Usp18 driven enforced viral replication in dendritic cells contributes to break of immunological tolerance in autoimmune diabetes. *PLoS Pathog* 9:e1003650
168. Hou S, Qi J, Zhang Q, Liao D, Li Q, et al. 2013. Genetic variants in the JAK1 gene confer higher risk of Behcet's disease with ocular involvement in Han Chinese. *Hum Genet* 132:1049-58
169. Polgar N, Csongei V, Szabo M, Zambo V, Melegh BI, et al. 2012. Investigation of JAK2, STAT3 and CCR6 polymorphisms and their gene-gene interactions in inflammatory bowel disease. *Int J Immunogenet* 39:247-52
170. Prager M, Buttner J, Haas V, Baumgart DC, Sturm A, et al. 2012. The JAK2 variant rs10758669 in Crohn's disease: altering the intestinal barrier as one mechanism of action. *Int J Colorectal Dis* 27:565-73
171. Tripathi P, Hong X, Caruso D, Gao P, Wang X. 2014. Genetic determinants in the development of sensitization to environmental allergens in early childhood. *Immun Inflamm Dis* 2:193-204
172. Fortune MD, Guo H, Burren O, Schofield E, Walker NM, et al. 2015. Statistical colocalization of genetic risk variants for related autoimmune diseases in the context of common controls. *Nat Genet* 47:839-46
173. Li Z, Gakovic M, Ragimbeau J, Eloranta ML, Ronnblom L, et al. 2013. Two rare disease-associated tyk2 variants are catalytically impaired but signaling competent. *J Immunol* 190:2335-44
174. Meuwissen ME, Schot R, Buta S, Oudesluijs G, Tinschert S, et al. 2016. Human USP18 deficiency underlies type 1 interferonopathy leading to severe pseudo-TORCH syndrome. *J Exp Med* 213:1163-74
175. Zhang X, Bogunovic D, Payelle-Brogard B, Francois-Newton V, Speer SD, et al. 2015. Human intracellular ISG15 prevents interferon-alpha/beta over-amplification and auto-inflammation. *Nature* 517:89-93
176. Speer SD, Li Z, Buta S, Payelle-Brogard B, Qian L, et al. 2016. ISG15 deficiency and increased viral resistance in humans but not mice. *Nat Commun* 7:11496
177. Wilmes S, Beutel O, Li Z, Francois-Newton V, Richter CP, et al. 2015. Receptor dimerization dynamics as a regulatory valve for plasticity of type I interferon signaling. *J Cell Biol* 209:579-93
178. Arimoto KI, Lochte S, Stoner SA, Burkart C, Zhang Y, et al. 2017. STAT2 is an essential adaptor in USP18-mediated suppression of type I interferon signaling. *Nat Struct Mol Biol* 24:279-89
179. Gauzzi MC, Velazquez L, McKendry R, Mogensen KE, Fellous M, Pellegrini S. 1996. Interferon-alpha-dependent activation of Tyk2 requires phosphorylation of positive regulatory tyrosines by another kinase. *J. Biol. Chem.* 271:20494-500
180. Richter MF, Dumenil G, Uze G, Fellous M, Pellegrini S. 1998. Specific contribution of Tyk2 JH regions to the binding and the expression of the interferon alpha/beta receptor component IFNAR1. *J Biol Chem* 273:24723-9

181. Desmet FO, Hamroun D, Lalande M, Collod-Beroud G, Claustres M, Beroud C. 2009. Human Splicing Finder: an online bioinformatics tool to predict splicing signals. *Nucleic Acids Res* 37:e67
182. Buchner DA, Trudeau M, Meisler MH. 2003. SCNM1, a putative RNA splicing factor that modifies disease severity in mice. *Science* 301:967-9
183. Dondi E, Pattyn E, Lutfalla G, Van Ostade X, Uze G, et al. 2001. Down-modulation of type 1 interferon responses by receptor cross-competition for a shared Jak kinase. *J Biol Chem* 276:47004-12
184. Dendrou CA, Cortes A, Shipman L, Evans HG, Attfield KE, et al. 2016. Resolving TYK2 locus genotype-to-phenotype differences in autoimmunity. *Sci Transl Med* 8:363ra149
185. Floss DM, Klocker T, Schroder J, Lamertz L, Mrotzek S, et al. 2016. Defining the functional binding sites of interleukin 12 receptor beta1 and interleukin 23 receptor to Janus kinases. *Mol Biol Cell* 27:2301-16
186. Sohn SJ, Barrett K, Van Abbema A, Chang C, Kohli PB, et al. 2013. A restricted role for TYK2 catalytic activity in human cytokine responses revealed by novel TYK2-selective inhibitors. *J Immunol* 191:2205-16
187. Works MG, Yin F, Yin CC, Yiu Y, Shew K, et al. 2014. Inhibition of TYK2 and JAK1 ameliorates imiquimod-induced psoriasis-like dermatitis by inhibiting IL-22 and the IL-23/IL-17 axis. *J Immunol* 193:3278-87
188. Consortium GT. 2015. Human genomics. The Genotype-Tissue Expression (GTEx) pilot analysis: multitissue gene regulation in humans. *Science* 348:648-60
189. Nagafuchi S, Kamada-Hibio Y, Hirakawa K, Tsutsu N, Minami M, et al. 2015. TYK2 Promoter Variant and Diabetes Mellitus in the Japanese. *EBioMedicine* 2:744-9
190. Marroqui L, Dos Santos RS, Floyel T, Grieco FA, Santin I, et al. 2015. TYK2, a Candidate Gene for Type 1 Diabetes, Modulates Apoptosis and the Innate Immune Response in Human Pancreatic beta-Cells. *Diabetes* 64:3808-17
191. Censin JC, Nowak C, Cooper N, Bergsten P, Todd JA, Fall T. 2017. Childhood adiposity and risk of type 1 diabetes: A Mendelian randomization study. *PLoS Med* 14:e1002362
192. Behnia R, Munro S. 2005. Organelle identity and the signposts for membrane traffic. *Nature* 438:597-604
193. Lemmon MA. 2008. Membrane recognition by phospholipid-binding domains. *Nat Rev Mol Cell Biol* 9:99-111
194. Progida C, Bakke O. 2016. Bidirectional traffic between the Golgi and the endosomes - machineries and regulation. *J Cell Sci* 129:3971-82
195. Nascimbeni AC, Codogno P, Morel E. 2017. Phosphatidylinositol-3-phosphate in the regulation of autophagy membrane dynamics. *FEBS J* 284:1267-78
196. Payelle-Brogard B, Pellegrini S. 2009. Biochemical monitoring of the early endocytic traffic of the type I interferon receptor. *J. IFN & Cytok. Res.* In press
197. Marijanovic Z, Ragimbeau J, van der Heyden J, Uze G, Pellegrini S. 2007. Comparable potency of IFNalpha2 and IFNbeta on immediate JAK/STAT activation but differential down-regulation of IFNAR2. *Biochem J* 407:141-51
198. Chmiest D, Sharma N, Zanin N, Viaris de Lesegno C, Shafaq-Zadah M, et al. 2016. Spatiotemporal control of interferon-induced JAK/STAT signalling and gene transcription by the retromer complex. *Nat Commun* 7:13476
199. Prchal-Murphy M, Semper C, Lassnig C, Wallner B, Gausterer C, et al. 2012. TYK2 kinase activity is required for functional type I interferon responses in vivo. *PLoS One* 7:e39141

200. Basters A, Geurink PP, Rocker A, Witting KF, Tadayon R, et al. 2017. Structural basis of the specificity of USP18 toward ISG15. *Nat Struct Mol Biol* 24:270-8
201. Ye Y, Akutsu M, Reyes-Turcu F, Enchev RI, Wilkinson KD, Komander D. 2011. Polyubiquitin binding and cross-reactivity in the USP domain deubiquitinase USP21. *EMBO Rep* 12:350-7

Résumé

In recent years, the pervasive action of type I IFN (IFN-α/β, here IFN-I) in human physiology and pathology has become evident. Actors of the immediate defence against viruses, IFN-I contribute to immune cell functions by orchestrating innate and adaptive immune responses. However, if the IFN-I system is dysregulated, altered immune responses and damaging processes can ensue as in the rare mendelian interferonopathies, several inflammatory and auto-immune diseases (AID) and some chronic viral infections. The evolution from beneficial to pathogenic IFN, which promotes persistent inflammation, immune cell dysfunction and tissue injury, remains poorly defined. On this basis, my thesis work has focused on the study of three elements of the IFN response pathway, with the view that their fine functional analyses could bring light onto how dysregulation may occur.

TYK2 belongs to the Janus protein tyrosine kinase family and is involved in signaling of several immunoregulatory cytokines, such as type I IFN (IFN-α/β) and type III IFNs, IL-6, IL-10, IL-12 and IL-23. Depending on the specific receptor complex, TYK2 is co-activated with either JAK1 or JAK2. A detailed molecular characterization of the interplay between the two juxtaposed enzymes is missing. In my study, I characterized TYK2 I684S and TYK2 P1104A, two rare human variants that have been associated with susceptibility to autoimmune diseases. I found that both variants are catalytically impaired but rescue signaling in response to IFN-I in fibroblasts. My results, coupled with additional functional study of JAK1-P1084A, support a model of non-hierarchical activation of Janus kinases where one catalytically competent JAK is sufficient for signaling provided that its partner, even if inactive, behaves as scaffold. Given the multitude of TYK2-activating cytokines, the cell type-specific dependence for TYK2 and the catalytic defect of the two disease-associated variants, I proposed that these two natural variants are relevant in complex immune disorders. Indeed, in addition to be associated with AID, a strong enrichment of TYK2 P1104A homozygosity was recently recorded in a cohort of patients with infection-predisposing primary immunodeficiency. My signaling studies showed that EBV-B cells homozygous for this variant exhibit mildly decreased IFN-I and IL-10 response, but abolished IL-23 signaling.

I studied two additional TYK2 variants (rs12720270, rs2304256) that have been associated with AID. Interestingly, from public eQTL datasets it appears that the rs2304256 minor allele correlates with elevated *TYK2* mRNA expression in many tissues. I found that both minor alleles promote retention of Exon8 and that an engineered TYK2 mutant lacking the Exon8-encoded segment is unable to bind the receptor subunit IFNAR1, though it retains catalytic activity. I propose that this partial loss of function is due to loss of integrity of the FERM-SH2 domain and/or an alteration of a potential lipid-binding surface.

In the second part of my thesis work I contributed to dissecting the molecular mechanism that tunes down IFN-I response in primary cells derived from rare USP18- and ISG15-deficient patients that suffered of severe and mild interferonopathy, respectively. This work substantiated the role of USP18 as the essential negative feedback regulator of IFN-I particularly in the central nervous system. It also highlighted a novel function of the ubiquitin-like protein ISG15 in restraining IFN-I response in humans, but not in mice. Molecular analysis showed that USP18 tunes down IFN signaling by modulating IFNAR1 recruitment or altering the dynamics of receptor dimerization.